MycoKeys 85: 1–30 (2021)
doi: 10.3897/mycokeys.85.70829
https://mycokeys.pensoft.net

RESEARCH ARTICLE

A peer-reviewed open-access journal
MycoKeys
Launched to accelerate biodiversity research

Two new asexual genera and six new asexual species in the family Microthyriaceae (Dothideomycetes, Ascomycota) from China

Min Qiao[1], Hua Zheng[1,2], Ji-Shu Guo[1,2], Rafael F. Castañeda-Ruiz[3], Jian-Ping Xu[1,4], Jie Peng[1,2], Ke-Qin Zhang[1], Ze-Fen Yu[1]

1 *Laboratory for Conservation and Utilization of Bio-resources, Key Laboratory for Microbial Resources of the Ministry of Education, Yunnan University, Kunming, Yunnan, 650091, China* **2** *School of Life Sciences, Yunnan University, Kunming, Yunnan, 650091, China* **3** *Instituto de Investigaciones Fundamentales en Agricultura Tropical "Alejandro de Humboldt" (INIFAT), 17200, La Habana, Cuba* **4** *Department of Biology, McMaster University, Hamilton, Ontario, L8S 4K1, Canada*

Corresponding author: Zefen Yu (zfyu@ynu.edu.cn)

Academic editor: Xinlei Fan | Received 29 June 2021 | Accepted 9 November 2021 | Published 29 November 2021

Citation: Qiao M, Zheng H, Guo J-S, Castañeda-Ruiz RF, Xu J-P, Peng J, Zhang K-Q, Yu Z-F (2021) Two new asexual genera and six new asexual species in the family Microthyriaceae (Dothideomycetes, Ascomycota) from China. MycoKeys 85: 1–30. https://doi.org/10.3897/mycokeys.85.70829

Abstract

The family Microthyriaceae is represented by relatively few mycelial cultures and DNA sequences; as a result, the taxonomy and classification of this group of organisms remain poorly understood. During the investigation of the diversity of aquatic hyphomycetes from southern China, several isolates were collected. These isolates were cultured and sequenced and a BLAST search of its LSU sequences against data in GenBank revealed that the closest related taxa are in the genus *Microthyrium*. Phylogenetic analyses, based on the combined sequence data from the internal transcribed spacers (ITS) and the large subunit (LSU), revealed that these isolates represent eight new taxa in Microthyriaceae, including two new genera, *Antidactylaria* **gen. nov.** and *Isthmomyces* **gen. nov.** and six new species, *Antidactylaria minifimbriata* **sp. nov.**, *Isthmomyces oxysporus* **sp. nov.**, *I. dissimilis* **sp. nov.**, *I. macrosporus* **sp. nov.**, *Triscelophorus anisopterioideus* **sp. nov.** and *T. sinensis* **sp. nov**. These new taxa are described, illustrated for their morphologies and compared with similar taxa. In addition, two new combinations are proposed in this family.

Keywords

Aquatic hyphomycetes, asexual genera, Microthyriaceae, phylogeny

Introduction

The family Microthyriaceae (Microthyriales, Dothideomycetes) was established by Saccardo (1883), containing foliar epiphytes and saprobes on dead leaves and stems (Wu et al. 2011a). This family is characterised by having superficial, flattened thyriothecia, with cells of the upper wall radiating in a parallel arrangement from the central ostiole opening; the ostiole may or may not be surrounded by setae. Asci are fusiform or obclavate to cylindro-clavate, bitunicate and fissitunicate and ascospores are two-celled, hyaline to brown often with ciliate appendages (Ashton 2009; Wu et al. 2011a; Hyde et al. 2013). Ashton et al. (2009) estimated that there were 54 genera and 278 species in the family. In a subsequent series of papers, Wu et al. (2010, 2011a, b, c 2014) revised Microthyriaceae by examining the generic type species and restricted Microthyriaceae to the species with morphological characteristics similar to *Microthyrium* Desm. Based on morphological characteristics, 11 genera and about 230 species were listed in this family (Wijayawardene et al. 2014), but in a subsequent outline of Ascomycota, only nine genera were accepted (Wijayawardene et al. 2018a). Recent studies accepted 11 genera in this family (Hongsanan et al. 2020; Wijayawardene et al. 2020).

Microthyriaceae have been poorly studied and there are few DNA sequences in public databases for this group of fungi. In the expanded multigene phylogeny of the Dothideomycetes, Microthyriaceae was not included because of the paucity of DNA sequences (Schoch et al. 2006). In the class-wide phylogenetic assessment of Dothideomycetes, Schoch et al. (2009) included Microthyriaceae, based on *Microthyrium microscopicum* Desm. (type species of Microthyriaceae). One major contributing reason for the absence of DNA sequences is that few living cultures are available. As a result, researchers might have assumed that many of these species were obligate parasites and could not be cultured (Wu et al. 2011a). Later, Hongsanan et al. (2014) isolated cultures of *Chaetothyriothecium elegans* Hongsanan & K.D. Hyde and *Tumidispora shoreae* Hongsanan & K.D. Hyde (Ariyawansa et al. 2015), but failed to observe anamorphs of the two species. Wu et al. (2014) tried to isolate fresh cultures of *Microthyrium propagulensis* H.X. Wu & K.D. Hyde, but did not observe the germination of ascospores. Based on these situations, asexual genera of Microthyriaceae were recorded only from the literature. Before Wu revised Microthyriaceae, *Asterostomula* Theiss. and seven other genera were described as asexual morphs (Hyde et al. 2011; Wijayawardene et al. 2012). With the exclusion of many genera from Microthyriaceae (Wu et al. 2010, 2011a, b, c), only *Hansfordiella* S. Hughes was retained as an asexual genus in Microthyriaceae (Wijayawardene et al. 2018a), but this connection was not confirmed by molecular data because sequences of *Hansfordiella* were unavailable. Moreover, *Hansfordiella* was recorded as the asexual state of *Trichothyrium* Speg., which belongs to Trichothyriaceae (Ashton 2009; Hyde et al. 2011, 2013; Wijayawardene et al. 2012, 2017).

In the early 1990s, molecular methods, in particular DNA sequence data, provided opportunities for phylogenetic inference and have made a significant impact on the taxonomy and classification of fungi (Shenoy et al. 2007). More importantly,

sequence analysis can potentially place an asexual-state taxon within an order or even link it with a teleomorph genus without having to observe the latter (e.g. in Berbee and Taylor 2001). The linkages between asexual and sexual genera have accumulated during implementation of the "One fungus: One name" concept, allowing the asexual genera to be placed in a natural biological framework of fungi (Wijayawardene et al. 2014, 2018a; Maharachchikumbura et al. 2015). However, the phylogenetic position of about 1530 genera in Ascomycota still remains incertae sedis (Wijayawardene et al. 2018a).

Aquatic hyphomycetes colonise allochthonous organic matter in fresh waters and are closely involved in the decomposition and conversion of biopolymers in aquatic habitats (Brlocher 1992). They are a polyphyletic group of fungi, mainly consisting of asexual morphs of Ascomycota and Basidiomycota, which have been identified, based on conidium morphology and conidiogenesis (Belliveau and Barlocher 2005). Molecular approaches applied to phylogeny of aquatic hyphomycetes place some genera in a defined class and found multiple origins of aquatic hyphomycetes. Specifically, seven strains (five species) of *Tetracladium* De Wild. showed close relationships to the Ascomycete orders Onygenales, Erysiphales and Leotiales (Nikolcheva 2002), but subsequently, Baschien (2006) found *Tetracladium* located in Leotiomycetes, based on combined ITS and 28S analyses. Besides, studies of 31 species of aquatic hyphomycetes placed the majority (74%) within the Leotiomycetes (Belliveau and Barlocher 2005; Campbell et al. 2006). Duarte et al. (2015) constructed an ITS phylogenetic tree for 79 aquatic hyphomycetes, and found *Tricladium* Ingold and *Triscelophorus* Ingold are not monophyletic. Of course, with the availability of more and more reference sequences and the establishment of backbone trees of some classes, new aquatic hyphomycetes related to monophyly have been published with confirmed phylogenetic positions (Pratibha et al. 2015; Liu et al. 2016; Su et al. 2016; Qiao et al. 2018a; Wijayawardene et al. 2018a). Although these studies promoted phylogenetic development of aquatic hyphomycetes, the phylogenetic positions of most aquatic hyphomycetes have not been determined at the family level (Wijayawardene et al. 2018a).

In recent years, we have investigated the diversity and phylogeny of aquatic hyphomycetes from southern China which is a hot spot of world biodiversity, such as Yunnan, Sichuan, Guizhou, Guangdong and Hainan Provinces. Many new species collected from these regions have been described (Yang et al. 2011, 2012; Bai et al. 2013; Li et al. 2013, 2014; Guo et al. 2015, 2019; Qiao et al. 2017a, b, 2018b, 2019a, b, c, 2020; Peng et al. 2016; Yu et al. 2019; Zheng et al. 2020a, 2021a). In addition, several interesting isolates were collected. These isolates were cultured and sequenced and a BLAST search of its LSU sequences against data in GenBank revealed that the closest related taxa are in the genus *Microthyrium*. Based on the phylogenetic analysis combined with the internal transcribed spacers (ITS) and the large subunit (LSU) gene sequences and morphological features, two new genera and six new species are proposed within Microthyriaceae. In addition, we also collected *Isthmolongispora quadricellularis* isolates and describe and illustrate it here.

Methods

Collection of samples, fungal isolation and morphological characterisation

Submerged leaves were collected from streams in Guangdong, Hainan Provinces and Tibet region. Samples were preserved in zip-locked plastic bags, labelled and transported to the laboratory at 4 °C. Each leaf was cut into several 3–4 × 4–5 cm-sized fragments, then these fragments were incubated on corn meal agar (CMA; 20 g cornmeal, 18 g agar, 40 mg streptomycin, 30 mg ampicillin, 1 litre distilled water) plates for 5 days at room temperature. Individual conidia were isolated using a sterilised toothpick under a BX51 microscope and cultivated on CMA plates. Morphological characteristics were observed from cultures growing on CMA and potato dextrose agar plates (PDA; 200 g potato, 20 g dextrose, 18 g agar, 1 litre distilled water) after incubation at 25 °C for one week. Microscopic photographs coming from CMA medium were taken with an Olympus BX51 microscope connected to a DP controller digital camera.

The pure cultures and dried cultures were deposited in the Herbarium of the Laboratory for Conservation and Utilization of Bio-Resources, Yunnan University, Kunming (YMF) and the China General Microbiological Culture Collection Center (CGMCC).

DNA extraction, PCR amplification and sequencing

Genomic DNA was extracted from fresh mycelia grown on PDA at 25 °C as described by Turner et al. (1997). Fragments of the internal transcribed spacers (ITS) and the large subunit nuclear ribosomal RNA gene (LSU rRNA) were amplified with the following primer pairs: ITS4 and ITS5 for ITS (White et al. 1990) and LROR/LR7 (Vilgalys and Hester 1990), respectively. Each 25 µl PCR reaction volume consisted of 12.5 µl T5 Super PCR Mix (Beijing TsingKe Biotech Co., Ltd., Beijing, China), 1 µl of forward primer (10 µM), 1 µl of reverse primer (10 µM), 1µl DNA template, 5 µl of PCR buffer and 4.5 µl sterile water. The PCR thermal cycle programmes for the amplifications of these three DNA fragments followed those described in Su et al. (2016). PCR products were visualised on 1% agarose gel stained with Goldview (Geneshun Biotech, China) with D2000 DNA ladder (Realtimes Biotech, Beijing, China) and were then purified using a commercial Kit (Bioteke Biotechnology Co., Ltd., Beijing, China). DNA forward and reverse sequencing was performed with a LI-COR 4000L automatic sequencer with the same primers, using a Thermo Sequenase-kit as described by Kindermann et al. (1998). Finally, these new obtained sequences were deposited in the GenBank database at the National Center for Bio-technology Information (NCBI) and the accession numbers are listed in Table 1.

Table 1. Species, strains and their corresponding GenBank accession numbers of sequences used for phylogenetic analyses. Newly-generated sequences are in bold.

Name	Strain	GenBank accession number	
		LSU	ITS
Antidactylaria ampulliforma	CBS223.59	MH869386	MH857845
Antidactylaria ampulliforma	P004	EU107302	—
Antidactylaria ampulliforma	P038	EU107303	—
Antidactylaria minifimbriata	CGMCC 3.18825 = YMF 1.04578	**MK577808**	**MK569506**
Chaetothyriothecium elegans	CPC 21375	KF268420	—
Hamatispora phuquocensis	VICCF 1219	LC064073	LC064074
Heliocephala elegans	MUCL 39003	HQ333478	HQ333478
Heliocephala gracilis	MUCL 41200	HQ333479	HQ333479
Heliocephala natarajanii	MUCL 43745	HQ333480	HQ333480
Heliocephala zimbabweensis	MUCL 40019	HQ333481	HQ333481
Isthmomyces dissimilis	CGMCC 3.18826 = YMF 1.04604	**MK577811**	**MF740794**
Isthmomyces lanceatus	CBS 622.66	MH870563	MH858897
Isthmomyces lanceatus	YMF 1.04514	**MK577813**	**MK577895**
Isthmomyces lanceatus	CGMCC 3.18827	**MK577814**	**MK577896**
Isthmomyces macrosporus	YMF 1.04518 = CGMCC 3.18824 = YMF 1.04794	**MK577812**	**MF740796**
Isthmomyces oxysporus	CGMCC 3.18821 = YMF 1.04513	**MK577810**	**MF740793**
Lichenopeltella pinophylla	CBS 143816	MG844152	—
Microthyrium buxicola	MFLUCC 15-0212	KT306551	—
Microthyrium buxicola	MFLUCC 15-0213	KT306552	—
Microthyrium chinense	HKAS 92487	KY911453	—
Microthyrium fici-septicae	NCYUCC 19-0038	MW063251	—
Microthyrium fici-septicae	MFLUCC 20-0174	MW063252	—
Microthyrium ilicinum	CBS 143808	MG844151	—
Microthyrium macrosporum	CBS 143810	MG844159	—
Microthyrium microscopicum	CBS 115976	GU301846	—
Microthyrium propagulensis	IFRD 9037	KU948989	—
Natipusilla decorospora	AF236-1	HM196369	—
Natipusilla naponense	AF217-1	HM196371	—
Neoanungitea eucalypti	CBS 143173	MG386031	MG386031
Neoscolecobasidium agapanthi	CPC 28778	KY173517	KY173426
Ochroconis dracaenae	CPC 26115	KX228334	KX228283
Parazalerion indica	CBS 125443	MH874977	MH863483
Phaeotrichum benjaminii	CBS 541.72	AY004340	MH860561
Pseudomicrothyrium thailandicum	MFLU 14-0286	MT741680	—
Pseudopenidiella gallaica	CBS 121796	LT984843	LT984842
Pseudopenidiella piceae	CBS 131453	JX069852	JX069868
Schismatomma decolorans	DUKE 47570	AY548815	AY548808
Scolecobasidium tropicale	CBS 380.87	KF156102	—
Sympoventuria capensis	CBS 120136	KF156104	DQ885906
Trichodelitschia bisporula	CBS 262.69	GU348996	MH859305
Triscelophorus anisopteriodeus	CGMCC 3.18978 = YMF 1.04267	**MK577818**	**MK569511**
Triscelophorus monosporus	CBS 440.54	MH868925	—
Triscelophorus sinensis	YMF 1.04065	**MK577820**	**MK569513**
Tumidispora shoreae	MFLUCC 12-0409	KT314073	—
Tumidispora shoreae	MFLUCC 14-0574	KT314074	—
Venturia inaequalis	CBS 594.70	GU301879	KF156040
Zeloasperisporium ficusicola	MFLUCC 15-0221	KT387733	—
Zeloasperisporium hyphopodioides	CBS 218.95	EU035442	EU035442
Zeloasperisporium siamense	IFRDCC 2194	JQ036228	—

Sequence alignment and phylogenetic analysis

Preliminary searches with newly-generated LSU and ITS gene sequences of these isolates against National Center for Biotechnology Information (NCBI) by the Basic Local Alignment Search Tool (BLAST) determined species closely related to our isolates. Based on this information, sequences of ITS and LSU were downloaded from Microthyriaceae and four sister orders belonging to Dothideomycetes, including 48 strains representing 35 species (Table 1), according to recent studies (Hongsanan et al. 2020; Iturrieta-González et al. 2020). *Schismatomma decolorans* (Erichsen) Clauzade & Vězda was used as the outgroup taxon.

For Microthyriaceae, the phylogenetic analysis was based on the combined ITS and LSU sequences. DNA sequence data of ITS and LSU were aligned using Clustal X 1.83 (Thompson et al. 1997) with the default parameters, then the consensus sequences were manually adjusted and linked through BioEdit v.7.0 (Hall 1999). Manual gap adjustments were carried out to improve the alignment and ambiguously-aligned regions were also excluded. We finally obtained the combined sequence matrix (Fasta file) generated by BioEdit v.7.0, containing 1119 nucleotide positions from two genes and the matrix was uploaded to TreeBASE (www.treebase.org; accession number: S28086). Bayesian Inference (BI) and Maximum Likelihood (ML) were used in this study for phylogenetic analyses. BI analysis was conducted with MrBayes v.3.2.2 (Ronquist et al. 2012) with NEXUS files converted by MEGA6 (Tamura et al. 2013). The Akaike Information Criterion (AIC) implemented in jModelTest 2.0 (Posada 2008) was used to select the best fit models after likelihood score calculations were done. GTR+F+I+G4 was estimated as the best-fit model under the output strategy of AIC. The parameters used were two simultaneous runs of 1,000,000 generations, four Markov chains, sampled every 500 generations. The 50% majority-rule consensus tree and posterior probability values (PP) were calculated after discarding the first 25% of the samples. ML analysis was computed by RAxML (Stamatakis 2006), using the GTR-GAMMA model. Maximum Likelihood bootstrap proportions (MLBP) were computed with 1000 replicates. Trees were visualised in FigTree 1.4.3 (http://tree.bio.ed.ac.uk/software/Figtree/, June 2021). Bayesian Inference posterior probabilities (BIPP) ≥ 0.9 and Maximum Likelihood bootstrap proportions (MLBP) ≥ 70% are indicated at nodes.

Results

Phylogenetic analyses

The phylogenic tree, based on a combined sequence of the LSU and ITS, indicated that eight isolates belong to the Microthyriaceae (Fig. 1). After detailed observations of morphological features, these isolates were considered as six new species and one known species. In this tree, five isolates grouped with *Isthmolongispora lanceata* CBS 622.66 with

good support (MLBP/BIPP = 100%/1.0). Combined with morphological differences, we proposed the new genus *Isthmomyces* to accommodate the three new species, designated as *I. dissimilis*, *I. macrosporus* and *I. oxysporus* and a new combination *I. lanceatus*. Two isolates, which clustered with *Triscelophorus monosporus* CBS 440.54 (MLBP/BIPP = 91%/1.0), were considered as two new *Triscelophorus* species, designated as *Triscelophorus anisopteriodeus* and *T. sinensis*. The isolate YMF 1.04578 is phylogenetically close to *Isthmolongispora ampulliformis* (MLBP/BIPP = 77%/0.96). Considering morphological characters, we proposed a new genus *Antidactylaria* to accommodate the new species *A. minifimbriata* and the new combination *A. ampulliforma*.

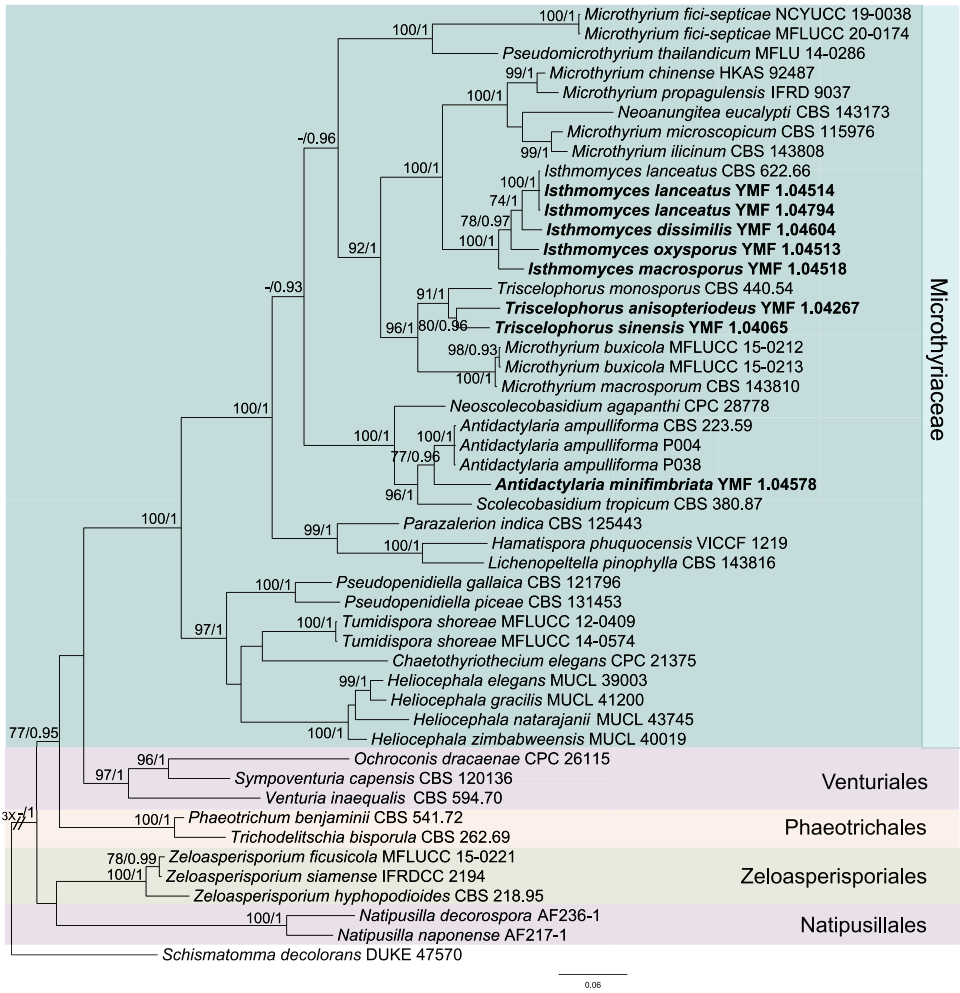

Figure 1. Phylogenetic tree generated by the Maximum Likelihood (ML) analysis using combined sequences of the nuclear large subunit (LSU) and the internal transcribed spacers (ITS) gene. Bootstrap support values for ML over 70% and Bayesian posterior probabilities greater than 0.9 are indicated above or below the nodes as MLBP/BIPP. *Schismatomma decolorans* strain DUKE 47570 is used as the outgroup. Novel species are indicated in bold.

Taxonomy

Microthyriaceae Sacc., Syll. fung. (Abellini) 2: 658 (1883).
MycoBank No: 81008

Description. Hyde et al. 2013.

Type genus. *Microthyrium* Desm., Annls Sci. Nat., Bot., sér. 2 15: 137 (1841).

Notes. Microthyriales only contains a single family Microthyriaceae, based on morphology and phylogeny. Currently, eleven genera are accepted in Microthyriaceae, including three asexual genera (Hongsanan et al. 2020; Wijayawardene et al. 2020). The asexual morph of this family is characterised by having micronematous or macronematous, unbranched or branched, septate conidiophores, mono- to polyblastic, determinate or sympodial, clavate, subcylindrical, ampulliform or ovoid conidiogenous cells and solitary or in branched chains, acrogenous or acropleurogenous, aseptate to multi-septate conidia. In this study, we erected two new asexual genera, *Antidactylaria* and *Isthmomyces* and recognised six new asexual species in Microthyriaceae, based on DNA sequences at two gene fragments. In addition, two new combinations are proposed in Microthyriaceae combined morphology and phylogeny.

***Antidactylaria* Z.F. Yu, M. Qiao & R.F. Castañeda, gen. nov.**
Index Fungorum number: IF555876
Facesoffungi Number No: FoF05734

Etymology. Greek, *Anti*, meaning against, Latin, *dactylaria*, referring to the genus *Dactylaria*.

Description. Asexual morph hyphomycetous. *Mycelium* superficial and immersed. *Conidiophores* macronematous, erect, unbranched, septate, hyaline, sometimes reduced to conidiogenous cells. *Conidiogenous cells* denticulate, polyblastic, sympodial elongated, integrated, terminal determinate or indeterminate, hyaline. Conidial secession rhexolytic. *Conidia* solitary, acrogenous, narrow obclavate, cylindrical to fusiform, navicular, attenuate towards the apex, rostrate, unicellular or septate, hyaline or subhyaline, smooth-walled, with a minute basal frill. Sexual state: unknown.

Type species. *Antidactylaria minifimbriata* Z.F. Yu, M. Qiao & R.F. Castañeda.

Notes. *Antidactylaria* is superficially similar to the genus *Dactylaria* Sacc. in morphology. The genus *Dactylaria*, typified with *D. purpurella* (Sacc.) Sacc., is characterised by unbranched, septate, hyaline or pigmented conidiophores, denticulate, integrated, mostly terminal, sympodially extending conidiogenous cells and cylindrical, fusiform, filiform, ellipsoid, clavate, obclavate, unicellular or septate, hyaline or pale pigmented conidia that are liberated with schizolytic secession (Goh and Hyde 1997; Paulus et al. 2003; Seifert et al. 2011). However, the rhexolytic conidial secession, observed in *Antidactylaria*, is absent in *Dactylaria*. Paulus et al. (2003) discussed the conidiogenous event as an important criterion for generic delimitation. In addition,

phylogeny analysis showed that *Antidactylaria* species belong to Microthyriales, while *Dactylaria* species belong to Helotiales.

***Antidactylaria ampulliforma* (de Hoog & Hennebert) Z.F. Yu, M. Qiao & R.F. Castañeda, comb. nov.**
MycoBank No: 108094

Isthmolongispora ampulliformis (Tubaki) de Hoog & Hennebert, Proc. K. Ned. Akad. Wet., Ser. C, Biol. Med. Sci. 86(3): 346 (1983)
Diplorhinotrichum ampulliforme Tubaki, J. Hattori bot. Lab. 20: 159 (1958)

Description. Matsush. 1975

Notes. *Antidactylaria ampulliforma* was originally isolated by Tubaki from leaves of *Cocos nucifera* and was described as *Diplorhinotrichum* species (Tubaki 1958). In 1983, de Hoog and Hennebert included it in the genus *Isthmolongispora* after examining its morphological character. In this study, *A. ampulliforma* is phylogenetically close to *A. minifimbriata* and they are very similar in morphology. Therefore, we assigned it in the newly-established genus *Antidactylaria* as a new combination.

***Antidactylaria minifimbriata* Z.F. Yu, M. Qiao & R.F. Castañeda, sp. nov.**
Index Fungorum number: IF556121
Facesoffungi Number No: FoF05735
Figs 2, 9a

Etymology. Latin, *mini*, meaning very small, minute, *fimbriata*, referring to edged, delicately toothed, fringe or frill that remained on the conidial base after rhexolytic secession.

Description. Asexual morph hyphomycetous. *Colonies* on CMA white to rosy buff, reverse buff, attaining 2.7 cm diam. after 20 days at 25 °C. *Mycelium* partly superficial, partly immersed, composed of branched, slender, septate, hyaline, smooth-walled hyphae. *Conidiophores* semi-macronematous, mononematous, cylindrical, straight or slightly flexuous, unbranched, 0–1(–2)-septate, hyaline or pale brown, smooth, sometimes reduced to conidiogenous cells. *Conidiogenous cells* polyblastic, sympodial elongated, terminal, denticulate, denticles cylindrical, minute fringed. *Conidia* solitary, acrogenous, narrow obclavate, cylindrical to fusiform, attenuate, rostrate or caudate towards the apex, 27.7–40 × 2.5–3.3 µm, rostrum 10–19 × 1–1.8 µm, 2-septate, hyaline to subhyaline, smooth-walled, with a minute basal frill. Sexual state: unknown.

Type. China, Hainan Province, Diaoluoshan National Forest Park, on submerged leaves, April 2014, Z.F Yu. Holotype YMF 1.04578, preserved in a metabolically-inactive state (deep freezing) in the Conservation and Utilization of Bio-Resources in Yunnan. Ex-type culture CGMCC 3.18825.

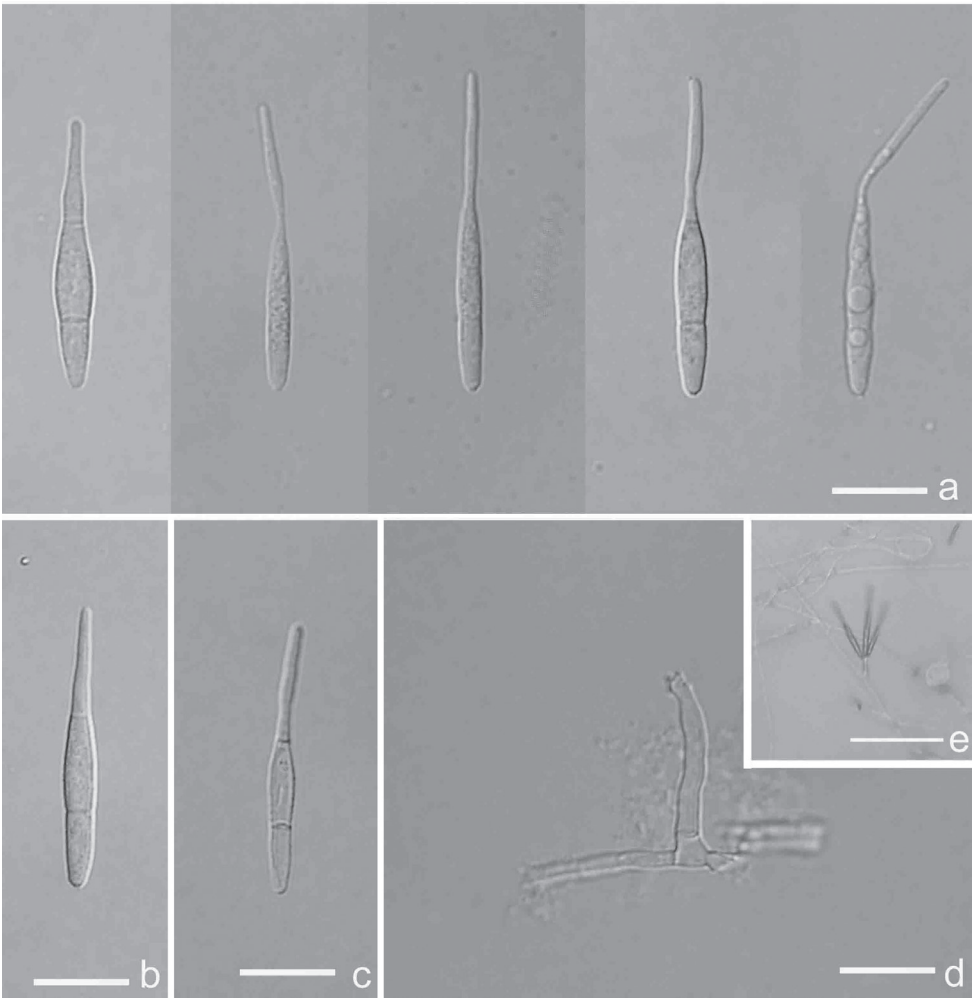

Figure 2. *Antidactylaria minifimbriata* (Holotype YMF 1.04578) **a–c** conidia **d** conidiophore and conidiogenous cell **e** conidia on conidiophore under low objective. Scale bars: 10 μm (**a–d**); 50 μm (**e**).

Notes. Morphologically, *Antidactylaria minifimbriata* is similar to *A. ampulliforma* (= *Isthmolongispora ampulliformis*) in conidial shape, but can be easily distinguished from it by having wider conidia (2.5–3.3 vs. 2.0–2.5 μm) and longer rostrum (10.0–19.0 vs. 6.0–10.0 μm) (Yen et al. 2017).

***Isthmomyces* Z. F. Yu, M. Qiao & R. F. Castañeda, gen. nov.**
Index Fungorum number: IF556126
Facesoffungi Number No: FoF05740

Etymology. Latin, *isthmus*, Greek (isthmós, "neck") meaning a narrow cellular structure that connects two larger bodies or cells, Greek, *myces*, referring to fungus.

Description. Asexual morph hyphomycetous. *Mycelium* superficial and immersed. *Conidiophores* macronematous, mononematous, erect, unbranched, smooth, pale brown or hyaline, septate, sometimes reduced to conidiogenous cells. *Conidiogenous cells* polyblastic, denticulate, integrated, terminal, sympodial extended. *Conidial secession* schizolytic. *Conidia* acrogenous, isthmosporous, composed two cellular isthmic-segment obclavate, clavate, pyriform, obpyriform, lageniform, subulate fusiform to navicular to lanceolate, unicellular or septate, smooth, hyaline, connected by a very narrow, distinct or inconspicuous isthmus. Sexual state: unknown.

Type species. *Isthmomyces oxysporus* Z.F. Yu, M. Qiao & R.F. Castañeda.

Notes. *Isthmomyces* is similar to the genus *Isthmolongispora* Matsush. in morphology. *Isthmolongispora* was established with *I. intermedia* Matsush. as type species (Matsushima 1971). The genus is characterised by denticulate, sympodially-extending conidiogenous cells and isthmospore conidia made of two or several cellular structures, which are connected by very narrow isthmuses. In this study, specimens with two and more cellular isthmic-segments were collected, respectively. Phylogenetic analysis inferred from two loci showed that our isolates grouped together with *Isthmomyces lanceatus* (*Isthmolongispora lanceata*) in Microthyriaceae. Combining morphological character and phylogenetic analysis, we finally erected the new genus *Isthmomyces* to accommodate these isolates and *I. lanceata*.

***Isthmomyces dissimilis* Z. F. Yu, M. Qiao & R. F. Castañeda, sp. nov.**

Index Fungorum number: IF556129

Facesoffungi Number No: FoF05743

Figs 3, 9b

Etymology. Latin, *dissimilis*, referring to the variation of the conidial shape related to the generic concept of the genus.

Description. Asexual morph hyphomycetous. *Colonies* on CMA white to dark salmon, reverse pale yellow, attaining 2.5 cm diam. after 20 days at 25 °C. *Mycelium* superficial or immersed, composed of branched, septate, brown, hyphae. *Conidiophores* macronematous, mononematous, erect, straight, unbranched or slightly branched, 0–1- septate, smooth, subhyaline13.8–51 × 2.3–3.2 μm. *Conidiogenous cells* polyblastic, ampulliform to cylindrical, sympodial extended, integrated, terminal, subhyaline. *Conidia* acrogenous, isthmospore, with inconspicuous isthmus, (isthmus mostly reduced to being constricted at the septa) subhyaline, guttulate, smooth, composed of 2–3-cellular isthmic-segments, more or less symmetrical: A) the larger isthmospore with 2-cellular isthmic-segments: i) basal isthmic-segment cylindrical-fusiform, truncate below, 1–3 septate, 35–60 × 4–4.5 μm, ii) apical isthmic-segment fusiform, rounded at the tip, 0–2 septate, 17–36.5 × 4–4.5 μm; total long 70–95 μm. B) the smaller isthmospore with 2-cellular isthmic-segments: i) basal isthmic-segment cylindrical-fusiform, truncate below, 0–1 septate, 23–33 × 3.5–4.5 μm; ii) apical isthmic-segment fusiform,

rounded at the tip, 0–1 septate, 17–22 × 3.5–4.5 μm; total long 47–57 μm. C) isthmospore with 3-cellular isthmic-segments: i) basal isthmic-segment fusiform, truncate below, 2–3-septate, 18.5–38.5 × 2.8–5.0 μm; ii) central isthmic-segment cylindrical-fusiform, 2–3-septate, 20.1–44.5 × 3.0–6.2 μm; iii) apical isthmic-

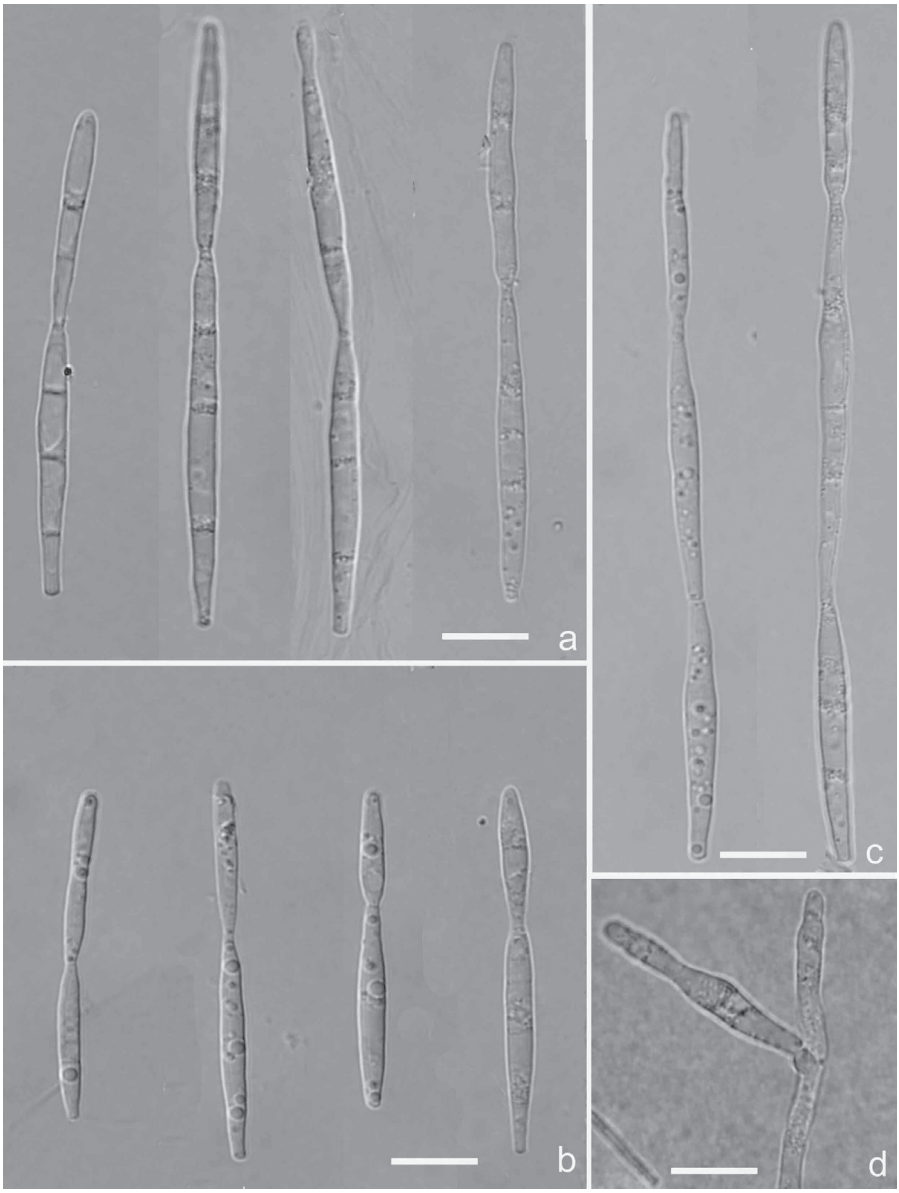

Figure 3. *Isthmomyces dissimilis* (Holotype YMF 1.04604) **a** the larger isthmospore with 2-cellular isthmic-segments **b** the smaller isthmospore with 2-cellular isthmic-segments **c** isthmospores with 3-cellular isthmic-segments **d** conidiogenous cell and developing conidia. Scale bars: 10 μm (**a–d**).

segment fusiform, rounded or obtuse at the tip, 0–2-septate, 17.4–31.6 × 2.3–4.8 μm. Sexual state: unknown.

Type. **China**, Hainan Province, Diaoluo Mountain Nature Reserve, on submerged leaves, August 2015, J. Peng. Holotype YMF 1.04604, preserved in a metabolically-inactive state (deep freezing) in the Conservation and Utilization of Bio-Resources in Yunnan. Ex-type culture CGMCC 3.18826.

Notes. The new species, *Isthmomyces dissimilis*, varies in conidial shape. Although it has 3-cellular isthmic-segment conidia, its isthmic-segment is not as distinct as *Isthmolongispora* species. However, the cells of *Isthmolongispora* are bead-like, while those of *I. dissimilis* are cylindrical to fusiform.

Isthmomyces lanceatus **(de Hoog & Hennebert) Z. F. Yu & R. F. Castañeda, comb. nov.**
Index Fungorum number: IF556158
Facesoffungi Number No: FoF05757
Figs 4, 9c

Isthmolongispora lanceata de Hoog & Hennebert, Proc. K. Ned. Akad.Wet., Ser. C, Biol. Med. Sci. 86(3): 343 (1983).

Description. Asexual morph hyphomycetous. *Colonies* on CMA white to dark salmon, reverse pale brown, attaining about 2 cm diam. after 20 days at 25 °C. *Mycelium* partly superficial, partly immersed, composed of branched, septate, slender, hyaline hyphae. *Conidiophores* macronematous, mononematous, cylindrical, erect, straight, unbranched, 0–1- septate, smooth, hyaline, up to 30 μm long, 3–3.5 μm wide. *Conidiogenous cells* polyblastic, cylindrical, denticulate, sympodial extended, integrated, terminal, hyaline. *Blastoconidia* isthmospore, somewhat fusiform, hyaline or subhyaline, smooth, thin-walled, 21.3–39.7 μm long, strongly constricted at the median septum, narrow, tiny, made of two cellular isthmic-segments: i) basal isthmic-segment narrow-clavate, sometimes cylindrical-clavate, truncated at the base, unicellular, 0–1-septate, 12.5–18.5 × 3.0–4.8 μm; ii) apical isthmic-segment broadly obclavate, obspathulate, rounded at the tip, unicellular, 0–1-septate, 13.0–30.0 × 2.3–3.8 μm. *Arthroconidia* often formed in the aerial mycelium, disarticulated from fertile hyphae. Sexual state: unknown.

Type. **China**, Tibet, Nanyigou Scenic Area, on submerged leaves, October 2016, Z.F. Yu, YMF 1.04794 = CGMCC 3.18827. **China**, Yunnan Province, Jade Dragon Snow Mountain, on submerged leaves, September 2015, J. Peng, YMF 1.04514.

Notes. *Isthmomyces lanceatus* was first isolated by Beverwijk from leaf of *Castanea vesca* in steam (Hoog and Hennebert 1983). However, the taxonomic status of this species was Ascomycota *incertae sedis*. In this study, this is the first report of *I. lanceatus* isolated from Asia. Morphologically, the conidia of our isolates are larger than the holotype CBS 622.66. Our phylogenetic analysis of combined LSU and ITS sequences reveals that the phylogenetic position of *I. lanceatus* is in Microthyriaceae and *I. lanceatus* is close to *I. dissimilis* in this tree.

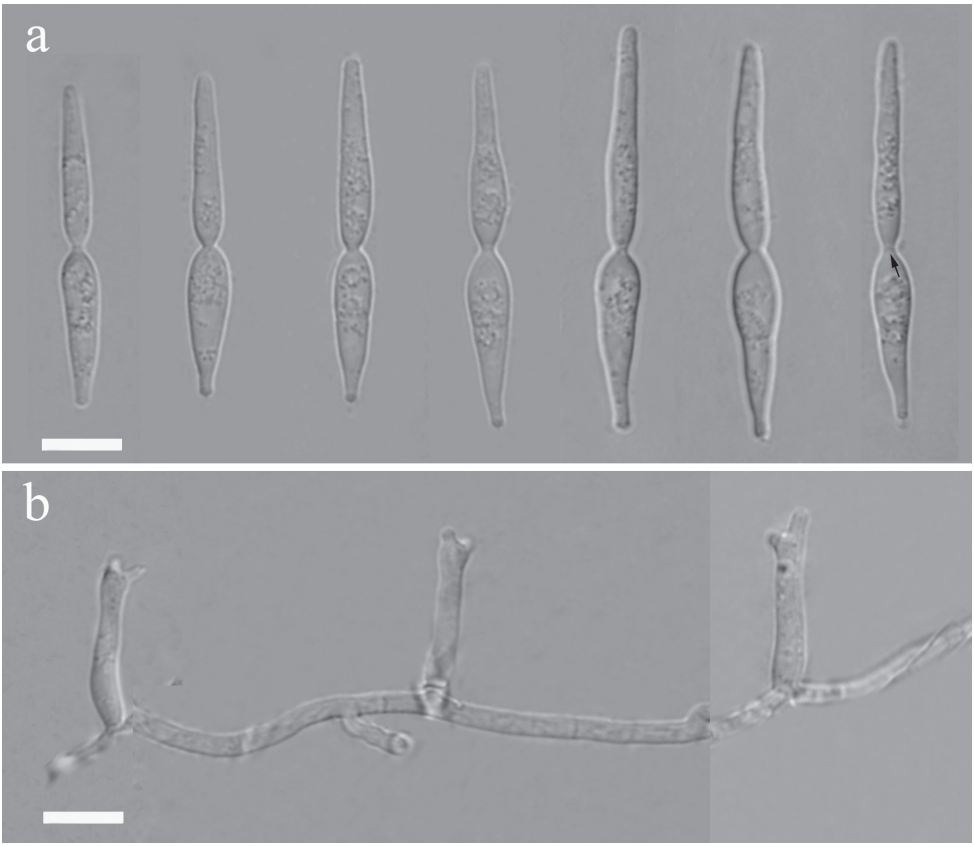

Figure 4. *Isthmomyces lanceatus* (YMF 1.04794) **a** conidia **b** conidiophores and conidiogenous cells. Scale bars: 10 μm (**a, b**). The arrow indicates septum inside isthmic-segments.

***Isthmomyces macrosporus* Z. F. Yu, M. Qiao & R. F. Castañeda, sp. nov.**
Index Fungorum number: IF556128
Facesoffungi Number No: FoF05742
Figs 5, 9d

Etymology. Greek, *macrosporus*, referring to the large, great conidia.

Description. Asexual morph hyphomycetous. *Colonies* on PDA amber to fawn, reverse fawn, attaining 2 cm diam. after 20 days at 25 °C. *Mycelium* mostly immersed, composed of branched, septate, slender, colourless hyphae. *Conidiophores* macronematous, mononematous, cylindrical, erect, straight, unbranched, 0–1-septate, smooth, pale brown, 25–35 × 3.0–3.5 μm. *Conidiogenous cells* polyblastic, cylindrical, denticulate, sympodial extended, integrated, terminal, pale brown or subhyaline. *Conidia* acrogenous, isthmospore, long fusiform, hyaline, smooth, 36.5–73.0 μm long, strongly constricted at the conspicuous, narrow, tiny central isthmus, sometime not differentiated, composed of two cellular isthmic-segments: i) basal isthmic-segment clavate, truncated at the base, 1-septate, hyaline or subhyaline, smooth, 19.2–31.1 ×

4.5–6.7 μm; ii) apical isthmic-segment 0–1-septate, narrow obclavate, sometimes subobspathulate, rounded at the tip, unicellular, guttulate, hyaline or subhyaline, smooth, 21.1–42.0 × 3.3–5.4 μm. Sexual state: unknown.

Type. China, Hainan Province, Limu Mountain National Conservation Area, on submerged leaves, April 2015, J. Peng. Holotype YMF 1.04518, preserved in a

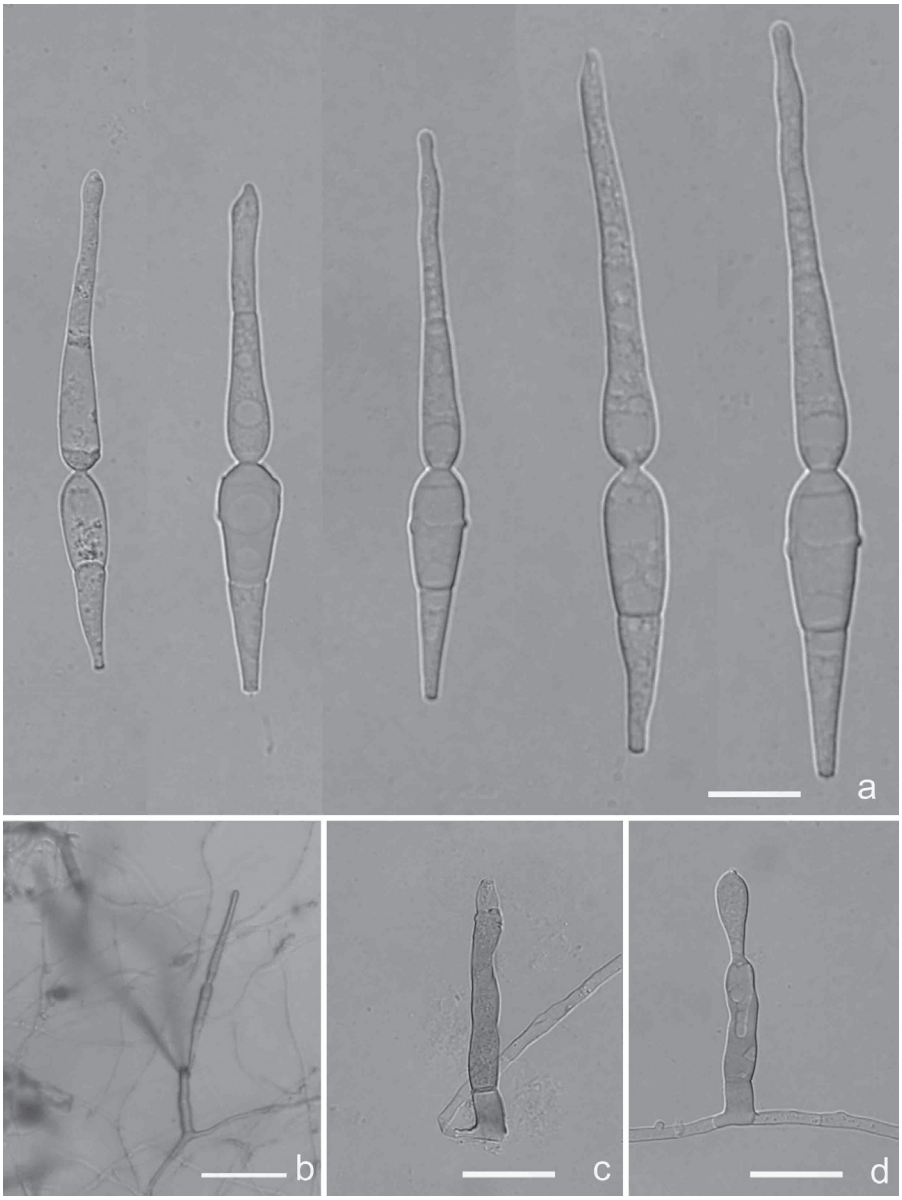

Figure 5. *Isthmomyces macroporus* (Holotype YMF 1.04518) **a** conidia **b** conidiophore with conidia under low objective **c** conidiophore and conidiogenous cell **d** conidiophore and developing conidia. Scale bars: 10 μm (**a, c, d**); 50 μm (**b**).

metabolically-inactive state (deep freezing) in the Conservation and Utilization of Bio-Resources in Yunnan. Ex-type culture CGMCC 3.18824.

Notes. Phylogenetically, *Isthmomyces macrosporus* is close to *I. dissimilis* and *I. lanceatus*. However, *I. macrosporus* is different from all species within this genus by having larger conidia, obviously brown conidiophores and few denticulate conidiogenous cells (Hoog and Hennebert 1983).

***Isthmomyces oxysporus* Z. F. Yu, M. Qiao & R. F. Castañeda, sp. nov.**
Index Fungorum number: IF556127
Facesoffungi Number No: FoF05741
Figs 6, 9e

Etymology. Greek, *oxys*, meaning sharp, keen, *sporum*, referring to the conidia.

Description. Asexual morph hyphomycetous. *Colonies* on CMA pale mouse grey to dark mouse grey, reverse olivaceous-grey, attaining about 2 cm diam. after 20 days at 25 °C. *Mycelium* mostly immersed, composed of branched, septate, subhyaline to hyaline hyphae. *Conidiophores* macronematous, mononematous, cylindrical, erect, smooth, 0–1-septate, subhyaline to hyaline, mostly reduced to conidiogenous cells, up to 30 μm long, 2.5–3 μm wide, arising from the creeping hyphae. *Conidiogenous cells* polyblastic, cylindrical, denticulate, integrated, terminal, sympodial extended, hyaline. *Conidia* isthmospore, fusiform, hyaline, smooth, 20.5–25.5 μm long, strongly constricted at the narrow, tiny central isthmus, composed of two cellular isthmic-segments: i) basal isthmic-segment broadly clavate to clavate, unicellular, hyaline 9.7–13 × 2.0–4.0 μm; ii) apical isthmic-segment narrow obclavate to obclavate, obpyriform or rarely lecythiform, unicellular, hyaline, 9.0–13.0 × 2.0–3.0 μm. Sexual state: unknown.

Type. China, Hainan Province, Diaoluo Mountain Natural Reserve, on submerged leaves, August 2015, J. Peng. Holotype YMF 1.04513, preserved in a metabolically-inactive state (deep freezing) in the Conservation and Utilization of Bio-Resources in Yunnan. Ex-type culture CGMCC 3.18821.

Notes. Morphologically, *Isthmomyces oxysporus* resembles *Isthmolongispora asymmetrica* Aramb. & Cabello in having both tapering isthmic-segment ends, but *Is. asymmetrica* has asymmetrical conidia, in which the basal isthmic-segment is longer (17–20 μm long) (Arambarri et al. 1987). Besides, *I. oxysporusis* is somewhat similar to *Is. rotundata* Matsush. in conidial sizes, but the apical isthmic-segments in *Is. rotundatus* are rounded at the tip (Matsushima 1987).

***Triscelophorus* Ingold, Trans. Br. mycol. Soc. 26(3–4): 151 (1943).**
MycoBank No: 10320

Description. Ingold 1943.

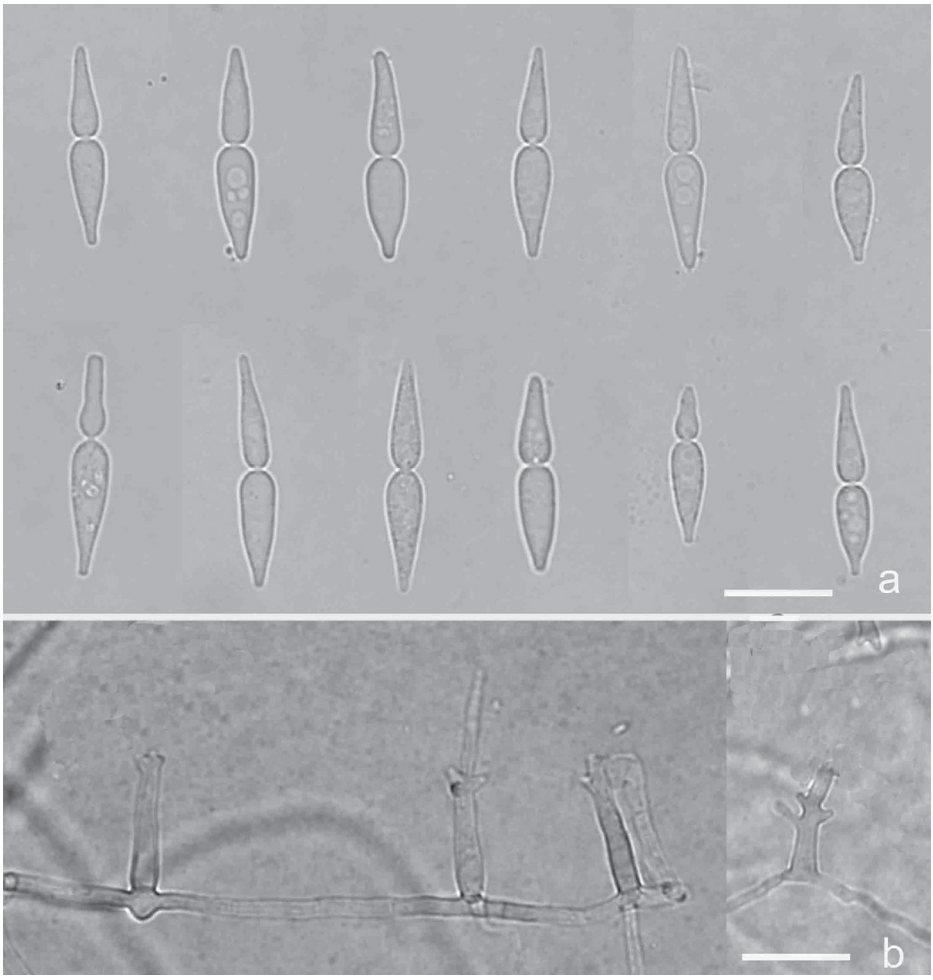

Figure 6. *Isthmomyces oxysporus* (Holotype YMF 1.04513) **a** conidia **b** conidiophores and conidiogenous cells. Scale bars: 10 μm (**a, b**).

Type species. *Triscelophorus monosporus* Ingold, Trans. Br. mycol. Soc. 26(3–4): 152 (1943).

Notes. *Triscelophorus* was established by Ingold, with *T. monosporus* as type species (Ingold 1943). The genus is characterised by macronematous, mononematous, erect, straight or flexuous, sometimes sinuate, septate, unbranched or sparingly branched, hyaline, smooth conidiophores. The conidiogenous cells are monoblastic, sometimes sympodially extended, integrated, hyaline that produce a solitary, acrogenous, septate, staurospore composed of a main axis and 3 or more branches verticillate arranged from the basal cell of the main axis (Ingold 1943; Seifert et al. 2011). Duarte et al. (2015) found that *Triscelophorus* was polyphyletic, based on ITS analysis, but our phylogenetic analysis, based on two-loci and ITS, showed the genus should be monophyletic. For more details, refer to Discussion.

***Triscelophorus anisopteriodeus* Z. F. Yu, M. Qiao & R. F. Castañeda, sp. nov.**
Index Fungorum number: IF556148
Facesoffungi Number No: FoF05747
Figs 7, 9f

Etymology. Latin, *anisopteriodeus*, referring to the resemblance of the conidial body to an adult of *Anisoptera* sp.

Description. Asexual morph hyphomycetous. *Colonies* on CMA, attaining about 1 cm diam. after 20 days at 25 °C, light smoky grey. Reverse smoky grey. *Mycelium* superficial and immersed, composed of branched, septate, hyaline hyphae. *Conidiophores* macronematous, mononematous, cylindrical, erect, flexuous, unbranched, smooth, hyaline, up to 20–110 μm long. *Conidiogenous cells* monoblastic, cylindrical, terminal, integrated, determinate, smooth, hyaline. *Conidia* solitary, acrogenous, staurospore, septate, composed of a main axis and 2–4 lateral branches: i) the main axis elongate obclavate, 2–4-septate, straight, smooth, hyaline, 31.2–48 × 3–5.2 μm; ii) 2–4-lateral branches obclavate to broad obclavate, straight, smooth, hyaline, all arising divergent, unequal, from the basal cell of the main axis: ii a) upper two lateral branches, 2–3-septate, 8.2–38.7 × 2.5–4.8 μm, more or less opposite, arranged just below the supra-basal septum; ii b) lower lateral branches, 0–1-septate, 14–20 × 5–5.5 μm, sequential opposite arranged near the middle of the basal cell. Sexual state: unknown.

Type. China, Hainan Province, Limu Mountain Nature Reserve, on submerged leaves, April 2015, J. Peng. Holotype YMF 1.04267, preserved in a metabolically-inactive state (deep freezing) in the Conservation and Utilization of Bio-Resources in Yunnan. Ex-type culture CGMCC 3.18978.

Notes. *Triscelophorus anisopteriodeus* is differentiated from other known *Triscelo-2*like a dragonfly-shape (Seifert et al. 2011). Four lateral branches are not arising from the same level at the basal cell of main axis. Two shorter ones are lower and two longer ones are upper. Amongst conidia of *Triscelophorus* spp., three lateral branches are often growing in a whorl, while 2 lateral branches are in pairs. Four lateral branches in pairs in *T. anisopteriodeus* make it easily recognisable. Morphologically, *T. anisopteriodeus* is similar to *Triramulispora duobinibrachiata* K. Ando in conidial shape, but *T. anisopteriodeus* has larger size of conidia (main axis: 31.2–48 × 3–5.2 vs. 19–36 × 2.5–3.5 μm) and more septa in branches (Ando 1993).

***Triscelophorus sinensis* Z. F. Yu, M. Qiao & R. F. Castañeda, sp. nov.**
Index Fungorum number: IF558520
Figs 8, 9g

Etymology. Latin, *sinensis*, referring to the country of origin, China.

Description. Asexual morph hyphomycetous. *Colonies* on CMA, attaining about 1 cm diam. after 20 days at 25 °C, pale mouse grey to dark mouse grey. *Mycelium* superficial and immersed, composed of branched, septate, hyaline hyphae. *Conidiophores*

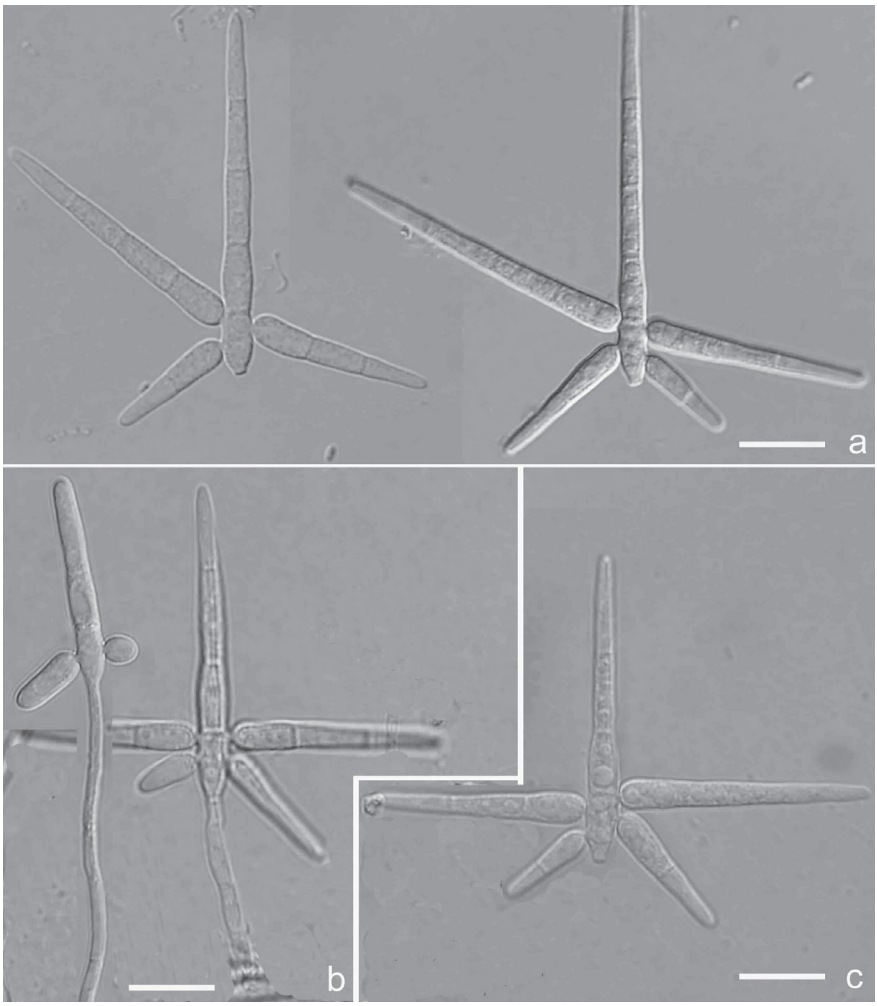

Figure 7. *Triscelophorus anisopteriodeus* (Holotype YMF 1.04267) **a, c** conidia **b** conidiophores with conidia. Scale bars: 10 μm (**a–c**).

macronematous, mononematous, lateral or terminal, cylindrical, erect, flexuous, separate, smooth, hyaline, up to 12–38 μm long, 1.0–2.4 μm wide. *Conidiogenous cells* monoblastic, cylindrical, terminal, integrated, determinate, smooth, hyaline. *Conidia* solitary, acrogenous, staurospore, septate, composed of a main axis and 2–3 lateral branches: i) the main axis obclavate, 2(–3)-septate, slightly constricted at the septa, straight, smooth, hyaline, 17.5–30.0 × 3.5–5.0 μm; ii) 2–3-lateral branches obclavate, (0–)1-septate, slightly constricted at the septa, straight, smooth, hyaline, 8.5–21.0 × 3.0–4.5 μm, arising from the basal cell of the main axis arranged in a regular or irregular verticillate. Sexual state: unknown.

Type. China, Guangdong Province, Guangzhou, on submerged leaves, September 2011, G.Z. Yang. Holotype YMF 1.04065, preserved in a metabolically-inactive state (deep freezing) in the Conservation and Utilization of Bio-Resources in Yunnan.

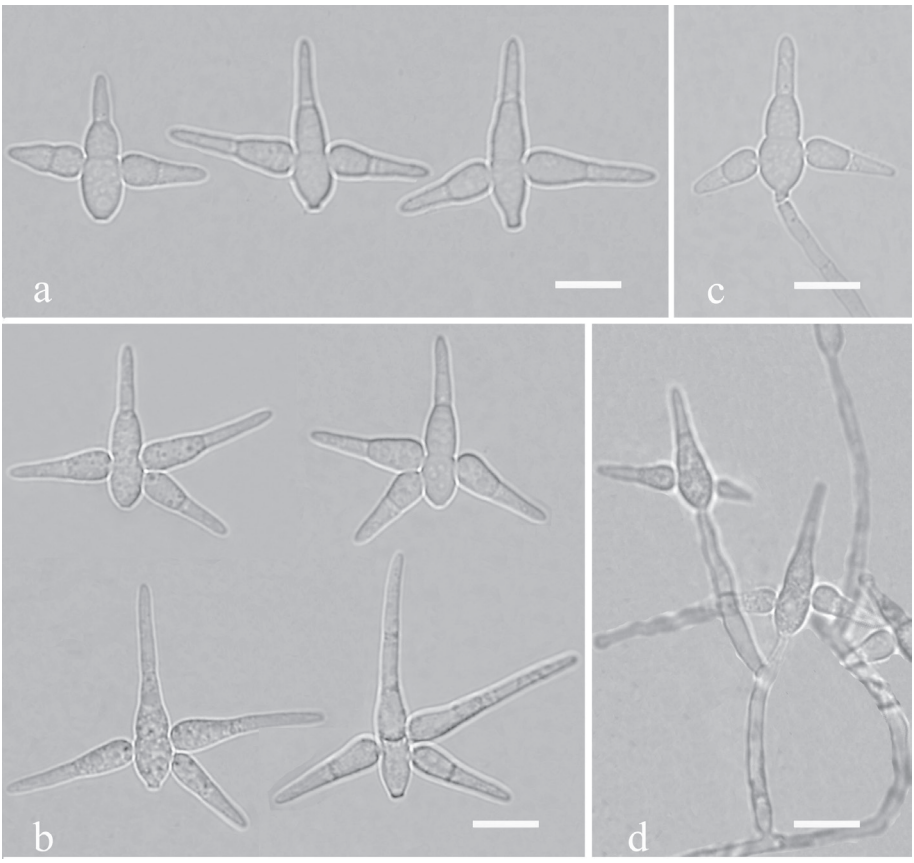

Figure 8. *Triscelophorus sinensis* (Holotype YMF 1.04065) **a, b** conidia **c, d** conidiophores with conidia. Scale bars: 10 μm (**a–d**).

Notes. In morphology, *Triscelophorus sinensis* is somewhat similar to *T. ponapensis* in conidia, both having 2–3 lateral arms (Matsushima 1981). However, *T. ponapensis* has shorter (main axis: 12–26 μm; lateral arms: 8–15 μm) and more septate (main axis: 2–4-septate; lateral arms: 1–4-septate) conidia.

Isthmolongispora quadricellularia **Matsush., Icon. microfung. Matsush. lect. (Kobe): 90 (1975).**
MycoBank No: 315952
Fig. 10

Description. Asexual morph hyphomycetous. *Colonies* on CMA white, gradually turning brown, reverse white to pale brown, attaining about 2.5 cm diam. after 20 days at 25 °C. *Mycelium* partly superficial, partly immersed, composed of branched, septate, slender, hyaline hyphae. *Conidiophores* macronematous, mononematous, cylindrical, erect, straight, unbranched, aseptate, smooth, hyaline, 3.9–9.0 × 2.0–3.2 μm.

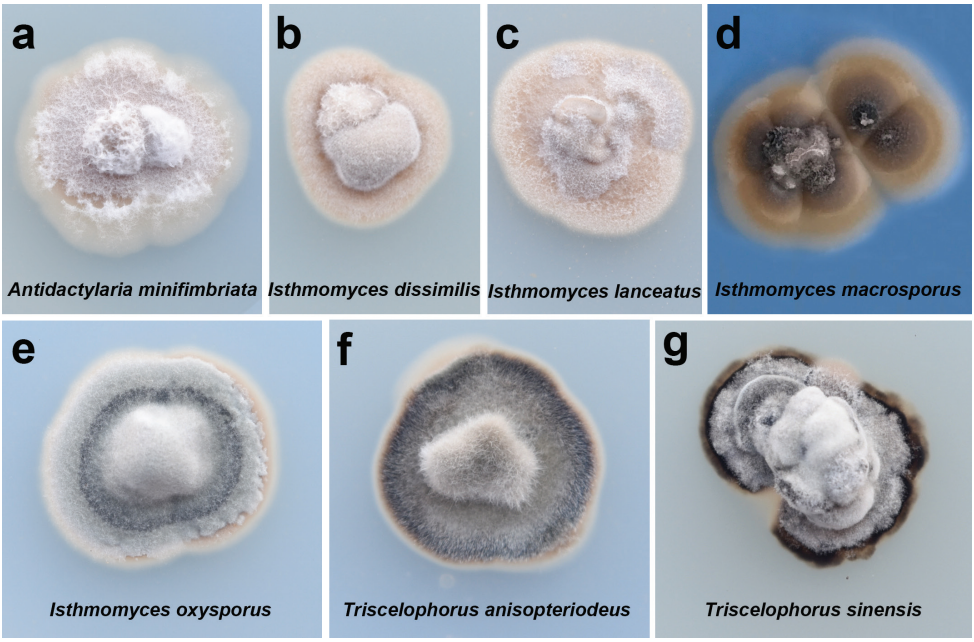

Figure 9. Cultural characters of all species in this study after 20 days on PDA at 25 °C.

Conidiogenous cells short, terminal, cylindrical, denticulate, integrated, hyaline. *Conidia* solitary, smooth, beaded, tapering towards both ends, 4–7-celled, generally 5–6-celled, hyaline, 44–88 × 3.5–5.0 μm. Sexual state: unknown.

Type. China, Hainan Province, Jianfengling National Nature Reserve, on submerged leaves, Jun 2011, G.Z. Yang, YMF 1.04794, YMF 1.04011, YMF 1.04016, YMF 1.04019, preserved in a metabolically-inactive state (deep freezing) in the Conservation and Utilization of Bio-Resources in Yunnan.

Notes. *Isthmolongispora quadricellularia* was first described by Matsush. in 1975 from Japan. Subsequently, this species has been isolated from leaves many times in Taiwan. However, no sequences of *I. quadricellularia* are available in the public database. In this study, it is the first time that *I. quadricellularia* has been isolated from the aquatic environment. In addition, we also submitted sequence data for this species to the public database (SSU: MT507103–105; LSU: MT507107–110; ITS: OL412746–749).

Discussion

China is considered an important reservoir of Asian biodiversity (Myers et al. 2000); it is estimated that this area harbours an inestimable diversity of fungi. In recent years, more and more new genera and species have been identified and classified for the application of phylogenetic analysis and have led to a significant expansion of species in Dothidomycetes (Zheng et al. 2019, 2020b, 2021b; Yang et al. 2021). However, comparatively speaking, aquatic hyphomycetes have been poorly investigated. In recent years, we have

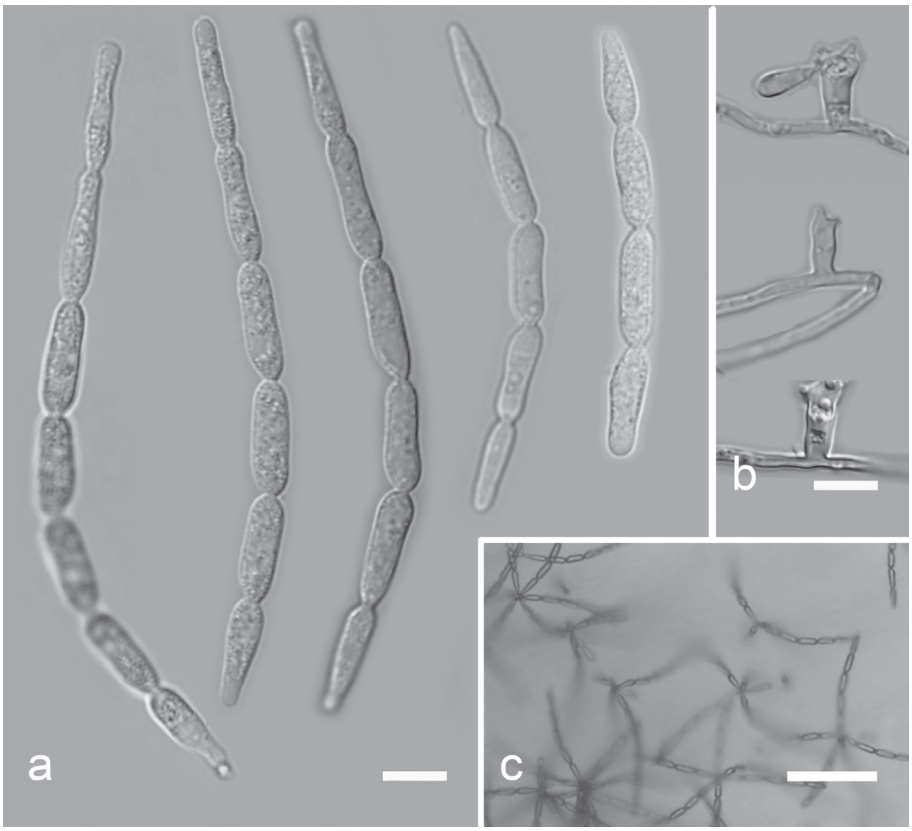

Figure 10. *Isthmolongispora quadricellularia* (YMF 1.04794) **a** conidia **b** conidiophores and conidiogenous cells **c** conidia under low power microscopy. Scale bars: 10 μm (**a, b**); 50 μm (**c**).

been investigating the diversity of aquatic hyphomycetes from southern China. During this process, several interesting isolates have been collected. After studying in detail, two new asexual genera and six new asexual species have been described in Microthyriaceae.

Triscelophorus Ingold was established with *T. monosporus* Ingold as type species; now, eight species have been accepted in this genus (Ingold 1943; Wijayawardene et al. 2017). However, the positions of *Triscelophorus* in ordinal and familial levels are still unclear. In this study, two isolates which have similarity to *Triscelophorus* species in morphology were collected. For further study, the two isolates were identified as two new species of *Triscelophorus*, named as *T. anisopteriodeus* and *T. sinensis*. Moreover, phylogenetic analysis of combined LSU and ITS sequences places *Triscelophorus* in Microthyriaceae (Fig. 1).

Isthmolongispora Matsush. was established in 1971 and, so far, eleven species were accepted in this genus (Matsushima 1971; Wijayawardene et al. 2018b, 2020). In this study, ten isolates have similarity to some *Isthmolongispora* species. Of these, four isolates were identified as *Isthmolongispora quadricellularis*, based on morphology. The combined LSU and ITS tree (Fig. 1) showed that the other six isolates formed two clades in Microthyriaceae. Comparing their morphological differences between species of the two clades,

we established two new genera *Antidactylaria* and *Isthmomyces*. *Antidactylaria* includes a new species *A. minifimbriata* and a new combination *A. ampulliforma* and is phylogenetically close to two asexual species *Scolecobasidium tropicum* Matsush. and *Neoscolecobasidium agapanthi* Crous. *Isthmomyces* includes three new species, *I. dissimilis*, *I. oxysporus and I. macrosporus* and a new combination *I. lanceatus*. Phylogenetically, *Isthmomyces* is near to the sexual genus *Microthyrium* and the asexual genus *Neoanungitea*. Although *Ishmomyces* is closely related to *Microthyrium*, their ITS sequence similarity is low, so we cannot determine the connection between them. Based on the two-gene tree, we speculated that *Isthmolongispora* is polyphyletic. So far, at least 14 genera of aquatic hyphomycetes have shown to be polyphyletic using sequence information from a single or two genes (Nikolcheva 2002; Tsui et al. 2006; Baschien 2006; Campbell et al. 2006; Duarte et al. 2015).

With increasingly widespread use of molecular techniques, multi-genes were concatenated to resolve phylogenetic affiliations and taxonomic placements at family or higher ranks. For example, SSU, LSU, *tef*1, *rpb*1 and *rpb*2 were combined to assess phylogeny (Schoch et al. 2006, 2009; Wijayawardene et al. 2014). However, sequence data and cultures of many aquatic hyphomycetes were unavailable. By 2013, over 300 aquatic hyphomycete species had been described, based on conidia morphology and conidiogenesis. However, fewer than 50 species had published ITS sequences in the International Nucleotide Sequence Database (Duarte et al. 2013). In addition, most of these species with ITS sequences were considered Ascomycota genera are *incertae sedis* because of the limitations of ITS as a phylogenetic marker for these organisms.

Molecular phylogeny of freshwater fungi in Dothideomycetes has been studied by Shearer et al. (2009) using SSU and LSU for 84 isolates representing 29 genera. The results showed that the majority of freshwater Dothideomycetes belonged to Pleosporomycetidae, including four clades comprised of only freshwater taxa, while the remaining freshwater taxa were distributed amongst other clades. In the largest phylogenetic assessment of Dothideomycetes up to 2009, members of the class from various ecological niches were included and freshwater taxa were in different clades (Schoch et al. 2009). Unfortunately, like other studies, though representative, these two studies of Dothideomycetes and freshwater ascomycetes had very few aquatic asexual genera. In the paper of Shearer et al. (2009), only 10 asexual genera were included, while in the paper of Schoch et al. (2009), only four asexual genera were included (*Monotosporella* S. Hughes and *Beverwykella* Tubaki belonging to Melanommataceae G. Winter, while *Helicomyces* Link and *Helicosporium* Nees belonging to Tubeufiaceae). Amongst the accepted genera of Dothideomycetes, only 11 aquatic or aero-aquatic asexual genera have been described as belonging to different families of the subclass Pleosporomycetidae (Wijayawardene et al. 2014). Our study provides the molecular evidence for asexual aquatic fungi.

Conclusions

This study described two new asexual genera and six new asexual species of aquatic hyphomycetes. Our phylogenetic analyses placed several other aquatic genera in the family Microthyriaceae. Though we failed to connect teleomorphs and anamorphs

at genus level, our results showed close phylogenetic relationships between aquatic hyphomycetes and Microthyriaceae at the family rank. This study also revealed the importance of obtaining pure cultures of aquatic fungi and multiple gene sequences from them to identify the origins and phylogenetic positions of aquatic hyphomycetes and their relationships with their terrestrial relatives.

Acknowledgements

This work was financed by the National Natural Science Foundation Program of PR China (31770026, 31760012). We are grateful to reviewers for critically reviewing the manuscript and for providing helpful suggestions to improve this paper.

References

Ando K (1993) Three new species of staurosporous hyphomycetes from Japan. Transactions of the Mycological Society of Japan 34(4): 399–408.

Arambarri A, Cabello M, Mengascini A (1987) Systematic study of the Hyphomycetes from Santiago River (Buenos Aires Province, Argentina). Mycotaxon 29: 29–35.

Ariyawansa H, Hyde K, Jayasiri S, Buyck B, Chen XH (2015) Fungal diversity notes 111–252—taxonomic and phylogenetic contributions to fungal taxa. Fungal Diversity 75(1): 27–274. https://doi.org/10.1007/s13225-015-0346-5

Ashton H (2009) Ainsworth and Bisby's Dictionary of the Fungi (10th edn.). Reference Reviews 23(5): 42–42. https://doi.org/10.1108/09504120910969104

Bai YL, Li JY, Qiao M, Qian WY, Yang GZ, Yu ZF (2013) *Setosynnema yunnanense* sp. nov. from submerged decaying leaves. Mycotaxon 125: 81–85. https://doi.org/10.5248/125.81

Baschien CML, Szewzyk U (2006) Phylogeny of selected aquatic hyphomycetes based on morphological and molecular data. Nova Hedwigia 83(3): 311–352. https://doi.org/10.1127/0029-5035/2006/0083-0311

Belliveau MJR, Barlocher F (2005) Molecular evidence confirms multiple origins of aquatic hyphomycetes. Mycological Research 109: 1407–1417. https://doi.org/10.1017/S0953756205004119

Berbee ML, Taylor JW (2001) Fungal molecular evolution: gene trees and geologic time. In: McLaughlin DJ, McLaughlin EG, Lemke PA (Eds) Systematics and evolution. Springer Berlin Heidelberg, The Mycota (A Comprehensive Treatise on Fungi as Experimental Systems for Basic and Applied Research), vol 7B. https://doi.org/10.1007/978-3-662-10189-6_10

Bärlocher F (1992) Research on aquatic hyphomycetes: historical background and overview. In: Bärlocher F (Ed.) The Ecology of Aquatic Hyphomycetes. Springer Berlin Heidelberg, Ecological Studies (Analysis and Synthesis). https://doi.org/10.1007/978-3-642-76855-2_1

Campbell J, Shearer C, Marvanova L (2006) Evolutionary relationships among aquatic anamorphs and teleomorphs: *Lemonniera*, *Margaritispora*, and *Goniopila*. Mycological Research 110(9): 1025–1033. https://doi.org/10.1016/j.mycres.2006.04.012

de Hoog GS, Hennebert GL (1983) Taxonomy of the *Dactylaria* complex III. A pleomorphic species of *Isthmolongispora*. Proc Konink Nederland Akad Wetenschappen, Ser C, 86: 343–346.

Duarte S, Batista D, Barlocher F, Cassio F, Pascoal C (2015) Some new DNA barcodes of aquatic hyphomycete species. Mycoscience 56(1): 102–108. https://doi.org/10.1016/j.myc.2014.04.002

Duarte S, Sahadevan S, Barlocher F, Pascoal C, F Cássio (2013) A decade's perspective on the impact of DNA sequencing on aquatic hyphomycete research. Fungal Biology Reviews 27(1): 19–24. https://doi.org/10.1016/j.fbr.2013.02.003

Goh TK, Hyde KD (1997) A revision of *Dactylaria*, with description of *D. tunicata* sp. nov. from submerged wood in Australia. Mycological Research 101(10): 1265–1272. https://doi.org/10.1017/S0953756297004000

Guo JS, Zhang Z, Qiao M, Yu ZF (2019) *Phalangispora sinensis* sp. nov. from Yunnan, China and two new members of Wiesneriomycetaceae. International Journal of Systematic and Evolutionary Microbiology 69(10): 3207–3213. https://doi.org/10.1099/ijsem.0.003612

Guo MT, Qiao M, Li JY, Wang W, Yu ZF (2015) *Verticicladus hainanensis*, a new aquatic hyphomycete. Mycotaxon 130(1): 275–278. https://doi.org/10.5248/130.275

Hall TA (1999) BioEdit: a user-friendly biological sequence alignment editor and analysis program for Windows 95/98/NT. Nucleic Acids Symposium Series 41: 95–98.

Hongsanan S, Hyde KD, Phookamsak R, Wanasinghe DN, McKenzie EHC, Sarma VV, Lücking R, Boonmee S, Bhat JD, Liu N-G, Tennakoon DS, Pem D, Karunarathna A, Jiang S-H, Jones GEB, Phillips AJL, Manawasinghe IS, Tibpromma S, Jayasiri SC, Sandamali D, Jayawardena RS, Wijayawardene NN, Ekanayaka AH, Jeewon R, Lu Y-Z, Phukhamsakda C, Dissanayake AJ, Zeng X-Y, Luo Z-L, Tian Q, Thambugala KM, Dai D, Samarakoon MC, Chethana KWT, Ertz D, Doilom M, Liu J-K, Pérez-Ortega S, Suija A, Senwanna C, Wijesinghe SN, Niranjan M, Zhang S-N, Ariyawansa HA, Jiang H-B, Zhang J-F, Norphanphoun C, de Silva NI, Thiyagaraja V, Zhang H, Jadson DP, Bezerra JDP, Miranda-González R, Aptroot A, Kashiwadani H, Harishchandra D, Sérusiaux E, Abeywickrama PD, Bao D-F, Devadatha B, Wu H-X, Moon KH, Gueidan C, Schumm F, Bundhun D, Mapook A, Monkai J, Bhunjun CS, Chomnunti P, Suetrong S, Chaiwan N, Dayarathne MC, Yang J, Rathnayaka AR, Xu J-C, Zheng J, Liu G, Feng Y, Xie N (2020) Refined families of Dothideomycetes: orders and families incertae sedis in Dothideomycetes. Fungal Diversity 105: 17–318. https://doi.org/10.1007/s13225-020-00462-6

Hyde KD, Jones EBG, Liu JK, Ariyawansha H, Bochm E, Boonmee S, Braun U, Chomnunti P, Crous P, Dai DQ, Diederich P, Dissanayake A, Doilom M, Doveri F, Hongsanan S, Jayawardena R, Lawrey JD, Li YM, Liu YX, Liucking R, Monkai J, Nelsen MP, Phookamsak R, Muggia L, Pang KL, Senanayake I, Shearer CA, Wijayawardene N, Wu HX, Thambugala M, Suetrong S, Tanaka K, Wikee S, Zhang Y, Hudson BA, Alias SA, Aptroot A, Bahkali AH, Bezerra LJ, Bhat JD, Camporesi E, Chukeatirote E, Hoog SD, Gueidan C, Hawksworth DL, Hirayama K, Kang JC, Knudsen K, Li WJ, LiuZY, McKenzie EHC, Miller AN, Nadeeshan D, Phillip AJL, Mapook A, Raja HA, Tian Q, Zhang M, Scheuer C, Schumm F, Taylor J, Yacharoen S, Tibpromma S, Wang Y, Yan J, Li X (2013) Families of Dothideomycetes. Fungal Diversity 63: 1–313. https://doi.org/10.1007/s13225-013-0263-4

Hyde KD, McKenzie EHC, Ko TW (2011) Towards incorporating anamorphic fungi in a natural classification–checklist and notes for 2010. Mycosphere 2(1): 1–88.

Ingold CT (1943) *Triscelophorus monosporus* N.Gen., N.SP., an aquatic hyphomycete. Transactions of the British Mycological Society 26(3): 148. [IN144–152,IN144]

Iturrieta-González I, García D, Guarro J, Gené J (2020) *Heliocephala variabilis* and *Pseudopenidiella vietnamensis*: two new hyphomycetous species in the Microthyriaceae (Dothideomycetes) from Vietnam. Microorganisms 8: e478. https://doi.org/10.3390/microorganisms8040478

Kindermann J, El-Ayouti Y, Samuels GJ, Kubicek CP (1998) Phylogeny of the genus *Trichoderma* based on sequence analysis of the internal transcribed spacer region 1 of the rDNA cluster. Fungal Genetics and Biology 24: 298–309. https://doi.org/10.1006/fgbi.1998.1049

Li JY, Qian WY, Qiao M, Bai YL, Yu ZF (2013) A new *Drechslerella* species from Hainan, China. Mycotaxon 125: 183–188. https://doi.org/10.5248/125.183

Li JY, Qiao M, Peng J, Qian WY, Yang GZ, Yu ZF (2014) *Uncispora hainanensis* sp. nov. isolated from decayed leaves. Mycotaxon 129(2): 473–476. https://doi.org/10.5248/129.473

Liu JK, Yang J, Maharachchikumbura SSN, McKenzie EHC, Jones EBG, Hyde KD, Liu ZY (2016) Novel chaetosphaeriaceous hyphomycetes from aquatic habitats. Mycological Progress 15(10–11): 1157–1167. https://doi.org/10.1007/s11557-016-1237-1

Maharachchikumbura SSN, Hydc KD, Joncs EGB, McKcnzic EHC, Huang SK, Abdcl-Wahab MA, Daranagama DA, Dayarathnc M, D'souza MJ, Goonasckara ID, Hongsanan S, Jayawardcna RS, Kirk PM, Konta S, Liu JK, Liu ZY, Norphanphoun C, Pang KL, Pcrcra RH, Scnanayakc IC, Shang Q, Shcnoy BD, Xiao Y, Bahkali AH, Kang J, Somrothipol S, Suctrong S, Wen T, Xu J (2015) Towards a natural classification and backbonc tree for Sordariomycetes. Fungal Diversity 72(1): 199–301. https://doi.org/10.1007/s13225-015-0331-z

Matsushima T (1971) Microfungi from the Solomon Islands and Papua-New Guinea. Published by author, Kobe.

Matsushima T (1981) Matsushima Mycological Memoirs No. 5. Matsushima Fungus Collection. Published by author, Kobe, 19 pp.

Matsushima T (1987) Matsushima Mycological Memoirs No. 5. Matsushima Fungus Collection. Published by author, Kobe, 100 pp. https://doi.org/10.2307/3807737

Myers N, Mittermeier RA, Mittermeier CG, da Fonseca GAB, Kent J (2000) Biodiversity hotspots for conservation priorities. Nature 403(6772): 853–858. https://doi.org/10.1038/35002501

Nikolcheva LGBF (2002) Phylogeny of *Tetracladium* based on 18S rDNA. Czech Mycology 53: 285–295. https://doi.org/10.33585/cmy.53404

Paulus B, Gadek P, Hyde KD (2003) Two new species of *Dactylaria* (anamorphic fungi) from Australian rainforests and an update of species in *Dactylaria* sensu lato. Fungal Diversity 14: 143–156. https://doi.org/10.1002/yea.955

Peng J, Chang D, Huang Y, Yu ZF (2016) *Nawawia oviformis* sp. nov. from China. Mycotaxon 131(4): 735–738. https://doi.org/10.5248/131.735

Posada D (2008) jModelTest: Phylogenetic model averaging. Molecular Biology and Evolution 25(7): 1253–1256. https://doi.org/10.1093/molbev/msn083

Pratibha J, Nguyen HDT, Mel'nik VA, Bhat DJ, White GP, Seifert KA (2015) Lectotypification, epitypification, and molecular phylogeny of the synnematous hyphomycete

Pseudogliophragma indicum, the second genus in the Wiesneriomycetaceae. Mycoscience 56(4): 387–395. https://doi.org/10.1016/j.myc.2014.12.002

Qiao M, Du X, Bian ZH, Peng J, Yu ZF (2017a) *Ellisembia pseudokaradkensis* sp. nov. from Hainan, China. Mycotaxon 132(4): 813–817. https://doi.org/10.5248/132.813

Qiao M, Guo JS, Tian WG, Yu ZF (2018b) *Ellisembia hainanensis* sp. nov. from Hainan, China. Mycotaxon 133(1): 97–101. https://doi.org/10.5248/133.97

Qiao M, Huang Y, Deng C, Yu ZF (2017b) *Tripospermum sinense* sp. nov. from China. Mycotaxon 132(3): 513–517. https://doi.org/10.5248/132.513

Qiao M, Li DW, Yu ZF, Zhang K, Castaneda-Ruiz RF (2019a) *Spadicoides matsushimae* sp. nov., and *Anisospadicoides* gen. nov. for two atypical *Spadicoides* species. Mycotaxon 134(1): 161–167. https://doi.org/10.5248/134.161

Qiao M, Li WJ, Huang Y, Xu JP, Zhang L, Yu ZF (2018a) *Classicula sinensis*, a new species of Basidiomycetous aquatic hyphomycetes from southwest China. MycoKeys (40): 1–12. https://doi.org/10.3897/mycokeys.40.23828

Qiao M, Tian WG, Castaneda-Ruiz AF, Xu JP, Yu ZF (2019b) Two new species of *Verruconis* from Hainan, China. MycoKeys (48): 41–53. https://doi.org/10.3897/mycokeys.48.32147

Qiao M, Zheng H, Lv RL, Yu ZF (2020) Neodactylariales, Neodactylariaceae (Dothideomycetes, Ascomycota): new order and family, with a new species from China. MycoKeys (73): 69–85. https://doi.org/10.3897/mycokeys.73.54054

Qiao M, Zheng H, Zhang Z, Yu ZF (2019c) *Seychellomyces sinensis* sp. nov. from China. Mycotaxon 134(2): 391–398. https://doi.org/10.5248/134.391

Ronquist F, Teslenko M, van der Mark P, Ayres DL, Darling A, Höhna S, Larget B, Liu L, Suchard MA, Huelsenbeck JP (2012) MrBayes 3.2: efficient bayesian phylogenetic inference and model choice across a large model space. Systematic Biology 61(3): 539–542. https://doi.org/10.1093/sysbio/sys029

Saccardo PA (1883) Sylloge Fungorum (Abellini). Italy, Pavia 4: 1–815.

Schoch CL, Crous PW, Groenewald JZ, Boehm EWA, Burgess TI, De Gruyter J, De Hoog GS, Dixon LJ, Grube M, Gueidan C, Harada Y, Hatakeyama S, Hirayama K, Hosoya T,Huhndorf SM, Hyde KD, Jones EBG, Kohlmeyer J, Kruys Å, Li YM, Lücking R, Lumbsch HT, Marvanová L, Mbatchou JS, McVay AH, Miller AN, Mugambi GK,Muggia L, Nelsen MP, Nelson P, Owensby CA, Phillips AJL, Phongpaichit S, Pointing SB, Pujade-Renaud V, Raja HA, Plata ER, Robbertse B, Ruibal C, Sakayaroj J, Sano T, Selbmann L, Shearer CA, Shirouzu T, Slippers B, Suetrong S, Tanaka K, Volkmann-Kohlmeyer B, Wingfield MJ, Wood AR, Woudenberg JHC, Yonezawa H, Zhang Y, Spatafora JW (2009) A class-wide phylogenetic assessment of Dothideomycetes. Studies in Mycology 64: 1–15. https://doi.org/10.3114/sim.2009.64.01

Schoch CL, Shoemaker RA, Seifert KA, Hambleton S, Spatafora JW, Crous PW (2006) A multigene phylogeny of the Dothideomycetes using four nuclear loci. Mycologia 98(6): 1041–1052. https://doi.org/10.3852/mycologia.98.6.1041

Seifert K, Morgan-Jones G, Gams W, Kendrick B (2011) The genera of hyphomycetes. CBS Biodiversity Series 9: 997.

Shearer CA, Raja HA, Miller AN, Nelson P, Tanaka K,Hirayama K, Marvanova L, Hyde KD, Zhang Y (2009) The molecular phylogeny of freshwater Dothideomycetes. Studies in Mycology 64: 145–153. https://doi.org/10.3114/sim.2009.64.08

Shenoy BD, Jeewon R, Hyde KD (2007) Impact of DNA sequence-data on the taxonomy of anamorphic fungi. Fungal Diversity 26(1): 1–54. https://doi.org/10.1002/yea.1503

Stamatakis A (2006) RAxML-VI-HPC: maximum likelihood-based phylogenetic analyses with thousands of taxa and mixed models. Bioinformatics 22(21): 2688–2690. https://doi.org/10.1093/bioinformatics/btl446

Su HY, Hyde KD, Maharachchikumbura SSN, Ariyawansa HA, Luo ZL, Promputtha I, Tian Q, Lin CG, Shang QJ, Zhao YC (2016) The families Distoseptisporaceae fam. nov., Kirschsteiniotheliaceae, Sporormiaceae and Torulaceae, with new species from freshwater in Yunnan Province. China. Fungal Diversity 80(1): 375–409. https://doi.org/10.1007/s13225-016-0362-0

Tamura K, Stecher G, Peterson D, Filipski A, Kumar S (2013) MEGA6: molecular evolutionary genetics analysis version 6.0. Molecular Biology & Evolution 30(12): 2725–2729. https://doi.org/10.1093/molbev/mst197

Thompson JD, Gibson TJ, Plewniak F, Jeanmougin F, Higgins DG (1997). The CLUSTAL_X windows interface: flexible strategies for multiple sequence alignment aided by quality analysis tools. Nucleic Acids Research 25(24): 4876–4882. https://doi.org/10.1093/nar/25.24.4876

Tsui CKM, Sivichai S, Berbee ML (2006) Molecular systematics of *Helicoma*, *Helicomyces* and *Helicosporium* and their teleomorphs inferred from rDNA sequences. Mycologia 98(1): 94–104. https://doi.org/10.3852/mycologia.98.1.94

Tubaki K (1958) Studies on the Japanese hyphomycetes. V. Leaf and stem group with a discussion of the classification of hyphomycetes and their perfect stages. Journal of the Hattori Botanical Laboratory 20: 142–244.

Turner D, Kovacs W, Kuhls K, Lieckfeldt E, Peter B, Arisan-Atac I, Strauss J, Samuels GJ, Börner T, Kubicek CP (1997) Biogeography and phenotypic variation in *Trichoderma* sect *Longibrachiatum* and associated *Hypocrea* species. Mycological Research 101: 449–459. https://doi.org/10.1017/S0953756296002845

Vilgalys R, Hester M (1990) Rapid genetic identification and mapping of enzymatically amplified ribosomal DNA from Several *Cryptococcus* Species. Journal of Bacteriology 172(8): 4238–4246. https://doi.org/10.1128/jb.172.8.4238-4246.1990

White TJ, Bruns T, Lee S, Taylor J (1990) Amplification and direct sequencing of fungal ribosomal RNA genes for phylogenetics. PCR Protocols: a Guide to Methods and Applications 18: 315–322. https://doi.org/10.1016/B978-0-12-372180-8.50042-1

Wijayawardene NN, McKenzie EHC, Hyde KD (2012) Towards incorporating anamorphic fungi in a natural classification-checklist and notes for 2011. Mycosphere 3(2): 157–228. https://doi.org/10.5943/mycosphere/3/2/5

Wijayawardene NN, Crous PW, Kirk PM, Hawksworth DL, Boonmee S, Braun U, Dai DQ, D'souza MJ, Diederich P, Dissanayake A (2014) Naming and outline of Dothideomycetes–2014 including proposals for the protection or suppression of generic names. Fungal Diversity 69: 1–55. https://doi.org/10.1007/s13225-014-0309-2

Wijayawardene NN, Hyde KD, Rajeshkumar KC, Hawksworth DL, Madrid H, Kirk PM, Braun U, Singh RV, Crous PW, Kukwa M, Lücking R, Kurtzman CP, Yurkov A, Haelewaters D, Aptroot A, Lumbsch HT, Timdal E, Ertz D, Etayo J, Phillips AJL, Groenewald JZ, Papizadeh M, Selbmann L, Dayarathne MC, Weerakoon G, Jones EBG, Suetrong S, Tian

Q, Castañeda-Ruiz RF, Bahkali AH, Pang KL, Tanaka K, Dai DQ, Sakayaroj J, Hujslová M, Lombard L, Shenoy BD, Suija A, Maharachchikumbura SSN, Thambugala KM, Wanasinghe DN, Sharma BO, Gaikwad S, Pandit G, Zucconi L, Onofri S, Egidi E, Raja HA, Kodsueb R, Cáceres MES, Pérez-Ortega S, Fiuza PO, Monteiro JS, Vasilyeva LN, Shivas RG, Prieto M, Wedin M, Olariaga I, Lateef AA, Agrawal Y, Fazeli SAS, Amoozegar MA, Zhao GZ, Pfiegler WP, Sharma G, Oset M, Abdel-Wahab MA, Takamatsu S, Bensch K, de Silva NI, De Kesel A, Karunarathna A, Boonmee S, Pfster DH, Lu YZ, Luo ZL, Boonyuen N, Daranagama DA, Senanayake IC, Jayasiri SC, Samarakoon MC, Zeng XY, Doilom M, Quijada L, Rampadarath S, Heredia G, Dissanayake AJ, Jayawardana RS, Perera RH, Tang LZ, Phukhamsakda C, Hernández-Restrepo M, Ma X, Tibpromma S, Gusmao LFP, Weerahewa D, Karunarathna SC (2017) Notes for genera: Ascomycota. Fungal Diversity 86(1): 1–594. https://doi.org/10.1007/s13225-017-0386-0

Wijayawardene NN, Hyde KD, Lumbsch HT, Liu JK, Maharachchi-kumbura SSN, Ekanayaka AH, Tian Q, Phookamsak R (2018a) Outline of Ascomycota: 2017. Fungal Diversity 88(1): 167–263. https://doi.org/10.1007/s13225-018-0394-8

Wijayawardene NN, Hyde KD, McKenzie EHC, Wang Y (2018b) Notes for genera update-Ascomycota: 6822–6917. Mycosphere 9(6): 1222–1234. https://doi.org10.5943/mycosphere/9/6/11

Wijayawardene NN, Hyde KD, Al-Ani LKT, Tedersoo L, Haelewaters D, Rajeshkumar KC, Zhao RL, Aptroot A, Leontyev DV, Saxena RK, Tokarev YS, Dai DQ, Letcher PM, Stephenson SL, Ertz D, Lumbsch HT, Kukwa M, Issi IV, Madrid H, Phillips AJL, Selbmann L, Pfliegler WP, Horváth E, Bensch K, Kirk PM, Kolaříková K, Raja HA, Radek R, Papp V, Dima B, Ma J, Malosso E, Takamatsu S, Rambold G, Gannibal PB, Triebel D, Gautam AK, Avasthi S, Suetrong S, Timdal E, Fryar SC, Delgado G, Réblová M, Doilom M, Dolatabadi S, Pawłowska J, Humber RA, Kodsueb R, Sánchez-Castro I, Goto BT, Silva DKA, de Souza FA, Oehl F, da Silva GA, Silva IR, Błaszkowski J, Jobim K, Maia LC, Barbosa FR, Fiuza PO, Divakar PK, Shenoy BD, Castañeda-Ruiz RF, Somrithipol S, Lateef AA, Karunarathna SC, Tibpromma S, Mortimer PE, Wanasinghe DN, Phookamsak R, Xu J, Wang Y, Tian F, Alvarado P, Li DW, Kušan I, Matočec N, Maharachchikumbura SSN, Papizadeh M, Heredia G, Wartchow F, Bakhshi M, Boehm E, Youssef N, Hustad VP, Lawrey JD, Santiago ALCMA, Bezerra JDP, Souza-Motta CM, Firmino AL, Tian Q, Houbraken J, Hongsanan S, Tanaka K, Dissanayake AJ, Monteiro JS, Grossart HP, Suija A, Weerakoon G, Etayo J, Tsurykau A, Vázquez V, Mungai P, Damm U, Li QR, Zhang H, Boonmee S, Lu YZ, Becerra AG, Kendrick B, Brearley FQ, Motiejūnaitė J, Sharma B, Khare R, Gaikwad S, Wijesundara DSA, Tang LZ, He MQ, Flakus A, Rodriguez-Flakus P, Zhurbenko MP, McKenzie EHC, Stadler M, Bhat DJ, Liu JK, Raza M, Jeewon R, Nassonova ES, Prieto M, Jayalal RGU, Erdoğdu M, Yurkov A, Schnittler M, Shchepin ON, Novozhilov YK, Silva-Filho AGS, Liu P, Cavender JC, Kang Y, Mohammad S, Zhang LF, Xu RF, Li YM, Dayarathne MC, Ekanayaka AH, Wen TC, Deng CY, Pereira OL, Navathe S, Hawksworth DL, Fan XL, Dissanayake LS, Kuhnert E, Grossart HP, Thines M (2020) Outline of Fungi and fungus-like taxa. Mycosphere 11(1): 1060–1456. https://doi.org/10.5943/mycosphere/11/1/8

Wu HX, Li YM, Chen H, Hyde KD (2010) Studies on Microthyriaceae: some excluded genera. Mycotaxon 113: 147–156. https://doi.org/10.5248/113.147

Wu HX, Schoch CL, Boonmee S, Bahkali AH, Chomnunti P, Hyde KD (2011a) A reappraisal of Microthyriaceae. Fungal Diversity 51(1): 189–248. https://doi.org/10.1007/s13225-011-0143-8

Wu HX, Hyde KD, Chen H (2011b) Studies on Microthyriaceae: placement of *Actinomyxa*, *Asteritea*, *Cirsosina*, *Polystomellina* and *Stegothyrium*. Cryptogamie Mycologie 32(1): 3–12. https://doi.org/10.7872/crym.v32.iss1.2012.003

Wu HX, Jaklitsch WM, Voglmayr H, Hyde KD (2011c) Epitypification, morphology, and phylogeny of *Tothia fuscella*. Mycotaxon 118: 203–211. https://doi.org/10.5248/118.203

Wu HX, Li YM, Ariyawansa HA, Li WJ, Yang H, Hyde K D (2014) A new species of *Microthyrium* from Yunnan, China. Phytotaxa 176(1): 213–218. https://doi.org/10.11646/phytotaxa.176.1.21

Yang GZ, Lu J, Yu ZF, Zhang KQ, Qiao M (2011). *Uncispora sinensis*, a new species from China. Mycotaxon 116: 171–174. https://doi.org/10.5248/116.171

Yang GZ, Lu KP, Yang Y, Ma LB, Qiao M, Zhang K Q, Yu ZF (2012) *Sympodioplanus yunnanensis*, a new aquatic species from submerged decaying leaves. Mycotaxon 120: 287–290. https://doi.org/10.5248/120.287

Yang XQ, Ma SY, Peng ZX, Wang ZQ, Qiao M, Yu Z (2021) Diversity of *Plectosphaerella* within aquatic plants from southwest China, with *P. endophytica* and *P. sichuanensis* spp. nov. MycoKeys 80: 57–75. https://doi.org/10.3897/mycokeys.80.64624

Yen LTH, Inaba S, Tsurumi Y, Nhung NTH, Hop DV, Ando K (2017). Leaf litter fungi isolated in Bach Ma National Park, Vietnam. Vietnam Journal of Science and Technology 55: 37–44. https://doi.org/10.15625/2525-2518/55/1A/12380

Yu ZF, Lv YF, Feng B, Qiao M (2019) *Lemonniera yulongensis* sp. nov. from Yunnan, China. Mycotaxon 134(1): 177–181. https://doi.org/10.5248/134.177

Zheng H, Zhang ZN, Wen ZJ, Castaeda-Ruiz RF, Yu ZF (2019) *Blastosporium persicolor* gen. et sp. nov., a new helotialean fungus. MycoKeys 51: 55–64. https://doi.org/10.3897/mycokeys.51.30798

Zheng H, Wan Y, Li J, Castaeda-Ruiz RF, Yu ZF (2020a) *Phialolunulospora vermispora* (Chaetosphaeriaceae, Sordariomycetes), a novel asexual genus and species from freshwater in southern China. MycoKeys 76: 17–30. https://doi.org/10.3897/mycokeys.76.57410

Zheng H, Yang XQ, Deng JS, Xu JP, Yu ZF (2020b) *Beltrania sinensis* sp. nov., an endophytic fungus from China and a key to species of the genus. International Journal of Systematic and Evolutionary Microbiology 70(2): 1178–1185. https://doi.org/10.1099/ijsem.0.003897

Zheng H, Li J, Guo JS, Qiao M, Yu ZF (2021a) *Anacraspedodidymum submersum* sp. nov. (Chaetosphaeriaceae, Chaetosphaeriales), a new species of freshwater hyphomycetes from southwest China. International Journal of Systematic and Evolutionary Microbiology 71(2). https://doi.org/10.1099/ijsem.0.004650

Zheng H, Qiao M, Lv YF, Du X, Zhang KQ, Yu ZF (2021b) New species of *trichoderma* isolated as endophytes and saprobes from southwest China. Journal of Fungi 7(6): 467. https://doi.org/10.3390/jof7060467

MycoKeys 85: 31–56 (2021)
doi: 10.3897/mycokeys.85.73107
https://mycokeys.pensoft.net

RESEARCH ARTICLE

A peer-reviewed open-access journal
MycoKeys
Launched to accelerate biodiversity research

Two new species of *Diaporthe* (*Diaporthaceae*, *Diaporthales*) associated with tree cankers in the Netherlands

Ning Jiang[1,3], Hermann Voglmayr[2], Chun-Gen Piao[1], Yong Li[1]

1 *Key Laboratory of Forest Protection of National Forestry and Grassland Administration, Institute of Forest Ecology, Environment and Nature Conservation, Chinese Academy of Forestry, Beijing 100091, China* **2** *Department of Botany and Biodiversity Research, University of Vienna, Rennweg 14, A-1030 Vienna, Austria* **3** *The Key Laboratory for Silviculture and Conservation of the Ministry of Education, Beijing Forestry University, Beijing 100083, China*

Corresponding author: Yong Li (ylx78@hotmail.com)

Academic editor: N Wijayawardene | Received 17 August 2021 | Accepted 9 November 2021 | Published 29 November 2021

Citation: Jiang N, Voglmayr H, Piao C-G, Li Y (2021) Two new species of *Diaporthe* (Diaporthaceae, Diaporthales) associated with tree cankers in the Netherlands. MycoKeys 85: 31–56. https://doi.org/10.3897/mycokeys.85.73107

Abstract

Diaporthe (*Diaporthaceae*, *Diaporthales*) is a common fungal genus inhabiting plant tissues as endophytes, pathogens and saprobes. Some species are reported from tree branches associated with canker diseases. In the present study, *Diaporthe* samples were collected from *Alnus glutinosa*, *Fraxinus excelsior* and *Quercus robur* in Utrecht, the Netherlands. They were identified to species based on a polyphasic approach including morphology, pure culture characters, and phylogenetic analyses of a combined matrix of partial ITS, *cal*, *his3*, *tef1* and *tub2* gene regions. As a result, four species (viz. *Diaporthe pseudoalnea* **sp. nov.** from *Alnus glutinosa*, *Diaporthe silvicola* **sp. nov.** from *Fraxinus excelsior*, *D. foeniculacea* and *D. rudis* from *Quercus robur*) were revealed from tree branches in the Netherlands. *Diaporthe pseudoalnea* differs from *D. eres* (syn. *D. alnea*) by its longer conidiophores. *Diaporthe silvicola* is distinguished from *D. fraxinicola* and *D. fraxini-angustifoliae* by larger alpha conidia.

Keywords

Two new taxa, *Diaporthe pseudoalnea*, *Diaporthe silvicola*, taxonomy, two new taxa

Introduction

Diaporthe (syn. *Phomopsis*) is the type genus of *Diaporthaceae* in *Diaporthales*, commonly occurring as plant endophytes, pathogens and saprobes (Udayanga et al. 2014, 2015; Guarnaccia et al. 2017, 2018a, 2018b; Tibpromma et al. 2018; Yang et al. 2020; Dissanayake et al. 2020; Jiang et al. 2021). The sexual morph is characterized by immersed perithecial ascomata and an erumpent pseudostroma with more or less elongated perithecial necks, unitunicate clavate to cylindrical asci, and fusoid, ellipsoid to cylindrical, hyaline uni- to bicellular ascospores (Udayanga et al. 2011; Senanayake et al. 2017). The asexual morph is characterized by ostiolate conidiomata, with cylindrical phialides producing up to three types of hyaline, aseptate conidia (Udayanga 2011; Gomes et al. 2013; Yang et al. 2018), and was previously classified as *Phomopsis*. Following the "one fungus one name" nomenclature, Rossman et al. (2015) recommended to use *Diaporthe* based on priority, necessitating the transfer of numerous *Phomopsis* species to *Diaporthe*.

Species of *Diaporthe* are known to cause plant diseases including dieback, canker, leaf spot, fruit rot, pod blights and seed decay. For example, *D. citri*, *D. cytosporella* and *D. foeniculina* caused melanose and stem end rot diseases of *Citrus* spp. (Udayanga et al. 2014), while *Daporthe lithocarpi* caused leaf spot disease of *Castanea henryi* in China (Jiang et al. 2021). Up to 19 *Diaporthe* species were confirmed to be associated with pear cankers in China (Guo et al. 2020), and eight species of *Diaporthe* were found to be the casual agents of Chinese grapevine dieback (Manawasinghe et al. 2019). Seven *Diaporthe* species were reported from blueberry twig blight and dieback diseases in Portugal (Hilário et al. 2020). *Diaporthe biconispora* and an additional six species were identified as endophytes from healthy *Citrus* tissues in China (Huang et al. 2015). *Diaporthe constrictospora* and an additional 11 species were isolated as saprobes from dead wood in karst formations in China (Dissanayake et al. 2020).

Diaporthe species were previously classified mainly based on host association and morphology (Rehner and Uecker 1994; Santos and Phillips 2009; Udayanga et al. 2011, 2014). However, several taxonomic studies of *Diaporthales* proved that phylogeny based on multiple genes is suitable to separate species (Voglmayr et al. 2012, 2017; Fan et al. 2018; Jiang et al. 2019, 2020; Jaklitsch and Voglmayr 2019, 2020). Species of *Diaporthe* are now characterised and circumscribed both by morphology and phylogeny of multi-locus DNA data, which revealed many cryptic species in recent years (Diogo et al. 2010; Lombard et al. 2014; Gao et al. 2016, 2017; Long et al. 2019; Yang et al. 2020, 2021; Zapata et al. 2020; Huang et al. 2021). To clarify the species boundaries of the *Diaporthe eres* complex, the Genealogical Phylogenetic Species Recognition principle (GCPSR) and the coalescent-based model Poisson Tree Processes (PTPs) were employed, which suggested that the *Diaporthe eres* species complex actually represents only a single species, *D. eres* (Hilário et al. 2021).

In the present study, *Diaporthe* samples from cankered branches of several tree species were collected in the Netherlands, and identified based on modern taxonomic

approaches. As a result, two new species and two known species were identified, and the new species are described and illustrated herein.

Materials and methods

Collection, examination and isolation

The fresh specimens of cankered branches were sampled from *Alnus glutinosa*, *Fraxinus excelsior* and *Quercus robur* in Utrecht, the Netherlands. Morphological characteristics of the conidiomata were determined under a Nikon AZ100 dissecting stereomicroscope. More than 20 conidiomata were sectioned, and 50 conidia were randomly selected for measurement using a Leica compound microscope (LM, DM 2500). Isolates were obtained by removing a mucoid conidial mass from conidiomata, spreading the suspension onto the surface of 1.8 % potato dextrose agar (PDA), and incubated at 25 °C for up to 24 h. Single germinating conidia were removed and plated onto fresh PDA plates. Cultural characteristics of isolates incubated on PDA in the dark at 25 °C were recorded, including the colony color and conidiomata structures. The cultures were deposited in the China Forestry Culture Collection Center (CFCC; http://www.cfcc-caf.org.cn/), and the specimens in the herbarium of the Chinese Academy of Forestry (CAF; http://museum.caf.ac.cn/).

DNA extraction, PCR amplification and phylogenetic analyses

Genomic DNA was extracted from colonies grown on cellophane-covered PDA using a cetyltrimethylammonium bromide (CTAB) method (Doyle and Doyle 1990). DNA was checked by electrophoresis in 1 % agarose gel, and the quality and quantity were measured using a NanoDrop 2000 (Thermo Scientific, Waltham, MA, USA). Five partial loci, including the 5.8S nuclear ribosomal DNA gene with the two flanking internally transcribed spacer (ITS) regions, the calmodulin (*cal*), the histone H3 (*his3*), the translation elongation factor 1-alpha (*tef1*) and the beta-tubulin (*tub2*) genes were amplified by the primer pairs and polymerase chain reaction (PCR) process listed in Table 1. The PCR products were assayed via electrophoresis in 2 % agarose gels. DNA sequencing was performed using an ABI PRISM 3730XL DNA Analyser with a Big-

Table 1. Genes used in this study with PCR primers and process.

Locus	PCR primers	PCR: thermal cycles: (Annealing temp. in bold)	Reference
ITS	ITS1/ITS4	(95 °C: 30 s, **48 °C**: 30 s, 72 °C: 1 min) × 35 cycles	White et al. 1990
cal	CAL228F/CAL737R	(95 °C: 15 s, **54 °C**: 20 s, 72 °C: 1 min) × 35 cycles	Carbone and Kohn 1999
his3	CYLH3F/H3-1b	(95 °C: 30 s, **57 °C**: 30 s, 72 °C: 1 min) × 35 cycles	Crous et al. 2004 Glass and Donaldson 1995
tef1	EF1-728F/EF1-986R	(95 °C: 15 s, **54 °C**: 20 s, 72 °C: 1 min) × 35 cycles	Carbone and Kohn 1999
tub2	T1(Bt2a)/Bt2b	(95 °C: 30 s, **55 °C**: 30 s, 72 °C: 1 min) × 35 cycles	Glass and Donaldson 1995; O'Donnell and Cigelnik 1997

Dye Terminator Kit v.3.1 (Invitrogen, USA) at the Shanghai Invitrogen Biological Technology Company Limited (Beijing, China).

The quality of the amplified nucleotide sequences was checked and the sequences assembled using SeqMan v.7.1.0. Reference sequences were retrieved from the National Center for Biotechnology Information (NCBI), based on recent publications on the genus *Diaporthe* (Dissanayake et al. 2021; Gao et al. 2021; Huang et al. 2021; Sun et al. 2021, Wang et al. 2021; Yang et al. 2021). Sequences were aligned using MAFFT v. 6 (Katoh and Toh 2010) and corrected manually using MEGA 7.0.21. The best-fit nucleotide substitution models for each gene were selected using jModelTest v. 2.1.7 (Darriba et al. 2012) under the Akaike Information Criterion.

The phylogenetic analyses of the combined gene regions were performed using Maximum Likelihood (ML) and Bayesian Inference (BI) methods. ML was implemented on the CIPRES Science Gateway portal (https://www.phylo.org) using RAxML-HPC BlackBox 8.2.10 (Stamatakis 2014), employing a GTRGAMMA substitution model with 1000 bootstrap replicates. While BI was performed using a Markov Chain Monte Carlo (MCMC) algorithm in MrBayes v. 3.0 (Ronquist et al. 2003). Two MCMC chains, started from random trees for 1000000 generations and trees, were sampled every 100th generation, resulting in a total of 10000 trees. The first 25 % of trees were discarded as burn-in of each analysis. Branches with significant Bayesian Posterior Probabilities (BPP) were estimated in the remaining 7500 trees. Phylogenetic trees were viewed with FigTree v.1.3.1 and processed by Adobe Illustrator CS5. The nucleotide sequence data of the new taxa were deposited in GenBank and are listed in Table 2.

Results

Phylogenetic analyses

The five-gene sequence dataset (ITS, *cal*, *his3*, *tef1* and *tub2*) was analysed to infer the interspecific relationships within *Diaporthe*. The dataset consisted of 307 sequences including one outgroup taxon, *Diaporthella corylina* (CBS 121124). A total of 2649 characters including gaps (516 for ITS, 576 for *cal*, 526 for *his3*, 507 for *tef1* and 524 for *tub2*) were included in the phylogenetic analysis. Of these characters, 844 were constant, 318 were variable and parsimony-uninformative, and 1487 were parsimony-informative. The topologies resulting from ML and BI analyses of the concatenated dataset were congruent (Fig. 1). Isolates from the present study formed four individual clades representing four species of *Diaporthe*, of which isolates CFCC 54192, M35, M40-1 and M84 from *Quercus robur* represent *D. foeniculacea*, while CFCC 54193 and M86 from *Q. robur* represent *D. rudis*. CFCC 54191 and M79 from *Fraxinus excelsior* and CFCC 54190 and M2A from *Alnus glutinosa* represent two new species which are here described as *D. silvicola* and *D. pseudoalnea*, respectively.

Table 2. Isolates and GenBank accession numbers used in the phylogenetic analyses of *Diaporthe*.

Species	Strain	Host	Origin	GenBank accession numbers				
				ITS	*cal*	*his3*	*tef1*	*tub2*
Diaporthe acaciigena	CBS 129521	*Acacia retinodes*	Australia	KC343005	KC343247	KC343489	KC343731	KC343973
D. acericola	MFLUCC 17-0956	*Acer negundo*	Italy	KY964224	KY964137	NA	KY964180	KY964074
D. acerigena	CFCC 52554	*Acer tataricum*	China	MH121489	MH121413	MH121449	MH121531	NA
D. acerigena	CFCC 52555	*Acer tataricum*	China	MH121490	MH121414	MH121450	MH121532	NA
D. acuta	PSCG 047	*Pyrus pyrifolia*	China	MK626957	MK691125	MK726161	MK654802	MK691225
D. acutispora	LC6161	*Coffea*	China	KX986764	KX999274	KX999235	KX999155	KX999195
D. alangii	CFCC 52556	*Alangium kurzii*	China	MH121491	MH121415	MH121451	MH121533	MH121573
D. alangii	CFCC 52557	*Alangium kurzii*	China	MH121492	MH121416	MH121452	MH121534	MH121574
D. albosinensis	CFCC 53066	*Betula albosinensis*	China	MK432659	MK442979	MK443004	MK578133	MK578059
D. albosinensis	CFCC 53067	*Betula albosinensis*	China	MK432660	MK442980	MK443005	MK578134	MK578060
D. alleghaniensis	CBS 495.72	*Betula alleghaniensis*	Canada	MH121502	MH121426	MH121462	MH121544	MH121584
D. ambigua	CBS 114015	*Pyrus communis*	South Africa	KC343010	KC343252	KC343494	KC343736	KC343978
D. ampelina	STE-U 2660	*Vitis vinifera*	France	NA	AY745026	NA	AY745056	NA
D. amygdali	CBS 126679	*Prunus dulcis*	Portugal	MH864208	KC343264	KC343506	KC343748	KC343990
D. anacardii	CBS 720.97	*Anacardium occidentale*	East Africa	KC343024	KC343266	KC343508	KC343750	KC343992
D. angelicae	CBS 111592	*Heracleum sphondylium*	Austria	KC343027	KC343269	KC343511	KC343753	KC343995
D. apiculatum	CFCC 53068	*Rhus chinensis*	China	MK432651	MK442973	MK442998	MK578127	MK578054
D. apiculatum	CFCC 53069	*Rhus chinensis*	China	MK432652	MK44297	MK442999	MK578128	MK578055
D. aquatica	IFRDCC 3051	*Aquatic habitat*	China	JQ797437	NA	NA	NA	NA
D. arctii	DP0482	*Arctium lappa*	Austria	KJ590736	KJ612133	KJ659218	KJ590776	KJ610891
D. arecae	CBS 161.64	*Areca catechu*	India	KC343032	KC343274	KC343516	KC343758	KC344000
D. arengae	CBS 114979	*Arenga engleri*	Hong Kong	MF773664	KC343276	KC343518	KC343760	KC344002
D. aseana	MFLUCC 12-0299a	Unknown	Thailand	KT459414	KT459464	NA	KT459448	KT459432
D. asheicola	CBS 136967	*Vaccinium ashei*	Chile	KJ160562	KJ160542	NA	KJ160594	KJ160518
D. aspalathi	CBS 117169	*Aspalathus linearis*	South Africa	KC343036	KC343278	KC343520	KC343762	KC344004
D. australafricana	CBS 111886	*Vitis vinifera*	Australia	KC343038	KC343280	KC343522	KC343764	KC344006
D. australiana	CBS 146457	*Macadamia*	Australia	MN708222	NA	NA	MN696522	MN696530
D. baccae	CBS 136972	*Vaccinium corymbosum*	Italy	MK370623	MG281695	MF418264	KJ160597	MF418509

Species	Strain	Host	Origin	GenBank accession numbers				
				ITS	*cal*	*his3*	*tef1*	*tub2*
D. batatas	CBS 122.21	*Ipomoea batatas*	USA	KC343040	KC343282	KC343524	KC343766	KC344008
D. bauhiniae	CFCC 53071	*Bauhinia purpurea*	China	MK432648	MK442970	MK442995	MK578124	MK578051
D. bauhiniae	CFCC 53072	*Bauhinia purpurea*	China	MK432649	MK442971	MK442996	MK578125	MK578052
D. bauhiniae	CFCC 53073	*Bauhinia purpurea*	China	MK432650	MK442972	MK442997	MK578126	MK578053
D. beilharziae	BRIP 54792	*Indigofera australis*	Australia	JX862529	NA	NA	JX862535	KF170921
D. benedicti	SBen914	*Diaporthe benedicti*	USA	KM669929	KM669862	NA	KM669785	NA
D. betulae	CFCC 50469	*Betula platyphylla*	China	KT732950	KT732997	KT732999	KT733016	KT733020
D. betulae	CFCC 50470	*Betula platyphylla*	China	KT732951	KT732998	KT733000	KT733017	KT733021
D. betulicola	CFCC 51128	*Betula albo-sinensis*	China	KX024653	KX024659	KX024661	KX024655	KX024657
D. betulicola	CFCC 51129	*Betula albo-sinensis*	China	KX0246554	KX024660	KX024662	KX0246556	KX024658
D. betulina	CFCC 52560	*Betula albo-sinensis*	China	MH121495	MH121419	MH121455	MH121537	MH121577
D. betulina	CFCC 52561	*Betula albo-sinensis*	China	MH121496	MH121420	MH121456	MH121538	MH121578
D. biconispora	ZJUD62	*Citrus maxima*	China	KJ490597	NA	KJ490539	KJ490476	KJ490418
D. biguttulata	ZJUD47	*Citrus limon*	China	KJ490582	NA	KJ490524	KJ490461	KJ490403
D. bohemiae	CBS 143347	*Vitis vinifera*	Czech Republic	MK300012	MG281710	MG281361	MG281536	MG281188
D. brasiliensis	CBS 133183	*Aspidosperma tomentosum*	Brazil	KC343042	KC343284	KC343526	KC343768	KC344010
D. caatingaensis	URM7485	*Tacinga inamoena*	Brazil	KY085927	KY115598	NA	KY115604	KY115601
D. camelliae-sinensis	SAUCC194.92	*Camellia sinensis*	China	MT822620	MT855699	MT855588	MT855932	MT855817
D. canthii	CPC 19740	*Canthium inerme*	South Africa	JX069864	NA	NA	NA	NA
D. caryae	CFCC 52563	*Carya illinoinensis*	China	MH121498	MH121422	MH121458	MH121540	MH121580
D. caryae	CFCC 52564	*Carya illinoinensis*	China	MH121499	MH121423	MH121459	MH121541	MH121581
D. cassines	CPC 21916	*Cassine peragua*	South Africa	KF777155	NA	NA	KF777244	NA
D. caulivora	CBS 127268	*Glycine max*	Croatia	MH864501	KC343287	KC343529	KC343771	KC344013
D. cercidis	CFCC 52565	*Cercis chinensis*	China	MH121500	MH121424	MH121460	NA	MH121582
D. cercidis	CFCC 52566	*Cercis chinensis*	China	MH121501	MH121425	MH121461	NA	MH121583
D. chamaeropis	CBS 454.81	*Chamaerops humilis*	Greece	KC343048	KC343290	KC343532	KC343774	KC344016
D. charlesworthii	BRIP 54884m	*Rapistrum rugostrum*	Australia	KJ197288	NA	NA	KJ197250	KJ197268
D. chensiensis	CFCC 52567	*Abies chensiensis*	China	MH121502	MH121426	MH121462	MH121544	MH121584
D. chensiensis	CFCC 52568	*Abies chensiensis*	China	MH121503	MH121427	MH121463	MH121545	MH121585
D. chongqingensis	PSCG 435	*Pyrus pyrifolia*	China	MK626916	MK691209	MK726257	MK654866	MK691321

Species	Strain	Host	Origin	GenBank accession numbers				
				ITS	*cal*	*his3*	*tef1*	*tub2*
D. chrysalidocarpi	SAUCC194.35	*Chrysalidocarpus lutescens*	China	MT822563	MT855646	MT855532	MT855760	MT855876
D. cichorii	MFLUCC 17-1023	*Cichorium intybus*	Italy	KY964220	KY964133	NA	KY964176	KY964104
D. cinnamomi	CFCC 52569	*Cinnamomum*	China	MH121504	NA	MH121464	MH121546	MH121586
D. cinnamomi	CFCC 52570	*Cinnamomum*	China	MH121505	NA	MH121465	MH121547	MH121587
D. cissampeli	CPC 27302	*Cissampelos capensis*	South Africa	KX228273	NA	KX228366	NA	KX228384
D. citri	AR3405	*Citrus*	USA	KC843311	KC843157	KJ420881	KC843071	KC843187
D. citri	CFCC 53079	*Citrus sinensis*	China	MK573940	MK574579	MK574595	MK574615	MK574635
D. citriasiana	CGMCC 3.15224	*Citrus unshiu*	China	JQ954645	KC357491	KC490515	JQ954663	KC357459
D. citrichinensis	CGMCC 3.15225	*Citrus*	China	JQ954648	KC357494	NA	JQ954666	NA
D. collariana	MFLU 17-2770	*Magnolia champaca*	Thailand	MG806115	MG783042	NA	MG783040	MG783041
D. compactum	LC3083	*Camellia sinensis*	China	KP267854	NA	KP293508	KP267928	NA
D. conica	CFCC 52571	*Alangium chinense*	China	MH121506	MH121428	MH121466	MH121548	MH121588
D. conica	CFCC 52572	*Alangium chinense*	China	MH121507	MH121429	MH121467	MH121549	MH121589
D. constrictospora	CGMCC 3.20096	Unknown	China	MT385947	MT424718	MW022487	MT424682	MT424702
D. convolvuli	CBS 124654	*Convolvulus arvensis*	Turkey	KC343054	KC343296	KC343538	KC343780	KC344022
D. coryli	CFCC 53083	*Corylus mandshurica*	China	MK432661	MK442981	MK443006	MK578135	MK578061
D. coryli	CFCC 53084	*Corylus mandshurica*	China	MK432662	MK442982	MK443007	MK538176	MK578062
D. corylicola	CFCC 53986	*Corylus heterophylla*	China	MW839880	MW836684	MW836717	MW815894	MW883977
D. corylicola	CFCC 53987	*Corylus heterophylla*	China	MW839867	MW836685	MW836718	MW815895	MW883978
D. crotalariae	CBS 162.33	*Crotalaria spectabilis*	USA	MH855395	JX197439	KC343540	GQ250307	KC344024
D. crousii	CAA 823	*Vaccinium corymbosum*	Portugal	MK792311	MK883835	MK871450	MK828081	MK837932
D. cucurbitae	DAOM 42078	*Cucumis*	Canada	KM453210	NA	KM453212	KM453211	KP118848
D. cuppatea	CBS 117499	*Aspalathus linearis*	South Africa	MH863021	KC343299	KC343541	KC343783	KC344025
D. cynaroidis	CBS 122676	*Protea cynaroides*	South Africa	KC343058	KC343300	KC343542	KC343784	KC344026
D. cytosporella	FAU461	*Citrus limon*	Italy	KC843307	KC843141	NA	KC843116	KC843221
D. diospyricola	CPC 21169	*Diospyros whyteana*	South Africa	KF777209	NA	NA	NA	NA
D. discoidispora	ZJUD89	*Citrus unshiu*	China	KJ490624	NA	KJ490566	KJ490503	KJ490445
D. dorycnii	MFLUCC 17-1015	*Dorycnium hirsutum*	Italy	KY964215	NA	NA	KY964171	KY964099
D. drenthii	CBS 146453	*Macadamia*	Australia	MN708229	NA	NA	MN696526	MN696537
D. elaeagni-glabrae	LC4802	*Elaeagnus glabra*	China	KX986779	KX999281	KX999251	KX999171	KX999212

Species	Strain	Host	Origin	GenBank accession numbers				
				ITS	*cal*	*his3*	*tef1*	*tub2*
D. ellipicola	CGMCC 3.17084	*Lithocarpus glaber*	China	KF576270	NA	NA	KF576245	KF576294
D. endophytica	CBS 133811	*Schinus terebinthifolius*	Brazil	KC343065	KC343307	KC343549	KC343791	KC344033
D. eres	CBS 146.46	*Alnus*	Netherlands	KC343008	KC343250	KC343492	KC343734	KC343976
D. eres	CBS 121004	*Juglans*	USA	KC343134	KC343376	KC343618	KC343860	KC344102
D. eres	CGMCC 3.17081	*Lithocarpus glabra*	China	KF576282	NA	NA	KF576257	KF576306
D. eres	CFCC 51632	*Camptotheca acuminata*	China	KY203726	KY228877	KY228881	KY228887	KY228893
D. eres	CBS 139.27	*Celastrus*	USA	KC343047	KC343289	KC343531	KC343773	KC344015
D. eres	CBS 143349	*Vitis vinifera*	United Kingdom	MG281017	MG281712	MG281363	MG281538	MG281190
D. eres	AR5193	*Ulmus*	Germany	KJ210529	KJ434999	KJ420850	KJ210550	KJ420799
D. eres	CFCC 52575	*Castanea mollissima*	China	MH121510	NA	MH121470	MH121552	MH121592
D. eres	CFCC 52576	*Castanea mollissima*	China	MH121511	MH121432	MH121471	MH121553	MH121593
D. eres	CFCC 52577	*Acanthopanax senticosus*	China	MH121512	MH121433	MH121472	MH121554	MH121594
D. eres	CFCC 52578	*Sorbus*	China	MH121513	MH121433	MH121473	MH121555	MH121595
D. eres	CFCC 52579	*Juglans regia*	China	MH121514	NA	MH121474	MH121556	NA
D. eres	CFCC 52580	*Melia azedarace*	China	MH121515	NA	MH121475	MH121557	MH121596
D. eres	CFCC 52581	*Rhododendron simsii*	China	MH121516	NA	MH121476	MH121558	MH121597
D. eres	MAFF 625034	*Pyrus pyrifolia*	Japan	NA	KJ435023	KJ420868	NA	KJ420819
D. eres	AR5211	*Hedera helix*	France	KJ210538	KJ435043	KJ420875	KJ210559	KJ420828
D. eres	CGMCC 3.17089	*Lithocarpus glabra*	China	KF576267	NA	NA	KF576242	KF576291
D. eres	MFLUCC 17-0963	*Lonicera*	Italy	KY964190	KY964116	NA	KY964146	KY964073
D. eres	DAOM 695742	*Picea ruben*	Canada	KU552025	NA	NA	KU552023	KU574615
D. eres	MFLUCC 16-0113	*Prunus persica*	China	KU557563	NA	KU557611	KU557631	KU55758
D. eres	CBS 144.27	*Spiraea*	USA	KC343144	KC343386	KC343628	KC343870	KC344112
D. eres	CBS 587.79	*Pinus parviflora var*	Japan	KC343153	KC343395	KC343637	KC343879	KC344121
D. eres	CBS 338.89	*Hedera helix*	Yugoslavia	KC343152	KC343394	KC343636	KC343878	KC344120
D. eres	MFLU 17-0646	*Rosa*	United Kingdom	MG828895	MG829274	NA	MG829270	MG843877
D. eucalyptorum	CBS 132525	*Eucalyptus*	China	MH305525	NA	NA	NA	NA
D. foeniculacea	CBS 111553	*Foeniculum vulgare*	Spain	MH854926	KC343343	KC343585	KC343827	KC344069
D. foeniculacea	**CFCC 54192**	***Quercus robur***	**Netherlands**	**MZ727033**	**NA**	**MZ753474**	**MZ816339**	**MZ753483**
D. foeniculacea	**M35**	***Quercus robur***	**Netherlands**	**MZ727034**	**NA**	**MZ753475**	**MZ816340**	**MZ753484**

Species	Strain	Host	Origin	GenBank accession numbers				
				ITS	*cal*	*his3*	*tef1*	*tub2*
D. foeniculacea	**M40-1**	***Quercus robur***	**Netherlands**	**MZ727035**	**NA**	**MZ753476**	**MZ816341**	**MZ753485**
D. foeniculacea	**M84**	***Quercus robur***	**Netherlands**	**MZ727036**	**NA**	**MZ753477**	**MZ816342**	**MZ753486**
D. fraxini-angustifoliae	BRIP 54781	*Fraxinus angustifolia*	Australia	JX862528	KT459462	NA	JX862534	NA
D. fraxinicola	CFCC 52582	*Fraxinus chinensis*	China	MH121517	MH121435	NA	MH121560	NA
D. fraxinicola	CFCC 52583	*Fraxinus chinensis*	China	MH121518	MH121436	NA	MH121559	NA
D. fulvicolor	PSCG 051	*Pyrus pyrifolia*	China	MK626859	MK691132	MK726163	MK654806	MK691236
D. fusicola	CGMCC 3.17087	*Lithocarpus glabra*	China	KF576281	KF576233	NA	KF576256	KF576305
D. ganjae	CBS 180.91	*Cannabis sativa*	USA	KC343112	KC343354	KC343596	KC343838	KC344080
D. ganzhouensis	CFCC 53087	Unknown	China	MK432665	MK442985	MK443010	MK578139	MK578065
D. ganzhouensis	CFCC 53088	Unknown	China	MK432666	MK442986	MK443011	MK578140	MK578066
D. garethjonesii	MFLUCC 12-0542a	Unknown	Thailand	KT459423	KT459470	NA	KT459457	KT459441
D. goulteri	BRIP 55657a	*Helianthus annuus*	Australia	KJ197290	NA	NA	KJ197252	KJ197270
D. grandiflori	SAUCC194.84	*Heterostemma grandiflorum*	China	MT822612	MT855691	MT855580	MT855809	MT855924
D. guangxiensis	JZB320087	*Vitis vinifera*	China	MK335765	MK736720	NA	MK500161	MK523560
D. gulyae	BRIP 54025	*Helianthus annuus*	Australia	NA	NA	NA	JN645803	KJ197271
D. guttulata	CGMCC 3.20100	Unknown	China	MT385950	MW022470	MW022491	MT424685	MT424705
D. helianthi	CBS 592.81	*Helianthus annuus*	Serbia	KC343115	KC343357	KC343599	KC343841	KC344083
D. heliconiae	SAUCC194.77	*Heliconia metallica*	China	MT822605	MT855684	MT855573	MT855802	MT855917
D. heterophyllae	CPC 26215	*Acacia heterophylla*	France	MG600222	MG600218	MG600220	MG600224	MG600226
D. heterostemmatis	SAUCC194.85	*Heterostemma grandiflorum*	China	MT822613	MT855692	MT855581	MT855810	MT855925
D. hickoriae	CBS 145.26	*Carya glabra*	USA	KC343118	KC343360	NA	KC343844	KC344086
D. hispaniae	CBS 143351	*Vitis vinifera*	Spain	MG281123	MG281820	MG281471	MG281644	MG281296
D. hongkongensis	CBS 115448	*Dichroa febrifuga*	China	MK304388	KC343361	KC343603	KC343845	KC344087
D. hubeiensis	JZB320123	*Vitis vinifera*	China	MK335809	MK500235	NA	MK523570	MK500148
D. incompleta	LC6754	*Camellia sinensis*	China	KX986794	KX999289	KX999265	KX999186	KX999226
D. inconspicua	CBS 133813	*Maytenus ilicifolia*	Brazil	NA	KC343365	KC343607	KC343849	KC344091
D. infecunda	CBS 133812	*Schinus terebinthifolius*	Brazil	KC343126	KC343368	KC343610	KC343852	KC344094
D. irregularis	CGMCC 3.20092	Unknown	China	MT385951	MT424721	NA	MT424686	MT424706
D. isoberliniae	CPC 22549	*Isoberlinia angolensis*	Zambia	KJ869190	NA	NA	NA	KJ869245
D. juglandicola	CFCC 51134	*Juglans mandshurica*	China	KU985101	KX024616	KX024622	KX024628	KX024634

Species	Strain	Host	Origin	GenBank accession numbers				
				ITS	*cal*	*his3*	*tef1*	*tub2*
D. kadsurae	CFCC 52586	*Kadsura longipedunculata*	China	MH121521	MH121439	MH121479	MH121563	MH121600
D. kadsurae	CFCC 52587	*Kadsura longipedunculata*	China	MH121522	MH121440	MH121480	MH121564	MH121601
D. kochmanii	BRIP 54033	*Helianthus annuus*	Australia	NA	NA	NA	JN645809	NA
D. kongii	BRIP 54031	*Helianthus annuus*	Australia	NA	NA	NA	NA	KJ197272
D. lenispora	CGMCC 3.20101	Unknown	China	MT385952	MW022472	MW022493	MT424687	MT424707
D. litchicola	BRIP 54900	*Litchi chinensis*	Australia	LC041036	NA	NA	JX862539	NA
D. litchii	SAUCC194.22	*Litchi chinensis*	China	MT822550	MT855635	MT855519	MT855747	MT855863
D. lithocarpus	CGMCC 3.15175	*Lithocarpus glabra*	China	KC135104	KF576235	NA	KC153095	KF576311
D. longicolla	FAU599	*Glycine max*	USA	KJ590728	KJ612124	KJ659188	KJ590767	KJ610883
D. longispora	CBS 194.36	*Ribes*	Canada	MH855769	KC343377	KC343619	KC343861	KC344103
D. lusitanicae	CBS 123212	*Foeniculum vulgare*	Portugal	MH863279	KC343378	KC343620	KC343862	KC344104
D. lutescens	SAUCC194.36	*Chrysalidocarpus lutescens*	China	MT822564	MT855647	MT855533	MT855761	MT855877
D. macadamiae	CBS 146455	*Macadamia*	Australia	MN708230	NA	NA	MN696528	MN696539
D. macintoshii	BRIP 55064a	*Rapistrum rugosum*	Australia	KJ197289	NA	NA	KJ197251	KJ197269
D. mahothocarpus	CGMCC 3.15181	*Lithocarpus glabra*	China	KC153096	NA	NA	KC153087	KF576312
D. malorum	CAA 734	*Malus domestica*	Portugal	KY435638	KY435658	KY435648	KY435627	KY435668
D. masirevicii	BRIP 54256	*Glycine max*	Australia	KJ197277	NA	NA	KJ197238	KJ197256
D. mayteni	CBS 133185	*Maytenus ilicifolia*	Brazil	KC343139	KC343381	KC343623	KC343865	KC344107
D. maytenicola	CPC 21896	*Maytenus acuminata*	South Africa	KF777157	NA	NA	NA	KF777250
D. mediterranea	SAUCC194.111	*Machilus pingii*	China	MT822639	MT855718	MT855606	MT855836	MT855951
D. melastomatis	SAUCC194.55	*Melastoma malabathricum*	China	MT822583	MT855664	MT855551	MT855780	MT855896
D. melonis	CBS 435.87	*Glycine soja*	Indonesia	KC343141	KC343383	KC343625	KC343867	KC344109
D. middletonii	BRIP 54884e	*Rapistrum rugosum*	Australia	KJ197286	NA	NA	KJ197248	KJ197266
D. minima	CGMCC 3.20097	Unknown	China	MT385953	MT424722	MW022496	MT424688	MT424708
D. minusculata	CGMCC 3.20098	Unknown	China	MT385957	MW022475	MW022499	MT424692	MT424712
D. miriciae	BRIP 54736j	*Helianthus annuus*	Australia	KJ197282	NA	NA	KJ197244	KJ197262
D. multigutullata	CFCC 53095	*Citrus maxima*	China	MK432645	MK442967	MK442992	MK578121	MK578048
D. multigutullata	CFCC 53096	*Citrus maxima*	China	MK432646	MK442968	MK442993	MK578122	MK578049
D. musigena	CBS 129519	*Musa*	Australia	KC343143	KC343385	KC343267	KC343869	KC344111
D. neoarctii	CBS 109490	*Ambrosia trifida*	USA	KC343145	KC343387	KC343629	KC343871	KC344113

Species	Strain	Host	Origin	GenBank accession numbers				
				ITS	*cal*	*his3*	*tef1*	*tub2*
D. neoraonikayaporum	MFLUCC 14-1136	*Tectona grandis*	Thailand	KU712449	KU749356	NA	KU749369	KU743988
D. nothofagi	BRIP 54801	*Nothofagus cunninghamii*	Australia	JX862530	NA	NA	JX862536	KF170922
D. novem	CBS 127269	*Glycine max*	Croatia	KC343155	KC343397	KC343639	KC343881	KC344123
D. ocoteae	CPC 26217	*Ocotea bullata*	France	KX228293	NA	NA	NA	KX228388
D. oraccinii	LC3166	*Camellia sinensis*	China	KP267863	NA	KP293517	KP267937	KP293443
D. ovalispora	ZJUD93	*Citrus limon*	China	KJ490628	NA	KJ490570	KJ490507	KJ490449
D. ovoicicola	CGMCC 3.17093	*Lithocarpus glabra*	China	KF576265	KF576223	NA	KF576240	KF576289
D. oxe	CBS 133186	*Maytenus ilicifolia*	Brazil	KC343164	KC343406	KC343648	KC343890	KC344132
D. padina	CFCC 52590	*Padus racemosa*	China	MH121525	MH121443	MH121483	MH121567	MH121604
D. padina	CFCC 52591	*Padus racemosa*	China	MH121526	MH121444	MH121484	MH121568	MH121605
D. pandanicola	MFLUCC 17-0607	*Pandanaceae*	Thailand	MG646974	NA	NA	NA	MG646930
D. paranensis	CBS 133184	*Maytenus ilicifolia*	Brazil	KC343171	KC343413	KC343655	KC343897	KC344139
D. parapterocarpi	CPC 22729	*Pterocarpus brenanii*	Zambia	KJ869138	NA	NA	NA	KJ869248
D. parvae	PSCG 035	*Pyrus bretschneideri*	China	MK626920	MK691169	MK726211	MK654859	MK691249
D. pascoei	BRIP 54847	*Persea americana*	Australia	MK111097	NA	NA	JX862538	KF170924
D. passiflorae	CPC 19183	*Passiflora edulis*	Netherlands	JX069860	NA	NA	NA	NA
D. passifloricola	CPC 27480	*Passiflora foetida*	Malaysia	KX228292	NA	KX228367	NA	KX228387
D. penetriteum	LC3215	*Camellia sinensis*	China	KP267879	NA	NA	KP293532	KP267953
D. perjuncta	CBS 109745	*Ulmus glabra*	Austria	KC343172	KC343414	KC343656	KC343898	KC344140
D. perseae	CBS 151.73	*Persea gratissima*	Netherlands	KC343173	KC343415	NA	NA	NA
D. pescicola	MFLUCC 16-0105	*Prunus persica*	China	KU557555	KU557603	NA	KY400831	KU557579
D. phaseolorum	AR4203	*Phaseolus vulgaris*	USA	KJ590738	KJ612135	KJ659220	KJ590739	KJ610893
D. phillipsii	CAA 817	*Vaccinium corymbosum*	Portugal	MK792305	MK883831	MK871445	MK828076	MN000351
D. podocarpi-macrophylli	LC6155	*Podocarpus macrophyllus*	Japan	KX986774	KX999278	KX999246	KX999167	KX999207
D. pometiae	SAUCC194.72	*Pometia pinnata*	China	MT822600	MT855679	MT855568	MT855797	MT855912
D. pseudoalnea	**CFCC 54190**	***Alnus glutinosa***	**Netherlands**	**MZ727037**	**MZ753468**	**MZ781302**	**MZ816343**	**MZ753487**
D. pseudoalnea	**M2A**	***Alnus glutinosa***	**Netherlands**	**MZ727038**	**MZ753469**	**MZ753478**	**MZ816344**	**MZ753488**
D. pseudomangiferae	CBS 101339	*Mangifera indica*	Dominican Republic	KC343181	KC343423	KC343665	KC343907	KC344149
D. pseudophoenicicola	CBS 176.77	*Mangifera indica*	Iraq	KC343183	KC343425	KC343667	KC343909	KC344151

Species	Strain	Host	Origin	GenBank accession numbers				
				ITS	*cal*	*his3*	*tef1*	*tub2*
D. pseudotsugae	MFLU 15-3228	*Pseudotsuga menziesii*	Italy	KY964225	KY964138	NA	KY964181	KY964108
D. psoraleae	CPC 21634	*Psoralea pinnata*	South Africa	KF777158	NA	NA	KF777245	KF777251
D. psoraleae-pinnatae	CPC 21638	*Psoralea pinnata*	South Africa	KF777159	NA	NA	NA	KF777252
D. pterocarpicola	MFLUCC 10-0580a	*Pterocarpus indicus*	Thailand	JQ619887	JX197433	NA	JX275403	JX275441
D. pungensis	SAUCC194.112	*Elaeagnus pungens*	China	MT822640	MT855719	MT855607	MT855837	MT855952
D. pyracanthae	CAA483	*Pyracantha coccinea*	Portugal	KY435635	KY435645	KY435656	KY435625	KY435666
D. racemosae	CPC 26646	*Euclea racemosa*	South Africa	MG600223	MG600219	MG600221	MG600225	MG600227
D. raonikayaporum	CBS 133182	*Spondias mombin*	Brazil	KC343188	KC343430	KC343672	KC343914	KC344156
D. ravennica	MFLUCC 16-0997	*Clematis vitalba*	Italy	NA	NA	NA	MT394670	NA
D. rhusicola	CPC 18191	*Rhus pendulina*	South Africa	JF951146	NA	NA	NA	NA
D. rosae	MFLUCC 17-2658	*Rosa*	United Kingdom	MG828894	MG829273	NA	NA	MG843878
D. rosiphthora	COAD 2914	*Rosa*	Brazil	MT311197	MT313691	NA	MT313693	NA
D. rossmaniae	CAA 762	*Vaccinium corymbosum*	Portugal	MK792290	MK883822	MK871432	MK828063	MK837914
D. rostrata	CFCC 50062	*Juglans mandshurica*	China	KP208847	KP208849	KP208851	KP208853	KP208855
D. rostrata	CFCC 50063	*Juglans mandshurica*	China	KP208848	KP208850	KP208852	KP208854	KP208856
D. rudis	AR3422	*Laburnum anagyroides*	Austria	KC843331	KC843146	NA	KC843090	KC843177
D. rudis	**CFCC 54193**	***Quercus robur***	**Netherlands**	**MZ727039**	**MZ753470**	**MZ753479**	**MZ816345**	**MZ753489**
D. rudis	**M86**	***Quercus robur***	**Netherlands**	**MZ727040**	**MZ753471**	**MZ753480**	**MZ816346**	**MZ753490**
D. saccarata	CBS 116311	*Protea repens*	South Africa	KC343190	KC343432	KC343674	KC343916	KC344158
D. sackstonii	BRIP 54669b	*Helianthus annuus*	Australia	KJ197287	NA	NA	KJ197249	KJ197267
D. salicicola	BRIP 54825	*Salix purpurea*	Australia	JX862531	NA	NA	JX862537	KF170923
D. sambucusii	CFCC 51986	*Sambucus williamsii*	China	KY852495	KY852499	KY852503	KY852507	KY852511
D. sambucusii	CFCC 51987	*Sambucus williamsii*	China	KY852496	KY852500	KY852504	KY852508	KY852512
D. schimae	CFCC 53103	*Schima superba*	China	MK442640	MK442962	MK442987	MK578116	MK578043
D. schimae	CFCC 53104	*Schima superba*	China	MK442641	MK442963	MK442988	MK578117	MK578044
D. schimae	CFCC 53105	*Schima superba*	China	MK442642	MK442964	MK442989	MK578118	MK578045
D. schini	CBS 133181	*Schinus terebinthifolius*	Brazil	KC343191	KC343433	KC343675	KC343917	KC344159
D. schisandrae	CFCC 51988	*Schisandra chinensis*	China	KY852497	KY852501	KY852505	KY852509	KY852513
D. schisandrae	CFCC 51989	*Schisandra chinensis*	China	KY852498	KY852502	KY852506	KY852510	KY852514
D. schoeni	MFLU 15-1279	*Schoenus nigricans*	Italy	KY964226	KY964139	NA	KY964182	KY964109

Species	Strain	Host	Origin	GenBank accession numbers				
				ITS	*cal*	*his3*	*tef1*	*tub2*
D. sclerotioides	CBS 296.67	*Cucumis sativus*	Netherlands	MH858974	KC343435	KC343677	KC343919	KC344161
D. searlei	CBS 146456	*Macadamia*	Australia	MN708231	NA	NA	NA	MN696540
D. sennae	CFCC 51636	*Senna bicapsularis*	China	KY203724	KY228875	NA	KY228885	KY228891
D. sennae	CFCC 51637	*Senna bicapsularis*	China	KY203725	KY228876	NA	KY228886	KY228892
D. sennicola	CFCC 51634	*Senna bicapsularis*	China	KY203722	KY228873	KY228879	KY228883	KY228889
D. sennicola	CFCC 51635	*Senna bicapsularis*	China	KY203723	KY228874	KY228880	KY228884	KY228890
D. serafiniae	BRIP 55665a	*Helianthus annuus*	Australia	KJ197274	NA	NA	KJ197236	KJ197254
D. shaanxiensis	CFCC 53106	*on branches of liana*	China	MK432654	MK442976	MK443001	MK578130	NA
D. shaanxiensis	CFCC 53107	*on branches of liana*	China	MK432655	MK432977	MK432002	MK578131	NA
D. siamensis	MFLUCC 10-0573a	*Dasymaschalon*	Thailand	NA	JQ619897	NA	JX275393	JX275429
D. silvicola	**CFCC 54191**	***Fraxinus excelsior***	**Netherlands**	**MZ727041**	**MZ753472**	**MZ753481**	**MZ816347**	**MZ753491**
D. silvicola	**M79**	***Fraxinus excelsior***	**Netherlands**	**MZ727042**	**MZ753473**	**MZ753482**	**MZ816348**	**MZ753492**
D. sojae	FAU635	*Glycine max*	USA	KJ590719	KJ612116	KJ659208	KJ590762	KJ610875
D. spartinicola	CPC 24951	*Spartium junceμm*	Spain	KR611879	NA	KR857696	NA	KR857695
D. spinosa	PSCG 383	*Pyrus pyrifolia*	China	MK626849	MK691129	MK726156	MK654811	MK691234
D. sterilis	CBS 136969	*Vaccinium corymbosum*	Italy	KJ160579	KJ160548	MF418350	KJ160611	KJ160528
D. stictica	CBS 370.54	*Buxus sampervirens*	Italy	KC343212	KC343454	KC343696	KC343938	KC344180
D. subclavata	ZJUD95	*Citrus unshiu*	China	KJ490630	NA	KJ490572	KJ490509	KJ490451
D. subcylindrospora	KUMCC 17-0151	Unknown	China	MG746629	NA	NA	MG746630	MG746631
D. subellipicola	KUMCC 17-0153	Unknown	China	MG746632	NA	NA	MG746633	MG746634
D. subordinaria	CBS 464.90	*Plantago lanceolata*	South Africa	KC343214	KC343456	KC343698	KC343940	KC344182
D. taoicola	MFLUCC 16-0117	*Prunus persica*	China	KU557567	NA	NA	KU557636	KU557591
D. tectonae	MFLUCC 12-0777	*Tectona grandis*	Thailand	KU712430	KU749345	NA	KU749359	KU743977
D. tectonendophytica	MFLUCC 13-0471	*Tectona grandis*	Thailand	KU712439	KU749354	NA	KU749367	KU743986
D. tectonigena	MFLUCC 12-0767	*Camellia sinensis*	China	KX986782	KX999284	KX999254	KX999174	KX999214
D. terebinthifolii	CBS 133180	*Schinus terebinthifolius*	Brazil	KC343216	KC343458	KC343700	KC343942	KC344184
D. ternstroemia	CGMCC 3.15183	*Ternstroemia gymnanthera*	China	KC153098	NA	NA	KC153089	NA
D. thunbergii	MFLUCC 10-0576a	*Thunbergia laurifolia*	Thailand	JQ619893	JX197440	NA	JX275409	NA
D. thunbergiicola	MFLUCC 12-0033	*Thunbergia laurifolia*	Thailand	KP715097	NA	NA	KP715098	NA
D. tibetensis	CFCC 51999	*Juglandis regia*	China	MF279843	MF279888	MF279828	MF279858	MF279873

Species	Strain	Host	Origin	GenBank accession numbers				
				ITS	*cal*	*his3*	*tef1*	*tub2*
D. tibetensis	CFCC 52000	*Juglandis regia*	China	MF279844	MF279889	MF279829	MF279859	MF279874
D. torilicola	MFLUCC 17-1051	*Torilis arvensis*	Italy	KY964212	KY964127	NA	KY964168	KY964096
D. toxica	CBS 534.93	*Lupinus angustifolius*	Australia	KC343220	KC343462	KC343704	KC343946	KC344188
D. tulliensis	BRIP 62248a	*Theobroma cacao*	Australia	KR936130	NA	NA	KR936133	KR936132
D. ueckerae	FAU656T	*Cucumis melo*	USA	KJ590726	KJ612122	KJ659215	KJ590747	KJ610881
D. ukurunduensis	CFCC 52592	*Acer ukurunduense*	China	MH121527	MH121445	MH121485	MH121569	NA
D. ukurunduensis	CFCC 52593	*Acer ukurunduense*	China	MH121528	MH121446	MH121486	MH121570	NA
D. undulata	LC6624	Unknown	China	KX986798	NA	KX999269	KX999190	KX999230
D. unshiuensis	ZJUD52	*Citrus unshiu*	China	KJ490587	NA	KJ490529	KJ490466	KJ490408
D. unshiuensis	CFCC 52594	*Carya illinoensis*	China	MH121529	MH121447	MH121487	MH121571	MH121606
D. unshiuensis	CFCC 52595	*Carya illinoensis*	China	MH121530	MH121448	MH121488	MH121572	MH121607
D. vaccinii	CBS 160.32	*Oxycoccus macrocarpos*	USA	MH121502	MH121426	MH121462	MH121544	MH121584
D. vangueriae	CBS 137985	*Vangueria infausta*	Zambia	KJ869137	NA	NA	NA	KJ869247
D. vawdreyi	BRIP 57887a	*Psidium guajava*	Australia	KR936126	NA	NA	KR936129	KR936128
D. velutina	LC4421	*Neolitsea*	China	KX986790	NA	KX999261	KX999182	KX999223
D. verniciicola	CFCC 53109	*Vernicia montana*	China	MK573944	MK574583	MK574599	MK574619	MK574639
D. verniciicola	CFCC 53110	*Vernicia montana*	China	MK573945	MK574584	MK574600	MK574620	MK574640
D. viniferae	JZB320071	*Vitis vinifera*	China	MK341551	MK500119	NA	MK500107	MK500112
D. virgiliae	CMW 40748	*Virgilia oroboides*	South Africa	KP247556	NA	NA	NA	KP247575
D. xishuangbanica	LC6707	*Camellia sinensis*	China	KX986783	NA	KX999255	KX999175	KX999216
D. xunwuensis	CFCC 53085	Unknown	China	MK432663	MK442983	MK443008	MK578137	MK578063
D. xunwuensis	CFCC 53086	Unknown	China	MK432664	MK442984	MK443009	MK578138	MK578064
D. yunnanensis	LC6168	Unknown	China	KX986796	KX999290	KX999267	KX999188	KX999228
D. zaobaisu	PSCG 031	*Pyrus bretschneideri*	China	MK626922	NA	MK726207	MK654855	MK691245
Diaporthella corylina	CBS 121124	*Corylus*	NA	KC343004	KC343246	KC343488	KC343730	KC343972

Note: NA, not applicable. Strains in this study are marked in bold.

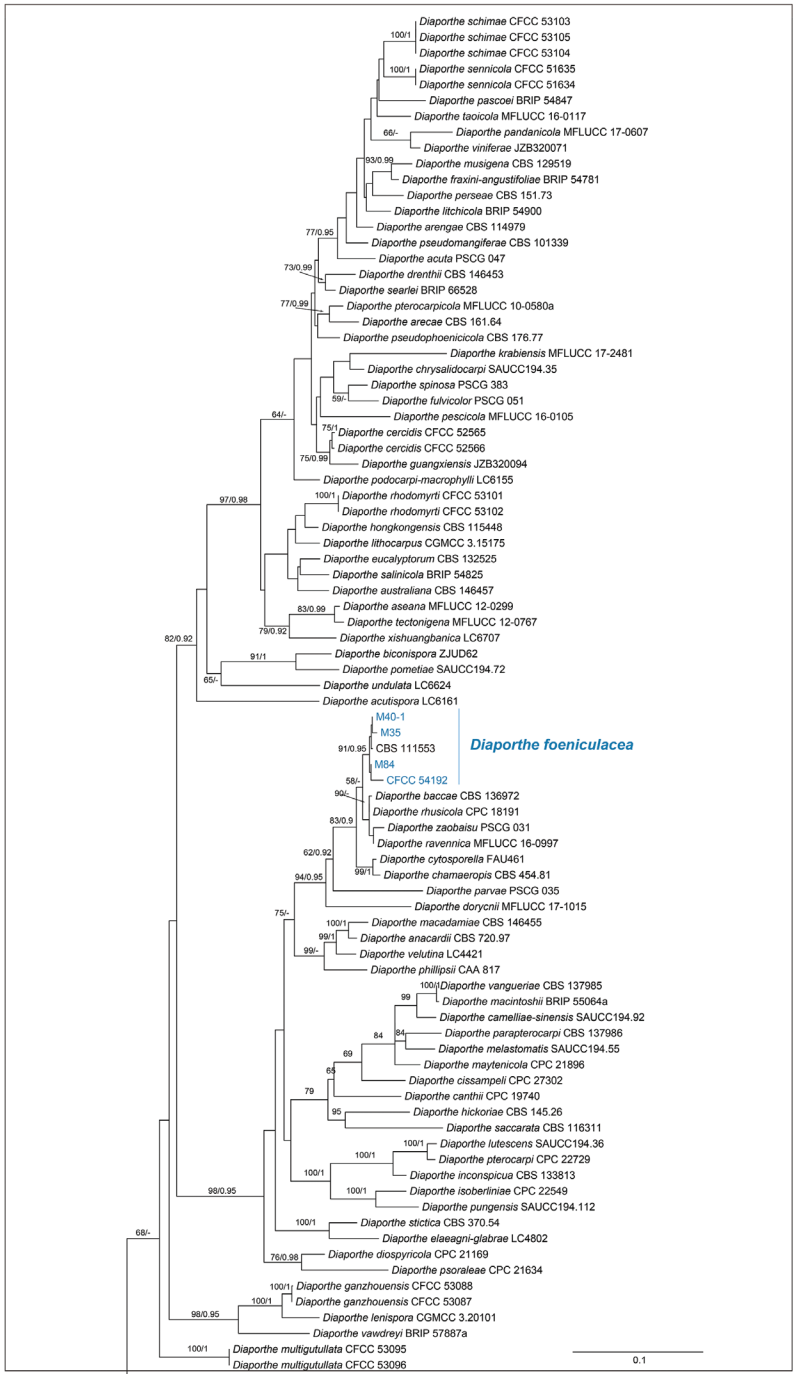

Figure 1. Phylogram of *Diaporthe* resulting from a maximum likelihood analysis based on a combined matrix of ITS, *cal*, *his3*, *tef1* and *tub2*. Numbers above the branches indicate ML bootstraps (left, ML BS ≥ 50 %) and Bayesian Posterior Probabilities (right, BPP ≥ 0.75). The tree is rooted with *Diaporthella corylina*. Isolates from present study are marked in blue.

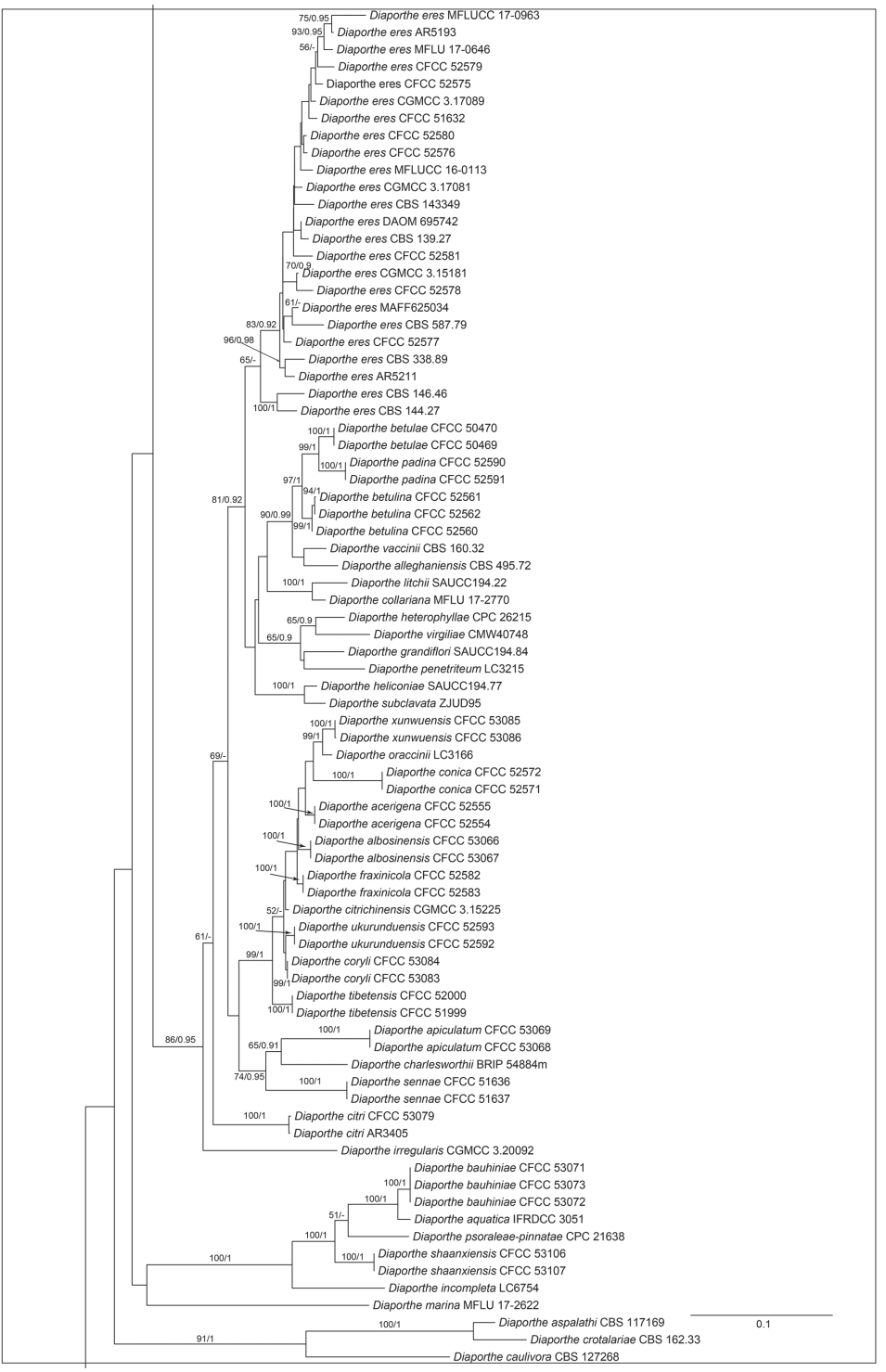

Figure 1. Continued.

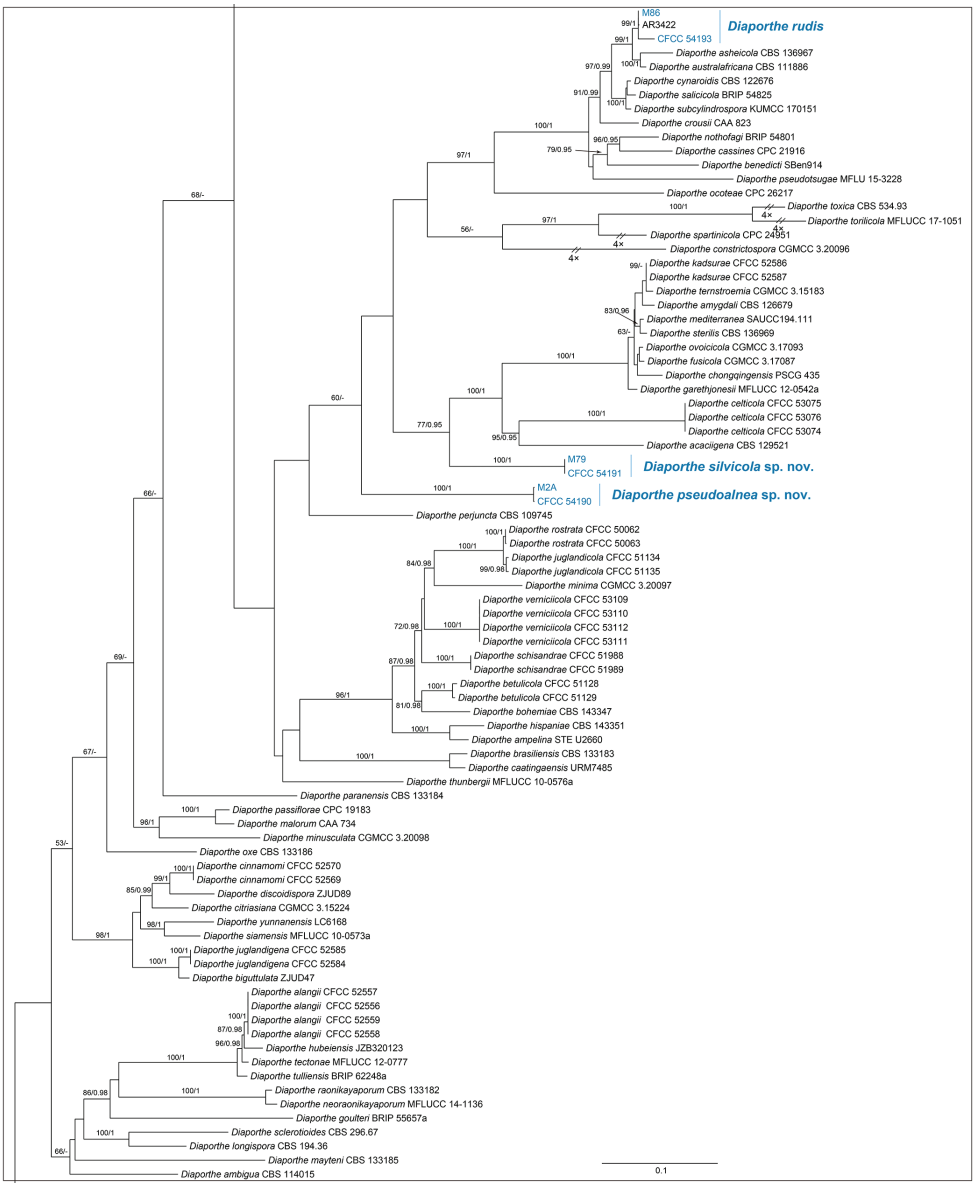

Figure 1. Continued.

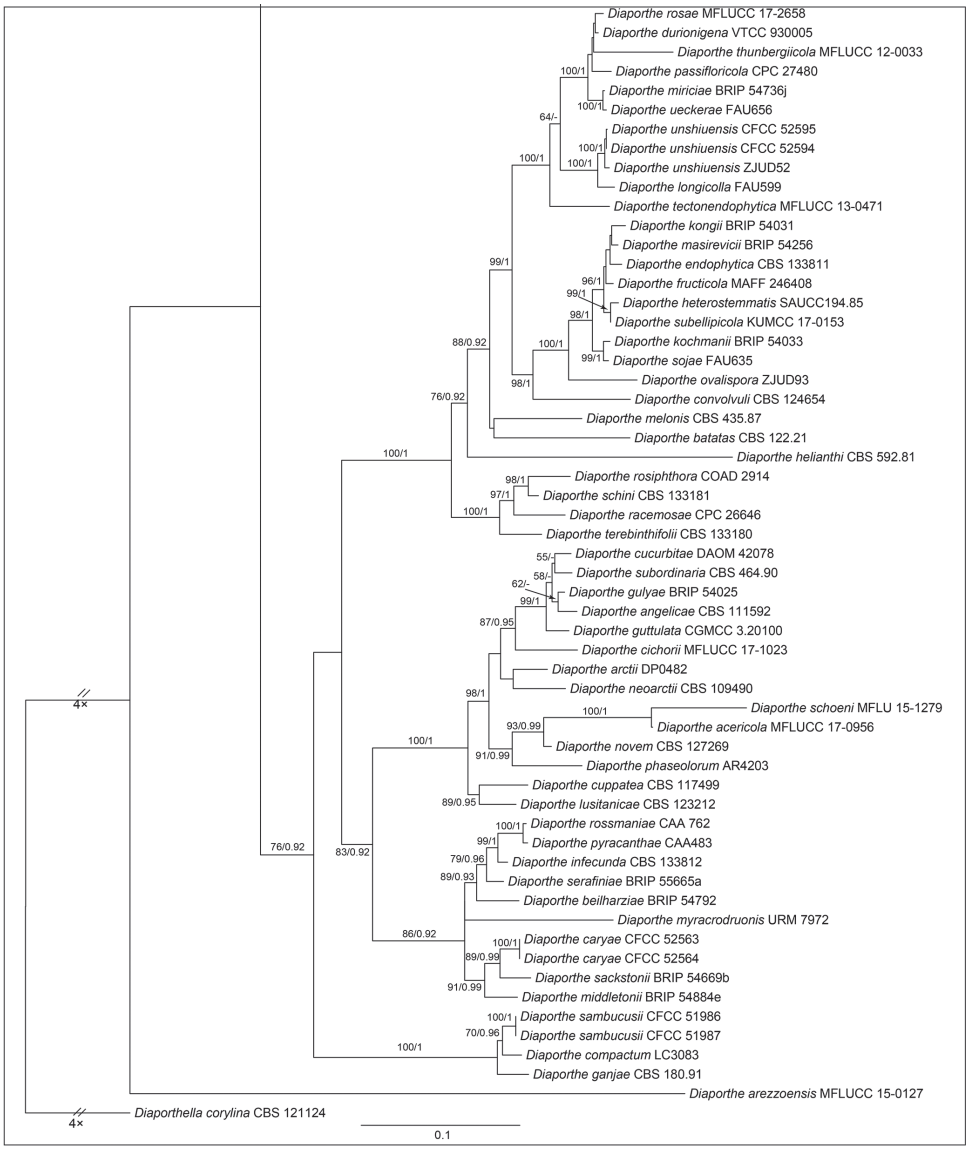

Figure 1. Continued.

Taxonomy

Diaporthe pseudoalnea **N. Jiang, sp. nov.**
MycoBank: 840714
Fig. 2

Etymology. With reference to *D. alnea*, which was described from the same host genus, *Alnus*.

Description. Conidiomata pycnidial, discoid, immersed in bark, scattered, erumpent through the bark surface, with a solitary locule. Locule 800–1250 µm diam., undivided. Conidiophores 22–68.5 × 1.5–3 µm (av. = 39.8 × 2.2 µm, n = 50), cylindrical, attenuate towards the apex, hyaline, slightly brown at base, phialidic, unbranched, straight or slightly curved. Alpha conidia (5.8–)7.1–8.9(–11.2) × (1.5–)1.8–2.2(–2.7) µm (av. = 7.9 × 2.0 µm, n = 50), L/W = 3.2–4.7 (av. = 3.8, n = 50), hyaline, aseptate, subcylindrical with a nearly rounded apex, multi-guttulate, sometimes acute at both ends. Beta conidia not observed.

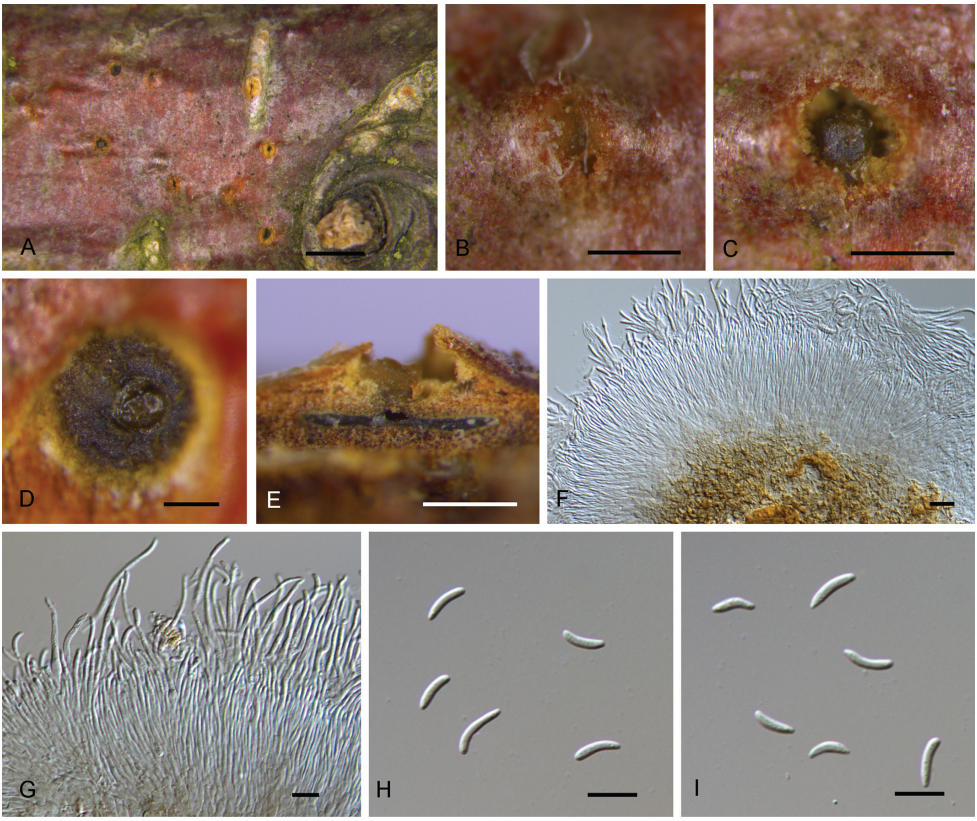

Figure 2. *Diaporthe pseudoalnea* from *Alnus glutinosa* **A–C** habit of conidiomata on branches **D** transverse section of conidiomata **E** longitudinal section through conidiomata **F, G** conidiophores and conidia **H, I** conidia. Scale bars: 2 mm (**A**), 500 µm (**B, C, E**), 200 µm (**D**), 10 µm (**F–I**).

Culture characters. Colonies are initially white with fluffy aerial mycelium, becoming dirty white after 2 weeks, and conidiomata are randomly distributed with orange conidial drops oozing out of the ostioles.

Specimens examined. NETHERLANDS. Utrecht City, on branches of *Alnus glutinosa*, 5°11'32" E, 52°05'22" N, 8 Apr. 2019, *N. Jiang* (holotype CAF800005 = JNH0001; ex-type living culture: CFCC 54190; other living culture: M2A).

Notes. *Diaporthe nivosa* and *D. alnea* were recorded from the host genus *Alnus*. Udayanga et al. (2014) investigated the lectotype of *Diaporthe nivosa* and revealed it as a *Melanconis* species based on a well-developed ectostromata and the ascospores characteristics, and Jaklitsch and Voglmayr (2020) treated it as a synonym of *Melanconis marginalis* ssp. *marginalis*. *D. alnea* has been reported from the Czech Republic, Germany, the Netherlands and the USA, and both sexual and asexual morphs have been described (Udayanga et al. 2014). However, applying the GCPSR principle, *D. alnea* has recently been considered to be a synonym of *Diaporthe eres* (Hilário et al. 2021), which has also been confirmed in our analyses where the ex-epitype isolate CBS 146.46 of *D. alnea* is placed within the *D. eres* clade (Fig. 1). *Diaporthe pseudoalnea* morphologically differs from *D. alnea* (now *D. eres*) by its longer conidiophores (22–68.5 × 1.5–3 μm in *D. pseudoalnea* vs. 9–16 × 1–2 μm in *D. alnea*; Udayanga et al. 2014). In our multi-gene analyses, *D. pseudoalnea* forms a distinct phylogenetic lineage which is placed remotely from the isolate CBS 146.46 of *D. alnea* (Fig. 1).

Diaporthe silvicola **N. Jiang, sp. nov.**

MycoBank: 840715

Fig. 3

Etymology. Name from "*silva*" = forest and "*-cola*" = inhabiting; with reference to its woody host.

Description. Conidiomata pycnidial, conical, immersed in bark, scattered, erumpent through the bark surface, with a solitary locule. Locule 450–700 μm diam., undivided. Conidiophores 6.5–25 × 1.5–4 μm (av. = 15.4 × 2.4 μm, n = 50), cylindrical, attenuate towards the apex, hyaline, slightly brown, phialidic, unbranched, slightly curved. Alpha conidia (9.2–)10.1–12.3(–13.5) × (3.8–)4.2–4.9(–5.2) μm (av. = 11.5 × 4.5 μm, n = 50), L/W = 2.0–3.2 (av. = 2.5, n = 50), hyaline, aseptate, fusiform to oval, multi-guttulate, acute at both ends. Beta conidia not observed.

Culture characters. Colonies are initially white, aerial mycelium turning grey at edges of plate, yellowish pigmentation developing in centre, conidiomata not produced until 2 weeks.

Specimens examined. NETHERLANDS. Utrecht City, on branches of *Fraxinus excelsior* in the forest ecosystem, 5°10'36" E, 52°05'32" N, 6 Jun. 2019, *N. Jiang* (holotype CAF800006 = JNH0002; ex-type living culture: CFCC 54191; other living culture: M79).

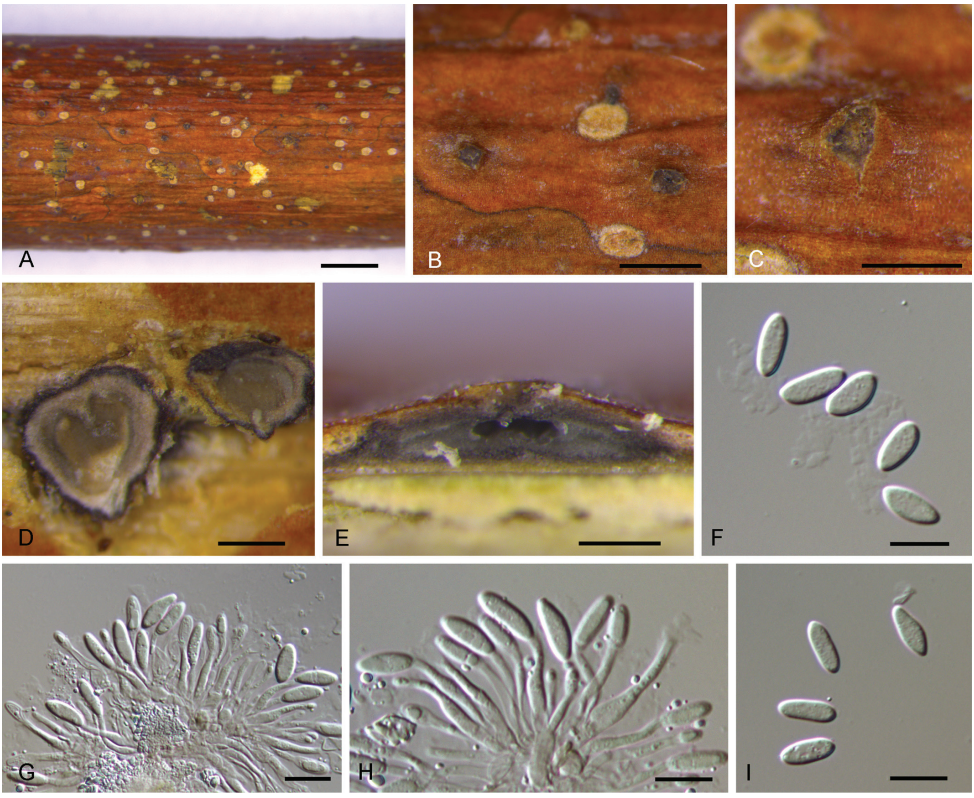

Figure 3. *Diaporthe silvicola* from *Fraxinus excelsior* **A–C** habit of conidiomata on branches **D** transverse section of conidiomata **E** longitudinal section through conidiomata **F, I** conidia **G, H** conidiophores and conidia. Scale bars: 2 mm (**A**), 1 mm (**B**), 500 µm (**C**), 200 µm (**D, E**), 10 µm (**F–I**).

Notes. *Diaporthe fraxini-angustifoliae* was reported from *Fraxinus angustifolia* subsp. *oxycarpa* cv. Claret Ash in Australia (Tan et al. 2013). *D. fraxinicola* was described from *Fraxinus chinensis* in China (Yang et al. 2018). However, *D. silvicola* from *Fraxinus excelsior* in Netherlands differs from *D. fraxini-angustifoliae* and *D. fraxinicola* by obviously larger alpha conidia (9.2–13.5 × 3.8–5.2 µm in *D. silvicola* vs. 4–10 × 2–3 µm in *D. fraxini-angustifoliae* vs. 7–10 × 2.9–3.2 µm in *D. fraxinicola*; Tan et al. 2013; Yang et al. 2018).

Discussion

In this study, branch-inhabiting *Diaporthe* species were sampled from *Alnus glutinosa*, *Fraxinus excelsior* and *Quercus robur* in Utrecht, the Netherlands. Ten *Diaporthe* isolates were obtained and identified based on five combined loci (ITS, *cal*, *his3*, *tef1* and *tub2*), as well as morphological characters from the natural substrates. The phylogenetic and morphological analyses revealed *Diaporthe pseudoalnea* sp. nov. from *Alnus*

glutinosa, *Diaporthe silvicola* sp. nov. from *Fraxinus excelsior*, and *D. foeniculacea* and *D. rudis* from *Quercus robur.*

Phylogenetic analyses were conducted based on a combined DNA sequence matrix of five loci (ITS, *cal*, *his3*, *tef1* and *tub2*) reported as useful markers to distinguish species of *Diaporthe* (Udayanga et al. 2014, 2015; Guarnaccia et al. 2017, 2018a, 2018b; Tibpromma et al. 2018; Yang et al. 2020; Dissanayake et al. 2020; Huang et al. 2021; Sun et al. 2021, Wang et al. 2021). The two novel species in this study can be distinguished from the other known species by all genes studied, but most effectively by *cal*, *his3*, *tef1* and *tub2.* The multi-locus phylogenetic analysis grouped the isolates in two new clades, which support the introduction of the new species.

The utility of host association for *Diaporthe* species identification is limited because several species have wide host ranges (e.g., *D. ere* inhabits 282 different hosts; *D. rudis* inhabits 44 different hosts), and multiple *Diaporthe* species can infect a single host (e.g., nineteen *Diaporthe* species are associated with pear cankers in China) (Guo et al. 2020; Farr and Rossman 2021). Thus, a polyphasic approach of morphological, cultural, ecological and molecular data to identify *Diaporthe* samples or to introduce new species is essential.

Acknowledgements

This research was funded by the National Microbial Resource Center of the Ministry of Science and Technology of the People's Republic of China (NMRC-2021-7).

References

Carbone I, Kohn LM (1999) A method for designing primer sets for speciation studies in filamentous ascomycetes. Mycologia 3: 553–556. https://doi.org/10.2307/3761358

Crous PW, Groenewald JZ, Risède JM, Simoneau P, Hywel-Jones NL (2004) *Calonectria* species and their *Cylindrocladium* anamorphs: species with sphaeropedunculate vesicles. Studies in Mycology 50: 415–430.

Darriba D, Taboada GL, Doallo R, Posada D (2012) jModelTest 2: more models, new heuristics and parallel computing. Nature Methods 9: 772. https://doi.org/10.1038/nmeth.2109

Diogo E, Santos JM, Phillips AJ (2010) Phylogeny, morphology and pathogenicity of *Diaporthe* and *Phomopsis* species on almond in Portugal. Fungal Diversity 44: 107–115. https://doi.org/10.1007/s13225-010-0057-x

Dissanayake AJ, Chen YY, Liu JK (2020) Unravelling *Diaporthe* species associated with woody hosts from karst formations (Guizhou) in China. Journal of Fungi 6: 251. https://doi.org/10.3390/jof6040251

Doyle JJ, Doyle JL (1990) Isolation of plant DNA from fresh tissue. Focus 12: 13–15.

Fan XL, Bezerra JDP, Tian CM, Crous PW (2018) Families and genera of diaporthalean fungi associated with canker and dieback of tree hosts. Persoonia 40: 119–134. https://doi.org/10.3767/persoonia.2018.40.05

Farr DF, Rossman AY (2021) Fungal Databases, U.S. National Fungus Collections, ARS, USDA. Retrieved August 3, 2021, from https://nt.ars-grin.gov/fungaldatabases/

Gao H, Pan M, Tian CM, Fan XL (2021) *Cytospora* and *Diaporthe* species associated with hazelnut canker and dieback in Beijing, China. Frontiers in Cellular and Infection Microbiology 11: 664366. https://doi.org/10.3389/fcimb.2021.664366

Gao YH, Liu F, Cai L (2016) Unravelling *Diaporthe* species associated with *Camellia*. Systematics and Biodiversity 14: 102–117. https://doi.org/10.1080/14772000.2015.1101027

Gao YH, Liu F, Duan W, Crous PW, Cai L (2017) *Diaporthe* is paraphyletic. IMA Fungus 8: 153–187. https://doi.org/10.5598/imafungus.2017.08.01.11

Glass NL, Donaldson GC (1995) Development of primer sets designed for use with the PCR to amplify conserved genes from filamentous ascomycetes. Applied and Environmental Microbiology 61(4): 1323–1330. https://doi.org/10.1128/AEM.61.4.1323-1330.1995

Gomes RR, Glienke C, Videira SIR, Lombard L, Groenewald JZ, Crous PW (2013) *Diaporthe*: a genus of endophytic, saprobic and plant pathogenic fungi. Persoonia 31: 1–41. https://doi.org/10.3767/003158513X666844

Guarnaccia V, Crous PW (2017) Emerging citrus diseases in Europe caused by species of *Diaporthe*. IMA Fungus 8: 317–334. https://doi.org/10.5598/imafungus.2017.08.02.07

Guarnaccia V, Crous PW (2018a) Species of *Diaporthe* on *Camellia* and *Citrus* in the Azores Islands. Phytopathologia Mediterranea 57: 307–319. https://doi.org/10.14601/Phytopathol_Mediterr-23254

Guarnaccia V, Groenewald JZ, Woodhall J, Armengol J, Cinelli T, Eichmeier A, Ezra D, Fontaine F, Gramaje D, Gutierrez-Aguirregabiria A, Kaliterna J, Kiss L, Larignon P, Luque J, Mugnai L, Naor V, Raposo R, Sándor E, Váczy KZ, Crous PW (2018b) *Diaporthe* diversity and pathogenicity revealed from a broad survey of grapevine diseases in Europe. Persoonia 40: 135–153. https://doi.org/10.3767/persoonia.2018.40.06

Guo YS, Crous PW, Bai Q, Fu M, Yang MM, Wang XH, Du YM, Hong N, Xu WX, Wang GP (2020) High diversity of *Diaporthe* species associated with pear shoot canker in China. Persoonia 45: 132–162. https://doi.org/10.3767/persoonia.2020.45.05

Hilário S, Amaral IA, Gonçalves MF, Lopes A, Santos L, Alves A (2020) *Diaporthe* species associated with twig blight and dieback of *Vaccinium corymbosum* in Portugal, with description of four new species. Mycologia 112: 293–308. https://doi.org/10.1080/00275514.2019.1698926

Hilário S, Gonçalves MF, Alves A (2021) Using genealogical concordance and coalescent-based species delimitation to asess species boundaries in the *Diaporthe eres* complex. Journal of Fungi 7: 507. https://doi.org/10.3390/jof7070507

Huang F, Udayanga D, Wang X, Hou X, Mei X, Fu Y, Hyde KD, Li HY (2015) Endophytic *Diaporthe* associated with *Citrus*: A phylogenetic reassessment with seven new species from China. Fungal Biology 119: 331–347. https://doi.org/10.1016/j.funbio.2015.02.006

Huang ST, Xia JW, Zhang XG, Sun WX (2021) Morphological and phylogenetic analyses reveal three new species of *Diaporthe* from Yunnan, China. MycoKeys 78: 49–77. https://doi.org/10.3897/mycokeys.78.60878

Jaklitsch WM, Voglmayr H (2019) European species of *Dendrostoma* (*Diaporthales*). MycoKeys 59: 1–26. https://doi.org/10.3897/mycokeys.59.37966

Jaklitsch WM, Voglmayr H (2020) The genus *Melanconis* (*Diaporthales*). MycoKeys 63: 69–117. https://doi.org/10.3897/mycokeys.63.49054

Jiang N, Fan XL, Crous PW, Tian CM (2019) Species of *Dendrostoma* (*Erythrogloeaceae*, *Diaporthales*) associated with chestnut and oak canker diseases in China. MycoKeys 48: 67–96. https://doi.org/10.3897/mycokeys.48.31715

Jiang N, Fan XL, Tian CM, Crous PW (2020) Reevaluating *Cryphonectriaceae* and allied families in *Diaporthales*. Mycologia 112: 267–292. https://doi.org/10.1080/00275514.2019.1698925

Jiang N, Fan XL, Tian CM (2021) Identification and characterization of leaf-inhabiting fungi from *Castanea* plantations in China. Journal of Fungi 7: 64. https://doi.org/10.3390/jof7010064

Katoh K, Toh H (2010) Parallelization of the MAFFT multiple sequence alignment program. Bioinformatics 26: 1899–1900. https://doi.org/10.1093/bioinformatics/btq224

Lombard L, Van Leeuwen GCM, Guarnaccia V, Polizzi G, Van Rijswick PC, Karin Rosendahl KC, Gabler J, Crous PW (2014) *Diaporthe* species associated with *Vaccinium*, with specific reference to Europe. Phytopathologia Mediterranea 53: 287–299. https://doi.org/10.14601/Phytopathol_Mediterr-14034

Long H, Zhang Q, Hao YY, Shao XQ, Wei XX, Hyde KD, Wang Y, Zhao DG (2019) *Diaporthe* species in south-western China. MycoKeys 57: 113–127. https://doi.org/10.3897/mycokeys.57.35448

Manawasinghe IS, Dissanayake AJ, Li X, Liu M, Wanasinghe DN, Xu J, Zhao W, Zhang W, Zhou Y, Hyde KD, Brooks S, Yan J. (2019) High genetic diversity and species complexity of *Diaporthe* associated with grapevine dieback in China. Frontiers in Microbiology. 10: 1936. https://doi.org/ 10.3389/fmicb.2019.01936

O'Donnell K, Cigelnik E (1997) Two divergent intragenomic rDNA ITS2 types within a monophyletic lineage of the fungus *Fusarium* are nonorthologous. Molecular Phylogenetics and Evolution 7: 103–116. https://doi.org/10.1006/mpev.1996.0376

Rehner SA, Uecker FA (1994) Nuclear ribosomal internal transcribed spacer phylogeny and host diversity in the coelomycete *Phomopsis*. Canadian Journal of Botany 72: 1666–1674. https://doi.org/10.1139/b94-204

Ronquist F, Huelsenbeck JP (2003) MrBayes 3: Bayesian phylogenetic inference under mixed models. Bioinformatics 19: 1572–1574. https://doi.org/10.1093/bioinformatics/btg180

Rossman AY, Adams GC, Cannon PF, Castlebury LA, Crous PW, Gryzenhout M, Jaklitsch WM, Mejia LC, Stoykov D, Udayanga D (2015) Recommendations of generic names in *Diaporthales* competing for protection or use. IMA Fungus 6(1): 145–154. https://doi.org/10.5598/imafungus.2015.06.01.09

Santos JM, Phillips AJL (2009) Resolving the complex of *Diaporthe* (*Phomopsis*) species occurring on *Foeniculum vulgare* in Portugal. Fungal Diversity 34: 111–125.

Senanayake IC, Crous PW, Groenewald JZ, Maharachchikumbura SSN, Jeewon R, Phillips AJL, Bhat DJ, Perera RH, Li QR, Li WJ (2017) Families of *Diaporthales* based on morphological and phylogenetic evidence. Studies in Mycology 86: 217–296. https://doi.org/10.1016/j.simyco.2017.07.003

Stamatakis A (2014) RAxML version 8: a tool for phylogenetic analysis and post-analysis of large phylogenies. Bioinformatics 30: 1312–1313. https://doi.org/10.1093/bioinformatics/btu033

Sun W, Huang S, Xia J, Zhang X, Li Z (2021) Morphological and molecular identification of *Diaporthe* species in south-western China, with description of eight new species. MycoKeys 77: 65–95. https://doi.org/10.3897/mycokeys.77.59852

Tan YP, Edwards J, Grice KRE, Shivas RG (2013) Molecular phylogenetic analysis reveals six new species of *Diaporthe* from Australia. Fungal Diversity 61: 251–260. https://doi.org/10.1007/s13225-013-0242-9

Tibpromma S, Hyde KD, Bhat JD, Mortimer PE, Xu J, Promputtha I, Doilom M, Yang JB, Tang AMC, Karunarathna SC (2018) Identification of endophytic fungi from leaves of *Pandanaceae* based on their morphotypes and DNA sequence data from southern Thailand. MycoKeys 33: 25–67. https://doi.org/10.3897/mycokeys.33.23670

Udayanga D, Castlebury LA, Rossman AY, Chukeatirote E, Hyde KD (2015) The Diaporthe sojae species complex: Phylogenetic re-assessment of pathogens associated with soybean, cucurbits and other field crops. Fungal Biology 119: 383–407. https://doi.org/10.1016/j.funbio.2014.10.009

Udayanga D, Castlebury LA, Rossman AY, Hyde KD (2014) Species limits in *Diaporthe*: molecular re-assessment of *D. citri*, *D. cytosporella*, *D. foeniculina* and *D. rudis*. Persoonia 32: 83–101. https://doi.org/10.3767/003158514X679984

Udayanga D, Liu X, McKenzie EH, Chukeatirote E, Bahkali AH, Hyde KD (2011) The genus *Phomopsis*: biology, applications, species concepts and names of common phytopathogens. Fungal Diversity 50: 189–225. https://doi.org/10.1007/s13225-011-0126-9

Voglmayr H, Castlebury LA, Jaklitsch WM (2017) *Juglanconis* gen. nov. on *Juglandaceae*, and the new family *Juglanconidaceae* (*Diaporthales*). Persoonia 38: 136–155. https://doi.org/10.3767/003158517X694768

Voglmayr H, Rossman AY, Castlebury LA, Jaklitsch WM (2012) Multigene phylogeny and taxonomy of the genus *Melanconiella* (*Diaporthales*). Fungal Diversity 57: 1–44. https://doi.org/10.1007/s13225-012-0175-8

Wang X, Guo Y, Du Y, Yang Z, Huang X, Hong N, Wang, G (2021) Characterization of *Diaporthe* species associated with peach constriction canker, with two novel species from China. MycoKeys 80: 77–90. https://doi.org/10.3897/mycokeys.80.63816

White TJ, Bruns T, Lee S, Taylor J (1990) Amplification and direct sequencing of fungal ribosomal RNA genes for phylogenetics. PCR Protocols: A Guide to Methods and Applications 18: 315–322. https://doi.org/10.1016/B978-0-12-372180-8.50042-1

Yang Q, Fan XL, Guarnaccia V, Tian CM (2018) High diversity of *Diaporthe* species associated with dieback diseases in China, with twelve new species described. MycoKeys 39: 97–149. https://doi.org/10.3897/mycokeys.39.26914

Yang Q, Jiang N, Tian CM (2020) Three new *Diaporthe* species from Shaanxi Province, China. MycoKeys 67: 1–18. https://doi.org/ 10.3897/mycokeys.67.49483

Yang Q, Jiang N, Tian CM (2021) New species and records of *Diaporthe* from Jiangxi Province, China. MycoKeys 77: 41–64. https://doi.org/ 10.3897/mycokeys.77.59999

Zapata M, Palma MA, Aninat MJ, Piontelli E (2020) Polyphasic studies of new species of *Diaporthe* from native forest in Chile, with descriptions of *Diaporthe araucanorum* sp. nov., *Diaporthe foikelawen* sp. nov. and *Diaporthe patagonica* sp. nov. International Journal of Systematic and Evolutionary Microbiology 70(5): 3379–3390. https://doi.org/10.1099/ijsem.0.004183

MycoKeys 85: 57–71 (2021)
doi: 10.3897/mycokeys.85.75944
https://mycokeys.pensoft.net

RESEARCH ARTICLE

A peer-reviewed open-access journal
MycoKeys
Launched to accelerate biodiversity research

Morphological and molecular phylogenetic analyses reveal three species of *Colletotrichum* in Shandong province, China

Taichang Mu[1], Zhaoxue Zhang[1], Rongyu Liu[1], Shubin Liu[1], Zhuang Li[1], Xiuguo Zhang[1], Jiwen Xia[1]

1 *Shandong Provincial Key Laboratory for Biology of Vegetable Diseases and Insect Pests, College of Plant Protection, Shandong Agricultural University, Taian, 271018, China*

Corresponding author: Jiwen Xia (zhenjunxue@126.com)

Academic editor: Ajay Kumar Gautam | Received 29 September 2021 | Accepted 20 November 2021 | Published 8 December 2021

Citation: Mu T, Zhang Z, Liu R, Liu S, Li Z, Zhang X, Xia J (2021) Morphological and molecular phylogenetic analyses reveal three species of *Colletotrichum* in Shandong province, China. MycoKeys 85: 57–71. https://doi.org/10.3897/mycokeys.85.75944

Abstract

Colletotrichum has numerous host range and distribution. Its species are important plant pathogens, endophytes and saprobes. *Colletotrichum* can cause regular or irregular depressions and necrotic lesions in the epidermal tissues of plants. During this research *Colletotrichum* specimens were collected from Mengyin County, Shandong Province, China. A multi-locus phylogenetic analysis of ITS, GAPDH, CHS-1, ACT, TUB2, CAL and GS sequence data combined with morphology, revealed a new species and two known species, viz. *C. mengyinense* sp. nov., *C. gloeosporioides* and *C. pandanicola*, belonging to the *C. gloeosporioides* species complex. The new species is described and illustrated in this paper and compared with taxa in the *C. gloeosporioides* species complex.

Keywords

Colletotrichum, Glomerellaceae, multi-gene phylogeny, new species, taxonomy

Introduction

Colletotrichum species (Glomerellaceae, Glomerellales) is one of the ten economically most important fungal plant pathogens worldwide (Dean et al. 2012). It was first observed by Tode (1790), who divided it into *Vermicularia*. Corda (1831) established *Colletotrichum* based on the characteristic of the conidiomata with setae in *Vermicularia*.

Colletotrichum is based on the type species *Colletotrichum lineola* which was associated with a member of the *Apiaceae* (Jayawardena et al. 2017). The sexual morph belongs to *Glomerella*. The asexual morph is characterized by acervuli born in the skin of the host, often producing brown sharp setae, colorless or brown conidiophores with separate, conidia colorless, pseudomonas, cylindrical or crescent-shaped (Damm et al. 2009).

Currently, more than 900 epithets of *Colletotrichum* are listed in Index Fungorum (http://www.indexfungorum.org/; accessed 22 November 2021). *Colletotrichum* has been studied for more than 200 years and the classification of *Colletotrichum* has undergone major changes (Jayawardena et al. 2016). In order to clarify its complex nature, the species are classified into 14 species complexes (Bhunjun et al. 2021). Specifically, *C. gloeosporioides* has been considered as a complex species for a long time.

The name *C. gloeosporioides* was first proposed by Penzig based on *Vermicularia gloeosporioides* which was collected from *Citrus* in Italy (Weir et al. 2012). Early in the study of *C. gloeosporioides* species complex, taxonomic concepts used were based on apparent features such as morphological characters, host species, size and shape of conidia and appressoria, presence or absence of setae, aspect, color and growth rate in culture, whether or not the teleomorph develops, etc (Weir et al. 2012). Nonetheless, Sutton commented that "no progress in the systematics and identification of isolates belonging to this complex is likely to be made based on morphology alone". Fortunately, with the development of molecular systematics, gene method is applied to taxonomy of *Colletotrichum* complexes. Multi-gene phylogeny analysis is of great significance to the study of the classification of *C. gloeosporioides* species complex and related concepts of species (Cannon et al. 2012; Damm et al. 2012; Weir et al. 2012).

The aim of this study was to explore the diversity of *Colletotrichum* species from symptomatic leaves and diseased fruit of plants in Shandong Province, China. We present a new species and two known species, *C. mengyinense* sp. nov., *C. gloeosporioides* and *C. pandanicola* based on phylogenetic data and morphology.

Materials and methods

Isolation and morphological studies

The samples were collected from Mengyin County, Shandong Province, China. The strains of *Colletotrichum* were isolated from symptomatic leaves of *Rosa chinensis* and diseased fruit of *Juglans regia* using single spore and tissue isolation methods (Chomnunti et al. 2014). The spore suspension was obtained and spread onto PDA plate and incubated for one day under the biochemical incubator. After germination, the spores were transferred to a new PDA plate to obtain pure culture. Additionally, the surface sterilized plant tissue isolation was used to obtain sterile isolates from the host plant. About 25 mm^2 tissue fragments were taken from the margin of tissue lesions and

surface sterilized by consecutively immersing in 75% ethanol solution for 60 s, 5% sodium hypochlorite solution for 30 s, and then rinsed in sterile distilled water for 60 s (Gao et al. 2013; Liu et al. 2015). The surface sterilized plant tissue was dried with sterilized paper and moved on the PDA plate (Cai et al. 2009). All the PDA plates were incubated at biochemical incubator at 25 °C for 3–4 days, then hyphae were picked out of the periphery of the colonies and inoculated on to new PDA plates.

Following 5–14 days of incubation, morphological characters were recorded (Cai et al. 2009). Photographs of the colonies were taken at 7 days and 14 days using a digital camera (Canon G7X). Micromorphological characters of colonies were observed using stereomicroscope (Olympus SZX10) and microscope (Olympus BX53), both fitted with high definition color digital cameras to photo document conidia and so on of fungal structures. All *Colletotrichum* strains were stored in 10% sterilized glycerin and sterile water at 4 °C for deep studies in the future. Every specimen was deposited in the Herbarium of the Department of Plant Pathology, Shandong Agricultural University (HSAUP). Living cultures were deposited in the Shandong Agricultural University Culture Collection (SAUCC). Taxonomic information of the new taxa was submitted to MycoBank (http://www.mycobank.org).

DNA extraction and amplification

Genomic DNA was extracted from *Colletotrichum* fungal mycelia grown on PDA after 5–7 days, using a modified cetyltrimethylammonium bromide (CTAB) buffer, and then it was incubated at 65 °C for 30 min with occasional gentle inverting (Guo et al. 2000). Gene sequences were obtained from seven genes loci including the internal transcribed spacer regions with intervening 5.8S nrRNA gene (ITS), partial glyceraldehyde-3-phosphate dehydrogenase gene (GAPDH), partial chitin synthase 1 gene (CHS-1), partial actin gene (ACT), partial beta-tubulin gene (TUB2), partial calmodulin gene (CAL) and partial glutamine synthetase gene (GS) were amplified and sequenced using primers pairs (Table 1).

PCR was performed using an Eppendorf Master Thermocycler (Hamburg, Germany). Amplification reactions were performed in a 25 μL reaction volume which contained 12.5 μL 2× Taq Plus Master Mix II (Vazyme, Nanjing, China), 1 μL of each forward and reverse primer (10 μM) (Tsingke, Qingdao, China), and 1 μL template genomic DNA in amplifier, and were adjusted with distilled deionized water to a total volume of 25 μL. PCR parameters were as follows: 94 °C for 5 min, followed by 35 cycles of denaturation at 94 °C for 30 s, annealing at a suitable temperature for 30 s, extension at 72 °C for 1 min and a final elongation step at 72 °C for 10 min. The annealing temperature for each gene was 52 °C for ITS and GS, 59 °C for CAL, 60 °C for GAPDH, 58 °C for ACT and CHS-1, 55 °C for TUB2. The PCR products were visualized on 1% agarose electrophoresis gel. Sequencing was conducted by the Tsingke Company Limited (Qingdao, China) bi-directionally. Consensus sequences were obtained using MEGA 7.0 (Kumar et al. 2016). All sequences generated in this study were deposited in GenBank (Table 2).

Table 1. Gene regions and respective primer pairs used in the study.

Locus	Gene	Primer	Direction	Sequence (5'-3')
The internal transcribed spacer regions with intervening 5.8S nrRNA gene	ITS	ITS5	Forward	GGA AGT AAA AGT CGT AAC AAG G
		ITS4	Reverse	TCC TCC GCT TAT TGA TAT GC
Partial glyceraldehyde-3-phosphate dehydrogenase gene	GAPDH	GDF1	Forward	GCC GTC AAC GAC CCC TTC ATT GA
		GDR1	Reverse	GGG TGG AGT CGT ACT TGA GCA TGT
Partial chitin synthase 1 gene	CHS-1	CHS-79F	Forward	TGG GGC AAG GAT GCT TGG AAG AAG
		CHS-354R	Reverse	TGG AAG AAC CAT CTG TGA GAG TTG
Partial actin gene	ACT	ACT-512F	Forward	ATG TGC AAG GCC GGT TTC GC
		ACT-783R	Reverse	TAC GAG TCC TTC TGG CCC AT
Partial beta-tubulin gene	TUB2	Bt-2a	Forward	GGT AAC CAA ATC GGT GCT GCT TTC
		Bt-2b	Reverse	ACC CTC AGT GTA GTG ACC CTT GGC
Partial calmodulin gene	CAL	CL1	Forward	GAR TWC AAG GAG GCC TTC TC
		CL2A	Reverse	TTT TTG CAT CAT GAG TTG GAC
		CL1C	Forward	GAA TTC AAG GAG GCC TTC TC
		CL2C	Reverse	CTT CTG CAT CAT GAG CTG GAC
Partial glutamine synthetase gene	GS	GSLF3	Forward	GAT ACG CCT CTT CCA GCG TT
		GSLR1	Reverse	AGR CGC ACA TTG TCA GTA TCG

Phylogenetic analyses

Novel sequences were generated from the nine strains in this study, and all reference available sequences of *Colletotrichum* species were downloaded from GenBank. Multiple sequence alignments for ITS, GAPDH, CHS-1, ACT, TUB2, CAL and GS were constructed and carried out using the MAFFT v.7.11 online programme (http://mafft.cbrc.jp/alignment/server/, Katoh et al. 2019) with the default settings, and manually corrected where necessary. To establish the identity of the isolates at species level, phylogenetic analyses were conducted individually for each locus and then as combined analyses of seven loci (ITS, GAPDH, CHS-1, ACT, TUB2, CAL and GS). Phylogenetic analyses were based on maximum likelihood (ML) and Bayesian.

Inference (BI) for the multi-locus analyses. For BI, the best evolutionary model for each partition was determined using MrModeltest v. 2.3 (Nylander 2004) and incorporated into the analyses. ML and BI were run on the CIPRES Science Gateway portal (https://www.phylo.org/) using RaxML-HPC2 on XSEDE (8.2.12) (Miller et al. 2012; Stamatakis 2014) and MrBayes on XSEDE (3.2.7a), respectively (Huelsenbeck and Ronquist 2001; Ronquist and Huelsenbeck 2003; Ronquist et al. 2012). For ML analyses the default parameters were used and BI was carried out using the rapid bootstrapping algorithm with the automatic halt option. Bayesian analyses included seven parallel runs of 5,000,000 generations, with the stop rule option and a sampling frequency of 1000 generations. The burn-in fraction was set to 0.25 and posterior probabilities (PP) were determined from the remaining trees. The resulting trees were plotted using FigTree v. 1.4.4 (http://tree.bio.ed.ac.uk/software/figtree) and edited with Adobe Illustrator CS6.0. New sequences generated in this study were deposited at GenBank (https://www.ncbi.nlm.nih.gov; Table 2).

Table 2. Species and GenBank accession numbers of DNA sequences used in this study with new sequences in bold.

Species	Strain/Isolate	Host/Substrate	GenBank accession number						
			ITS	GAPDH	CHS-1	ACT	TUB2	CAL	GS
Colletotrichum aenigma	ICMP 18608*	*Persea americana*	JX010244	JX010044	JX009774	JX009443	JX010389	JX009683	JX010078
C. aeschynomenes	ICMP 17673*=ATCC 201874	*Aeschynomene virginica*	JX010176	JX009930	JX009799	JX009483	JX010392	JX009721	JX010081
C. alatae	CBS 304.67*=ICMP 17919	*Dioscorea alata*	JX010190	JX009990	JX009837	JX009471	JX010383	JX009738	JX010065
C. alienum	ICMP 12071*	*Malus domestica*	JX010251	JX010028	JX009882	JX009572	JX010411	JX009654	JX010101
C. aotearoa	ICMP 18735	*Hedychium gardnerianum*	JX010221	JX010023	JX009880	JX009500	JX010424	JX009620	JX010115
C. arecicola	hb8	*Areca catechu*	MW561344	MW557464	-	-	MW557482	-	-
C. artocarpicola	MFLUCC18-1167*	*Artocarpus heterophyllus*	MN415991	MN435568	MN435569	MN435570	MN435567	-	-
C. asianum	ICMP 18580*=CBS 130418	*Coffea arabica*	FJ972612	JX010053	JX009867	JX009584	JX010406	FJ917506	JX010096
C. australianum	BRIP 63695	*Capsicum annuum*	KU923677	MN442115	MW092000	MN442105	KU923693	-	KU923737
C. boninense (outgroup)	CBS 123755*	*Crinum asiaticum* var. *sinicum*	JQ005153	JQ005240	JQ005327	JQ005501	JQ005588	-	-
C. camelliae	ICMP 10643	*Camellia* × *williamsi*	JX010224	JX009908	JX009891	JX009540	JX010436	JX009630	JX010119
C. changpingense	MFLUCC 15-0022*	*Fragaria* × *ananassa*	KP683152	KP852469	KP852449	KP683093	KP852490	-	-
C. chiangmaiense	MFLUCC 18-0945	*Magnolia garrettii*	MW346499	MW548592	MW623653	MW655578	-	-	-
C. chrysophilum	CMM4268*	*Musa* sp.	KX094252	KX094183	KX094083	KX093982	KX094285	KX094063	KX094204
C. ciggaro	ICMP 19122	*Vaccinium* sp.	JX010228	JX009950	JX009902	JX009536	JX010433	JX009744	JX010134
C. clidemiae	ICMP 18658*	*Clidemia hirta*	JX010265	JX009989	JX009877	JX009537	JX010438	JX009645	JX010129
C. cobbittiense	BRIP66219	*Cordyline stricta* × *Cordyline australis*	MH087016	MH094133	MH094135	MH094134	MH094137	-	-
C. conoides	CAUG17*	*Capsicum annuum*	KP890168	KP890162	KP890156	KP890144	KP890174	-	-
C. cordylinicola	MFLUCC090551*=ICMP 18579	*Cordyline fruticosa*	JX010226	JX009975	JX009864	HM470235	JX010440	HM470238	JX010122
C. dracaenigenum	MFLUCC 19-0430*	*Dracaena fragrans*	MN921250	MT215577	MT215575	MT313686	-	-	-
C. endophytica	CAUG28	*Capsicum annuum*	KP145441	KP145413	KP145385	KP145329	KP145469	-	-
C. fici-septicae	MFLU 19-27708*	*Ficus septica*	MW114367	MW183774	MW177701	MW151585	-	-	-
C. fructicola	MFLU 090228*	*Coffea arabica*	FJ972603	FJ972578	-	FJ907426	FJ907441	FJ917508	FJ972593
C. fructivorum	CBS 133125*	*Vaccinium macrocarpon*	JX145145	-	-	-	JX145196	-	-
C. gloeosporioides	IMI356878*=ICMP 17821	*Citrus sinensis*	JX010152	JX010056	JX009818	JX009531	JX010445	JX009731	JX010085
	ICMP 19121	*Citrus limon*	JX010148	JX010054	JX009903	JX009558	-	JX009745	-
	SAUCC200952	***Juglans regia***	**MW786743**	**MW876474**	**MW883689**	**MW883698**	**MW888973**	**MW922541**	**MW888964**
	SAUCC200954	***Juglans regia***	**MW786744**	**MW876475**	**MW883690**	**MW883699**	**MW888974**	**MW922542**	**MW888965**
	SAUCC201001	***Juglans regia***	**MW786745**	**MW876477**	**MW883692**	**MW883701**	**MW888976**	**MW922544**	**MW888967**
C. grevilleae	CBS 132879*	*Grevillea* sp.	KC297078	KC297010	KC296987	KC296941	KC297102	KC296963	-
C. grossum	CAUG7*	*Capsicum* sp.	KP890165	KP890159	KP890153	KP890141	KP890171	KP890147	-
C. hebeiense	MFLUCC130-726*	*Vitis vinifera*	KF156863	KF377495	KF289008	KF377532	KF288975	-	-
C. hedericola	MFLU 15-0689	*Hedera helix*	MN631384	-	MN635794	MN635795	-	-	-
C. helleniense	CBS 142418*	*Poncirus trifoliata*	KY856446	KY856270	KY856186	KY856019	KY856528	-	-
C. henanense	LF238*	*Camellia sinensis*	KJ955109	KJ954810	-	KM023257	KJ955257	KJ954662	KJ954960

Species	Strain/Isolate	Host/Substrate	GenBank accession number						
			ITS	GAPDH	CHS-1	ACT	TUB2	CAL	GS
C. horii	ICMP 10492	*Diospyros kaki*	GQ329690	GQ329681	JX009752	JX009438	JX010450	JX009604	JX010137
C. hystricis	CPC 28153*	*Citrus hystrix*	KY856450	KY856274	KY856190	KY856023	KY856532	-	-
C. jiangxiense	LF687*	*Camellia sinensis*	KJ955201	KJ954902	-	KJ954471	KJ955348	KJ954752	KJ955051
C. kahawae	IMI 319418*=ICMP 17816	*Coffea arabica*	JX010231	JX010012	JX009813	JX009452	JX010444	-	JX010130
C. ledongense	CGMCC3.18888*	*Quercus palustris*	MG242008	MG242016	MG242018	MG242014	MG242010	-	-
C. makassarense	CBS 143664a*=CPC 28612	*Capsicum annuum*	MH728812	MH728820	MH805850	MH781480	MH846563	-	-
C. mengyinense	**SAUCC200702***	***Rosa chinensis***	**MW786742**	**MW846240**	**MW883686**	**MW883695**	**MW888970**	**MW922538**	**MW888961**
	SAUCC200912	***Juglans regia***	**MW786689**	**MW876472**	**MW883687**	**MW883696**	**MW888971**	**MW922539**	**MW888962**
	SAUCC200913	***Juglans regia***	**MW786690**	**MW876473**	**MW883688**	**MW883697**	**MW888972**	**MW922540**	**MW888963**
	SAUCC200983	***Juglans regia***	**MW786642**	**MW876476**	**MW883691**	**MW883700**	**MW888975**	**MW922543**	**MW888966**
C. musae	CBS 116870*=ICMP 19119	*Musa* sp.	JX010146	JX010050	JX009896	JX009433	HQ596280	JX009742	JX010103
C. nupharicola	CBS 470.96*=ICMP 18187	*Nuphar lutea* subsp. *polysepala*	JX010187	JX009972	JX009835	JX009437	JX010398	JX009663	JX010088
C. pandanicola	MFLU 18-0003*	*Pandanus* sp.	MG646967	MG646934	MG646931	MG646938	MG646926	-	-
	SAUCC200204	***Juglans regia***	**MW786641**	**MW846239**	**MW883685**	**MW883694**	**MW888969**	**MW922537**	**MW888960**
	SAUCC201152	***Juglans regia***	**MW786746**	**MW876478**	**MW883693**	**MW883702**	**MW888977**	**MW922545**	**MW888968**
C. perseae	GA100*	*Persea americana*	KX620308	KX620242	-	KX620145	KX620341	KX620206	KX620275
C. proteae	CBS 132882*	*Protea* sp.	KC297079	KC297009	KC296986	KC296940	KC297101	KC296960	-
C. pseudotheobromicola	MFLUCC 18-1602	*Prunus avium*	MH817395	MH853675	MH853678	MH853681	MH853684	-	-
C. psidii	ICMP 19120	*Psidium* sp.	JX010219	JX009967	JX009901	JX009515	JX010443	JX009743	JX010133
C. queenslandicum	ICMP 1778*	*Carica papaya*	JX010276	JX009934	JX009899	JX009447	JX010414	JX009691	JX010104
C. rhexiae	CBS 133134*	*Rhexia virginica*	JX145128	-	-	-	JX145179	-	-
C. salsolae	ICMP 19051*	*Salsola tragus*	JX010242	JX009916	JX009863	JX009562	JX010403	-	-
C. siamense	ICMP 18578*	*Coffea arabica*	JX010171	JX009924	JX009865	FJ907423	JX010404	FJ917505	JX010094
	ICMP 19118	*Jasminum sambac*	HM131511	HM131497	JX009895	HM131507	JX010415	-	JX010105
C. syzygicola	MFLUCC10-0624*	*Syzygium samarangense*	KF242094	KF242156	-	KF157801	KF254880	KF254859	-
C. tainanense	CBS 143666*	*Capsicum annuum*	MH728818	MH728823	MH805845	MH781475	MH846558	-	-
C. temperatum	Coll883*	*Vaccinium macrocarpon*	JX145159	-	-	-	JX145211	-	-
C. theobromicola	ICMP 18649	*Theobroma cacao*	JX010294	JX010006	JX009869	JX009444	JX010447	JX009591	JX010139
C. ti	ICMP 4832*	*Cordyline* sp.	JX010269	JX009952	JX009898	JX009520	JX010442	JX009649	JX010123
C. tropicale	CBS 124949*=ICMP 18653	*Theobroma cacao*	JX010264	JX010007	JX009870	JX009489	JX010407	JX009719	JX010097
C. viniferum	GZAAS5.08601*	*Vitis vinifera*	JN412804	JN412798	-	JN412795	JN412813	-	-
C. wuxiense	CGMCC 3.17894*	*Camellia sinensis*	KU251591	KU252045	KU251939	KU251672	KU252200	-	KU252101
C. xanthorrhoeae	BRIP 45094*=ICMP 17903 = CBS 127831	*Xanthorrhoea preissii*	JX010261	JX009927	JX009823	JX009478	JX010448	JX009653	JX010138
C. yulongense	CFCC 50818*	*Vaccinium dunalianum*	MH751507	MK108986	MH793605	MH777394	MK108987	MH793604	MK108988
Colletotrichum sp.	BRIP 58074a	*Citrus australasica*	MK469999	MK470017	MW091975	MK470089	MK470053	-	MK470035

Strains marked with "*" are ex-type or ex-epitype.

Results

Phylogenetic analyses

Nine strains of *Colletotrichum* isolated from leaves of *Rosa chinensis* and fruit of *Juglans regia* in Mengyin County, Shandong Province, China, were grown in culture. Among the nine *Colletotrichum* isolates were identified a new species and two known species based on an analysis of combined ITS, GAPDH, CHS-1, ACT, TUB2, CAL and GS gene sequences composed of 69 isolates of *C. gloeosporioides* species complex and *C. boninense* (CBS 123755) as the outgroup taxon.

A total of 3953 characters including gaps were obtained in the phylogenetic analysis, viz. ITS: 1–619, GAPDH: 620–929, CHS-1: 930–1229, ACT: 1230–1542, TUB2: 1543–2288, CAL: 2289–3028, GS: 3029–3953. Of these characters, 2667 were constant, 674 were variable and parsimony-uninformative, and 612 were parsimony-informative.

The Bayesian analysis lasted 4,685,000 generations, resulting in 4686 total trees, of which 3515 trees were used to calculate the posterior probabilities. The BI posterior probabilities were plotted on the ML tree. For the BI and ML analyses, HKY+G for GAPDH and ACT, SYM+I+G for ITS, K80+I+G for CHS-1, GTR+G for GS and CAL, HKY+I for TUB2 were selected and incorporated into the analyses. The ML tree topology confirmed the tree topologies obtained from the BI analyses, and therefore, the ML tree is presented (Fig. 1).

ML bootstrap support values (≥ 50%) and Bayesian posterior probability (≥ 0.90) are shown as first and second position above nodes, respectively. The 70 strains were assigned to 60 species clades based on the seven gene loci phylogeny (Fig. 1). The nine strains studied here represented a novel species and two known species. The new species of *C. mengyinense* showed a close relationship to *C. fructicola* (MFLU 090228) with full support (ML-BS: 100% and BYPP: 1). The strains SAUCC200952, SAUCC200954 and SAUCC201001 belong to *C. gloeosporioides* (IMI356878) with full support (ML-BS: 100% and BYPP: 1) by the multi-locus phylogeny. The strains SAUCC200204 and SAUCC201152 belong to *C. pandanicola* (MFLU 18-0003) with good support (ML-BS: 94% and BYPP: 0.99) by the multi-locus phylogeny.

Taxonomy

Colletotrichum gloeosporioides **(Penz.) Penz. & Sacc., Atti Reale Ist. Veneto Sci. Lett. Arti., ser. 6, 2: 670. 1884**
Figure 2

Vermicudaria gloeosporioides Penz., Michelia 2: 450, 1882. Basionym.

Description. Lesion fruit, round or irregular, dark brown slightly sunken center, brown at margin. Asexual morph developed on PDA. A mass of orange conidia grows in the white my-

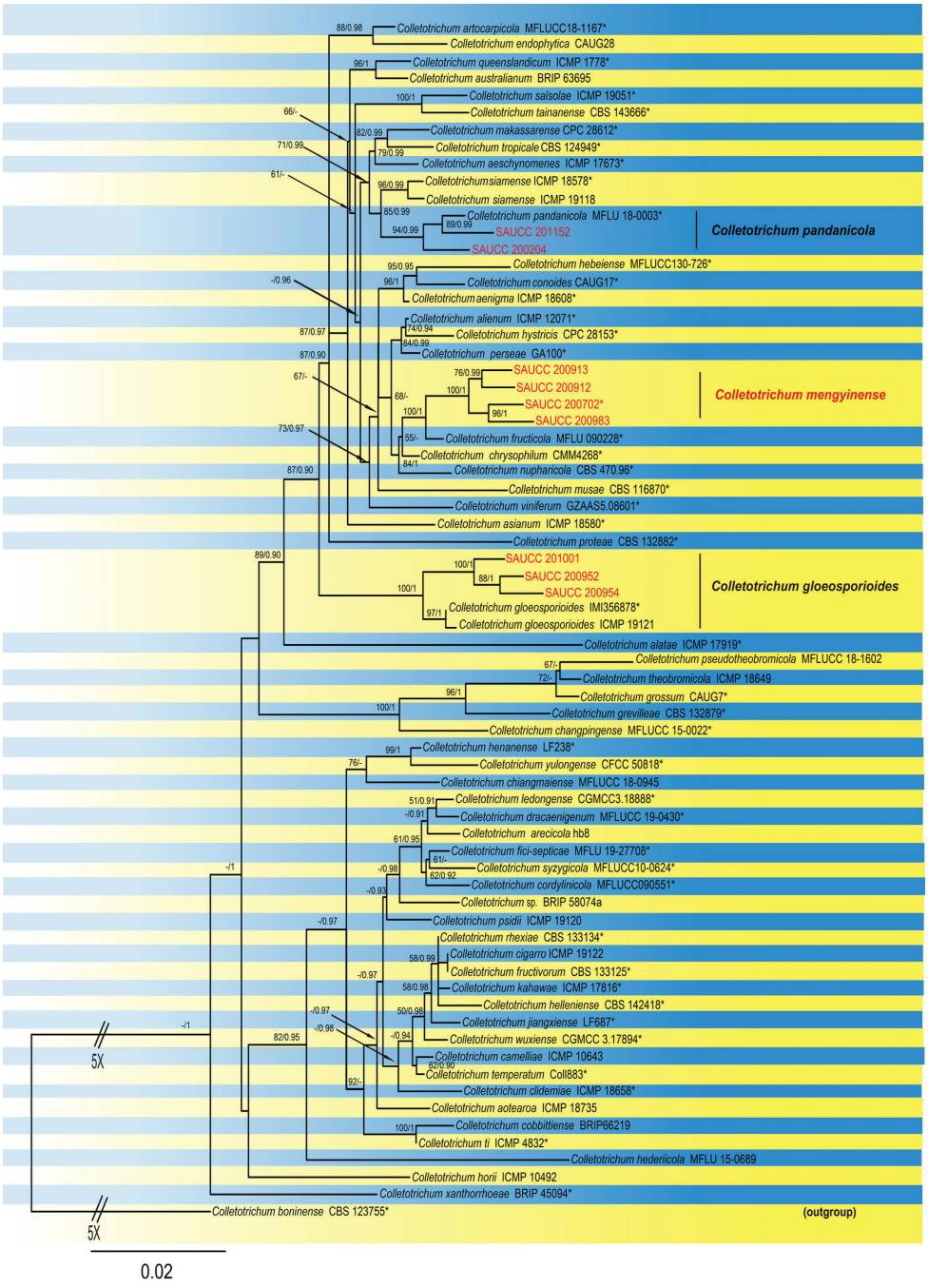

Figure 1. Phylogram of *Colletotrichum gloeosporioides* complex based on combined ITS, GAPDH, CHS-1, ACT, TUB2, CAL and GS genes. The ML and BI bootstrap support values above 50% and 0.90 BYPP are shown at the first and second position, respectively. Strains marked with "*" are ex-type or ex-epitype. Strains from this study are shown in red. Two branches were shortened to fit the page size-these are indicated by the symbol (//) with an indication number showing how many times they are shortened.

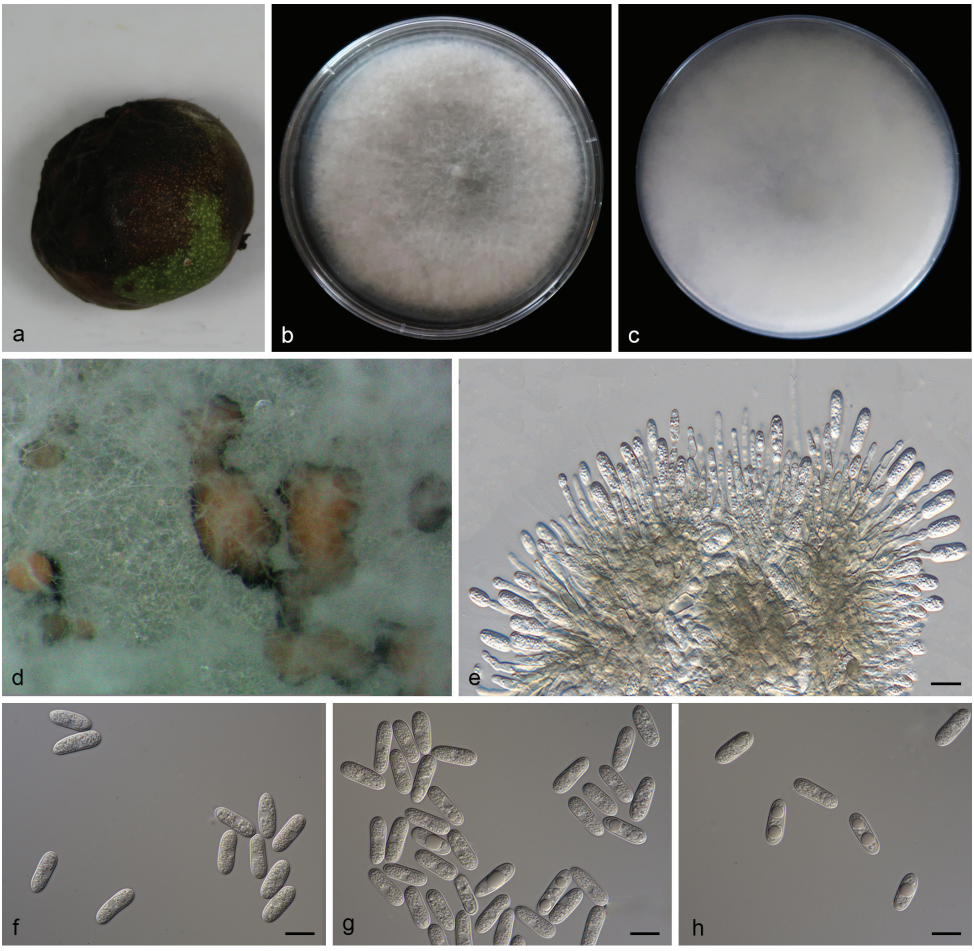

Figure 2. *Colletotrichum gloeosporioides* (SAUCC201001) **a** lesion fruit of host plant **b, c** surface (**b**) and reverse (**c**) sides of colony after incubation for 7 days on PDA **d** conidiomata **e** conidiophores, conidiogenous cells and conidia **f–h** conidia. Scale bars: 10 μm (**e–h**).

celium of PDA after 14 days in light at 25 °C. Conidia, hyaline, smooth-walled, subcylindrical, both ends round, 1–3-guttulate, contents granular. Conidia on PDA (10.6–16.5 × 4.3–5.3 μm, mean ± SD = 14.9 ± 1.5 × 4.9 ± 0.3 μm, L/W ratio = 3.0, n = 40). Sexual morph not observed. Conidiogenous cells subcylindrical, straight to curved, 4.7–12.7 × 3.1–4.0 μm, opening 1.5–2.0 μm diam. Conidiophores hyaline, smooth walled, septate, branched.

Culture characteristics. Colonies on PDA flat with entire margin, aerial mycelium white, floccose cottony; surface and reverse grayish in the center and white margin. PDA attaining max 81 mm in diameter after 7 days, at 25 °C, growth rate 8.7–11.5 mm/day. Colonies on SNA sparse hyphae, slow growth.

Specimens examined. China, Shandong Province: Mengyin County, Mengshan, on diseased fruit of *Juglans regia*, 25 July 2020, T.C. Mu, paratype HSAUP200952, ex-paratype living culture SAUCC200952. China, Shandong Province: Mengyin

County, Mengshan, on diseased fruit of *Juglans regia*, 25 July 2020, T.C. Mu, paratype HSAUP200954, ex-paratype living culture SAUCC200954. China, Shandong Province: Mengyin County, Mengshan, on diseased fruit of *Juglans regia* 25 July 2020, T.C. Mu, paratype HSAUP201001, ex-paratype living culture SAUCC201001.

Notes. *Colletotrichum gloeosporioides* was originally described as *Vermicularia gloeosporioides* on fruit of *Citrus sinensis* in Italy and this species placed in *Colletotrichum* by Corda (Weir et al. 2012; Cannon et al. 2008). In the present study, three strains (SAUCC200952, SAUCC200954 and SAUCC201001) are clustered to *C. gloeosporioides* clade in the combined phylogenetic tree (Fig. 1). Morphologically, our strains were similar to *C. gloeosporioides* by conidia (10.6–16.5 × 4.3–5.3 vs. 12.0–17.0 (–23.5) × 4.5–6.0 μm, mean： 14.9 × 4.9 vs. 14.4 × 5.6 μm). We therefore consider the isolated strain as *C. gloeosporioides*.

Colletotrichum mengyinense **T.C. Mu, J.W. Xia, X.G. Zhang & Z. Li, sp. nov.**
MycoBank No: 841265
Figure 3

Etymology. Named after Mengyin County where the fungus was collected.

Diagnosis. *Colletotrichum mengyinense* can be distinguished from the phylogenetically most closely related species *C. fructicola* (MFLU 090228) by its large conidia (12.5–15.7 × 4.8–6.1 vs. 9.7–14.0 × 3.0–4.3 μm), and five loci (2/509 in the ITS region, 1/139 GAPDH, 9/237 ACT, 8/410 TUB2 and 20/727 GS).

Type. China, Shandong Province: Mengyin County, on diseased leaves of *Rosa chinensis*, 25 July 2020, T.C. Mu, holotype HSAUP200702, ex-type living culture SAUCC200702.

Description. Leaf spots discoid to irregular, brown or tanned. Asexual morph developed on SNA. A yellowish or orange mass appearing just as accumulations of conidia on the surface of the medium of SNA after 14 days in light at 25 °C. Conidia one-celled, hyaline, smooth-walled, subcylindrical, both ends round, contents granular. Conidia on SNA (12.5–15.7 × 4.8–6.1 μm, mean ± SD = 14.3 ± 1.1 × 5.3 ± 0.4 μm, L/W ratio = 2.7, n = 40). Sexual morph not observed. Conidiogenous cells subcylindrical, hyaline, 5.3–15.5 × 2.9–4.9 μm, opening 1.7–2.5 μm diam. Conidiophores hyaline, smooth walled, septate, branched.

Culture characteristics. Colonies on PDA flat with entire margin, aerial mycelium white or gray, floccose cottony; surface and reverse gray in the center and grayish margin. PDA attaining 69.3–75.6 mm in diameter after 7 days, at 25 °C, growth rate 9.9–10.8 mm/day. Colonies on SNA sparse hyphae, slow growth.

Additional specimen examined. China, Shandong Province: Mengyin County, on diseased fruit of *Juglans regia*, 25 July 2020, T.C. Mu, paratype HSAUP200912, ex-paratype living culture SAUCC200912. China, Shandong Province: Mengyin County, on diseased fruit of *Juglans regia*, 25 July 2020, T.C. Mu, paratype HSAUP200913, ex-paratype living culture SAUCC200913. China, Shandong Province: Mengyin County, on diseased fruit of *Juglans regia*, 25 July 2020, T.C. Mu, paratype HSAUP200983, ex-paratype living culture SAUCC200983.

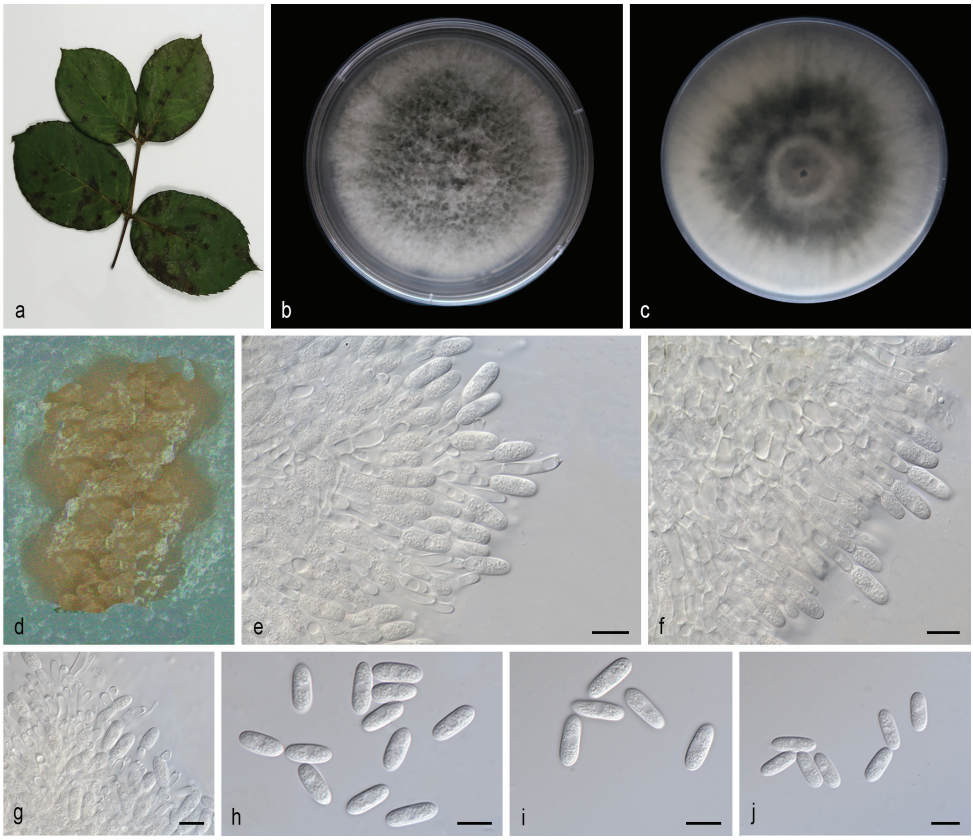

Figure 3. *Colletotrichum mengyinense* (SAUCC200702) **a** branch with leaves of host plant **b, c** surface (**b**) and reverse (**c**) sides of colony after incubation for 7 days on PDA **d** conidiomata **e-g** conidiophores, conidiogenous cells and conidia **h–j** conidia. Scale bars: 10 μm (**e–j**).

Notes. Phylogenetic analysis of a combined seven gene showed that *Colletotrichum mengyinense* formed an independent clade (Fig. 1) and is phylogenetically distinct from *C. fructicola* (Prihastuti et al. 2009). This species can be distinguished from *C. fructicola* by 40 different nucleotides (2/509 in the ITS region, 1/139 in the GAPDH region, 9/237 ACT, 8/410 TUB2 and 20/727 GS). What's more, *C. mengyinense* differs from *C. fructicola* in having large conidia (12.5–15.7 × 4.8–6.1 vs. 9.7–14.0 × 3.0–4.3 μm, mean: 14.3 × 5.3 vs. 11.53× 3.55 μm). Therefore, we establish this fungus as a novel species.

Colletotrichum pandanicola **Tibpromma & K.D. Hyde, MycoKeys 33:47. (2018)**
Figure 4

Description. Lesion fruit, round or irregular, dark brown slightly sunken center, brown at margin. Asexual morph developed on SNA. A mass of yellowish or orange

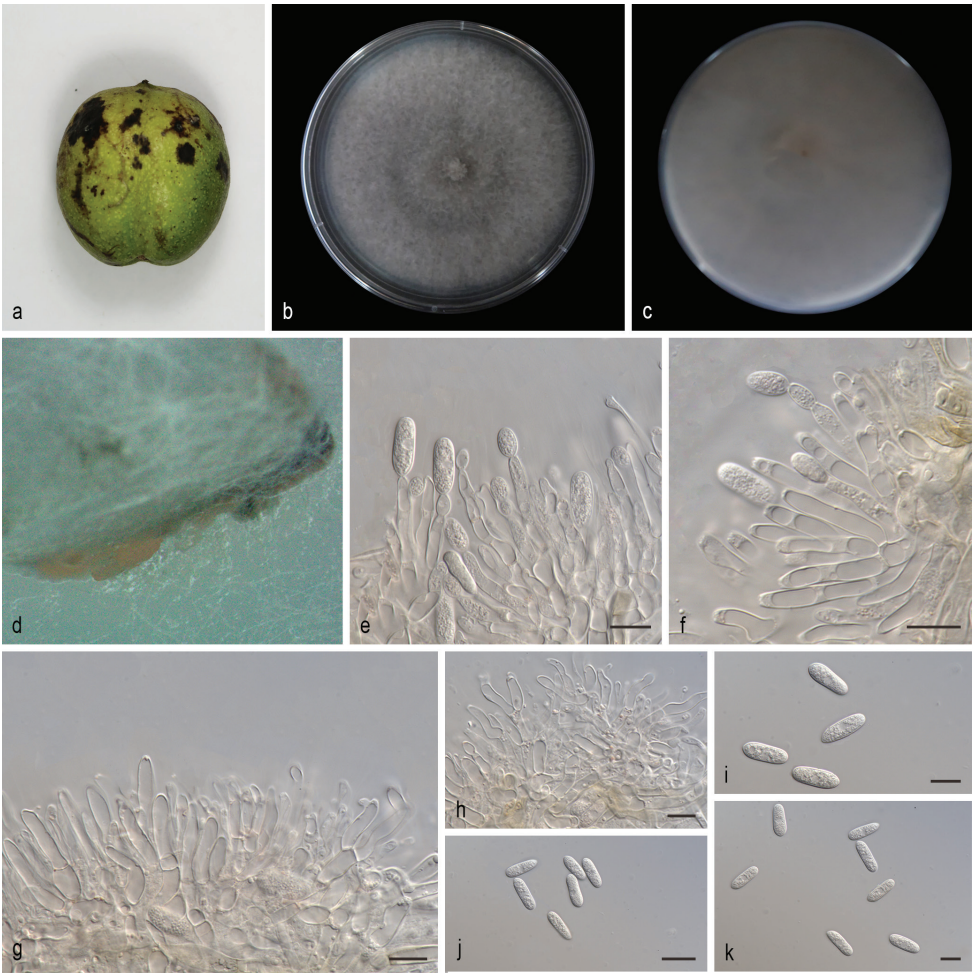

Figure 4. *Colletotrichum pandanicola* (SAUCC201152) **a** lesion fruit of host plant **b, c** surface (**b**) and reverse (**c**) sides of colony after incubation for 7 days on PDA **d** conidiomata **e, f** conidiophores, conidiogenous cells and conidia **g, h** conidiophores, conidiogenous cells **i–k** conidia. Scale bars: 10 μm (**e–k**).

creamy conidial droplets at the inoculum point on SNA after 14 days in light at 25 °C. Born in conidiomata, conidia first take an ovoid shape, then become subcylindrical with rounded ends, contents granular. Conidia on SNA (14.2–17.9 × 4.6–6.0 μm, mean ± SD = 16.1 ± 0.9 × 5.4 ± 0.3 μm, L/W ratio = 2.9, n = 40). Sexual morph not observed. Conidiogenous cells subcylindrical, hyaline, 5.5–23.9 × 2.6–6.3 μm, opening 1.1–1.5 μm diam. Conidiophores branched, hyaline, smooth walled, septate, some septa disappeared at the end, contents granular.

Culture characteristics. Colonies on PDA flat with entire margin, aerial mycelium white, floccose cottony; light gray in the center and pale white margin, reverse white to pale brownish. PDA attaining 58.1–82.6 mm in diameter after 7 days, at 25 °C, growth rate 8.3–11.8 mm/day. Colonies on SNA sparse hyphae, slow growth.

Specimens examined. China, Shandong Province: Mengyin County, Mengshan, on diseased fruit of *Juglans regia*. 25 July 2020, T.C. Mu, paratype HSAUP200204, ex-paratype living culture SAUCC200204. China, Shandong Province: Mengyin County, Mengshan, on diseased fruit of *Juglans regia*. 25 July 2020, T.C. Mu, paratype HSAUP201152, ex-paratype living culture SAUCC201152.

Notes. *Colletotrichum pandanicola* was originally described from the healthy leaves of *Pandanus* sp. (MFLU 18-0003, Pandanaceae) in Thailand (Tibpromma et al. 2018). In the present study, two strains (SAUCC200204 and SAUCC201152) are clustered to the *C. pandanicola* clade in the combined phylogenetic tree (Fig. 1). Morphologically, our strains were similar to *C. pandanicola* by conidia (14.2–17.9 × 4.6–6.0 vs. 9.0–18.0 × 4.0–8.0 μm, mean： 16.1 × 5.4 vs. 13.39 × 5.35 μm). We therefore consider the isolated strains as *C. pandanicola*.

Discussion

In this study, the *Colletotrichum* specimens of diseased leaves and fruits were collected in Mengyin, Shandong Province, China. A temperate monsoon climate and an abundance of fruit trees provide the proper conditions for anthracnose propagation. As a result, 70 reference sequences (including an outgroup taxon: *C. boninense* CBS 123755) were selected based on BLAST searches of NCBI's GenBank nucleotide database and were included in the phylogenetic analyses (Table 2).

Phylogenetic analyses based on seven combined loci (ITS, GAPDH, CHS-1, ACT, TUB2, CAL and GS), as well as morphological characters of the asexual morph obtained in culture, were contributed to knowledge of the diversity of *Colletotrichum* species in Shandong Province. Based on a large set of freshly collected specimens from Shandong province, China, nine strains of *Colletotrichum* species were isolated from two host genera (Table 2). A new species is proposed: *C. mengyinense*. In a previous report, *C. gloeosporioides* has been isolated from *Juglans regia* (Zhu et al. 2014). *Colletotrichum pandanicola* was described from *Pandanus* sp. (Pandanaceae) in Thailand (Tibpromma et al. 2018) and *C. pandanicola* is first reported from *Juglans regia* in China. In this study, we described and illustrated *C. gloeosporioides* and *C. pandanicola* again.

Previously, species identification of *Colletotrichum* was largely referred to the host-specificity and pure culture characteristics, leading to the chaos of names (Weir et al. 2012). On the other hand, based on a polyphasic approach and known morphology, more than one species of *Colletotrichum* can colonize a single host, while one species can be associated with different hosts (Damm et al. 2012). It revealed diversity of *Colletotrichum* species from different hosts. Our study supported this result. For example, *C. pandanicola* (SAUCC200204 and SAUCC201152) and *C. gloeosporioides* (SAUCC200952, SAUCC200954 and SAUCC201001) were collected from *Juglans regia*. In addition, isolates of *C. mengyinense* were obtained from two hosts (*Juglans regia* and *Rosa chinensis*). The morphological descriptions and molecular data for species of *Colletotrichum* represent an important resource and basis for plant pathologists and fungus taxonomists.

Acknowledgements

This work was supported by the National Natural Science Foundation of China (no. 31900014, 31750001 and 31770016).

References

Bhunjun CS, Phukhamsakda C, Jayawardena RS, Jeewon R, Promputtha I, Hyde KD (2021) Investigating species boundaries in *Colletotrichum*. Fungal Diversity 107: 107–127. https://doi.org/10.1007/s13225-021-00471-z

Cai L, Hyde KD, Taylor PWJ, Weir BS, Waller JM, Abang MM, Zhang ZJ, Yang YL, Phoulivong S, Liu ZY, Prihastuti H, Shivas RG, McKenzie EHC, Johnston PR (2009) A polyphasic approach for studying *Colletotrichum*. Fungal Diversity 39: 183–204.

Cannon PF, Buddie AG, Bridge PD (2008) The typification of *Colletotrichum gloeosporioides*. Mycotaxon 104: 189–204.

Cannon PF, Damm U, Johnston PR, Weir BS (2012) *Colletotrichum* - current status and future directions. Studies in Mycology 73: 181–213. https://doi.org/10.3114/SIM0014

Chomnunti P, Hongsanan S, Aguirre-Hudson B, Tian Q, Peršoh D, Dhami MK, Alias AS, Xu J, Liu X, Stadler M, Hyde KD (2014) The sooty moulds. Fungal Diversity 66: 1–36. https://doi.org/10.1007/S13225-014-0278-5

Corda ACI (1831) Die Pilze Deutschlands. In: Sturm J (Ed.) Deutschlands Flora in Abbildungen nach der Natur mit Beschreibungen. Sturm, Nürnberg 3(12): 33–64.

Damm U, Cannon PF, Woudenberg JH, Johnston PR, Weir BS, Tan YP, Shivas RG, Crous PW (2012) The *Colletotrichum boninense* species complex. Studies in Mycology 73: 1–36. https://doi.org/10.3114/sim0002

Damm U, Woudenberg JHC, Cannon PF, Crous PW (2009) *Colletotrichum* species with curved conidia from herbaceous hosts. Fungal Diversity 39: 45–87.

Dean R, Van Kan JA, Pretorius ZA, Hammond-Kosack KE, Di Pietro A, Spanu PD, Rudd JJ, Dickman M, Kahmann R, Ellis J, Foster GD (2012) The Top 10 fungal pathogens in molecular plant pathology. Molecular Plant Pathology13: 414–430. https://doi.org/10.1111/J.1364-3703.2011.00783.X

Gao YH, Sun W, Su YY, Cai L (2013) Three new species of *Phomopsis* in Gutianshan Nature Reserve in China. Mycological Progress 13: 111–121. https://doi.org/10.1007/S11557-013-0898-2

Guo LD, Hyde KD, Liew ECY (2000) Identification of endophytic fungi from *Livistona chinensis* based on morphology and rDNA sequences. New Phytologist 147: 617–630. https://doi.org/10.1046/J.1469-8137.2000.00716.X

Huelsenbeck JP, Ronquist F (2001) MRBAYES: Bayesian inference of phylogeny. Bioinformatics 17(17): 754–755. https://doi.org/10.1093/bioinformatics/17.8.754

Jayawardena RS, Hyde KD, Jeewon R, Li XH, Liu M, Yan JY (2016) Mycosphere Essay 6: Why is it important to correctly name *Colletotrichum* species? Mycosphere 7: 1076–1092. https://doi.org/10.5943/mycosphere/si/2c/1

Jayawardena RS, Camporesi E, Elgorban AM, Bahkali AH, Yan J, Hyde KD (2017) A new species of *Colletotrichum* from *Sonchus* sp. in Italy. Phytotaxa 314(1): 55–63. https://doi.org/10.11646/phytotaxa.314.1.3

Katoh K, Rozewicki J, Yamada KD (2019) MAFFT online service: multiple sequence alignment, interactive sequence choice and visualization. Briefings in Bioinformatics 20: 1160–1166. https://doi.org/10.1093/bib/bbx108

Kumar S, Stecher G, Tamura K (2016) MEGA7: Molecular Evolutionary Genetics Analysis Version 7.0 for bigger datasets. Molecular Biology and Evolution 33(7): 1870–1874. https://doi.org/10.1093/MOLBEV/MSW054

Liu F, Weir BS, Damm U, Crous PW, Wang Y, Liu B, Wang M, Zhang M, Cai L (2015) Unravelling *Colletotrichum* species associated with *Camellia*: employing ApMat and GS loci to resolve species in the *C. gloeosporioides* complex. Persoonia 35: 63–86. https://doi.org/10.3767/003158515X687597

Miller MA, Pfeiffer W, Schwartz T (2012) The CIPRES science gateway: enabling high-impact science for phylogenetics researchers with limited resources. Proceedings of the 1st Conference of the Extreme Science and Engineering Discovery Environment. Bridging from the extreme to the campus and beyond. Association for Computing Machinery 39: 1–8. https://doi.org/10.1145/2335755.2335836

Nylander JAA (2004) MrModeltest v. 2. Program distributed by the author. Evolutionary Biology Centre, Uppsala University.

Prihastuti H, Cai L, Chen H, Mckenzie EHC, Hyde KD (2009) Characterization of *Colletotrichum* species associated with coffee berries in northern Thailand. Fungal Diversity 39: 89–109.

Ronquist F, Huelsenbeck JP (2003) MrBayes 3: Bayesian phylogenetic inference under mixed models. Bioinformatics 19: 1572–1574. https://doi.org/10.1093/BIOINFORMATICS/BTG180

Ronquist F, Teslenko M, van der Mark P, Ayres DL, Darling A, Hohna S, Larget B, Liu L, Suchard MA, Huelsenbeck JP (2012) MrBayes 3.2: efficient Bayesian phylogenetic inference and model choice across a large model space. Systematic Biology 61: 539–542. https://doi.org/10.1093/sysbio/sys029

Stamatakis A (2014) RAxML Version 8: A tool for phylogenetic analysis and post-analysis of large phylogenies. Bioinformatics 30(9): 1312–1313. https://doi.org/10.1093/bioinformatics/btu033

Tibpromma S, Hyde KD, Bhat JD, Mortimer PE, Xu J, Promputtha I, Doilom M, Yang JB, Tang AMC, Karunarathna SC (2018) Identification of endophytic fungi from leaves of Pandanaceae based on their morphotypes and DNA sequence data from southern Thailand. MycoKeys: 25–67. https://doi.org/10.3897/mycokeys.33.23670

Tode HJ (1790) Fungi Mecklenburgenses Selecti. Fasc. 1. Nova Fungorum Genera Complectens. https://doi.org/10.5962/bhl.title.148599

Weir BS, Johnston PR, Damm U (2012) The *Colletotrichum gloeosporioides* species complex. Studies in Mycology 73: 115–180. https://doi.org/10.3114/sim0011

Zhu YF, Yin YF, Qu WW, Yang KQ (2014) Occurrence and Spread of the Pathogens on Walnut (*Juglans regia*) in Shandong Province, China. Acta Horticulturae 1050: 347–351. https://doi.org/10.17660/ACTAHORTIC.2014.1050.47

MycoKeys 85: 73–85 (2021)
doi: 10.3897/mycokeys.85.76040
https://mycokeys.pensoft.net

RESEARCH ARTICLE

A peer-reviewed open-access journal
MycoKeys
Launched to accelerate biodiversity research

New species and records of *Chapsa* (Graphidaceae) in China

Ming-Zhu Dou[1*], Min Li[1*], Ze-Feng Jia[1]

1 *College of Life Sciences, Liaocheng University, Liaocheng 252059, China*

Corresponding author: Ze-Feng Jia (zfia2008@163.com)

Academic editor: Thorsten Lumbsch | Received 5 October 2021 | Accepted 27 November 2021 | Published 10 December 2021

Citation: Dou M-Z, Li M, Jia Z-F (2021) New species and records of *Chapsa* (Graphidaceae) in China MycoKeys 85: 73–85. https://doi.org/10.3897/mycokeys.85.76040

Abstract

We studied the genus *Chapsa* in China based on morphological characteristics, chemical traits and molecular phylogenetic analysis. One species new to science (*C. murioelongata* M.Z. Dou & M. Li) and two records new to China were found (*C. wolseleyana* Weerakoon, Lumbsch & Lücking and *C. niveocarpa* Mangold). *Chapsa murioelongata* **sp. nov.** is characterised by its lobed thalline margin, orange discs with white pruina, clear hymenium, and submuriform and long ascospores. *Chapsa wolseleyana* was recombined into *Astrochapsa* based on phenotypic traits. Sequences of this species are for the first time reported here and phylogenetic analyses of three loci (mtSSU, ITS and nuLSU) supported the position of this species within *Chapsa*. A key for the *Chapsa* species known in China is provided.

Keywords

Ascomycota, lichenized fungi, phylogeny, taxonomy

Introduction

The lichen genus *Chapsa* (Graphidaceae) was first established by Massalongo (1860) with *C. indica* as the type species. This genus was ignored for a long time until 2006, when Frisch re-established *Chapsa*, based on the *Chroodiscus*-type apothecia, presence of periphysoids and *Chapsa*-type paraphyses. Frisch (2006) also provided a detailed description and delimitation of the genus *Chapsa*, which was widely recognised by

* These two authors contributed equally to this work.

subsequent researchers (Mangold 2008; Frisch and Kalb 2009; Rivas Plata et al. 2011; Sipman et al. 2012; Xu et al. 2016). The genus *Chapsa* was considered to be monophyletic in the beginning (Frisch 2006) but with further research, it was suspected to be polyphyletic (Mangold 2008; Papong et al. 2010). Subsequently, seven genera, *Astrochapsa* Parnmen, Lücking & Lumbsch, *Crutarndina* Parnmen, Lücking & Lumbsch, *Gintarasia* Kraichak, Lücking & Lumbsch, *Pseudochapsa* Parnmen, Lücking & Lumbsch, *Pseudotopeliopsis* Parnmen, Lücking & Lumbsch, *Myriochapsa* M. Cáceres, Lücking & Lumbsch and *Nitidochapsa* Parnmen, Lücking & Lumbsch were separated from *Chapsa*, based on a combination of molecular evidence, phenotypic and chemical characteristics (Parnmen et al. 2012, 2013; Kraichak et al. 2013).

Although China is rich in lichenised fungal species (Wei 2020), there are few studies and reports on the genus *Chapsa*. More than 60 species of *Chapsa* have been reported in the world, of which only three, *C. indica* A. Massal, *C. mirabilis* A. (Zahlbr.) Lücking and *C. leprocarp*a (Nyl.) Frisch, have so far been found in China (Rivas Plata et al. 2010; Xu et al. 2016; Jia and Lücking 2017; Kalb and Kalb 2017; Wijayawardene et al. 2017; de Lima et al. 2019).

During the study of *Chapsa* A. Massal. in southern China, one species, *C. murioelongata* was found new to science, and two species, *C. niveocarpa* Mangold and *C. wolseleyana* Weerakoon, Lumbsch & Lücking were found new to China. In our study, 26 sequences were newly generated from freshly collected specimens.

Materials and methods

Morphological and chemical analyses

The specimens were collected from southern China and deposited in the Fungarium, College of Life Sciences, Liaocheng University, China (LCUF). Morphological and anatomical characters of thalli and apothecia were examined and photographed under an Olympus SZX16 dissecting microscope and an Olympus BX53 compound microscope. The lichen secondary metabolites were detected and identified by thin-layer chromatography using solvent C (Orange et al. 2010; Jia and Wei 2016).

DNA extraction, PCR sequencing and phylogenetic analysis

Genomic DNA was extracted from ascomata using the Hi-DNA-secure Plant Kit (Tiangen, Beijing, China) according to the manufacturer's protocol. The nuLSU, ITS and mtSSU regions were amplified using the primer pair AL2R/LR6 (Mangold et al. 2008, Vilgalys and Hester 1990), ITS1F/ITS4 (Gardes and Bruns 1993, White et al. 1990) and mrSSU1/mrSSU3R (Zoller et al. 1999), respectively. The PCR amplification progress followed Dou et al. (2018) and the PCR products were sequenced by Biosune Inc. (Shanghai). The newly generated sequences were submitted to GenBank (Table1).

Table 1. Information for the sequences used in this study. Newly generated sequences are shown in bold.

Species	Specimen No.	Locality	ITS	nuLSU	mtSSU
Pseudochapsa phlyctidioides	Lumbsch 20500d	Fiji	–	JX465301	JX421005
Pseudochapsa dilatata	Luecking 32101	Venezuela	–	JX421446	JX420981
Pseudochapsa esslingeri	Caceres s.n.	Brazil	–	–	JX420983
Pseudochapsa esslingeri	Caceres 6006a	Brazil	–	–	JX420984
Pseudochapsa esslingeri	Rivas Plata 107C (F)	Peru	–	–	JX420985
Pseudochapsa esslingeri	Rivas Plata 809a (F)	Peru	–	–	JX420986
Chapsa alborosella	Luecking 31238a	Brazil	–	JX421439	JX420972
Chapsa alborosella	Luecking 25587	Guatemala	–	JX421440	JX420973
Chapsa soredicarpa	Luecking 31200	Brazil	–	JX421462	JX421011
Chapsa soredicarpa	Luecking 31240	Brazil	–	JX421463	JX421012
Chapsa sublilacina	Luecking RLD056	Mexico	–	HQ639624	HQ639600
Chapsa thallotrema	Lucking 32019	Venezuela	–	JX465319	JX421013
Chapsa indica	Parnmen018486(RAMK)	Thailand	–	JX465295	JX465280
Chapsa leprocarpa	GZ19531	China, Guizhou	**MW009079**	**MW007981**	**MW010276**
Chapsa leprocarpa	GZ19537	China, Guizhou	**MW009077**	**MW007984**	**MW010278**
Chapsa leprocarpa	GZ19536	China, Guizhou	**MW009080**	**MW007982**	**MW010274**
Chapsa niveocarpa	HN19508	China, Hainan	**MW009076**	**MW010272**	–
Chapsa niveocarpa	Lumbsch_19125k2(F) & Mangold (F)	Australia, Queensland	–	–	EU675274
Chapsa niveocarpa	Lumbsch 19151p & Mangold (F)	Australia, Queensland	–	FJ708487	EU075567
Chapsa patens	FJ19131	China, Fujian	**MT995055**	**MW007979**	**MW010275**
Chapsa patens	FJ19049	China, Fujian	**MW007918**	**MW007980**	–
Chapsa wolseleyana	FJ19158	China, Fujian	**MW009078**	**MW010273**	**MW010277**
Chapsa wolseleyana	FJ19148	China, Fujian	**MW009106**	**MW010270**	**MW010279**
Chapsa murioelongata	HN19222	China, Hainan	**MW009102**	**MW010271**	–
Chapsa murioelongata	HN19682	China, Hainan	**MW009103**	**MW010269**	–
Chapsa pulchra	CHAPUL19129t	Australia	–	KC020261	KC020255
Astrochapsa meridensis	Luecking 17770 (F)	Costa Rica	–	EU075655	EU075610
Astrochapsa mastersonii	Lumbsch 20500f	Fiji	–	–	JX420996
Astrochapsa zahlbruckneri	Papong 6516	Thailand	–	JX421467	–
Astrochapsa astroidea	Lumbsch 19166n & Mangold(F)	Australia, Queensland	–	EU075614	EU075566
Astrochapsa astroidea	Lumbsch 19750a	Thailand	–	JX421441	JX420974
Astrochapsa astroidea	Papong 6004	Thailand	–	JX421442	JX420975
Astrochapsa astroidea	Luecking 24006	Thailand	–	JX421443	JX420977
Astrochapsa astroidea	Luecking 24008	Thailand	–	JX421444	JX420978
Astrochapsa astroidea	Luecking 24011	Thailand	–	JX421445	JX465278
Chroodiscus coccineus	Herb. R. Luecking 2000	Costa Rica	–	AF465441	–

Multi-locus (ITS, mtSSU and nuLSU) phylogenetic analysis was performed. The combined analysis included 70 sequences (Table 1) representing 18 in-group taxa and one out-group taxon. As many species as possible of *Chapsa* s. lat. were contained in our data matrix including the taxa that were similar in morphology or sequence to the new species and the two records. We blasted sequences of the three species in GenBank and selected sequence-similar taxa on a pre-determined cut-off.

The alignment was undertaken by applying MAFFT 7 with the option of L-INS-I (Katoh and Standley 2013). The three single-locus alignments were concatenated in PhyloSuite v1.2.2 (Zhang et al. 2020). The concatenated data matrix comprised 3188 nucleotide sites (nuLSU 1405 bp, ITS 647 bp and mtSSU 1136 bp). In order to check the consistency between the three loci, incongruence length difference test (ILD Test) was carried out using PAUP. The P value of ILD Test was 0.65 (>0.5), so the three loci were

suitable for polygenic phylogeny. Construction of the ML (Maximum Likelihood) tree was undertaken by applying RAxML v.8.2.12 (Stamatakis 2014) and implementing a GTRGAMMA model. For BI (Bayesian Inference) analysis, PartitionFinder 2 (Lanfear et al. 2017) was used to determine the best-fit model for each partition. For the nuLSU region, we used GTR+I+G, for ITS, GTR+G, and for mtSSU, HKY+I+G. BI analysis was performed with MrBayes 3.2.7 (Ronquist et al 2012). Markov Chain Monte Carlo (MCMC) chains were run for 200,000 generations, sampling every 100th generation, at which point, the average standard deviation of split frequencies was 0.001738. ML bootstrap values (BS) ≥ 75% and Bayesian posterior probabilities (PP) ≥ 0.95 were considered as significantly supported.

Results and discussion

The BI and ML trees showed similar topologies and thus, only the BI tree was provided (Fig. 1). The three species were all monophyletic with a high support value: *C. mu-*

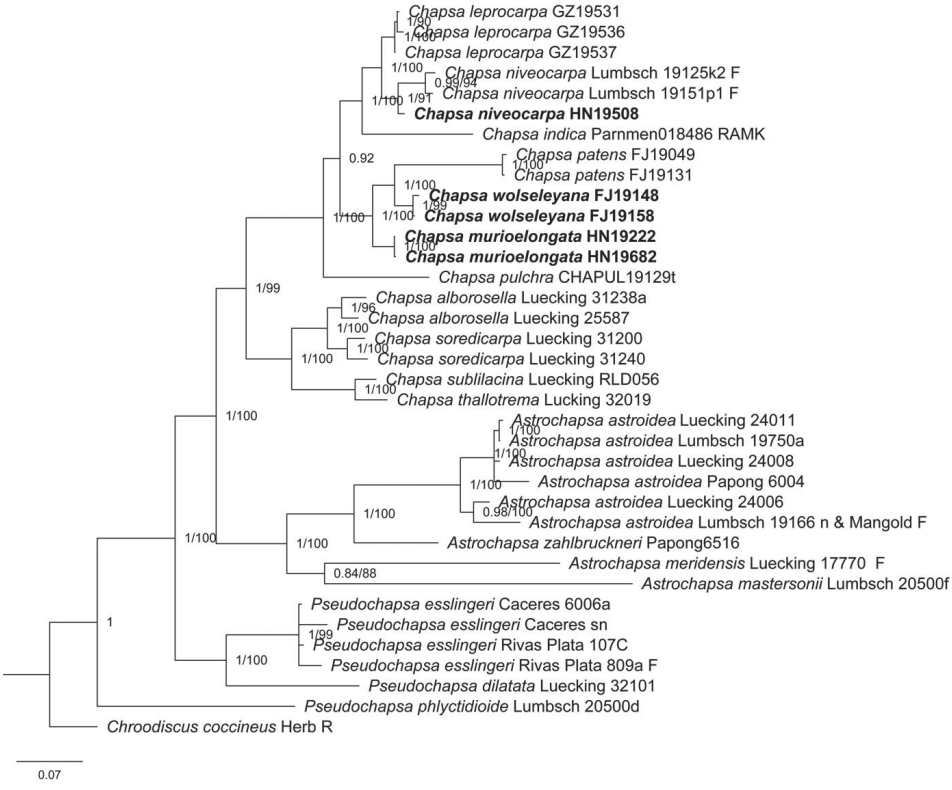

Figure 1. Bayesian phylogenetic tree generated from analysis of combined ITS, nuLSU and mtSSU. *Chroodiscus coccineus* is the out-group taxon. ML-bootstrap values/Bayesian posterior probabilities above 50% are written next to nodes.

rioelongata (100%, 1.00), *C. wolseleyana* (99%, 1.00) and *C. niveocarpa* (91%, 1.00). *Chapsa murioelongata* is sister to the clade consisting of *C. wolseleyana* and *C. patens* (Nyl.) Frisch. *Chapsa niveocarpa* HN19508 and *C. niveocarpa* Lumbsch form a well-supported clade and are sisters to *C. leprocarpa*.

Taxonomy

New species

***Chapsa murioelongata* M.Z. Dou & M. Li, sp. nov.**
Fungal Names: FN 570754
Figure 2

Etymology. The specific epithet *murioelongata* refers to the elongate, muriform ascospores.

Type. China. Hainan Province: Ledong County, Jianfengling National Forest Park, 18°42'39"N, 108°52'37"E, alt. 760 m, on bark, 09 Dec 2019, Y. H. Ju HN19222 (LCUF: holotype: HN19222; GenBank MW009102 for ITS and MW010271 for LSU).

Description. Thallus corticolous, crustose, olive-grey, surface dull, smooth to uneven, ecorticate. Apothecia erumpent, dispersed or two to four aggregated, rounded, 1–3 mm diam.; thalline margin lobed with white felt-like inner surface, lobes

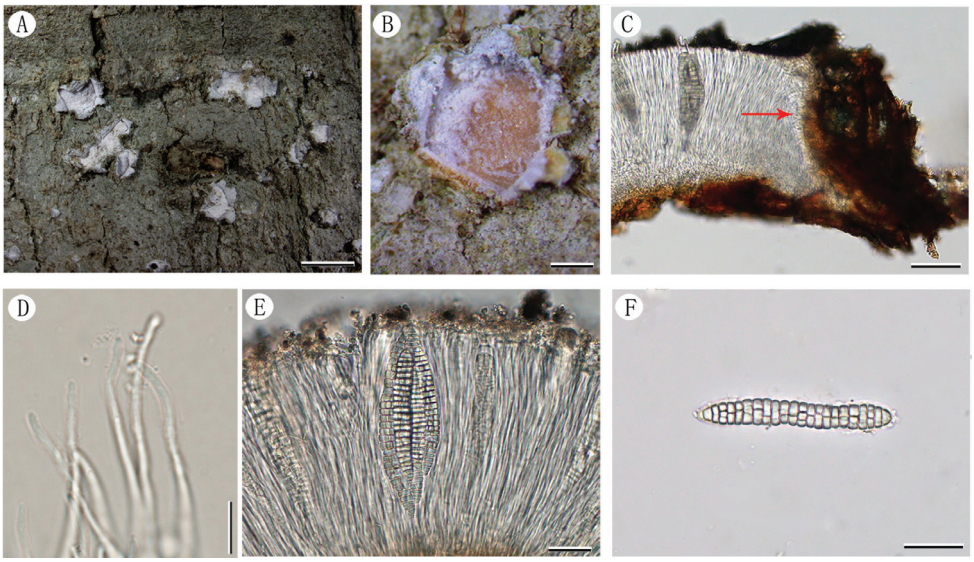

Figure 2. *Chapsa murioelongata* (LCUF HN19222) **A** habit of thallus with apothecia at different developmental stages **B** apothecium (the pruina of the disc partly scraped off) **C** section of apothecium with periphysoids (direction of arrow) **D** paraphyses **E** an ascus containing six ascospores **F** ascospore. Scale bars: 3 mm (**A**); 0.5 mm (**B**); 50 μm (**C**); 8 μm (**D**); 30 μm (**E**); 25 μm (**F**).

strongly backward curved; DISC flesh-coloured, covered by thick, white pruina. EXCIPLE 80–105 μm wide laterally, dark brown; EPIHYMENIUM 20–40 μm high, with coarse greyish granules; HYMENIUM clear, 110–170 μm high, non-amyloid; HYPOTHECIUM colourless, 10–30 μm high; PARAPHYSES simple, tips unbranched; PERIPHYSOIDES present, 5–30 μm long. ASCI 4–6 (8)-spored, clavate, 100–120 × 35–50 μm; ASCOSPORES hyaline, bacillary with rounded to subacute ends, submuriform with 20–25 transverse septa and 0–2 longitudinal septa per segment, 75–105 × 9.5–16 μm, non-halonate, I-. PYCNIDIA not observed.

Chemistry. Thallus K-, C-, PD-; no compounds detectable by TLC.

Ecology and distribution. On the bark in semi-exposed forest of Hainan Province.

Additional specimens examined. CHINA. Hainan Province: Changjiang County, Bawangling Nature Reserve, Yajia Scenic Area, 10°04'54"N, 109°07'04"E, alt. 810 m, on bark, 08 Dec 2019, Y. H. Ju HN19167 (LCUF); CHINA. Hainan Province: Lingshui County, Diaoluo Mountain, 18°43'35"N, 109°52'02"E, alt. 900 m, on bark, 14 Dec 2019, M. Li HN19682 (LCUF) (GenBank MW009103 for ITS and MW010269 for LSU).

Note. *Chapsa murioelongata* is characterised by its olive-grey thallus; white pruinose discs; distinct periphysoids; clear hymenium; 4–8-spored asci; submuriform ascospores with 20–25 transverse septa and 0–2 longitudinal septa per segment. *Chapsa microspora* Kalb, *C. asteliae* (Kantvilas & Vězda) Mangold, *Astrochapsa elongata* Poengs. & Lumbsch and *C. patens* are morphologically similar to the new species. *Chapsa microspora* can be distinguished from *C. murioelongata* by the smaller apothecia (0.6–1.2 mm diam.), transversely septate and smaller ascospores (7–9 × 4 μm) (Lumbsch et al. 2011). *Chapsa asteliae* differs in amyloid and shorter ascospores (30–80 μm) (Kantvilas and Vězda 2000; Mangold 2008). *Astrochapsa elongata* differs from *C. murioelongata* in having shorter ascospores (40–65 μm) and less longitudinal septa per segment (0–1) (Poengsungnoen et al. 2019). *Chapsa patens* differs from *C. murioelongata* chiefly in the single-spored asci and broader ascospores (22–35 μm) (Frisch et al. 2006).

Blast searches of nuLSU sequences indicate *Chapsa murioelongata* has close affinities with *C. patens* (98.36% identity), *C. wolseleyana* (95.63% identity), *C. leprocarpa* (91.97% identity) and *C. indica* (90.81% identity), so all these species were included in the phylogenetic analyses. *Chapsa murioelongata* was well separated from any other species in the tree and strongly supported as the monophyletic (PP = 1; ML = 100%).

New records

Chapsa wolseleyana Weerakoon, Lumbsch & Lücking, in Weerakoon, Rivas Plata, Lumbsch & Lücking, Lichenologist 44(3): 377 (2012)

Figure 3

Astrochapsa wolseleyana (Weerakoon, Lumbsch & Lücking) Parnmen, Lücking & Lumbsch, in Parnmen et al., PLoS ONE 7(12): 10 (2012)

Description. THALLUS crustose, corticolous, grey-brown, surface dull to slightly shiny, uneven, fissured. APOTHECIA erumpent, dispersed, sometimes two or three fused, most-

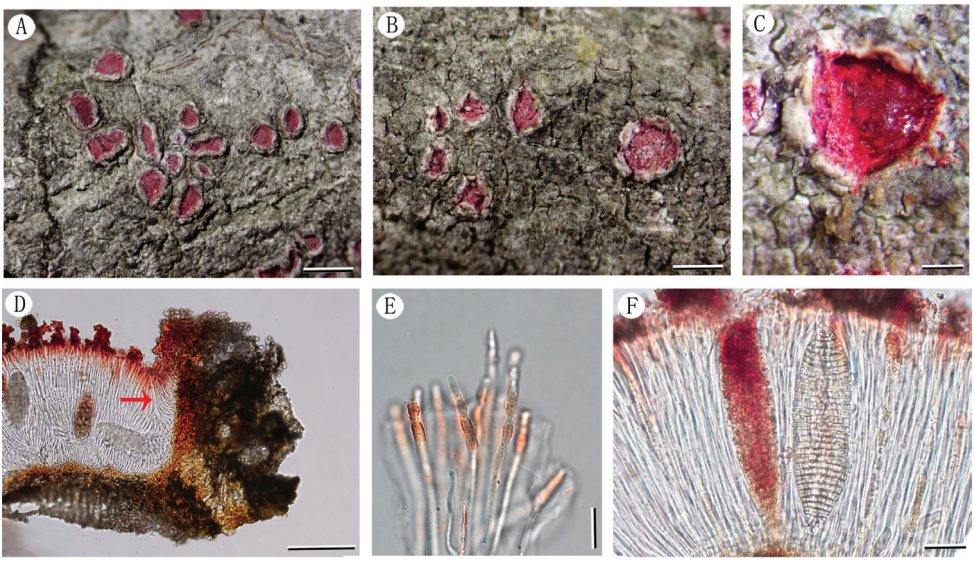

Figure 3. *Chapsa wolseleyana* (LCUF FJ19148-b) **A** habit of thallus with apothecia **B** apothecia at different developmental stages **C** apothecium (part of pruina scraped off) **D** section of apothecium with periphysoids (direction of arrow) **E** paraphyses **F** young and mature ascospores. Scale bars: 1.5 mm (**A**); 1 mm (**B**); 0.25 mm (**C**); 120 µm (**D**); 10 µm (**E**); 25 µm (**F**).

ly rounded to seldom slightly angular, 0.7–1.2 mm diam.; THALLINE MARGIN raised to lobulate, lobes erected to recurved, inner part brown, covered with rose-red or white pruina; DISC exposed, rose-red, covered with thick, rose-red pruina. EXCIPLE fused, cupular, laterally 180–250 µm wide, yellowish-brown to brown; EPIHYMENIUM rose-red with granules, 20–50 µm high, K+ green; HYMENIUM 140–230 µm high, clear, colourless, non-amyloid; HYPOTHECIUM indistinct; PARAPHYSES septate, tips rose-red and moniliform with oval or rectangular cells; PERIPHYSOIDES present, 50–100 µm long. ASCI clavate, 1-spored, 110–135 × 35–50 µm; ASCOSPORES densely muriform, oblong-ellipsoid, with hemispherical to roundish ends, 105–130 × 30–45 µm, first reddish, becoming hyaline to slightly olive-brown at maturity, I-. PYCNIDIA not observed.

Chemistry. No substances detected by TLC but apothecial disc with pigment producing K+ yellow-green efflux, suggesting presence of isohypocrelline.

Ecology and distribution. Growing on bark exposed to wind and high light intensity in montane forests. Worldwide distribution: Sri Lanka (Weerakoon et al. 2012) and newly reported for China.

Selected specimens examined. CHINA. Fujian Province: Quanzhou City, Jiuxian Mountain, Reflecting Pool, 25°42'57"N, 118°07'14"E, alt. 1540 m, on bark, 5 Jul 2019, F.Y. Liu FJ19148-b (LCUF) (GenBank MW009106 for ITS, MW010270 for LSU and MW010279 for SSU); CHINA. Fujian Province: Quanzhou City, Jiuxian Mountain, Natural Observation Path, 25°42'44"N, 118°07'17"E, alt. 1460 m, on bark, 25 Jul 2019, F.Y. Liu FJ19158 (LCUF) (GenBank MW009078 for ITS, MW010273 for LSU and MW010277 for SSU). CHINA. Fujian Province: Quanzhou City, Jiuxian Mountain,

Reflecting Pool, 25°42'57"N, 118°07'14"E, alt. 1540 m, on bark, 25 Jul 2019, F.Y. Liu FJ19127-2, same locality, FJ19128-2, FJ19141-2 (LCUF).

Note. *Chapsa wolseleyana* is characterised by its grey-brown, uneven thallus, apothecia with raised to lobed thalline margin, rose-red discs with similar coloured pruina, rose-red epihymenium and paraphyses tips, distinct periphysoids, 1-spored asci, muriform ascospores, red when young and hyaline to olive-brown when old. Only a few species of *Chapsa* have pigmented discs and among them *C. rubropulveracea* Hale ex Mangold, Lücking & Lumbsch is morphologically most similar to *C. wolseleyana*, but its thallus is farinose and its ascospores are 8 per ascus, smaller (15–20 ×5–6 μm) and transversely septate (Lumbsch et al. 2011).

Chapsa wolseleyana was transferred to *Astrochapsa*, based on a phenotype-based analysis (not molecular phylogeny) (Parnmen et al. 2012). However, our phylogenetic analysis shows that this species belongs in *Chapsa*, rather than *Astrochapsa. Chapsa wolseleyana* was associated phylogenetically with a strongly-supported clade (100/1) with *C. patens*, but with sufficient distance to be considered a distinct species. In addition, the latter differs from *C. wolseleyana* in having larger pale brown apothecia (up to 2 mm diam.) with white pruina, unpigmented epihymenium and unpigmented paraphyses adspersed with fine greyish to brownish granules, hyaline ascospores (Frisch et al. 2006; Joshi et al. 2012; Joshi et al. 2018).

Chapsa niveocarpa Mangold in Mangold, Elix & Lumbsch, Flora of Australia, 57:654 (2009)

Figure 4

Description. Thallus corticolous, crustose, pale grayish-green surface dull and fluctuating along the bark. Apothecia erumpent, solitary to fused, angular rounded to slightly elongate, 0.5–1.8 × 0.5–1.2 mm; thalline margin split and recurved, inside-with thick white pruina; disc exposed, yellowish-brown, covered by white pruina. Exciple laterally 12–75 μm wide, dark brown; epihymenium 10–20 μm high; hymenium 120–200 μm high, grey-brown, inspersed by granules, non-amyloid; hypothecium indistinct; paraphyses unbranched; tips distinctly thickened; periphysoides present, but obscured by granular inclusions. Asci 1-spored, clavate, 120–140 × 27–36 μm; ascospores densely muriform, with thick halo at both ends, oblong, hyaline, 115–135 × 25–34 μm, I-. Pycnidia not observed.

Chemistry. Thallus K-, C-, PD-; no compounds detectable by TLC.

Ecology and distribution. Growing on tree bark in tropical rainforests in altitudes ranging from 500 to 1100 m. Australia, Queensland (Mangold 2008); newly reported for China.

Selected specimens examined. China. Hainan Province: Wuzhishan City, Wuzhishan Nature Reserve, 18°54'13"N, 109°41'04"E, alt. 870 m, on bark, 12 Dec 2019,

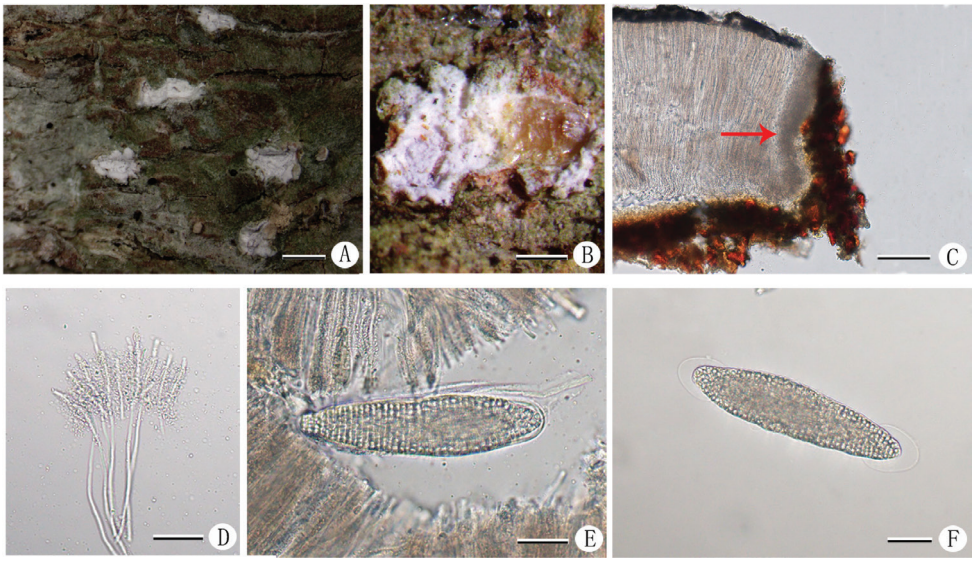

Figure 4. *Chapsa niveocarpa* (LCUF HN19508) **A** habit of thallus with apothecia **B** apothecium (part of pruina scraped off) **C** section of apothecium with periphysoids (direction of arrow) **D** paraphyses with hyaline granules **E** ascus **F** ascospore with halo. Scale bars: 1 mm (**A**); 0.5 mm (**B**); 50 µm (**C**); 25 µm (**D**); 30 µm (**E**); 25 µm (**F**).

M. Li HN19508 (LCUF) (GenBank MW009076 for ITS and MW010272 for LSU); China. Hainan Province: Wuzhishan City, Wuzhishan Nature Reserve, 18°53'13"N, 109°41'04"E, alt. 1020 m, on bark, 12 Dec 2019, M. Li HN19530 (LCUF); China. Hainan Province: Wuzhishan City, Wuzhishan Nature Reserve, 18°54'13'N, 109°41'04'E, alt. 870 m, on bark, 12 Dec 2019, M. Li HN19499 (LCUF); China. Hainan Province: Lingshui County, Diaoluo Mountain, 18°43'35"N, 109°52'02"E, alt. 900 m, on bark, 14 Dec 2019, M. Li HN19687 (LCUF); China. Hainan Province: Lingshui County, Diaoluo Mountain, 18°43'35"N, 109°52'02"E, alt. 900 m, on bark, 14 Dec 2019, M. Li HN19679 (LCUF).

Note. *Chapsa niveocarpa* is characterised by its crustose, pale greyish-green thallus; rounded to elongate apothecia, yellowish-brown discs with white pruina, obscured periphysoids, inspersed hymenium, 1-spored(rare 2-spored)ascus and muriform and hyalineascospores with halo. *Chapsa niveocarpa* is morphologically similar and phylogenetically related to *C. leprocarpa*, and both species occur on bark in tropical forests (Frisch 2006; Mangold 2008; Parnmen et al. 2012). *Chapsa leprocarpa* differs from *C. niveocarpa* in having a lower hymenium (100–130 µm) and smaller ascospores (up to 111 µm long) (Frisch 2006). The specimen (HN19508) we collected in China is allocated phylogenetically to a strongly-supported (1/91) clade with *C. niveocarpa*. The collections cited above are the first reports for China.

Key to *Chapsa* in China

1 Disc with red pruina; ascospores 1/ascus, muriform, 105–135 × 30–50 μm. ..... ***C. wolseleyana***
– Disc with white pruina **2**
2 Ascospores transversely septate; ascospores 4–8/ascus, 50–110 × 6–12 μm.... ..... ***C. indica***
– Ascospores (sub)muriform **3**
3 Hamathecium inspersed; ascospores 1/ascus, 80–190 × 20–50 μm ***4***
– Hamathecium clear..... **5**
4 Ascospores 1/ascus, 80–190 × 20–50 μm..... ***C. niveocarpa***
– Ascospores 8/ascus, 40–50 × 11–15 μm..... ***C. mirabilis***
5 Asci 4−6 (8)-spored; acsospores oblong to cylindrical with rounded to subacute ends, submuriform with 20–25 transverse septa and 0–2 longitudinal septa per segment, 75–105 × 9.5−16 μm ..... ***C. murioelongata***
– Asci 4-spored; acsospores oblong to slightly ellipsoid, with roundish ends, 60–130 × 20–40 μm..... ***C. leprocarpa***

Acknowledgements

This study was supported by the National Natural Science Foundation of China (31750001), Doctoral Initiation Fund of Liaocheng University (318051813) and Research Fund of Liaocheng University (318012011).

References

Dou MZ, Wu XH, Li M, Zhao X, Jia ZF (2018) *Gyalecta caudiospora* sp. nov. from China. Mycotaxon 133(4): 721–727. https://doi.org/10.5248/133.721

Frisch A (2006) Contribution towards a new systematic of the lichen family Thelotremataceae. I. The lichen family Thelotremataceae in Africa. Bibliotheca Lichenologica 92: 1–370.

Frisch A, Kalb K (2009) *Chapsa* species (Thelotremataceae) from Brazil. Bibliotheca Lichenologica 99: 133–142.

Gardes M, Bruns TD (1993) ITS primers with enhanced specificity for Basidiomycetes – application to the identification of mycorrhiza and rusts. Molecular Ecology 2: 113–118. https://doi.org/10.1111/j.1365-294X.1993.tb00005.x

Jia ZF, Lücking R (2017) Resolving the genus *Phaeographina* Müll. Arg. in China. Mycokeys 21(1): 13 –32.

Jia ZF, Wei JC (2016) Flora Lichenum Sinicorum, vol. 13. – Ostropales (I) – Graphidaceae 1. Science Press, Beijing, 21–22.

Joshi S, Upreti DK, Nayaka S (2012) The lichen genus *Chapsa* (Graphidaceae) in India. Mycotaxon 120: 23–24, 27, 31, 32. https://doi.org/10.5248/120.23

Joshi S, Upreti DK, Divakar PK, Lumbsch HT, Lücking R (2018) A re-evaluation of thelotremoid Graphidaceae (lichenized Ascomycota: Ostropales) in India. The Lichenologist 50(6): 634–639. https://doi.org/10.1017/S0024282918000439

Kalb J, Kalb K (2017) New lichen species from Thailand, new combinations and new additions to the Thai lichen biota. Phytotaxa 332 (2): 141–156. https://doi.org/10.11646/phytotaxa.332.2.2

Kantvilas G, Vězda A (2000) Studies on the lichen family Thelotremataceae in Tasmania. The genus *Chroodiscus* and its relatives. Lichenologist 32(4): 325–357. https://doi.org/10.1006/lich.2000.0274

Katoh K, Standley DM (2013) MAFFT multiple sequence alignment software version 7: improvements in performance and usability. Molecular Biology and Evolution 30: 772–780. https://doi.org/10.1093/molbev/mst010

Kraichak E, Parnmen S, Lücking R, Lumbsch HT (2013) *Gintarasia* and *Xalocoa*, two new genera to accommodate temperate to subtropical species in the predominantly tropical Graphidaceae (Ostropales, Ascomycota). Australian Systematic Botany 26: 466–474. https://doi.org/10.1071/SB13038

Lanfear R, Frandsen PB, Wright AM, Senfeld T, Calcott B (2017) PartitionFinder 2: new methods for selecting partitioned models of evolution for molecular and morphological phylogenetic analyses. Molecular Biology and Evolution 34(3): 772–773. https://doi.org/10.1093/molbev/msw260

Lima EL, Maia LC, Martins MCB, da Silva NL, Lücking R, da Silva Cáceres ME (2019) Five new species of Graphidaceae from the Brazilian Northeast, with notes on *Diorygma alagoense*. The Bryologist 122(3): 414–422. https://doi.org/10.1639/0007-2745-122.3.414

Lumbsch HT, Ahti T, Altermann S, De Paz GA, Aptroot A, Arup U et al. (2011) One hundred new species of lichenized fungi: a signature of undiscovered global diversity. Phytotaxa 18: 36–40. https://doi.org/10.11646/phytotaxa.18.1.1

Mangold A (2008) Taxonomic studies on members of Thelotrematoid Ostropales (Lichenized Ascomycota) in Australia. PhD Thesis, University of Duisburg, Essen.

Massalongo AB (1860) Esame comparativo di alcune genere di licheni. Atti dell´Istituto Veneto Scienze 5: 247–276.

Orange A, James PW, White FJ (2010) Microchemical methods for the identification of lichens. British Lichen Society, London, 101 pp.

Papong K, Boonpragob K, Mangold A, Divakar PK, Lumbsch HT (2010) Thelotremoid lichen species recently described from Thailand: a re-evaluation. The Lichenologist 42(2): 131–137. https://doi.org/10.1017/S0024282909990405

Parnmen S, Lücking R, Lumbsch HT (2012) Phylogenetic classification at generic level in the absence of distinct phylogenetic patterns of phenotypical variation: a case study in Graphidaceae (Ascomycota). PLoS ONE 7(12): e51392. https://doi.org/10.1371/journal.pone.0051392

Parnmen S, Cáceres MES, Lücking R, Lumbsch HT (2013) *Myriochapsa* and *Nitidochapsa*, two new genera in Graphidaceae (Ascomycota: Ostropales) for chroodiscoid species in the *Ocellularia* clade. The Bryologist 116(2): 127–133. https://doi.org/10.1639/0007-2745-116.2.127

Poengsungnoen V, Buaruang K, Vongshewarat K, Sangvichien K, Boonpragob K, Mongkolsuk P, Lumbsch HT (2019) Three new crustose lichens from Thailand. The Bryologist 122(3): 451–456. https://doi.org/10.1639/0007-2745-122.3.451

Rivas Plata R, Lücking R, Lumbsch HT (2011) A new classification for the family Graphidaceae (Ascomycota: Lecanoromycetes: Ostropales). Fungal Diversity 52(1): 107–121. https://doi.org/10.1007/s13225-011-0135-8

Rivas Plata R, Lücking R, Sipman HJM, Mangold A, Klab K, Lumbsch HT (2010) A worldwide key to the thelotremoid Graphidaceae, excluding the Ocellularia-Myriotrema-Stegobolus clade. The Lichenologist 42(2): e139185.

Ronquist F, Teslenko M, van der Mark P, Ayres DL, Darling A, Hohna S, Larget B, Liu L, Suchard MA, Huelsenbeck JP (2012) MrBayes 3.2: efficient Bayesian phylogenetic inference and model choice across a large model space. Systematic Biology 61: 539–542. https://doi.org/10.1093/sysbio/sys029

Sipman HJM, Lücking R, Aptroot A, et al. (2012) A first assessment of the Ticolichen biodiversity inventory in Costa Rica and adjacent areas: the thelotremoid Graphidaceae (Ascomycota: Ostropales). Phytotaxa 55: 1–214. https://doi.org/10.11646/phytotaxa.55.1.1

Stamatakis A (2014) RAxML version 8: A tool for phylogenetic analysis and post-analysis of large phylogenies. Bioinformatics 30(9): 1312–1313. https://doi.org/10.1093/bioinformatics/btu033

Vilgalys R, Hester M (1990) Rapid genetic identification and mapping of enzymatically amplifed ribosomal DNA from several *cryptococcus* species. Journal of Bacteriology 172(8): 4238–4246. https://doi.org/10.1128/JB.172.8.4238-4246.1990

Weerakoon G, Rivas Plata, Lumbsch HT, Lücking R (2012) Three new species of *Chapsa* (lichenized Ascomycota: Ostropales: Graphidaceae) from tropical Asia. The Lichenologist 44(3): 373–379. https://doi.org/10.1017/S0024282911000892

Wei JC (2020) The enumeration of lichenized fungi in China. China Forestry Publishing House, Beijing, 606 pp.

White T, Bruns T, Lee S, Taylor J (1990) Amplification and direct sequencing of fungal ribosomal RNA genes for phylogenetics. In: Innis MA, Gelfand DH, Snisky JJ, White TJ (Eds) PCR Protocols: a guide to methods and applications. Academic Press, New York, 315–322. https://doi.org/10.1016/B978-0-12-372180-8.50042-1

Wijayawardene NN, Hyde KD, Rajeshkumar KC, Hawksworth DL, Madrid H, Kirk PM, Braun U, Singh RV, Crous PW, Kukwa M, Lücking R, Kurtzman CP, Yurkov A, Haelewaters D, Aptroot A, Lumbsch HT, Timdal E, Ertz D, Etayo J, Phillips AJL, Groenewald JZ, Papizadeh M, Selbmann L, Dayarathne MC, Weerakoon G, Jones EBG, Suetrong S, Tian Q, Castañeda-Ruiz RF, Bahkali AH, Pang KL, Tanaka K, Dai DQ, Sakayaroj J, Hujslová M, Lombard L, Shenoy BD, Suija A, Maharachchikumbura SSN, Thambugala KM, Wanasinghe DN, Sharma BO, Gaikwad S, Pandit P, Zucconi L, Onofri S, Egidi E, Raja HA, Kodsueb R, Cáceres MES, Pérez-Ortega S, Fiuza PO, Monteiro JS, Vasilyeva LN, Shivas RG, Prieto M, Wedin M, Olariaga I, Lateef AA, Agrawal Y, Fazeli SAS, Amoozegar MA, Zhao GZ, Pfliegler WP, Sharma G, Oset M, Abdel-Wahab MA, Takamatsu S, Bensch K, de Silva NI, Kesel AD, Karunarathna A, Boonmee S, Pfister DH, Lu YZ, Luo ZL, Boonyuen N, Daranagama DA, Senanayake IC, Jayasiri SC, Samarakoon MC, Zeng XY, Doilom M, Quijada L, Rampadarath S, Heredia G, Dissanayake AJ, Jayawardana RS, Perera RH, Tang LZ, Phukhamsakda C, Hernández-Restrepo M, Ma X, Tibpromma S, Gusmao LFP,

Weerahewa D, Karunarathna SC (2017) Notes for genera: Ascomycota. Fungal Diversity 86: e96. https://doi.org/10.1007/s13225-017-0386-0

Xu LL, Wu QH, Wang QD, Jia ZF (2016) *Chapsa* (Graphidaceae, Ostropales), A lichen genus new to China. Journal of Tropical and Subtropical Botany 24(5): 495–498.

Zhang D, Gao FL, Jakovli I, Zou H, Wang GT (2020). Phylosuite: an integrated and scalable desktop platform for streamlined molecular sequence data management and evolutionary phylogenetics studies. Molecular Ecology Resources 20(1): 348–355. https://doi.org/10.1111/1755-0998.13096

Zoller S, Scheidegger C, Sperisen C (1999) PCR primers for the amplification of mitochondrial small subunit ribosomal DNA of lichen-forming ascomycetes. Lichenologist 31: 511–516. https://doi.org/10.1006/lich.1999.0220

MycoKeys 85: 87–108 (2021)
doi: 10.3897/mycokeys.85.71957
https://mycokeys.pensoft.net

RESEARCH ARTICLE

A peer-reviewed open-access journal
MycoKeys
Launched to accelerate biodiversity research

Two new *Inosperma* (Inocybaceae) species with unexpected muscarine contents from tropical China

Lun-Sha Deng[1], Rui Kang[2], Nian-Kai Zeng[1], Wen-Jie Yu[1], Cheng Chang[3], Fei Xu[4], Wang-Qiu Deng[5], Liang-Liang Qi[6], Yu-Ling Zhou[2], Yu-Guang Fan[1]

1 *Key Laboratory of Tropical Translational Medicine of Ministry of Education, Transgenic Laboratory, Tropical Environment and Health Laboratory, College of Pharmacy, Hainan Medical University, Haikou 571199, China* **2** *Hainan Institute for Food Control, Haikou 570314, China* **3** *Jilin Provincial Joint Key Laboratory of Changbai Mountain Biocoenosis and Biodiversity, Changbai Mountain Academy of Sciences, Yanbian 133613, China* **4** *Physical and Chemical Department, Ningxia Hui Autonomous Region Center for Disease Control and Prevention, Yinchuan 750004, China* **5** *State Key Laboratory of Applied Microbiology Southern China, Guangdong Provincial Key Laboratory of Microbial Culture Collection and Application, Guangdong Institute of Microbiology, Guangdong Academy of Sciences, Guangzhou 510070, China* **6** *Microbiology Research Institute, Guangxi Academy of Agriculture Sciences, Nanning 530007, China*

Corresponding author: Yu-Guang Fan (mycena@qq.com)

Academic editor: T. Lumbsch | Received 23 July 2021 | Accepted 24 November 2021 | Published 15 December 2021

Citation: Deng L-S, Kang R, Zeng N-K, Yu W-J, Chang C, Xu F, Deng W-Q, Qi L-L, Zhou Y-L, Fan Y-G (2021) Two new *Inosperma* (Inocybaceae) species with unexpected muscarine contents from tropical China. MycoKeys 85: 87–108. https://doi.org/10.3897/mycokeys.85.71957

Abstract

An accurate identification of poisonous mushrooms and the confirmation of the toxins involved are both of great importance in the treatment of mushroom poisoning incidents. In recent years, cases of mushroom poisoning by *Inosperma* spp. have been repeatedly reported from tropical Asia. It is urgent to know the real species diversity of *Inosperma* in this region. In the present study, we proposed two new *Inosperma* species from tropical Asia, namely *I. muscarium* and *I. hainanense*. They were described based on morphology and multilocus phylogeny. Detailed descriptions, color photographs and the discussion with other closely related species of the two new taxa were provided. In addition, a comprehensive muscarine determination of these two new species using ultrahigh performance liquid chromatography tandem mass spectrometry (UPLC-MS/MS) approach has been performed. Results showed that these two species were muscarine positive, with a content of 16.03 ± 1.23 g/kg in *I. muscarium* and a content of 11.87 ± 3.02 g/kg in *I. hainanense*, much higher than the known species *I. virosum*. Recovery of muscarine ranged from 93.45% to 97.25%, and the average recovery is 95.56%.

Keywords

Agaricales, muscarine, new species, phylogeny, taxonomy

Introduction

Muscarine $C_9H_{20}NO_2^+$, CAS number: 300–54–9, is a toxic alkaloid found in Inocybaceae, *Clitocybe* and several other mushroom genera (Patocka et al. 2021). The ingestion of muscarine-containing mushrooms would cause diaphoresis, salivation, urination, nausea, vomiting, gastrointestinal effects and muscular cramp, and fatal muscarinic syndromes like miosis, bronchoconstriction, and bradycardias in humans (Wilson 1947; Lurie et al. 2009; Chandrasekharan et al. 2020; Latha et al. 2020; Patocka et al. 2021), or even death (Pauli et al. 2005; Işıloğlu et al. 2009; Zosel et al. 2015). Many species of Inocybaceae are known to contain muscarine (Malone et al. 1962), especially in *Inocybe sensu stricto*, and *Pseudosperma* (Kosentka et al. 2013; Matheny et al. 2020). *Inosperma*, a genus in Inocybaceae, is supposed to contain only a small number of muscarine positive species (Kosentka et al. 2013). However, mushroom poisoning events caused by *Inosperma* species were repeatedly reported from tropical Asia in recent years (Chandrasekharan et al. 2020; Li et al. 2021; Parnmen et al. 2021). Accordingly, it is urgent to enrich the knowledge of species diversity of the genus and to detect their muscarine toxin contents in tropical Asia.

Inosperma was erected as a subgenus of *Inocybe* with *Inocybe calamistrata* (Fr.) Gillet as type (Kühner 1980), and is now treated as genus rank (Matheny et al. 2020). Members in this genus are characterized by small to medium-sized basidiomata, rimose to scaly pileus, often rubescent context, phaseoliform to subglobose basidiospores, thin-walled cheilocystidia, lack of pleurocystidia, and often with distinctive odors. *Inosperma* species are widespread and there are seventy-one taxa documented globally (http://www.indexfungorum.org, retrieved 7 Oct. 2021). The tropical elements of *Inosperma* comprise several recently described, and still a few undescribed taxa, which were divided into two separate Old World tropical clades (Kropp et al. 2013; Matheny et al. 2020; Aïgnon et al. 2021; Deng et al. 2021). Interestingly, most of the taxa from Old World tropical clade 1 were mainly distributed in western Africa (Matheny et al. 2020; Aïgnon et al. 2021), and species in Old World tropical clade 2 were mainly from tropical Asia (Deng et al. 2021).

During our field works around the tropical China, two new *Inosperma* species were discovered. The present study aims to describe these two new tropical species using a combined data of morphology and phylogeny, and to determine their muscarine contents, in order to provide an accurate data for the prevention and clinical treatment of potential *Inosperma* poisoning accidents.

Materials and methods

Research area and specimens sampling

Our collections were made from *Castanopsis* dominated forests in Hainan, Guangdong Provinces, and Guangxi Zhuang Autonomous Region of China, with a tropical or subtropical climate. Specimens were photographed in the field using a digital camera and

then described soon after collection. The specimens were dried through an electronic drier at 45 °C overnight, and were then preserved in plastic bags and sealed. After study, dried specimens were deposited in the Fungal Herbarium of Hainan Medical University (FHMU), Haikou City, Hainan Province of China, or in the Fungarium of Guangdong Institute of Microbiology (GDGM), Guangzhou, China.

Morphological study

Marcoscopic features were made from field notes and photographs. Color notations follow Kornerup and Wanscher (1978). Microscopic characters from dried materials mounted in KOH (5%) or mixed with Congo Red (1%) solution were observed with a microscope and photographed using a digital camera. Randomly selected twenty basidiospores and ten basidia for each specimen, the length and width of each basidiospore and basidium were measured, excluding the apiculus and sterigmata respectively (Kobayashi 2009). Numbers in square brackets [n/m/p] represent "n" basidiospores measured from "m" basidiomata of "p" specimens (Zhang et al. 2019). The dimensions of basidiospores and Q values are expressed as (a) b–c (d), "a" and "d" denote extreme values ("a" < 5^{th} percentile; "d" > 95^{th} percentile), while the ranges "b–c" means 5^{th} to 95^{th} percentile values. The quotient Q = length/width ratio for individual basidiospore, and Q_m means the average of Q values (Dramani et al. 2020).

DNA extraction, PCR and sequencing

Genomic DNA was extracted from dried specimens using the NuClean Plant Genomic DNA kit (ComWin Biotech, Beijing). The following primers were used: ITS1F/ITS4 for ITS (Gardes and Bruns 1993), LR0R/LR7 for LSU (Vilgalys and Herster 1990), bRPB2-6F/bRPB2-7.1R for *rpb2* (Matheny 2005). The volume of polymerase chain reaction (PCR) mixture solution was 25 μL, containing 9.5 μL dd H_2O, 12.5 μL 2×Taq Plus MasterMix (Dye), 1 μL of each primer, and 1 μL of template DNA. PCR conditions for ITS, LSU and *rpb2* followed Wang et al. (2021), that the conditions of PCR for three different gene regions are all the same as denaturation at 95 °C for 1 min at first, then followed by 35 cycles of denaturation at 95 °C for 30 s, annealing at 52 °C for 1 min, extension at 72 °C for 1 min, and a final extension at 72 °C for 8 min. Afterwards, the products of amplifications were sent to the Beijing Genomics Institute for purification and sequenced as soon as possible.

Analysis of sequence data

Sequences in this study were prepared and compared with closely related *Inosperma* sequences that were retrieved from GenBank (https://www.ncbi.nlm.nih.gov/) through BLAST tool (https://blast.ncbi.nlm.nih.gov/Blast.cgi) or literature survey (Larsson et al. 2009; Kropp et al. 2013; Horak et al. 2015; Nasser et al. 2017; Bau and Fan 2018; Matheny and Kudzma 2019; Matheny et al. 2020; Deng et al. 2021; Aïgnon et al.

2021; Cervini et al. 2021; Bandini et al. 2021). Then sequences from three genes were aligned respectively using MAFFT online service (https://mafft.cbrc.jp/alignment/server/) (Katoh et al. 2019) and were edited by BioEdit version 7.0.9.0 (Hall 1999). Two taxa in *Auritella* (*A. hispida* and *A. spiculosa*) were served as outgroups (Matheny et al. 2020). MrModeltest v2.3 was used to select the best-fit model for each gene partition for Bayes analysis (Nylander 2004). The datasets of each locus were combined in MEGA 5.02 (Tamura 2011). Maximum likelihood (ML) was inferred under partitioned models using W-IQ-TREE Web Service (http://iqtree.cibiv.univie.ac.at/), and the ultrafast bootstrapping was done with 1000 replicates (Trifinopoulos et al. 2016). Bayesian analysis was performed in MrBayes v.3.2.7a (Ronquist et al. 2012).

Muscarine toxin detection

Methods for sample preparation and analysis through UPLC-MS/MS were followed by Xu et al. (2020) with some modifications. Dried samples were ground to a fine power respectively, to 20 mg of each homogenised portion, 2 mL methanol-water solution (5:95 v/v) was added. The extraction was vortexed in a vortex mixer for 30 min, the mixture was further extracted by using an ultrasonic bath for another 30 min, and centrifuged for 5 min with 10000 rpm speed. Total supernatant was collected, using 0.22 μm organic filter membrane to filtrate for UPLC-MS/MS analysis and diluted with methanol-water (5:95, v/v) when necessary. The blank sample used here was *Lentinula edodes*. The optimal MS parameters and product ion confirmation settings followed Xu et al. (2020), while the chromatographic column we used was ACQUITY UPLC BEH Amide (2.1 mm × 100 mm, 1.7 μm). The muscarine content was estimated in the mushroom extract by using standard muscarine (Sigma-Aldrich, Chemical purity ≥ 98%). The analytical results are reported as Mean ± SD g/kg, where Mean is the average content of muscarine in the mushroom from each experimental species, and SD represents its standard deviation.

Results

Phylogenetic inference

The final multilocus dataset (Table 1) includes 94 taxa and 3130 characters, and 37 new sequences (14 ITS, 12 LSU and 11 *rpb2*) were generated in this study and then submitted to GenBank. The alignment was deposited in TreeBase (28515). The best-fit models for each gene selected by MrModelGUI are GTR+I+G equally. The Maximum likelihood (ML) and Bayesian analyses for the combined dataset provide a best scoring tree is shown in Fig. 1. Three ectomycorrhizal samples (KIC27, KI54, and KIB1) and an environmental sample grouped together with eight specimens of *I. muscarium*

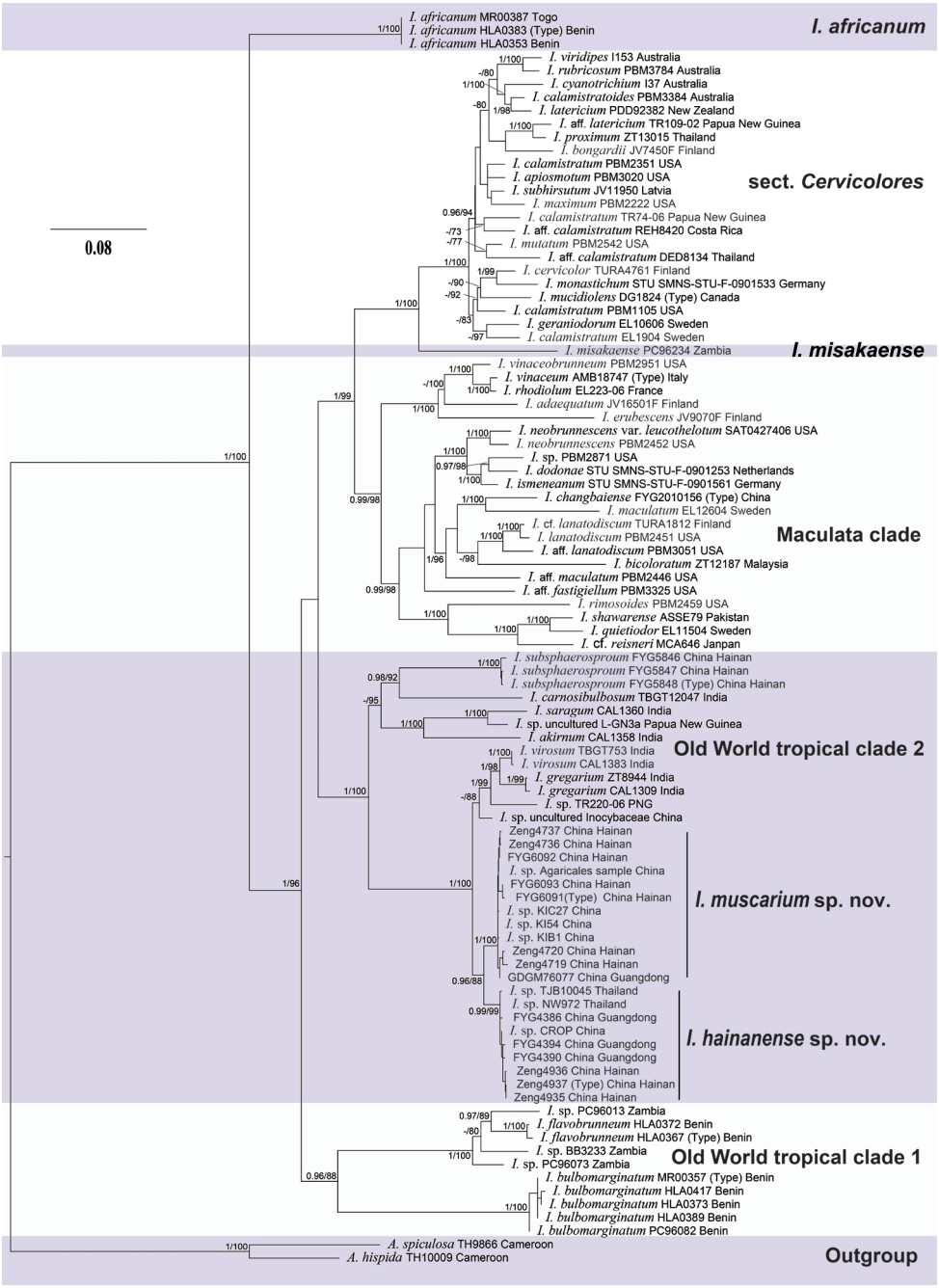

Figure 1. Phylogram generated by Bayesian Inference (BI) analyses based on sequences of a combined data set from nuclear genes (rDNA-ITS, nrLSU, and *rpb2*), rooted with *Auritella hispida* and *A. spiculosa.* Bayesian Inference posterior probabilities (BI-PP) ≥0.95 and ML bootstrap proportions (ML-BP) ≥70 are represented as BI-PP/ML-BP. *I. muscarium* sp. nov. and *I. hainanense* sp. nov. are two newly described taxa.

Table 1. Taxon sampling information and DNA sequences used for phylogenetic analyses

Taxa	Collection number/ Herbaium	Locality	GenBank accession number			Reference
			ITS	LSU	*rpb2*	
Auritella hispida	TH10009	Cameroon	KT378203	KT378207	KT378215	Matheny et al. (2020)
Auritella spiculosa	TH9866	Cameroon	KT378204	KT378206	KT378214	Matheny et al. (2020)
Inosperma adaequatum	JV16501F	Finland	–	AY380364	AY333771	Matheny et al. (2020)
Inosperma aff. *lanatodiscum*	PBM3051	USA	JQ801401	JN975026	JQ846485	Pradeep et al. (2016)
Inosperma aff. *calamistratum*	DED8134	Thailand	GQ892983	GQ892937	–	Pradeep et al. (2016)
Inosperma aff. *calamistratum*	REH8420	Costa Rica	JQ801390	JN975018	JQ846471	Pradeep et al. (2016)
Inosperma aff. *fastigiellum*	PBM3325	USA	JQ801399	JQ815419	JQ846477	Pradeep et al. (2016)
Inosperma aff. *latericium*	TR109-02	Papua New Guinea	JQ801405	JN975023	JQ846487	Pradeep et al. (2016)
Inosperma aff. maculatum	PBM2446	USA	DQ241778	AY745700	EU569863	Pradeep et al. (2016)
Inosperma africanum	MR00387	Togo	MN096189	MN097881	MT770739	Aïgnon et al. (2021)
Inosperma africanum	HLA0383 (Type)	Benin	MT534298	MT560733	–	Aïgnon et al. (2021)
Inosperma africanum	HLA0353	Benin	MT534299	–	–	Aïgnon et al. (2021)
Inosperma akirnum	CAL1358	India	KY440085	KY549115	KY553236	Matheny et al. (2020)
Inosperma apiosmotum	PBM3020	USA	JQ801385	JN975021	JQ846463	Matheny et al. (2020)
Inosperma bicoloratum	ZT12187	Malaysia	GQ892984	GQ892938	JQ846464	Pradeep et al. (2016)
Inosperma bongardii	JV7450F	Finland	–	EU555448	–	Pradeep et al. (2016)
Inosperma bulbomarginatum	MR00357 (Type)	Benin	MN096190	MN097882	MN200775	Aïgnon et al. (2021)
Inosperma bulbomarginatum	HLA0417	Benin	MT534300	MT560734	–	Aïgnon et al. (2021)
Inosperma bulbomarginatum	HLA0373	Benin	MT534301	–	–	Aïgnon et al. (2021)
Inosperma bulbomarginatum	HLA0389	Benin	MT534302	–	–	Aïgnon et al. (2021)
Inosperma bulbomarginatum	PC96082	Benin	JQ801412	JN975027	–	Aïgnon et al. (2021)
Inosperma calamistratoides	PBM3384	Australia	JQ801393	JQ815415	KJ729949	Pradeep et al. (2016)
Inosperma calamistratum	PBM1105	USA	JQ801386	JQ815409	JQ846466	Pradeep et al. (2016)
Inosperma calamistratum	EL1904	Sweden	AM882938	AM882938	–	Pradeep et al. (2016)
Inosperma calamistratum	PBM2351	USA	–	AY380368	AY333764	Pradeep et al. (2016)
Inosperma calamistratum	TR74-06	Papua New Guinea	JQ801391	JN975020	JQ846472	Pradeep et al. (2016)
Inosperma carnosibulbosum	TBGT12047	India	KT329448	KT329454	KT329443	Pradeep et al. (2016)
Inosperma cervicolor	TURA4761	Finland	JQ801395	JQ815417	JQ846474	Pradeep et al. (2016)
Inosperma cf. *lanatodiscum*	TURA1812	Finland	JQ408763	JQ319694	JQ846484	Pradeep et al. (2016)
Inosperma cf. *reisneri*	MCA646	Japan	–	EU555463	–	Pradeep et al. (2016)
Inosperma changbaiense	FYG2010156 (Type)	China	MH047251	MG844976	MT086755	Bau and Fan (2018)
Inosperma cyanotrichium	I37	Australia	JQ801396	JN975033	JQ846476	Pradeep et al. (2016)
Inosperma dodonae	SMNS-STU-F-0901253	Netherlands	MW647615	–	–	Bandini et al. (2021)
Inosperma erubescens	JV9070F	Finland		EU569846	–	Pradeep et al. (2016)
Inosperma flavobrunneum	HLA0372	Benin	MT534290	MT536756	–	Aïgnon et al. (2021)
Inosperma flavobrunneum	HLA0367 (Type)	Benin	MN096199	MT536754	–	Aïgnon et al. (2021)
Inosperma geraniodorum	EL10606	Sweden	FN550945	FN550945	–	Pradeep et al. (2016)
Inosperma gregarium	ZT8944	India	–	EU600903	EU600902	Pradeep et al. (2016)
Inosperma gregarium	CAL1309	India	KX852305	KX852306	KX852307	Latha and Manimohan. (2016)
Inosperma hainanense	**Zeng4936**	**China**	**MZ374069**	**MZ374760**	**MZ388103**	**The present study**
Inosperma hainanense	**Zeng4937 (Type)**	**China**	**MZ374070**	**MZ374761**	**MZ388104**	**The present study**
Inosperma hainanense	**Zeng4935**	**China**	**MZ374071**	**MZ374762**	**MZ388105**	**The present study**
Inosperma hainanense	**FYG4386**	**China**	**MZ374072**	–	–	**The present study**
Inosperma hainanense	**FYG4390**	**China**	**MZ374073**	**MZ374763**	–	**The present study**
Inosperma hainanense	**FYG4394**	**China**	**MZ374068**	–	–	**The present study**
Inosperma ismeneanum	STU:SMNS-STU-F-0901561	Germany	MW647625	–	–	Bandini et al. (2021)

Taxa	Collection number/ Herbaium	Locality	GenBank accession number			Reference
			ITS	LSU	*rpb2*	
Inosperma lanatodiscum	PBM2451	USA	JQ408759	JQ319690	JQ846483	Pradeep et al. (2016)
Inosperma latericium	PDD92382	New Zealand	GU233367	GU233413	–	Pradeep et al. (2016)
Inosperma maculatum	EL12604	Sweden	AM882964	AM882964	–	Pradeep et al. (2016)
Inosperma maximum	PBM2222	USA		EU569854	–	Pradeep et al. (2016)
Inosperma misakaense	PC96234	Zambia	JQ801409	EU569875	AY333767	Pradeep et al. (2016)
Inosperma monastichum	STU:SMNS-STU-F-0901533	Germany	MW647631	–	–	Bandini et al. (2021)
Inosperma mucidiolens	DG1824 (Type)	Canada	HQ201339	HQ201340	–	Pradeep et al. (2016)
Inosperma muscarium	**Zeng4720**	**China**	**MZ373978**	**MZ373988**	**MZ388089**	**The present study**
Inosperma muscarium	**Zeng4736**	**China**	**MZ373979**	**MZ373989**	**MZ388090**	**The present study**
Inosperma muscarium	**Zeng4737**	**China**	**MZ373980**	–	**MZ388091**	**The present study**
Inosperma muscarium	**Zeng4719**	**China**	**MZ373981**	**MZ373990**	**MZ388092**	**The present study**
Inosperma muscarium	**FYG6091 (Type)**	**China**	**MZ373982**	**MZ373991**	**MZ388093**	**The present study**
Inosperma muscarium	**FYG6092**	**China**	**MZ373983**	**MZ373992**	**MZ388094**	**The present study**
Inosperma muscarium	**FYG6093**	**China**	**MZ373984**	**MZ373993**	**MZ388095**	**The present study**
Inosperma muscarium	**GDGM76077**	**China**	**MZ520549**	**MZ520550**	**MZ542730**	**The present study**
Inosperma neobrunnescens	PBM2452	USA	–	EU569868	EU569867	Pradeep et al. (2016)
Inosperma neobrunnescens var. *leucothelotum*	SAT0427406	USA	JQ801411	JN975025	JQ846489	Pradeep et al. (2016)
Inosperma proximum	ZT13015	Thailand	EU600839	EU600840		Matheny et al. (2020)
Inosperma quietiodor	EL11504	Sweden	AM882960	AM882960		Pradeep et al. (2016)
Inosperma rhodiolum	EL223-06	France	FJ904175	FJ904175		Pradeep et al. (2016)
Inosperma rimosoides	PBM2459	USA	DQ404391	AY702014	DQ385884	Pradeep et al. (2016)
Inosperma rubricosum	PBM3784	Australia	KP308817	KP170990	KM406230	Pradeep et al. (2016)
Inosperma saragum	CAL1360	India	KY440103	KY549133	KY553249	Latha and Manimohan (2017)
Inosperma shawarense	ASSE79	Pakistan	KY616964	KY616966		Naseer et al. (2018)
Inosperma sp.	PBM2871	USA	HQ201348	HQ201348	JQ846475	Pradeep et al. (2016)
Inosperma sp.	BB3233	Zambia	JQ801415	EU600885		Pradeep et al. (2016)
Inosperma sp.	L-GN3a	Papua New Guinea	JX316732	JX316732		Pradeep et al. (2016)
Inosperma sp.	TJB10045	Thailand	KT600658	KT600659	KT600660	Pradeep et al. (2016)
Inosperma sp.	TR22006	Papua New Guinea	JQ801416	JN975017	JQ846496	Pradeep et al. (2016)
Inosperma sp.		China	LS983441			Unpublished
Inosperma sp.	CROP	China	MF532817			Unpublished
Inosperma sp.		China	LS975930			Unpublished
Inosperma sp.	NW972	Thailand	MN492637			Unpublished
Inosperma sp.	KIB1	China	JX456867			Unpublished
Inosperma sp.	KIC27	China	JX456949			Unpublished
Inosperma sp.	KI54	China	JX456860			Unpublished
Inosperma sp.	PC96013	Zambia	JQ801383	EU600883	EU600882	Pradeep et al. (2016)
Inosperma sp.	PC96073	Zambia	JQ801417	EU600870	EU600869	Pradeep et al. (2016)
Inosperma subhirsutum	JV11950	Latvia		EU555452	AY333763	Pradeep et al. (2016)
Inosperma subsphaerosproum	FYG5848 (Type)	China	MW403825	MW397171	MW404237	Deng et al. (2021)
Inosperma subsphaerosproum	FYG5847	China	MW403826	MW397172	MW404238	Deng et al. (2021)
Inosperma subsphaerosproum	FYG5846	China	MW403827	MW397173	MW404239	Deng et al. (2021)
Inosperma vinaceobrunneum	PBM2951	USA		HQ201353	JQ846478	Pradeep et al. (2016)
Inosperma vinaceum	AMB18747	Italy	MW561108	MW561120		Cervini et al. (2021)
Inosperma viridipes	I153	Australia	KP641646	KP171095	KM656139	Pradeep et al. (2016)
Inosperma virosum	TBGT753	India	KT329452	KT329458	KT329446	Pradeep et al. (2016)
Inosperma virosum	CAL1383	India	KY440108	KY549138	KY553253	Latha and Manimohan (2017)

with significant support (BP = 100%, PP = 1). In addition, two specimens (TJB10045 and NW972) from Thailand and an environmental sample (CROP denovo 1461) from China grouped together with six specimens of *I. hainanense* with high support (BP = 99%, PP = 0.99). The two new *Inosperma* species formed separate lineages and were sister with significant support (BP = 88%, PP = 0.96) to each other. These two new species formed a subclade in the Old World tropical clade 2. The subclade was sister to *I. virosum* (K.B. Vrinda, C.K. Pradeep, A.V. Joseph & T.K. Abraham ex C.K. Pradeep, K.B. Vrinda & Matheny) Matheny & Esteve-Rav., *I. gregarium* (K.P.D. Latha & Manimohan) Matheny & Esteve-Rav., and an undescribed specimen *I.* sp. (TR220-06) from Papua New Guinea with full support (BP = 100%, PP = 1).

Taxonomy

Inosperma muscarium **Y.G. Fan, L.S. Deng, W.J. Yu & N.K. Zeng, sp. nov.**
MycoBank: MB840527
Figures 2, 3

Etymology. "*muscarium*" refers to its high content of muscarine.

Holotype. China, Hainan Province, Ledong Li Autonomous County, Yinggeling substation of Hainan Tropical Rainforest National Park, under *Castanopsis* forest, at 19°1'20"N, 109°23'33"E, alt. 550 m, 26 April 2021, FYG6091 (FHMU3162), GenBank accession number: ITS (MZ373982); LSU (MZ373991) and *rpb2* (MZ388093).

Diagnosis. Basidiomata small to medium-sized. Pileus rimulose to rimose with an indistinct umbo, lamellae rather crowded. Basidiospores smooth, enlongate ellipsoid to ellipsoid. Cheilocystidia clavate. Under *Castanopsis* forest. Differs from *I. hainanense* by its more robust habit, elongate basidiospores, and narrower cheilocystidia.

Basidiomata. small to medium-sized. Pileus 25–60 mm diam., conical convex to convex when young, becoming broadly convex to plano-convex with a small indistinct umbo when mature, margin slightly incurved when young, becoming somewhat reflexed with age. Surface dry, smooth with distinct ivory white (5A1) veil layer around the disc when young, then appressed with indistinct veil remnants, fibrillose-rimulose elsewhere, margin usually strongly rimose with age; yellowish brown (5D8) to chocolate brown (5E8) around the center and on the fibrils, yellowish brown (5C6) elsewhere, yellowish brown (6C6) to slightly dark brown (6E7) all over the basidiomata when overmatured. Lamellae rather crowded, adnexed, initially pure white to pale off-white (4B1), becoming grayish white (5B1) to yellowish white (4A2), dirty yellow (4A3) to yellowish brown (5B4) when overmatured, 1.5–3 mm wide, edge fimbriate, faint serrate to somewhat wavy. Stipe 35–72 × 3–8 mm, central, solid, terete, equal with a slightly swollen apex and base; with sparse fibrils at apex, longitudinally fibrillose downwards the stipe, with white tomentose hyphae at the base; initially white

Figure 2. Basidiomata of *Inosperma muscarium* **a–e** basidiomata **f–h** rimose to rimulose pileus **i** lamellae **j–k** lamellae edge **l–m** stipe surface. **a–b, d, f–g, i–m** FHMU3162 (holotype) **c, e** FYG6092 (FHMU3163) **h** FYG6093 (FHMU3164). Scale bars: 10 mm (**a–m**). Photos by Y.-G. Fan.

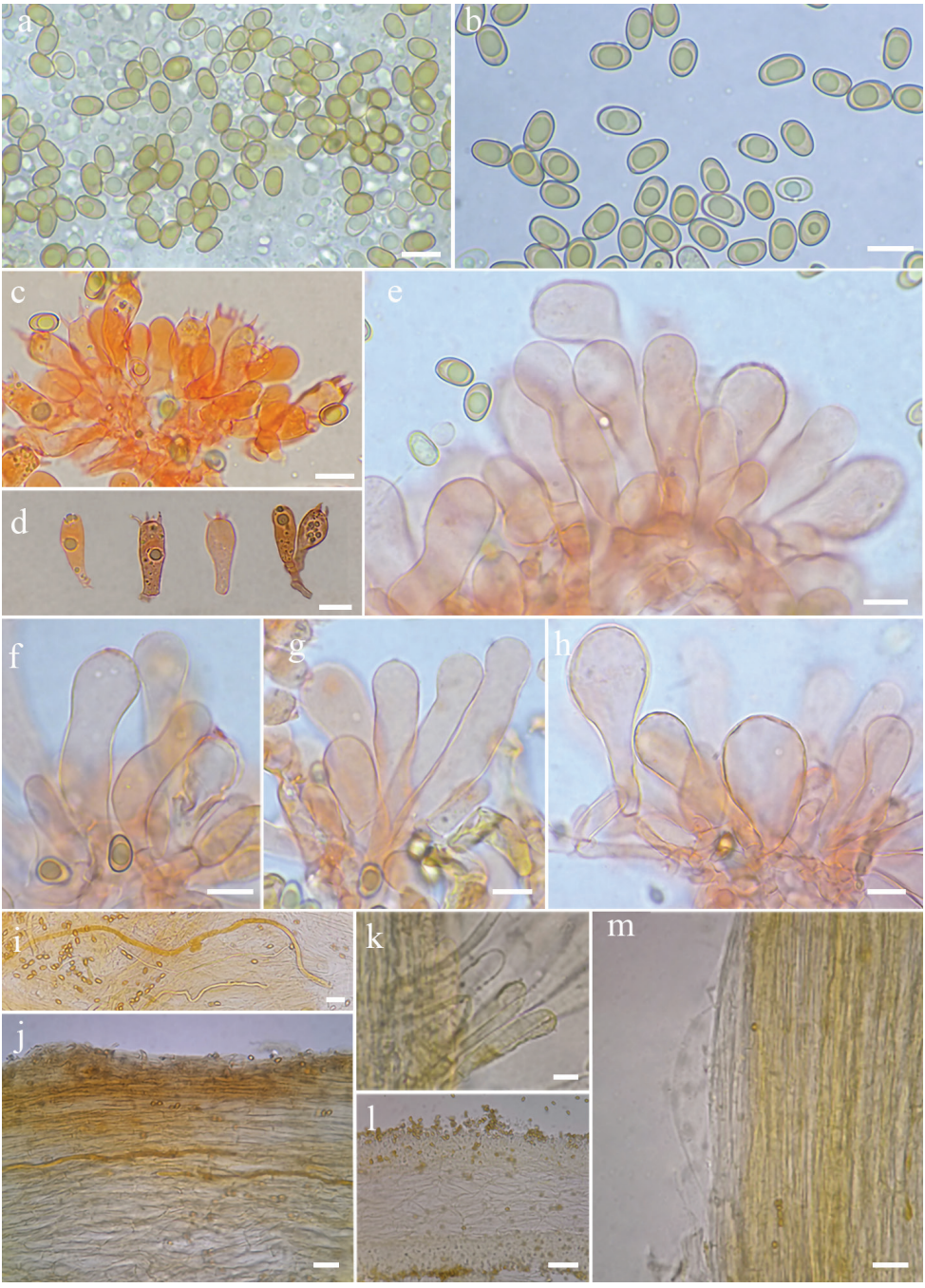

Figure 3. Microscopic features of *Inosperma muscarium* (FHMU3162, holotype) **a–b** basidiospores **c–d** basidia **e–h** cheilocystidia in clusters **i** oleiferous hyphae **j** pileipellis and pileal trama **k** terminal hyphae at the stipe apex **l** hymenophoral trama **m** stipitipellis and stipe trama. Scale bars: 10 μm (**a–m**). Photos by L.-S. Deng

(5A1) to cream white(3A2), yellowish (4A3) or brownish (5A3) with age, brown (5B6) to dark brown (5C5) when old. Context solid, fleshy in pileus, 0.5–1 mm thick at mid-radius, 1.5–4.5 mm under the umbo, white to ivory white (5A1) at first, becoming brownish white (5B2); fibrillose and striate in the stipe, white to yellowish (4A2) or flesh color (4B3). Odor fungoid, slightly grassy or mild.

Basidiospores. [180/9/9] 8–10(11) × 5–6 (6.5) μm, Q = (1.15)1.42–1.86(2.00), Q_m=1.63, mostly ellipsoid to enlongate ellipsoid, occasionally sub-phaseoliform, smooth, thick-walled, yellowish, apiculus small, indistinct, with a spherical to ellipsoid yellowish brown oil-droplet inside. Basidia 17–24 × 7–9 μm, clavate to broadly clavate, obtuse at apex, slightly tapering towards the base, 4-spored, sterigmata 2–4 μm in length, thin-walled, hyaline or pale yellow, with oily drops in various sizes with age. Pleurocystidia none. Lamella edge sterile. Cheilocystidia 36–50 × 9–14 μm, abundant and crowded, mostly clavate, broadly clavate to enlongate-clavate, rarely balloon-shaped, apices rounded to obtuse, or occasionally subcapitate, thin- to slightly thick-walled, septate, often constricted at septa, colorless to yellowish, sometimes with golden yellow inclusions. Hymenophoral trama 75–108 μm thick, sub-regular, colorless to yellowish, composed of thin-walled, smooth, cylindric to mostly inflated, hyphae 12–25 μm wide, somewhat constricted at the both ends of per hyphae. Pileipellis a cutis, sub-regular, composed of thin-walled, brown to yellowish brown, cylindrical, slightly encrusted hyphae 4–10 μm wide. Pileal trama colorless, regular to subregular, hyphae 12–25 μm wide. Stipitipellis a cutis, regularly arranged, occasionally with small clusters of terminal cheilocystidoid cells at the stipe apex, cheilocystidoid cells 31–47 × 9–10 μm, rare, clavate to enlongate clavate, hyaline or pale yellow, thin- to slightly thick-walled, some with golden yellow inclusions. Caulocystidia not observed. Oleiferous hyphae 4–13 μm wide, scattered in pileus and stipe tramal tissue, yellow or bright golden yellow, smooth, often bent, sometimes diverticulate. Clamp connections present, common in all tissues.

Habitat. Gregarious in clusters, usually scattered with numerous clusters under *Castanopsis* forest, late March to August in tropical China.

Known distribution. China (Hainan, Guangdong, Guangxi), Thailand.

Additional materials examined. China. Hainan Province, Ledong Li Autonomous County, Yinggeling substation of Hainan Tropical Rainforest National Forest Park, under *Castanopsis* forest, 13 August 2020, N.K. Zeng, Zeng4720 (FHMU3158); Same location, under *Castanopsis* forest, 14 August 2020, N.K. Zeng Zeng4736 (FHMU3159); Zeng4737 (FHMU3160), Same location, 26 April 2021, Y.G. Fan, L.S. Deng & Q.Q. Chen, FYG6092 (FHMU3163); FYG6093 (FHMU3164); FYG6094 (FHMU3173); Guangdong Province, Yangchun City, Gangmei Town, Lunshui Village, under *Castanopsis* forest, 29 March 2019, W.Y. Huang, GDGM76077; Guangxi Zhuang Autonomous Region: Wuzhou City, Cangwu Country, Wangfu Town, 23°40'28"N, 111°29'6"E, alt. 30 m, Under *Castanopsis* dominated forest, 29 May 2021, L.L. Qi, WSW10286, (FHMU3174).

Inosperma hainanense **Y.G. Fan, L.S. Deng, W.J. Yu & N.K. Zeng, sp. nov.**
MycoBank: MB840528
Figures 4, 5

Etymology. "*hainanense*" refers to the its type locality.

Holotype. China, Hainan Province, Changjiang Li Autonomous County, Bawangling substation of Hainan Tropical Rainforest National Park, under *Castanopsis* dominated forest, at 19°7'12.43"N, 109°7'6.29"E, alt. 630 m, 2 September, 2020, N.K. Zeng, Zeng4937 (FHMU3166), GenBank accession number: ITS (MZ374070); LSU (MZ374761) and *rpb2* (MZ388104).

Diagnosis. Distinguishes from *I. muscarium* by its slender basidiomata, ellipsoid to ovoid basidiospores, and mostly vesiculose cheilocystidia.

Basidiomata. small to medium-sized. Pileus 25–53 mm diam., conical to convex at young age, becoming applanate to uplifted with age, with a broad to subacute umbo, margin initially decurved, straight to somewhat wavy when mature; surface dry, smooth when young, fibrillose-rimulose elsewhere, strongly rimose towards the margin with age; chocolate brown (5D8) to somewhat dark brown (5F7) around the disc, straw yellow (4A6) to yellowish brown (4B5) elsewhere, background pallid to cream white (4B1), becoming brown (5B4) to dark brown (5C6) with age; Lamellae rather crowded, adnexed, initially ivory white (5A1) to grayish white (5B2), becoming dirty yellowish (5B5) to brownish (5C7) when matured, completely brown (5D6) after drying, 2–3 mm in width, edge fimbriate, slightly serrate. Stipe 40–72 × 3–5 mm, central, nearly terete, equal with a slightly swollen apex, base somewhat swollen; nearly smooth and longitudinally striate all over the stipe; initially ivory (5A1) to yellowish white (5A2) at the upper half, yellowish to brownish (4B5) downwards, becoming uniformly yellowish brown (4B7) to brown (4C7) with age. Context solid, fleshy in pileus, white to grayish white (4B1), pale brown under the umbo (4B2), 1–2 mm thick at mid-radius, 4–5 mm thick under the umbo, fibrillose in stipe, pallid to yellowish (4A2) or brownish (4B2), striate, shiny. Odor indistinct or slightly acid.

Basidiospores. [180/9/9] 8–9(10.5) × 5–7 μm, Q = (1.18)1.28–1.64 (1.78), Q_m = 1.43, mostly ellipsoid to ovoid, occasionally subphaseoliform, smooth, slightly thick-walled, brown to yellowish brown, apiculus small, indistinct, with a spherical to ellipsoid yellowish brown oil-droplet. Basidia 21–28 × 6–9 μm, clavate, often obtuse at apex, slightly tapered towards the base, thin-walled, 4-spored, sometimes 2-spored, sterigmata 4–6 μm in length, with spherical yellowish brown to golden yellow brown oily inclusions. Pleurocystidia absent. Lamella edge sterile. Cheilocystidia 34–55 × 15–25 μm, abundant and crowded, mostly obovoid to balloon-shaped, occasionally broadly clavate, rarely enlongate-clavate, thin- to slightly thick-walled (up to 1 μm thick); often rounded or slightly obtuse at apex, colorless to pale yellow, sometimes with golden yellow pigments. Hymenophoral trama 75–138 μm thick, sub-regular, hyaline to slightly yellow, composed of cylindric to inflated hyphae 20–33 μm wide, slightly constricted at septa. Pileipellis a cutis, hyphae 2.5–10 μm wide, thin-walled, pale yellow to yellowish brown, cylindrical, sometimes slightly encrusted. Pileal trama regular to subregular, hyphae 12–30 μm wide,

Figure 4. Basidiomata of *Inosperma hainanense* **a–e** basidiomata **f–g** rimose to rimulose pileus **h** lamellae **i** lamellae edge **j–k** stipe surface. **c** FHMU3166 (holotype) **a–b, d–g, i–k** FHMU6511 **h** FHMU3168. Scale bars: 10 mm (**a–k**). **a–b, d–k**: photos by L.-S. Deng; **c**: photos by N.-K. Zeng

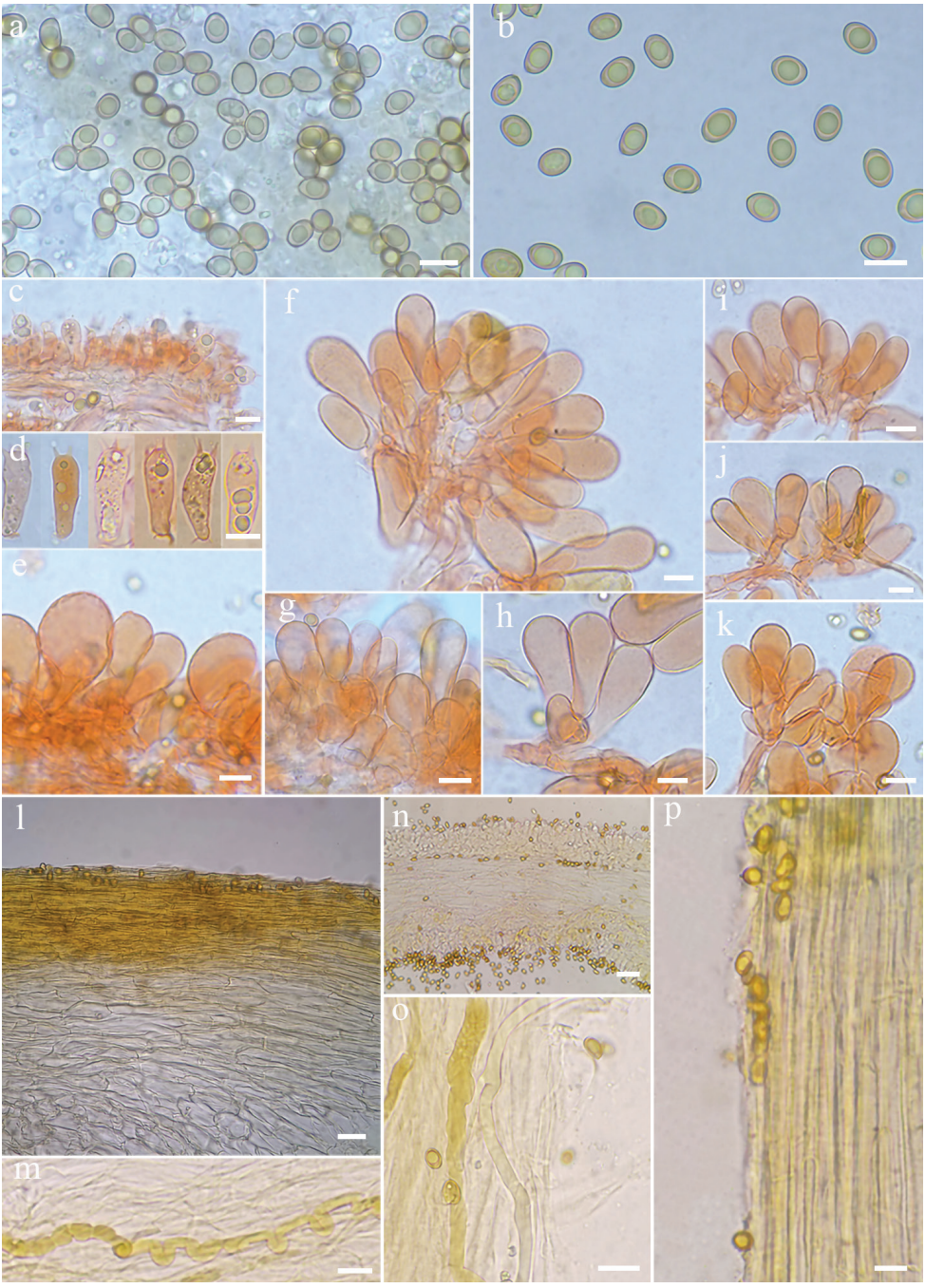

Figure 5. Microscopic features of *Inosperma hainanense* (FHMU3166, holotype) **a–b** basidiospores **c–d** basidia **e–k** cheilocystidia in clusters **l** pileipellis and pileal trama **n** hymenophoral trama **m, o** oleiferous hyphae **p** stipitipellis and stipe trama. Scale bars: 10 μm (**a–k**). Photos by L.-S. Deng

thin-walled, colorless. Stipitipellis a cutis, regularly arranged, walls yellowish to bright yellow. Oleiferous hyphae 2.5–10 μm wide, commonly scattered in pileus and stipe tramal tissues, straw yellow or bright golden yellow, smooth, often bent or diverticulate. Clamp connections observed in all tissues.

Habitat. Scattered or gregarious in small clusters under *Castanopsis* dominated forest, June to September in tropical China.

Known distribution. China (Hainan, Guangdong).

Additional materials examined. China. Hainan Province, Wuzhishan City, Maoyang Town, Maoyang Village, 11 August 2021, Y.G. Fan & L.S. Deng, FYG6440 (FHMU6513); Ganshiling Provincial Nature Reserve, L.S. Deng & Y.G. Fan, DLS0043 (FHMU6512); Changjiang Li Autonomous County, Bawangling substation of Hainan Tropical Rainforest National Park, under *Castanopsis* dominated forest, 2 September 2020, N.K. Zeng, Zeng4936 (FHMU3165); Zeng4935 (FHMU3167); Guangdong Province, Guangzhou City, Tianluhu Forest Park, 2 June 2019, Y.G. Fan & W.J. Yu, FYG4386 (FHMU3168); Shaoguan City, Danxiashan Nature Reserve, 4 June 2019, Y.G. Fan & W.J. Yu, FYG4388 (FHMU3175); 4390 (FHMU3169); FYG4394 (FHMU3170).

Muscarine detection

Representative chromatograms of muscarine were shown in Fig. 8. The muscarine toxin content was confirmed by linear equation according to the analysis of UPLC-MS/MS, it was found that both of the two new species contained muscarine toxin, and the content of *Inosperma muscarium* was 16.03 ± 1.23 g/kg while *I. hainanense* was 11.87 ± 3.02 g/kg. Muscarine was identified by comparing retention time (1.22 min) and relative deviation (0.82%) in the allowable relative range of 25 % base on the qualitative analysis. The calibration curve for muscarine generated during the validation was $y = 2083.17\ x – 209.297$ ($r = 0.9988$) for muscarine concentration in the range of 2–200 ng/mL (y represents the peak area, and x is muscarine concentration, r is correlation coefficient). Recovery of muscarine ranged from 93.45% to 97.25%, and the average recovery was 95.56%.

Discussion

New species delimitation

The phylogenetic results place both the two new species in the Old World tropical clade 2 in genus *Inosperma* (Kropp et al. 2013; Pradeep et al. 2016; Deng et al. 2021), and they are sister to each other with significant support (BP = 88%, PP = 0.96). Morphologically, they share yellowish brown pileus, longitudinally striate stipe, crowded lamellae, and elliptic basidiospores. It is really difficult to distinguish the two new species by their macromorphology, in spite of the fact that *I. hainanense* has a relatively more slender habit, more finely rimulose in pileus, and a smoother stipe surface. However, they could

be easily distinguished by their outlines of basidiospores and cheilocystidia. As is shown in Figs 6–7, *I. muscarium* has more elongated basidiospores in outline, as well as narrower cheilocystidia (*I. muscarium*: 36–50 × 9–14 µm; *I. hainanense*: 34–55 × 15–25 µm).

In Old World tropical clade 2, *I. gregarium* and *I. virosum*, both of which described from India, formed a sister lineage with the two new species. They also share fibrillose-

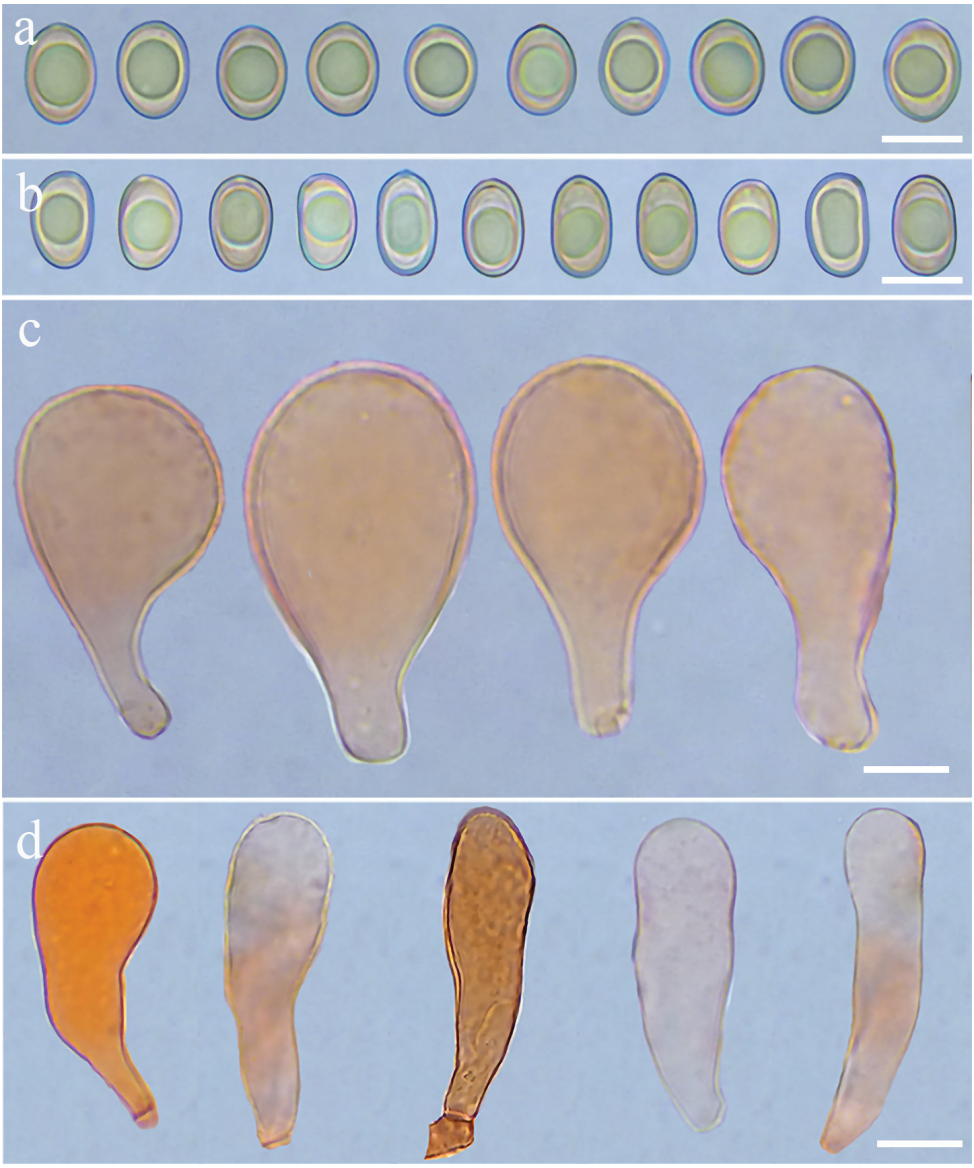

Figure 6. The comparisons of the two new species in their outline of basidiospores and cheilocystidia shape **a, c** basidiospores and cheilocystidia of *I. hainanense* (FHMU3162, holotype); **b, d** Basidiospores and cheilocystidia of *I. muscarium* (FHMU3166, holotype). Scale bars: 10 µm (**a–d**). Photos by L.-S. Deng

rimose pileus, longitudinally striate stipe, crowded lamellae, and elliptic basidiospores (Vrinda et al. 1996; Latha and Manimohan 2016). However, *I. gregarium* differs from the two new species by its smaller basidiospores (7–8.5 × 5–5.5 µm, Q = 1.3–1.8, Q_m = 1.6), versiform and longer cheilocystidia (24–60 × 16–24 µm), the presence of caulocystidia, and an association with Dipterocarpaceae trees (Latha and Manimohan 2016). *Inosperma virosum* differs in having smaller basidiospores (6.5–8.5 × 5–6 µm, Q = 1.3–1.6, Q_m = 1.4), and an association also with Dipterocarpaceae trees (Vrinda et al. 1996; Latha and Manimohan 2017). The remaining species in this subgrouping resemble the two new species to some extent; however, they have appressed-scaly or appressed-fibrillose pileus and different phylogenetic positions (Latha and Manimohan 2017).

There are eight described species in Old World tropical clade 2 so far, three of which were described from China in Fagaceae forest (Deng et al. 2021), and the rest five species were all described from India under Dipterocarpaceae forest or among ginger plants (Pradeep et al. 2016; Latha and Manimohan 2017). By our current knowledge, members in this subgrouping usually have medium-sized basidiomata, gregarious habit, appressed-scaly or fibrillose-rimose pileus, rather crowded lamellae, longitudinally striate stipe, non-changing context, subglobose to elliptic basidiospores, and the lack of distinctive odors (Pradeep et al. 2016; Latha and Manimohan 2017; Deng et al. 2021).

Muscarine toxin in Inosperma

The compound muscarine was initially isolated and identified from *Amanita muscaria* with the content at about 0.0003% of the fresh weight (Spoerke and Rumack 1994). However, muscarine was more commonly found in Inocybaceae and *Clitocybe* spp. with significant concentrations reached the highest record of 1.6%. (Lurie et

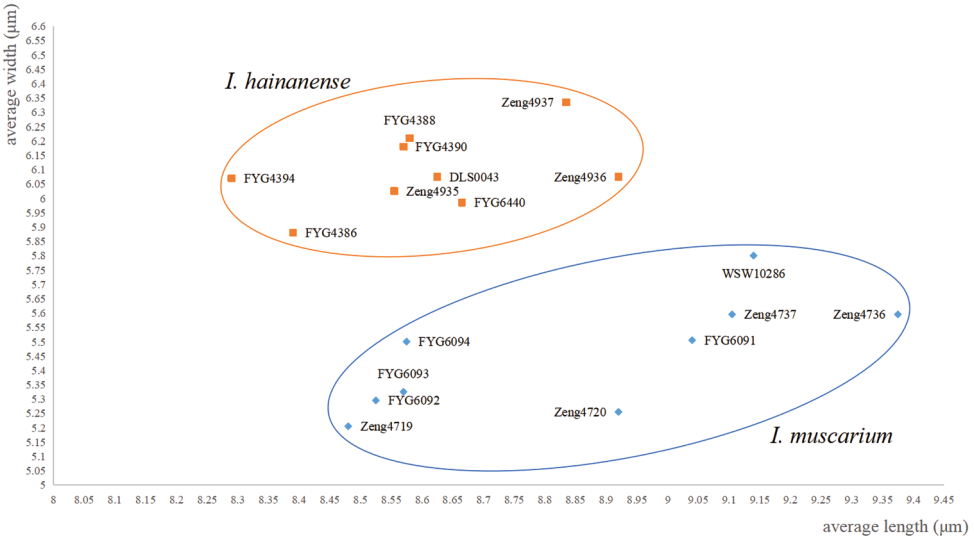

Figure 7. The comparisons of the two new species in their dimensions of basidiospores.

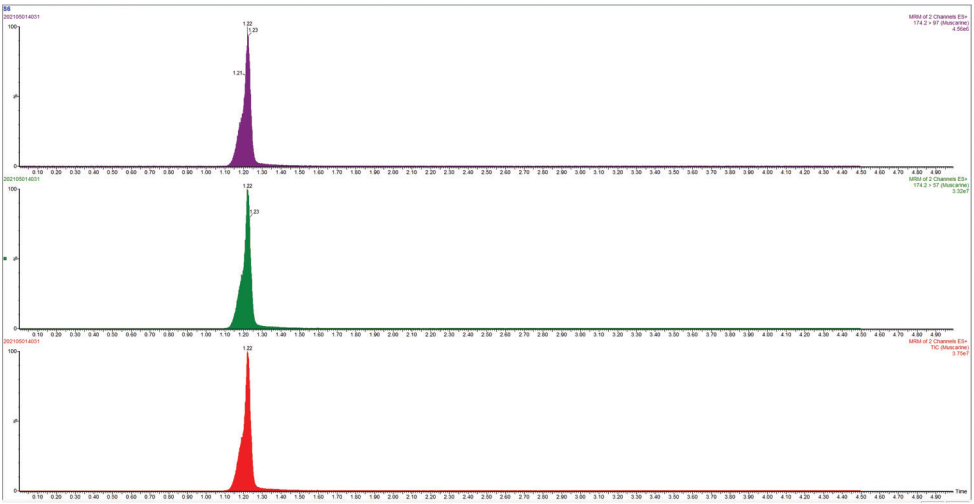

Figure 8. Representative chromatograms of muscarine.

al. 2009). Many Inocybaceae species were well known to contain muscarine (Peredy et al. 2014; Patocka et al. 2021), and various methods have been used to detect this toxin in the past years (Fahrig 1920; Eugster 1957; Brown et al. 1962; Robbers 1964; Kosentka et al. 2013; Latha et al. 2020). Five *Inosperma* species were reported as muscarine positive, including *I. cervicolor* (Pers.) Matheny & Esteve-Rav., *I. erubescens* (A. Blytt) Matheny & Esteve-Rav., *I. maculatum* (Boud.) Matheny & Esteve-Rav., *I. vinaceobrunneum* (Matheny, Ovrebo & Kudzma) Haelew. and *I. virosum* (K.B. Vrinda, C.K. Pradeep, A.V. Joseph & T.K. Abraham ex C.K. Pradeep, K.B. Vrinda & Matheny) Matheny & Esteve-Rav. (Kosentka et al. 2013; Latha et al. 2020). In addition, *I. carnosibulbosum* (C.K. Pradeep & Matheny) Matheny & Esteve-Rav., a species described from India, is probably a muscarine positive species due to a recent report of poisonous case (Chandrasekharan et al. 2020). Among these muscarine positive species in *Inosperma*, *I. virosum* described from India, is more extensively studied in toxin detection, toxicity in vitro using NCM460 colon epithelial cell line, toxic effects in vivo and pharmacokinetics of muscarine (Latha et al. 2020). The muscarine content of *I. virosum* is 270 or 300 mg/kg reported by separate studies (Sailatha et al. 2014; Latha et al. 2020).

Surprisingly, of the two new species we assayed, both of them have a high content of muscarine that is about 30 to 50 times higher than *I. virosum* (Sailatha et al. 2014; Latha et al. 2020). For humans, a lethal dose of muscarine is estimated from 40 mg to 495 mg (Pauli et al. 2005). Based on the muscarine concentrations of between 0.1% to 0.33% (dry weight) in Inocybaceae spp., a single mushroom can be lethal (Puschner 2018; Patocka et al. 2021). Consequently, the two new species proposed by the present study were considered to be more dangerous when mistakenly ingested by humans. In particular, for *I. muscarium*, a species often with a medium-sized basidiomata, a gregarious, large, discrete clusters habitat, and the lack of aposematic coloration make it extremely easily collected by local people as an edible mushroom. The publicity and

education of the two new species were essential to prevent mushroom poisoning from tropical areas where they distributed.

The accurate identification of poisonous mushrooms and the knowledge of toxin type and contents are crucial for the treatment of mushroom poisoning patients (Li et al. 2021). However, species identification can usually be difficult for doctors when faced with mushroom-poisoned patients, mainly because of the insufficient identification data of wild poisoning mushrooms (Hall et al. 1987). Our present study provides detailed knowledge for a better prevention of potential *Inosperma* poisoning from tropical Asia.

Acknowledgements

The authors thank Dr. Shuai Jiang, Mr. Yongqing Fu (Hainan tropical rainforest National Park, China) and Mr. Weiyong Huang (Yangchun Center for Disease Control and Prevention, China) for their kind help in field work, and to Dr. Junqing Yan (Jiangxi Agricultural University, China) and Dr. Yupeng Ge (Ludong University, China) for their kind help in the phylogenetic analysis. This work was supported by the National Natural Science Foundation of China (Grant Nos. 31860009 & 31400024), Hainan Basic and applied research project for cultivating high level talents (2019RC230), The Innovative Research Projects for Graduate Students in Hainan Medical University, Hainan China (HYYS2020-42), and Jilin Provincial Foundation for Excellent Scholars (20180520035JH). We also thank the anonymous reviewers for their corrections and suggestions to improve our work.

References

Aïgnon HL, Jabeen S, Naseer A, Yorou NS, Ryberg M (2021) Three new species of *Inosperma* (Agaricales, Inocybaceae) from Tropical Africa. MycoKeys 77(1): 97–116. https://doi.org/10.3897/mycokeys.77.60084

Bandini D, Oertel B, Eberhardt U (2021) Even more fibre-caps (2): Thirteen new species of the family Inocybaceae. Mycologia Bavarica 21: 27–98.

Bau T, Fan YG (2018) Three new species of *Inocybe* sect. *Rimosae* from China. Mycosystema 37(6): 693–702. http://dx.doi.org/10.13346/j.mycosystema.180033.

Brown J, Malone M, Stuntz D, Tyler V (1962) Paper chromatographic determination of muscarine in *Inocybe* species. Journal of Pharmaceutical Sciences 51(9): 853–856. https://doi.org/10.1002/jps.2600510908.

Cervini M, Carbone M, Bizio E (2021) *Inosperma vinaceum*, una nuova specie distinta da *I. rhodiolum* e *I. adaequatum*. Rivista di Micologia 63(3): 215–241.

Chandrasekharan B, Pradeep C, Vrinda B (2020) *Inocybe* poisoning from Kerala– a case study. Journal of Mycopathological Research 57(4): 255–258.

Deng LS, Yu WJ, Zeng NK, Liu LJ, Liu LY, Fan YG (2021) *Inosperma subsphaerosporum* (Inocybaceae), a new species from Hainan, tropical China. Phytotaxa 502(2): 169–178. http://dx.doi.org/10.11646/phytotaxa.502.2.5.

Dramani R, Hegbe ADMT, Tabe A, Badou AS, Furneaux B, Ryberg M, Yorou NS (2020) How are basidiospore size measurements affected by drying? Current Research in Environmental and Applied Mycology 10(1): 63–70. https://doi.org/10.5943/cream/10/1/7

Eugster CH (1957) Isolierung von muscarin aus *Inocybe Patouillardi* (Bres.) 4. Mitteilung ber Muscarin. Helvetica Chimica Acta 40(4): 886–887. http://dx.doi.org/10.1002/hlca.19570400403.

Fahrig C (1920) Über die Vergiftung durch pilze aus der gattung *Inocybe* (Rißpilze und Faserköpfe). Archiv Für Experimentelle Pathologie Und Pharmakologie 88(5): 227–246. http://dx.doi.org/10.1007/BF01864886.

Gardes M, Bruns TD (1993) ITS primers with enhanced specificity for basidiomycetes – application to the identification of mycorrhizae and rusts. Molecular Ecology 2(2): 113–118. https://doi.org/10.1111/j.1365-294X.1993.tb00005.x

Hall A, Spoerke D, Rumack B (1987) Mushroom poisoning: identification, diagnosis, and treatment. Pediatrics in review / American Academy of Pediatrics 8(10): 291–298. http://dx.doi.org/10.1542/pir.8-10-291.

Hall TA (1999) BioEdit: A user-friendly biological sequence alignment editor and analysis program for Windows 95/98/NT. Nucleic Acids Symposium Series 41(41): 95–98.

Horak E, Matheny PB, Desjardin DE, Soytong K (2015) The genus *Inocybe* (Inocybaceae, Agaricales, Basidiomycota) in Thailand and Malaysia. Phytotaxa 230(3): 201–238. http://dx.doi.org/10.11646/phytotaxa.230.3.1.

Işiloğlu M, Helfer S, Alli H, Yilmaz F (2009) A fatal *Inocybe* (Fr.) Fr. poisoning in mediterranean Turkey. Turkish Journal of Botany 33(1): 71–73. http://dx.doi.org/10.3906/bot-0605-2.

Katoh K, Rozewicki J, Yamada KD (2019) MAFFT online service: multiple sequence alignment, interactive sequence choice and visualization. Briefings in Bioinformatics 20(4): 1160–1166. https://doi.org/10.1093/bib/bbx108.

Kobayashi T (2009) Notes on the genus *Inocybe* of Japan. IV. Species having metuloids collected from Hokkaido, Honshu, and Kyushu. Mycoscience 50(3): 203–211. http://dx.doi.org/10.1007/s10267-008-0472-y

Kornerup A, Wanscher JH (1978) The methuen handbook of colour 3rd edn. Eyre Methuen Ltd. Reprint, London, 252 pp.

Kosentka P, Sprague S, Ryberg M, Gartz J, May A, Campagna S, Matheny P (2013) Evolution of the toxins muscarine and psilocybin in a family of mushroom-forming fungi. PLoS ONE 8(5): e64646. http://dx.doi.org/10.1371/journal.pone.0064646.

Kropp BR, Matheny PB, Hutchison LJ (2013) *Inocybe* section *Rimosae* in Utah: phylogenetic affinities and new species. Mycologia 105(3): 728–747. https://doi.org/10.3852/12-185.

Kühner R (1980) Les Hyménomycètesagaricoïdes (Agaricales, Tricholomatales, Plutéales, Russulales). Etude générale et classification. Bulletin de la Société Linnéenne de Lyon 50(4): 1–1927.

Larsson E, Ryberg M, Moreau PA, Mathiesen AD, Jacobsson S (2009) Taxonomy and evolutionary relationships within species of section *Rimosae* (*Inocybe*) based on ITS, LSU and mtSSU sequence data. Persoonia 23(1): 86–98. https://doi.org/10.3767/003158509X475913

Latha KPD, Manimohan P (2017) Inocybes of Kerala. SporePrint Books, Calicut, 181 pp.

Latha KPD, Manimohan P (2016) *Inocybe gregaria*, a new species of the Inosperma clade from tropical India. Phytotaxa 286(2): 107–115. http://dx.doi.org/10.11646/phytotaxa.286.2.5.

Latha S, Shivanna N, Naika M, Anilakumar K, Kaul A, Mittal G (2020) Toxic metabolite profiling of *Inocybe virosa*. Scientific Reports 10(1): 13669. https://doi.org/10.1038/s41598-020-70196-7.

Li HJ, Zhang HS, Zhang YZ, Zhou J, Yin Y, He Q, Jiang SF, Ma PB, Zhang YT, Wen K, Yuan Y, Lang N, Cheng BW, Lu JJ, Sun CY (2021). Mushroom poisoning outbreaks – China, 2020. China CDC Weekly 3(3): 41–45. https://doi.org/10.46234/ccdcw2021.014

Lurie Y, Wasser S, Taha M, Shehade H, Nijim J, Hoffmann Y, Basis F, Vardi M, Lavon O, Suaed S, Bisharat B, Bentur Y (2009) Mushroom poisoning from species of genus *Inocybe* (fiber head mushroom): A case series with exact species identification *Inocybe* mushroom poisoning. Clinical Toxicology 47(6): 562–565. https://doi.org/10.1080/15563650903008448.

Malone MH, Robichaud RC, Tyler Jr V, Brady LR (1962) Relative muscarinic content of thirty *Inocybe* species. Lloydia 25: 231–237.

Matheny PB (2005) Improving phylogenetic inference of mushrooms with RPB1 and RPB2 nucleotide sequences (*Inocybe*, Agaricales). Molecular Phylogenetics and Evolution 35(1): 1–20. http://dx.doi.org/10.1016/j.ympev.2004.11.014

Matheny PB, Hobbs AM, Esteve-Raventós F (2020) Genera of Inocybaceae: New skin for the old ceremony. Mycologia 112(1): 83–120. https://doi.org/10.1080/00275514.2019.1668906

Matheny PB, Kudzma LV (2019) New species of *Inocybe* (Inocybaceae) from eastern North America. The Journal of the Torrey Botanical Society 146(3): 213–235. https://doi.org/10.3159/TORREY-D-18-00060.1

Naseer A, Khalid AN, Smith ME (2017) *Inocybe shawarensis* sp. nov. in the Inosperma clade from Pakistan. Mycotaxon 132(4): 909–918. http://dx.doi.org/10.5248/132.909

Nylander J (2004) MrModeltest V2. program distributed by the author. Bioinformatics 24: 581–583. https://doi.org/10.1093/bioinformatics/btm388

Parnmen S, Nooron N, Leudang S, Sikaphan S, Polputpisatkul D, Pringsulaka O, Binchai S, Rangsiruji A (2021) Foodborne illness caused by muscarine-containing mushrooms and identification of mushroom remnants using phylogenetics and LC-MS/MS. Food Control 128(4): 108182. https://doi.org/10.1016/j.foodcont.2021.108182.

Patocka J, Wu R, Nepovimova E, Valis M, Wu W, Kuca K (2021) Chemistry and toxicology of major bioactive substances in *Inocybe* mushrooms. International Journal of Molecular Sciences 22(4): 2218. https://doi.org/10.3390/ijms22042218.

Pauli J, Foot C (2005) Fatal muscarinic syndrome after eating wild mushrooms. The Medical Journal of Australia 182(6): 294–295. https://doi.org/10.5694/j.1326-5377.2005.tb06705.x.

Peredy T, Bradford H (2014) Mushrooms, Muscarine. Encyclopedia of Toxicology 3: 416–417. https://doi.org/10.1016/B978-0-12-386454-3.00758-2.

Pradeep CK, Vrinda KB, Varghese SP, Korotkin HB, Matheny PB (2016) New and noteworthy species of *Inocybe* (Agaricales) from tropical India. Mycological Progress 15(3): 1–25. http://dx.doi.org/10.1007/s11557-016-1174-z.

Puschner B (2018) Mushroom Toxins. In: Gupta RC (Ed.) Veterinary toxicology: basic and clinical principles: 3rd edn. Acdemic Press, Hopkinsville, KY, 955–966. http://dx.doi.org/10.1016/B978-0-12-811410-0.00067-2.

Robbers JE, Brady L, Tyler Jr V (1964) A chemical and chemotaxonomic evaluation of *Inocybe* species. Lloydia 27: 192–202.

Ronquist F, Teslenko M, van der Mark P, Ayres DL, Darling A, Höhna S, Larget B, Liu L, Suchard MA, Huelsenbeck JP (2012) MrBayes 3.2: Efficient Bayesian Phylogenetic Inference and Model Choice across a Large Model Space. Systematic Biology 61: 539–542. https://doi.org/10.1093/sysbio/sys029

Sailatha S, Naveen S, Naika M, Anilakumar KR, Singh M (2014) Toxicological evaluation of *Inocybe virosa*. In: Manjit S, Ramesh U, Parkash SV, Ahlawat, OP, Satish K, Shwet K, Bindvi A, Mamta G (Eds) Proceedings of the 8th international conference on mushroom biology and mushroom products (icmbmp8) volume ii. Papers presented in 8th ICMBMP, NASC, New Delhi (India), November 2014, Yugantar Prakashan Pvt. Ltd., 467–472.

Spoerke DG, Rumack BH (1994) Handbook of mushroom poisoning: diagnosis and treatment. CRC Press, London, 456 pp.

Tamura K, Peterson D, Peterson N, Stecher G, Nei M, Kumar S (2011) Mega5: molecular evolutionary genetics analysis using maximum likelihood, evolutionary distance, and maximum parsimony methods. Molecular Biology and Evolution 28(10): 2731–2739. https://doi.org/10.1093/molbev/msr121

Trifinopoulos J, Nguyen LT, von Haeseler A, Minh BQ (2016) W-IQ-TREE: a fast online phylogenetic tool for maximum likelihood analysis. Nucleic Acids Research 44(W1): 1–4. https://doi.org/10.1093/nar/gkw256.

Vilgalys R, Hester M (1990) Rapid genetic identification and mapping of enzymatically amplified ribosomal DNA from several *Cryptococcus* species. Journal of Bacteriology 172(8): 4238–4246. https://doi.org/10.1128/jb.172.8.4238-4246.1990

Vrinda KB, Pradeep CK, Joseph AV, Abraham TK (1996) A new *Inocybe* (Cortinariaceae) from Kerala state, India. Mycotaxon 57: 171–174.

Wang SN, Hu YP, Chen JL, Qi LL, Zeng H, Ding H, Huo GH, Zhang LP, Chen FS, Yan JQ (2021) First record of the rare genus *Typhrasa* (Psathyrellaceae, Agaricales) from China with description of two new species. MycoKeys 79: 119–128. https://doi.org/10.3897/mycokeys.79.63700

Wilson D (1947) Poisoning by *Inocybe fastigiata*. British Medical Journal 2(4520): 297. https://doi.org/10.1136/bmj.2.4520.297

Xu F, Zhang YZ, Zhang YH, Guan GY, Zhang KP, Li HJ, Wang JJ (2020) Mushroom poisoning from *Inocybe serotina*: A case report from Ningxia, northwest China with exact species identification and muscarine detection. Toxion 179: 72–75. https://doi.org/10.1016/j.toxicon.2020.03.003.

Zhang M, Li TH, Wang CQ, Zeng NK, Deng WQ (2019) Phylogenetic overview of *Aureoboletus* (Boletaceae, Boletales), with descriptions of six new species from China. MycoKeys 61(1): 111–145. https://doi.org/10.3897/mycokeys.61.47520.

Zosel A, Stanton M, Klager A, Gummin D (2015) Death following ingestion of *Clitocybe* species mushroom. Clinical Toxicology 53(7): 735–736. https://doi.org/10.4172/2161-0495.1000308.

MycoKeys 85: 109–125 (2021)
doi: 10.3897/mycokeys.85.75309
https://mycokeys.pensoft.net

RESEARCH ARTICLE

A peer-reviewed open-access journal
MycoKeys
Launched to accelerate biodiversity research

Two new species of *Phallus* (Phallaceae) with a white indusium from China

Ting Li[1,2], Wang-Qiu Deng[1], Bin Song[1], Ming Zhang[1], Mu Wang[3], Tai-Hui Li[1]

1 *State Key Laboratory of Applied Microbiology Southern China, Guangdong Provincial Key Laboratory of Microbial Culture, Collection and Application, Institute of Microbiology, Guangdong Academy of Sciences, Guangzhou 510070, China* **2** *College of Science, Tibet University, Lhasa 850011, China* **3** *Tibet Agricultural and Animal Husbandry University, Nyingchi 860000, China.*

Corresponding authors: Mu Wang (wangmutb@163.com), Tai-Hui Li (mycolab@263.net)

Academic editor: K. Hosaka | Received 6 September 2021 | Accepted 29 November 2021 | Published 16 December 2021

Citation: Li T, Deng W-Q, Song B, Zhang M, Wang M, Li T-H (2021) Two new species of *Phallus* (Phallaceae) with a white indusium from China. MycoKeys 85: 109–125. https://doi.org/10.3897/mycokeys.85.75309

Abstract

Two new *Phallus* species, *P. cremeo-ochraceus* and *P. rigidiindusiatus* were discovered in southwestern and southern China, respectively. *Phallus cremeo-ochraceus* is morphologically characterized by its cream to ochraceous receptacle, white to very slightly pinkish indusium, white to pinkish pseudostipe and white to slightly purplish pink volva. *Phallus rigidiindusiatus* is characterized by a white to yellowish white receptacle, a strongly rigid indusium usually without serrated margin and smaller basidiospores than those of *P. serratus*. Phylogenetic positions of the two species are located in two independent lineages respectively. Detailed descriptions, color photographs, illustrations and a key to the related species are presented.

Keywords

Edible mushrooms, Gasteromycetes, *Phallus indusiatus*, phylogeny, taxonomy

Introduction

Phallus Junius ex L. (1798) is a well-known and widespread gasteroid genus from tropical to temperate zones. Studies based on molecular phylogenetic analyses about a dozen years ago have shown that the existence of an indusium and a perforate pore at top of receptacle has no phylogenetic significance at generic level, and members of *Dictyophora* Desv. (1809), which are mainly characterized by possession of an

indusium, should be merged into genus *Phallus* (Cabral et al. 2012; Moreno et al. 2013). In the last decade, quite a lot of species with or without an indusium have been discovered under the genus of *Phallus* (Mohanan 2011; Li et al. 2014; Rebriev et al. 2014; Adamčík et al. 2015; Li et al. 2016; Medeiros et al. 2017; Trierveiler-Pereira et al. 2017; Song et al. 2018; Cabral et al. 2019; Li et al. 2020a).

Thirty-one species, nearly one-third of the world's total members of known *Phallus* species, have been recorded in China, and sixteen of them were originally reported from there. Many of them are notably edible mushrooms, for instance, *Phallus fragrans* M. Zang, *P. haitangensis* H.L. Li, P.E. Mortimer, J.C. Xu & K.D. Hyde, *P. lutescens* T.H. Li, T. Li & W.Q. Deng and *P. luteus* (Liou & L. Hwang) T. Kasuya; and some have even been produced commercially, e. g. *P. dongsun* T.H. Li, T. Li, Chun Y. Deng, W.Q. Deng & Zhu L. Yang, *P. echinovolvatus* (M. Zang, D.R. Zheng & Z.X. Hu) Kreisel, *P. rubrovolvatus* (M. Zang, D.G. Ji & X.X. Liu) Kreisel and *P. serratus* H. Li Li, L. Ye, P.E. Mortimer, J.C. Xu & K.D. Hyde (Zang end Ji 1985, 1988; Kreisel 1996; Kasuya 2008; Li et al. 2014, 2016, 2020a).

In the past decades, *Phallus indusiatus* Vent. (1798), characterized by a white and touching-ground indusium, had been reported from the tropical and subtropical Africa and Asia, temperate China, Japan, South Pacific islands, Australia and South America (Dring 1964; Kobayasi 1965; Liu et al. 2005; Young 2005; Cabral et al. 2019). However, recent studies revealed that many collections named as "*Phallus indusiatus*" or "*Dictyophora indusiata* (Vent.) Desv. (1809)" were misidentified, and *P. indusiatus* might be only distributed in Brazil and adjacent countries in South America, rather than widespread from the temperate and subtropical zones (Zang end Ji 1985; Calonge et al. 2005; Song et al. 2018; Cabral et al. 2019). *Phallus indusiatus* s.s. has recently been redescribed with a neotype, which strongly suggested that the *P. indusiatus*-like species from other continents should be considered different taxa from *P. indusiatus* s.s. (Cabral et al. 2019).

During these years, the authors further investigated the diversity of *Phallus* species from China with some new collections. Based on detailed morphological data and DNA-based phylogenetic analyses, two additional new *P. indusiatus*-like species to science were confirmed, and then formally introduced in this study.

Materials and methods

Morphological studies

Fresh specimens of *Phallus* with white or nearly white indusium were collected from various sites in southern and southwestern China. Photographs of the basidiomata were taken in the field with digital cameras in natural light. Voucher samples were dried with an electronic dryer and deposited in the Fungorum of Guangdong Institute of Microbiology (GDGM), Guangzhou, China. Methods for morphological descriptions followed the previous study by Li et al. (2020a). Color codes mentioned in the description were referenced from Kornerup and Wanscher (1978). Basidiospore di-

mensions were given as: (a) b–c (d), in which b–c contains 90% of the measured values and a or d represent extreme values. Q denotes to length/width ratio of an individual basidiospore, Q_m refers to the average Q value of all basidiospores.

Molecular studies

Genomic DNA were extracted from the dried materials using Fungi Genomic DNA Purification Kit (Sangon Biotech Co., Ltd.) following the instructions. The nuclear ribosomal large subunit (LSU) and internal transcribed spacer (ITS) regions were amplified using primer pairs LROR/LR5 and ITS1-F/ITS4, respectively (Vilgalys and Hester 1990; White et al. 1990). Newly generated sequences in this study were deposited to GenBank (https://www.ncbi.nlm.nih.gov/genbank). Available sequences of related species of *Phallus* and *Mutinus* were retrieved from the databases of GenBank or Unite Community (https://unite.ut.ee/), whereafter, aligned and edited the matrix of sequences using MAFFT v.7 (Katoh and Standley 2013) and BioEdit v.7.0.9 (Hall 1999).

In order to infer the phylogenetic relationships among new species and other known taxa of *Phallus*, two analyses were run; one for the ITS dataset and the other for ITS and LSU concatenated dataset. Maximum Likelihood (ML) and Bayesian Inference (BI) analyses were performed with MEGA v.7.0 (Hall 2013) and MrBayes v.3.1.2 (Ronquist and Huelsenbeck 2003), respectively. The best substitution model (Tamura 3-parameter+G+I) was chosen for both ITS and concatenated ITS-LSU analyses. Bootstrap (BS) analysis was implemented with 1,000 replicates. BI was calculated with 4 million and 14 million generations for ITS and ITS-LSU datasets, respectively, and stoprule command with the value of stoprule set to 0.01. Trees were sampled every 100 generations and obtained using the sump and sumt commands with the first 25% generations discarded as burn-ins. Branches corresponding to partitions reproduced <50% BS replicates were collapsed; the confidence values of BI were estimated with Posterior probabilities (PP), and discarded the values without reaching 0.95 PP. Trees were edited using FigTree version 1.4.2.

Results

Molecular phylogenetic results

In this study, sixteen sequences were newly generated from specimens of *Phallus* spp. and deposited in GenBank (Table 1), all of which were collected from China. In phylogenetic analyses, ITS dataset included 66 sequences from 27 taxa; ITS-LSU concatenated dataset included 77 assembled sequences consisting of 32 taxa; *Mutinus zenkeri* (Henn.) E. Fisch. (1900) was chosen as the outgroup (ITS: KC128650; LSU: KC128654) (Table 1). The ITS dataset contained 771 nucleotide sites (gaps included), and the concatenated dataset (ITS-LSU) contained 1687 nucleotide sites (gaps included) for each sample, of which 766 were ITS, 921 were LSU. In MrBays analyses, BI generations reached 3,458,000 for ITS dataset and 13,007,000 for ITS-

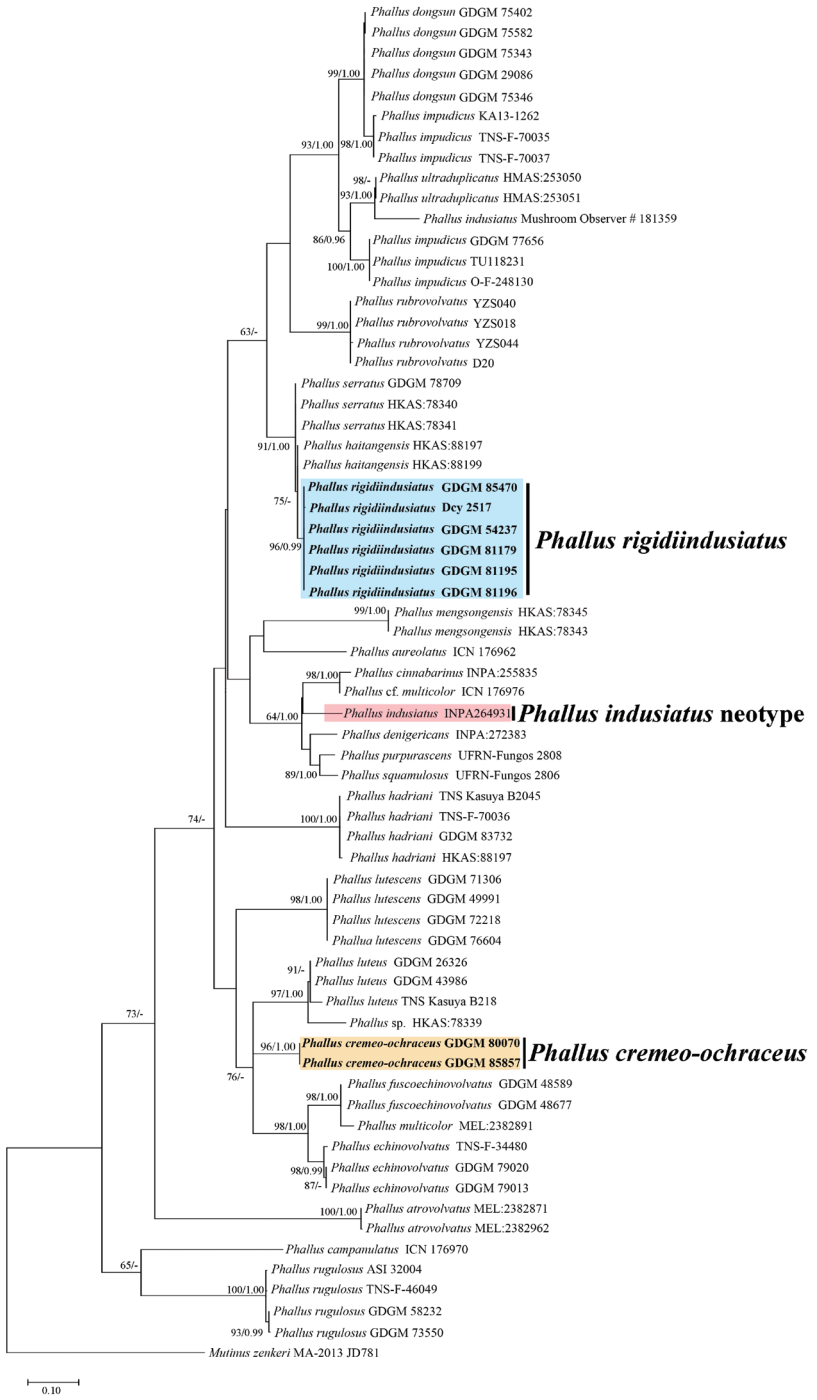

Figure 1. Phylogenetic overview of the genus *Phallus* inferred from ITS data using Maximum Likelihood (ML) and Bayesian Inference (BI). *Mutinus zenkeri* was selected as outgroup. Bootstrap values (≥50%) and Posterior probabilities (≥0.95) were presented around the branches.

LSU dataset as the value of stoprule became to 0.01, and the number of burn-in was 864.5 and 3251.75, respectively. Both ML and BI analyses had a very similar topological structure, but differed in minimum support values. Six collections (GDGM 54237, GDGM 81179, GDGM 81195, GDGM 81196, GDGM 85470 and Dcy 2517) are nested in a paraphyletic group containing *P. serratus* and *P. haitangensis* with strong supports (91%/1.00 BS/PP, Figure 1; 75%/0.99 BS/PP, Figure 2); while two other collections (GDGM 80700 and GDGM 85857), formed a monophyletic group containing *P. luteus*, *P. fuscoechinovolvatus*, *P. multicolor*, *P. echinovolvatus* with moderate supports in the ML analysis (76%/- BS/PP, Figure 1). However, in the ITS-LSU dataset analysis, both GDGM 80700 and GDGM 85857 separate from them and formed an independent clade with strong supports (99%/1.00 BS/PP, Figure 2).

Table 1. Sequences information of samples used for the ITS and ITS-LSU combined tree. Newly generated sequences were bold. The star "*" indicates the holotype or neotype specimens.

Name of the speices	Voucher/collection no.	Locality	LSU	ITS
Phallus atrovolvatus	MEL:2382871	Australia	KP012745	KP012745
	MEL:2382962	Australia	KP012823	KP012823
P. aureolatus	ICN 176962*	Brazil	MF372127	MF372135
P. calongei	AH31862	Pakistan	FJ785522	–
P. campanulatus	ICN 176970	Brazil	MF372130	MF372138
P. cinnabarinus	INPA:255835	–	–	KJ764821
P. costatus	MB02040	–	DQ218513	–
P. cremeo-ochraceus	**GDGM 80070***	**China**	**MZ890577**	**MZ890332**
	GDGM 85857	**China**	**MZ890578**	**MZ890333**
P. denigricans	INPA:272383*	Brazil	MG678455	MG678486
P. dongsun	GDGM 29086	China	MN264676	MN303794
	GDGM 75343	China	MN264678	MN303796
	GDGM 75346	China	MN264677	MN303795
	GDGM 75402*	China	MN264679	MN303797
	GDGM 75582	China	MN264680	MN303798
P. echinovolvatus	TNS-F-34480	Thailand	MF372129	MF372137
	GDGM 79020	China	–	MN523216
	GDGM 79013	China	MN611444	MN613536
P. fuscoechinovolvatus	GDGM 48589*	China	MF039585	MF039581
	GDGM 48677	China	MF039586	MF039583
P. hadriani	OSC KH 11092003-1 Reference material	–	NG_060067	NR_119579
	TNS Kasuya B2045	Japan	KP222544	KP222542
	TNS-F-70036	Japan	KU516107	KU516100
	GDGM 83732	China	MW031865	MW031862
P. haitangensis	HKAS:88197*	China	–	NR_155668
	HKAS:88199	China	–	KU705384
P. impudicus	CBS 294.53	U.K.	MH868748	–
	FO 46622	Germany	AY152404	–
	GDGM 77656	North Macedonia	MN264675	MN303793
	TU118231	Estonia	–	UDB015413
	O-F-248130	Norway	–	UDB038029
	KA13-1262	South Korea	–	KR673719
	TNS-F-70035	Japan	KU516106	KU516099
	TNS-F-70037	Japan	KU516108	KU516101
	KH-TGB11-1034 (TNS)	Japan	KF783249	–
	Mushroom Observer # 181359	Mexico	–	MF428417
	OSC36088	Japan	DQ218627	–

Name of the speices	Voucher/collection no.	Locality	LSU	ITS
P. indusiatus	INPA264931*	Brazil	MG678463	MG678502
P. lutescens	GDGM 49991	China	MN131077	MN131081
	GDGM 71306	China	MN131074	MN131080
	GDGM 72218*	China	NG_073753	NR_171847
	GDGM 76604	China	MN131076	MN131078
P. luteus	TNS Kasuya B218	Japan	KP222545	KP222543
	GDGM 26326	China	MT261793	MT261850
	GDGM 43986	China	MT261794	MT261851
P. mengsongensis	HKAS:78345	China	–	KF052625
	HKAS:78343*	China	–	NR_158805
P. merulinus	CJL-120214-03	Guiana	KF783250	–
P. multicolor	MEL:2382891	Australia	KP012762	KP012762
P. cf. *multicolor*	ICN 176976	Guiana	MF372128	MF372136
P. purpurascens	UFRN-Fungos 2808*	Brazil	MG678456	MG678487
P. ravenelii	UMO(USA-MO):0001	USA	KP779906	–
	CUW s.n	–	DQ218515	–
P. rigidiindusiatus	**GDGM 54237**	**China**	**MZ890579**	**MZ890334**
	GDGM 81179	**China**	**MZ890580**	**MZ890335**
	GDGM 81195	**China**	**MZ890581**	**MZ890336**
	GDGM 81196*	**China**	**MZ890582**	**MZ890337**
	GDGM 85470	**China**	**MZ890583**	**MZ890338**
	Dcy 2517	**China**	**MZ890584**	**MZ890339**
P. rubicundus	CLO 3220	USA	MK652718	–
	CLO 4473	USA	MK652720	–
P. rubrovolvatus	D20	China	–	MH381785
	YZS040	China	–	KF939503
	YZS018	China	–	KF939513
	YZS044	China	–	KF939515
P. rugulosus	TNS-F-46049	China, Taiwan	MF372134	MF372142
	ASI 32004	-	-	AF324169
	GDGM 58232	China	MT261858	MT361864
	GDGM 73550	China	MT261859	MT361865
P. serratus	HKAS:78341	China	–	KF052623
	HKAS:78340*	China	–	KF052622
	GDGM 78709	China	MZ508445	MZ508443
P. squamulosus	UFRN-Fungos 2806*	Brazil	–	MG678497
P. ultraduplicatus	HMAS:253050*	China	KJ591586	KJ591584
	HMAS:253051	China	KJ591587	KJ591585
Phallus sp.	HKAS:78339	China	–	KF052621
Mutinus zenkeri	MA-2013 JD781	São Tomé and Principe (Africa)	KC128654	KC128650

Taxonomy

Phallus cremeo-ochraceus **T. Li, T.H. Li & W.Q. Deng, sp. nov.**
MycoBank No: 840963
Figures 3, 5a–c

Diagnosis. Similar to *Phallus indusiatus* with an indusium almost touching ground, but mainly characterized by the cream to ochraceous receptacle, white to very slightly pinkish indusium and pseudostipe, white to pinkish volva, and basidiospores up to 4.0 × 1.7 µm.

Holotype. China. Guizhou Province, Libo County, Xiaoqikong Scenic Area (25°15'12"N, 107°44'16"E, alt. 428 m), Zhang Ming, 2 July 2020 (GDGM 80700).

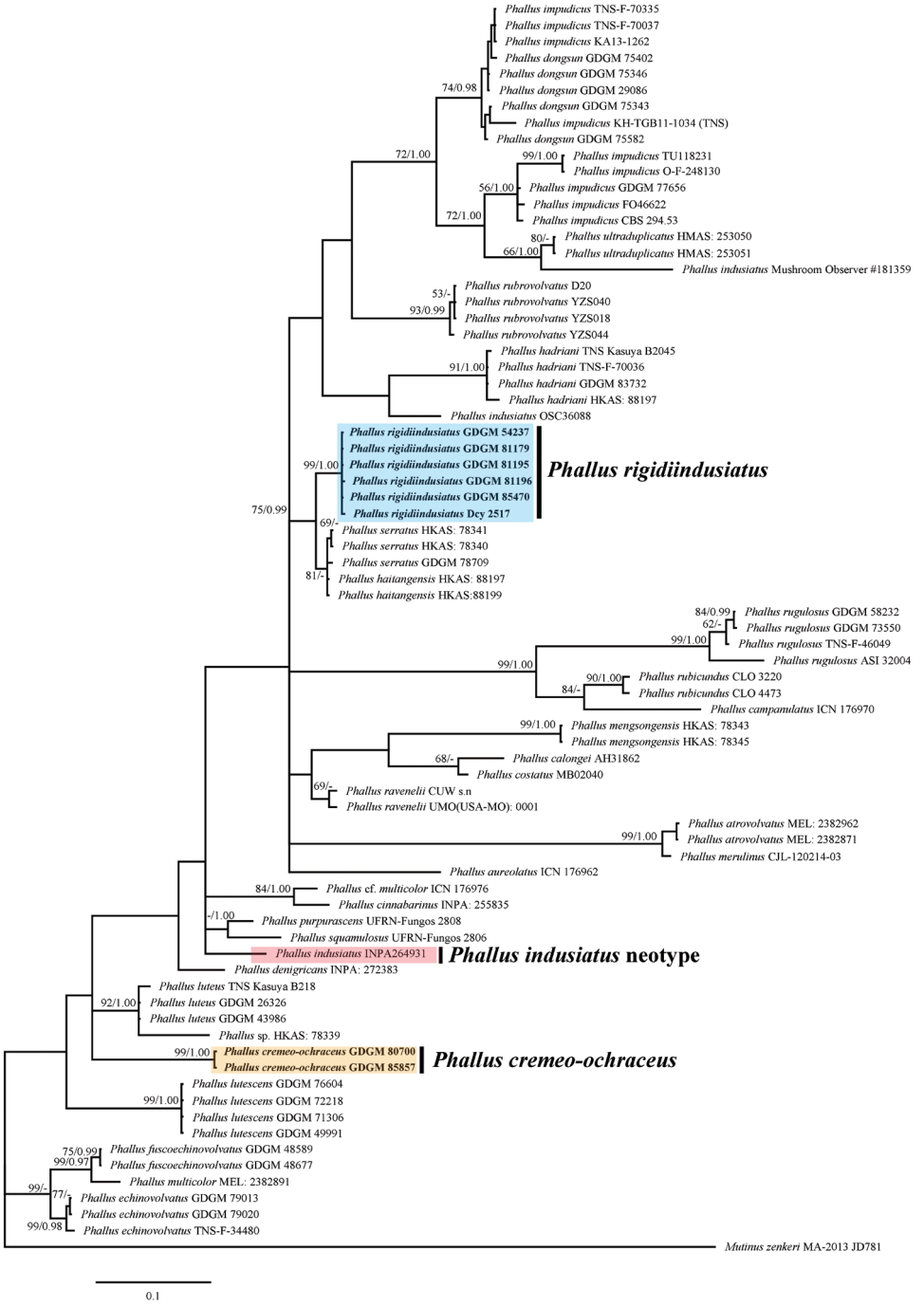

Figure 2. Phylogenetic overview of the genus *Phallus* inferred from concatenated data (ITS-LSU) using Maximum Likelihood (ML) and Bayesian Inference (BI). *Mutinus zenkeri* was selected as outgroup. Bootstrap values (≥50%) and Posterior probabilities (≥0.95) were presented around the branches.

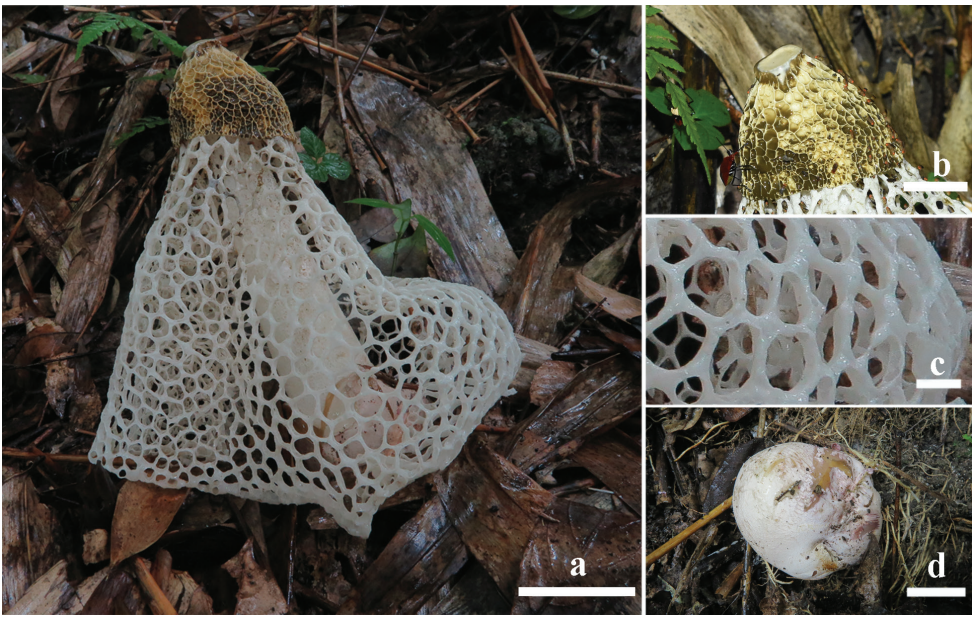

Figure 3. Basidiomata of *Phallus cremeo-ochraceus* **a-c** GDGM 80700 **d** GDGM 85857. Scale bars: 5 cm (**a**), 2 cm (**b, d**), 1 cm (**c**).

Immature basidioma globose to subglobose, 55 × 50 mm, white to pinkish (9A2), purplish pink (14A4) when injured, smooth to very slightly rimose-areolate, attached to substrate by pinkish white to pinkish (9A2) rhizomorphs. Exoperidium membranous; endoperidium gelatinous, hyaline. Expanded basidioma up to 240 mm high when fresh. Receptacle 42–50 mm high, 50–60 mm broad, campanulate, cream to ochraceous (4A3-5), reticulated with irregularly ridges up to 4.0 mm deep, covered with gleba; apex truncate, with a pale yellow (4A2), prominent disc up to 15 mm in diam. Gleba olive brown (4E4-6, 4F5-8), mucilaginous. Pseudostipe subcylindrical, constricted at apex, enlarged downwards, 200–220 mm high when mature, 22–27/32–38/40–45 mm broad (apex/middle/base), white (9A1) to slightly pinkish white (9A2), spongiform, hollow; pseudostipe wall 6–9 mm thick, usually consisting of small irregular chambers up to 3 mm. Volva obovate, 47–52 mm high, 40–45 mm broad, smooth, pinkish (9A2). Indusium well-developed, almost touching ground, white to very slightly pinkish, 190–210 mm in length, attached to the apex of pseudostipe, with polygonal to irregular meshes; meshes 7–20 mm wide, 2–4 mm thick. Rhizomorphs simple, yellowish white (4A2) to pinkish (9A2), 1–2 mm thick, about 20 mm long. Odour foetid (mainly from gleba). Taste mild.

Basidiospores (3.2–)3.5–3.8(–4.0) × 1.2–1.5(–1.7) μm, Q= (2.0–)2.3–2.7(–3.0), Q_m= 2.5 ± 0.5, cylindrical to long ellipsoid, hyaline and light olivaceous in H_2O and 5% KOH solution, inamyloid, thin-walled, smooth under light microscope. Hyphae of receptacle, pseudostipe and indusium hyaline or slightly yellowish, thin-walled,

pseudoparenchymatic, consisting of globose to subglobose or irregularly globose cells up to 30 μm in diam. Hyphae of volva tubular and branched, 4–8 μm in diam., thin-walled, smooth, septate, with clamp-connections. Hyphae of rhizomorphs filamentous, up to 8.0 μm in diam., thin-walled, smooth, septate, rarely branched.

Habitat and distribution. Solitary or scattered on soil with decaying litter under bamboo groves. So far known only from southwestern China (Guizhou). Season: July.

Etymology. With reference to the cream to ochraceous color of receptacle.

Additional specimens examined. China. Guizhou Province, Libo county, Xiaoqikong Scenic Area (25°15'46"N, 107°41'4"E, alt. 480 m), Zhang Ming, 2 July 2020, (GDGM 85857).

Phallus rigidiindusiatus **T. Li, T.H. Li & W.Q. Deng, sp. nov.**
MycoBank No: 840965
Figures 4, 5d–f

Diagnosis. Characterized by a well-developed indusium with thick meshes, morphologically similar to *Phallus serratus*, but different in its rigid, round or irregular meshes of indusium without serrated margin, and in smaller basidiospores.

Holotype. China. Guangdong Province, Jiangmen City, Yunkaishan National Nature Reserve. (22°17'57"N, 111°12'37"E, alt. 1350 m), Song Bin and Wen Huashu,10 June 2020 (GDGM 81196).

Immature basidioma globose to subglobose, 55–65 × 50–57 mm, white (1A1), slightly yellowish white (4A2) to orange white (7A2) or pinkish white (10A2), partially darker to grayish brown (7D3), smooth, attached to substrate by grayish violet (17D5-7) rhizomorphs. Exoperidium membranous; endoperidium gelatinous, hyaline. Expanded basidioma big-sized, 220–240 mm high when fresh. Receptacle 40–50 mm high, 50–60 mm broad, campanulate to subconical, white (1A1) to yellowish white (3A2), reticulated with irregularly ridges up to 4.5 mm deep, covered with gleba; apex truncate, perforated, or with a white spongy expansion up to 8 mm high, 10 mm in diam. Gleba yellowish brown to linoleum brown (5E5-7), mucilaginous. Pseudostipe subcylindrical, constricted at apex, enlarged toward base, white (1A1), spongiform, hollow, 170–190 mm high, 15–20/28–35/35–40 mm broad (apex/middle/base); pseudostipe wall 5–9 mm thick, usually consisting of small irregular chambers in 1–3 mm width. Volva obovate, 55–65 mm high, 50–60 mm broad, smooth, brownish orange (7C6) to light brown (7D8). Indusium well-developed, expanded to 3/4–5/6 portion of pseudostipe, white, up to 170 mm in length, attached to apex of pseudostipe, with rigid polygonal to irregular meshes becoming gradually smaller from top to bottom, margin entire; meshes usually not serrated at margin, 5–20 mm wide, up to 7 mm thick. Rhizomorphs simple, grayish orange (6C5) to brown (7E4), up to 3 mm thick, 4 cm long. Odour foetid (mainly from gleba). Taste mild.

Basidiospores (3.5–)3.7–4.2(–4.5) × 1.6–2.0(–2.3) μm, Q= (1.7–)2.1–2.4 (–2.6), Q_m= 2.3 ± 0.2, cylindrical to long ellipsoid, hyaline and light olivaceous in H_2O and

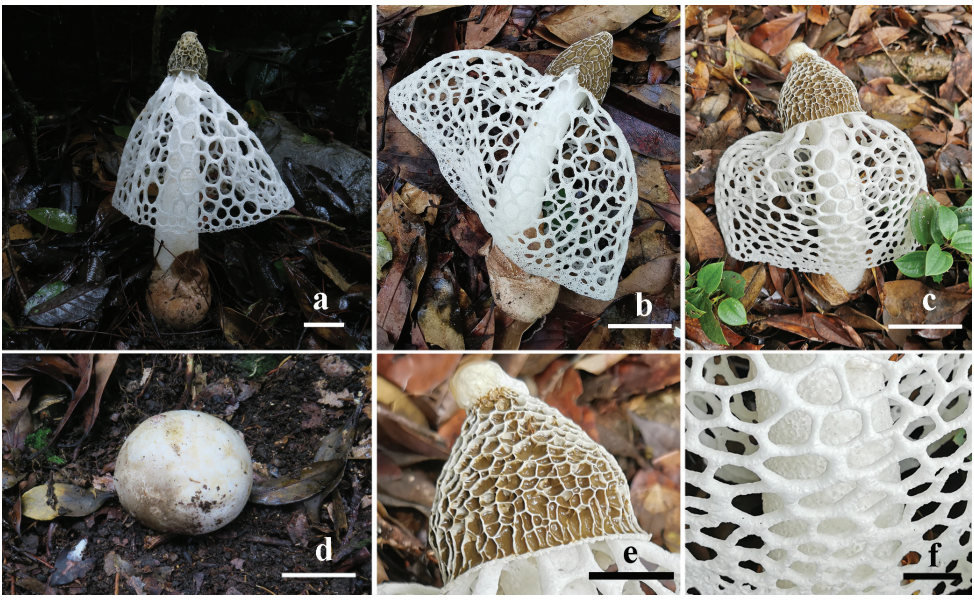

Figure 4. Basidiomata of *Phallus rigidiindusiatus*. **a** GDGM 54237 **b** GDGM 85470 **c, e, f** GDGM 81196 **d** 81195. Scale bars: 5 cm (**a-c**), 3 cm (**d**), 2 cm (**e**), 1 cm (**f**).

5% KOH solution, inamyloid, thin-walled, smooth, truncate at one end under light microscope. Hyphae of receptacle, pseudostipe and indusium hyaline, thin-walled, pseudoparenchymatic, consisting of globose to subglobose or irregularly globose structures, up to 25 μm in diam. Hyphae of volva tubular and branched, 3–5 μm in diam., thin-walled, smooth, septate, with clamp-connections. Hyphae of rhizomorphs filamentous, up to 6.0 μm in diam., thin-walled, smooth, septate, rarely branched.

Habitat and distribution. Solitary or scattered on soil with decaying litter in forests dominated by broad-leaved trees and bamboo groves. So far known only from southern China and southwestern China (Guizhou). Season: May to June.

Etymology. With reference to the rigid indusium.

Additional specimens examined. China. Hunan Province, Rucheng County, Jiulongjiang National Forest Park (25°26'49"N, 113°48'10"E, alt. 555 m), Huang Hao, 7 May 2015 (GDGM 54237); Guizhou Province, Duyun County, Doupengshan scenic place (26°21'17"N, 107°22'49"E, alt. 1300 m), Deng Chunying, 16 May 2020 (Dcy2517); Guangdong Province, Shaoguan City, Nanling National Nature Reserve (24°49'54"N, 113°7'22"E, alt. 994 m), Song Bin and Xie Dechun, 27 May 2021 (GDGM 85470); Guangdong Province, Jiangmen City, Yunkaishan National Nature Reserve. (22°15'22"N, 111°9'23"E, alt. 1480 m), Song Bin and Wen Huashu, 10 June 2020 (GDGM 81179); Guangdong Province, Jiangmen City, Yunkaishan National Nature Reserve. (22°17'58"N, 111°12'36"E, alt. 1420 m), Song Bin and Wen Huashu, 10 June 2020 (GDGM 81195).

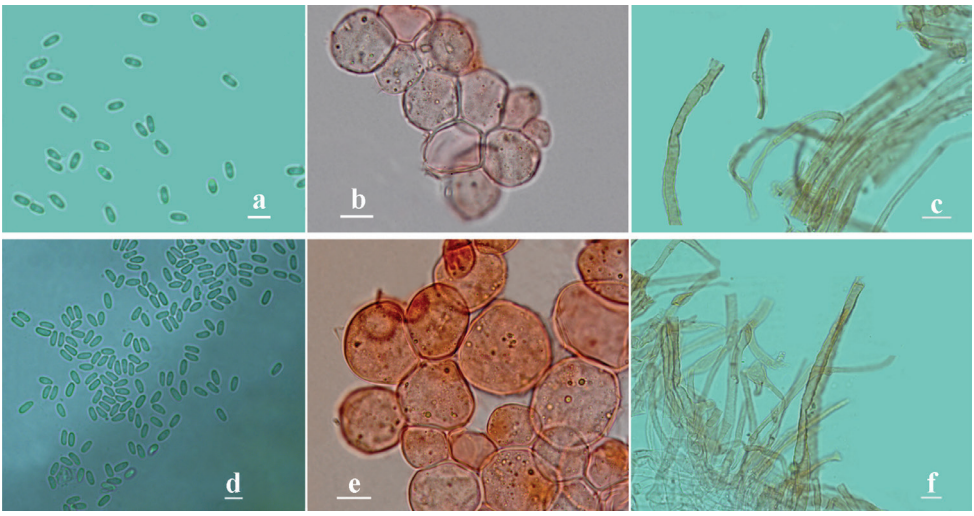

Figure 5. Characteristics of *Phallus cremeo-ochraceus* **a-c** and *Phallus rigidiindusiatus* **d-e** under the light microscope. **a, d** basidiospores **b, e** pseudoparenchymatous hyphae from pseudostipe **c, f** hyphae from volva. Scale bars 5 μm (**a–f**).

Discussion

Based on the ITS dataset *P. cremeo-ochraceus* nested in a group containing *P. luteus*, *P. echinovolvatus*, *P. fuscoechinovolvatus* and *P. multicolor* (Figure 1). However, in the ITS-LSU dataset *P. cremeo-ochraceus* separates from them and formed an independent clade (Figure 2). Therefore, the sister relationships of *P. cremeo-ochraceus* remain unclear. Morphologically, all of them have similar color in receptacle except *P. multicolor* and *P. luteus* which have a bright yellow to orange indusium (Berkeley and Broome 1883; Kasuya 2008).

Phylogenetically, *P. rigidiindusiatus* is closely related to *P. serratus* and *P. haitangensis* with strong support (Figures 1, 2). Morphologically, *P. serratus* resembles *P. rigidiindusiatus* in having a white and strongly reticulate receptacle, a white and well-developed indusium and a brownish-gray volva. However, *P. serratus* can be easily distinguished from the new species in having the serrated meshes of indusium and larger basidiospores (4–5 × 2–3 μm) (Li et al. 2014); *Phallus haitangensis* is another closely related taxon, which is different in its golden orange receptacle and a well-developed, light orange indusium (Li et al. 2016). Interestingly, *P. haitangensis* and *P. serratus* have distinct morphological characteristics but shared with a 98.4% similarity of ITS sequence (Li et al. 2014, 2016). Both two new species were separated from *P. indusiatus* in phylogenetical analyses.

Other *Phallus* species with a white indusium are relatively easier to be distinguished from the new species *P. cremeo-ochraceus* and *P. rigidiindusiatus* (Table 2). For example, the Chinese species *P. echinovolvatus* and *P. fuscoechinovolvatus* are distinguished by having

Table 2. Type location, receptacle, volva, indusium, and basidiospores of the *Phallus indusiatus*-like species.

Species name	Type location	Receptacle	Volva	Indusium	Basidiospores
Phallus cremeo-ochraceus	China, Guizhou	Pale yellow to light yellow, reticulated	Pinkish, smooth surface	Almost touching the ground	3.2–4.0×1.2–1.7 μm
P. echinovolvatus	China, Hunan	White to yellow, reticulated	Whitish or pale brown, with echinulate projections	Almost touching the ground	3.0–4.0×1.3–2.0 μm
P. fuscoechinovolvatus	China, Guangdong	Yellowish, reticulated	Dark brown or blackish, with many white to pale yellow echinules	Almost touching the ground	2.5–4.0×1.0–2.0 μm
P. indusiatus	Brazil, Pará	White, reticulated	White, with pinkish pigments	Extending to the ground	3.6–4.1×1.5–2.2 μm
P. merulinus	Indonesia, Java	White, minutely convoluted folds	Dull white	Expanded to 1/2 portion of pseudostipe	3.3–4.0×1.4–1.8 μm
P. rigidiindusiatus	Southern and Southwestern of China	White to yellowish, reticulated	Brownish orange to light brown, smooth surface	Expanded to 3/4–5/6 portion of pseudostipe, with rigid polygonal to irregular meshes, without serrated margin.	3.5–4.5×1.6–2.3 μm
P. rubrovolvatus	China, Yunnan	Yellowish, reticulated	Dark purple, smooth surface	Expanded to 1/2 portion of pseudostipe	3.7–4.0×1.5–2.5 μm
P. serratus	China, Yunnan	White, reticulated	Brownish-gray, without scales	Almost touching the ground, with the serrated margin in hole of indusium.	4.0–5.0×2.0–3.0 μm
P. ultraduplicatus	China, Liaoning	White, reticulated	Flesh-ocher	Short, 20–40 mm long,	4.0–5.0×1.5–2.0 μm

an obviously echinate volva (Zang et al. 1988; Song et al. 2018); and *P. atrovolvatus* Kreisel & Calonge, described from the Central America, can be easily distinguished by having a rugulose to merulioid receptacle, a black volva, and an indusium expanded to midway from the receptacle and volva (Calonge 2005). Although the Brazilian species *P. aureolatus* L. Trierveiler-Pereira & A.A.R. de Meijer has a rigid, white and almost touching ground indusium which is similar to that of *P. rigidiindusiatus*, it differs in having a rugulose to merulioid receptacle, a shorter pseudostipe (up to 10 cm high) and a shorter basidiospores (3.0–4.1 × 1.5–2.0 μm) (Trierveiler-Pereira et al. 2017).

Among the complex members of *P. indusiatus* s.l. published by Cabral et al. (2019), *P. denigricans* T.S. Cabral, B.D.B. Silva & Baseia has a volva varying from white to dark brown and basidiospores up to 4.6 × 2.5 μm; *Phallus purpurascens* T.S. Cabral, B.D.B. Silva & Baseia has a white receptacle, a purplish volva and larger basidiospores (4.4–5 × 2.5–3.4 μm); and *P. squamulosus* T.S. Cabral, B.D.B. Silva & Baseia is characterized by its squamous surfaces of immature basidioma and volva. Besides, *P. maderensis* Calonge, described from the Atlantic Island of Africa, has an interesting indusium attaching to the base of pseudostipe and is not hanging from the receptacle (Calonge et al. 2008); and *P. merulinus* (Berk.) Cooke from Indonesia differs in a rugose receptacle with minutely convoluted folds (Lloyd 1909). The Chinese species *P. rubrovolvatus* is distinguished by the red purple volva, although it also has a rigid indusium reaching on

the midway or 3/4 portion of the pseudostipe (Liu et al. 2005); and *P. ultraduplicatus* X.D. Yu, W. Lv, S.X. Lv, Xu H. Chen & Qin Wang from northeastern China has a shorter indusium hanging down less than 1/2 portion of the pseudostipe and longer and narrower basidiospores than those of *P. rigidiindusiatus* (Adamčík et al. 2015).

According to the original description, *Phallus indusiatus*, a South American species, is characterized by the campanulate and reticulated receptacle and the white indusium touching the ground (Ventenat 1798). However, it was not possible to find the original material in herbarium for comparison due to the unspecific information (Ventenat 1798). Recently, based on same characteristics as the original description, close geographical location with the same forest domain, and submitted the available molecular sequences to GenBank, a neotype of *P. indusiatus* was designated, which has a campanulate and reticulated receptacle, a white and fully developed indusium, a white volva and elongated and smooth basidiospores (3.6–4.1 × 1.5–2.2 μm); according to all known data about the *Phallus* taxa, its distribution is presumed to be restricted to South America (Cabral et al. 2019).

In phalloid fungi, macro-characters, such as the shape, the surface characters and color of the main structures (receptacle, pseudostipe, indusium, volva and rhizomorphs), are generally more important than micro-characters for infrageneric classification (Kreisel 1996). Therefore, if without any molecular phylogenetic analyses, two or more species shared similar macro-characters, then these could easily be confused for the same species. However, when geographical distribution has been taken into account as the taxonomic evidence, they tend to become easily distinguishable, because phalloid fungi have a passive basidiospore dispersal mechanism that depends mainly on insects as transporters, and this factor together with environmental conditions (such as temperature, humidity, illumination, soil nutrition and dominated plants) arguably limit their geographical distributions (Wilson et al. 2011). According to our previous studies, for example, quite a lot of Asian specimens labeled as "*P. impudicus*" were actually identical to *P. dongsun* from China, and *Phallus rubicundus* (Bosc) Fr. originally described from America was probably not naturally distributed in China, even in Asia (Li et al. 2020a, b). Therefore, morphological analyses and geographical distributions, as well as molecular phylogeny are the most useful evidences to identify the phalloid fungi. The two *Phallus indusiatus*-like species from China were proven as new to science with strong supports of those evidences in this study while the natural distribution of *P. indusiatus* in China becomes more suspicious.

Key to *Phallus* species with a white or nearly white indusium

1 Volva squamulose or echinulate **2**
– Volva smooth or nearly so, not squamulose or echinulate..... **4**
2 Volva surface squamulose, white ..... ***P. squamulosus***
– Volva surface obviously echinulate **3**
3 Volva dark brown or blackish..... ***P. fuscoechinovolvatus***
– Volva generally white ..... ***P. echinovolvatus***

4 Volva discoloring from white to dark brown ..... ***P. denigricans***
– Volva unchanging in color or only slightly discoloring, not discoloring to dark brown **5**
5 Receptacle rugulose to merulioid **6**
– Receptacle reticulate **8**
6 Volva black ..... ***P. atrovolvatus***
– Volva pinkish or white 7
7 Vovla pinkish; indusium almost touching ground ..... ***P. aureolatus***
– Volva white, with minutely convoluted folds; indusium not touching ground ..... ***P. merulinus***
8 Indusium attached to the base of the pseudostipe and free from receptacle ... . ***P. maderensis***
– Indusium attached to the apex of the pseudostipe **9**
9 Volva white ..... ***P. indusiatus***
– Volva colored **10**
10 Indusium shorter than 40 mm when mature ..... ***P. ultraduplicatus***
– Indusium longer than 40 mm when mature **11**
11 Receptacle cream to ochreous ..... ***P. cremeo-ochraceus***
– Receptacle white **12**
12 Indusium with obviously serrated meshes ..... ***P. serratus***
– Indusium with round or irregular meshes, but without obviously serrated meshes **13**
13 Volva brownish orange to light brown, not red to purple obviously; indusium strongly rigid; basidiospores narrower, (3.5–)3.7–4.2(–4.5) × 1.6–2.0(–2.3) μm ..... ***P. rigidiindusiatus***
– Volva obviously red to purple; basidiospores broader **14**
14 Volva deep red; basidiospores smaller, 3.7–4 × 2–2.5 μm .... ***P. rubrovolvatus***
– Volva purplish or becoming purple; basidiospores larger, 4.4–5 × 2.5–3.4 μm.. ..... ***P. purpurascens***

Acknowledgements

The authors express sincere gratitude to Dr. Chunying Deng, Mr. Guorui Zhong and Mr. Hao Huang for collecting the specimens, also to Dr. Chaoqun Wang and Dr. Md. Iqbal Hosen for their helpful suggestions on improving the morphological descriptions, molecular phylogenetic analyses, figure illustration and references. This work was funded by the National Natural Science Foundation of China (31800014, 31970016); the Science and Technology Planning Project of Guangdong Province, China (2019B121202005, 2018B020205001, 2018B030324001); the Science and Technology Planning Project of Guizhou Province, China [No. Qian Ke He Fu Qi (2019) 4007]; the project of macrofungi investigation in Shenzhen (SZCG2019191412) and the project of Macrofungal Investigation in Zhongshan (ZZ21901438). We also sincerely thank the two anonymous reviewers for their corrections and suggestions to improve the paper.

References

Adamčík S, Cai L, Chakraborty D, Chen XH, Cotter HVT, Dai DQ, Dai YC, Das K, Deng CY, Ghobad-Nejhad M, Hyde KD, Langer E, Latha DKP, Liu F, Liu SL, Liu TT, Lv W, Lv SX, Machado AR, Pinho DB, Pereira OL, Prasher IB, Rosado AWC, Qin J, Qin WM, Verma RK, Wang Q, Yang ZL, Yu XD, Zhou LW, Buyck B (2015) Fungal biodiversity profiles 1–10. Cryptogamie, Mycologie 36(2): 1–46. https://doi.org/10.7872/crym/v36.iss2.2015.121

Berkeley MJ, Broome CE (1883) List of fungi from Brisbane, Queensland: with descriptions of new species. Part II. Transactions of the Linnaean Society of London 2: 53–73. https://doi.org/10.1111/j.1095-8339.1883.tb00004.x

Cabral TS, Marinho P, Goto BT, Baseia IG (2012) *Abrachium*, a new genus in the Clathraceae, and *Itajahya* reassessed. Mycotaxon 119: 419–429. https://doi.org/10.5248/119.419

Cabral TS, Silva BDB, Martín MP, Clement CR, Hosaka K, Baseia IG (2019) Behind the veil-exploring the diversity in *Phallus indusiatus* s.l. (Phallomycetidae, Basidiomycota). MycoKeys 58: 103–127. https://doi.org/10.3897/mycokeys.58.35324

Calonge FD (2005) A tentative key to identify the species of *Phallus*. Boletín de la Sociedad Micológica de Madrid 29: 9–18.

Calonge FD, Menezes de Sequeira M, Freutas T, Rocha E, Franquinho L (2008) *Phallus maderensis* sp. nov., found in Madeira, Portugal. Boletín de la Sociedad Micológica de Madrid 32: 101–104.

Desvaux NA (1809) Observations on several genera to establish families of mushrooms. Journal de Botanique 2: 88–105.

Dring DM (1964) Gasteromycetes of west tropical Africa. Mycological Papers 15: 1–60.

Fischer ED (1900) Unterschungen zur vergleichenden Entwicklungsgeschchte und Systematik der Phalloideen. III serie, mit einem Anhang: Verwandtschaftsverhältnisse der Gasteromyceten. In: Allgemeine Schweizerische Gesellschaft für die Gesammten Naturwissenschaften. (Eds) Neue Denkschriften der Allgemeinen Schweizerischen Gesellschaft für die Gesammten Naturwissenschaften, band VI–XXXVI. Zürich: Druck von Zürcher & Furrer, 1–84.

Hall BG (2013) Building phylogenetic trees from molecular data with MEGA. Molecular Biology & Evolution 30(5): e1229. https://doi.org/10.1093/molbev/mst012

Hall TA (1999) BioEdit: a user-friendly biological sequence alignment editor and analysis program for Windows 95/98/NT. Nucleic Acids Symposium Series 41: 95–98.

Katoh K, Standley DM (2013) Mafft multiple sequence alignment software version 7: improvements in performance and usability. Molecular Biology & Evolution 30(4): 772–780. https://doi.org/10.1093/molbev/mst010

Kasuya T (2008) *Phallus luteus* comb. nov. a new taxonomic treatment of a tropical phalloid fungus. Mycotaxon 106: 7–13. https://doi.org/10.1007/S10267-008-0441-5

Kobayasi Y (1965) On the genus *Dictyophora*, especially on the East-Asiatic group. Transactions of the Mycological Society of Japan 6(1): 1–8.

Kornerup A, Wanscher JH (1978) Methuen handbook of colour. 3rd edn. Eyre Methuen, London, 196–265.

Kreisel H (1996) A preliminary survey of the genus *Phallus* sensu lato. Czech Mycology 48: 273–281. https://doi.org/10.33585/cmy.48407

Li HL, Ma XL, Mortimer PE, Karunarathna SC, Xu JC, Hyde KD (2016) *Phallus haitangensis*, a new species of stinkhorn from Yunnan Province, China. Phytotaxa 280(2): 116–128. https://doi.org/10.11646/phytotaxa.280.2.2

Li HL, Mortimer PE, Karunarathna SC, Xu JC, Hyde KD (2014) New species of *Phallus* from a subtropical forest in Xishuangbanna, China. Phytotaxa 163(2): 91–103. https://doi.org/10.11646/phytotaxa.163.2.3

Li T, Li TH, Deng WQ, Song B, Deng CY, Yang ZL (2020a) *Phallus dongsun* and *P. lutescens*, two new species of Phallaceae (Basidiomycota) from China. Phytotaxa 443(1): 19–37. https://doi.org/10.11646/phytotaxa.443.1.3

Li T, Li TH, Deng WQ, Song B (2020b) A taxonomic revision of two *Phallus* species distributed in and around South China. Acta Edulis Fungi 27(4): 155–163.

Linnaeus CV, Salvius L (1753) Species plantarum Vol. 2. Holmiae, Impensis Laurentii Salvii, Stockholm, 1178 pp.

Liu B, Fan L, Li JZ, Li TH, Song B, Liu JH (2005) Flora fungorum sinicorum Vol. 23. Science Press, Beijing, 137–171.

Lloyd CG (1909) Synopsis of the known phalloids. Bulletin of the Lloyd Library 13: 1–96.

Medeiros GS, Rodrigues ACM, Cruz RHSF, Melanda GCS, Carvalho Jr AA, Baseia IG (2017) *Phallus fluminensis* (Phallaceae, Basidiomycota), a new species of stinkhorn from the Brazilian Atlantic rainforest. Studies in Fungi 2(1): 191–198. https://doi.org/10.5943/sif/2/1/21

Mohanan C (2011) Macrofungi of Kerala. Kerala Forest Research Institute, Kerala, Indien. [ISBN 81–85041–73–3]

Moreno G, Khalid AN, Alvarado P (2009) A new species of *Phallus* from Pakistan. Mycotaxon 108: 457–462. https://doi.org/10.5248/108.457

Moreno G, Khalid AN, Alvarado P, Kreisel H (2013) *Phallus hadriani* and *P. roseus* from Pakistan. Mycotaxon 125: 45–51. https://doi.org/10.5248/125.45

Rebriev YA, Pham THG, Alexandrova AV (2014) *Phallus coronatus* sp. nov. from Vietnam. Mycotaxon 127: 93–96. http://dx.doi.org/10.5248/127.93

Ronquist F, Huelsenbeck JP (2003) Mrbayes 3: bayesian phylogenetic inference under mixed models. Bioinformatics 19(12): e1572. https://doi.org/10.1093/bioinformatics/btg180

Song B, Li T, Li TH, Huang QJ, Deng WQ (2018) *Phallus fuscoechinovolvatus* (Phallaceae, Basidiomycota), a new species with a dark spinose volva from southern China. Phytotaxa 334(1): 19–27. https://doi.org/10.11646/phytotaxa.334.1.3

Trierveiler-Pereira L, Meijer AAR, Reck MA, Kentaro H, Silveira RMB da (2017) *Phallus aureolatus* (Phallaceae, Agaricomycetes), a new species from the Brazilian Atlantic Forest. Phytotaxa 327: 223–236. https://doi.org/10.11646/phytotaxa.327.3.2

Wilson AW, Binder M, Hibbett DS (2011) Effects of gasteroid fruiting body morphology on diversification rates in three independent clades of fungi estimated using binary state speciation and extinction analysis. Evolution 65: 1305–1322. https://doi.org/10.1111/j.1558-5646.2010.01214.x

Ventenat EP (1798) Dissertation sur le genre *Phallus*. Mémoires de l'institut National Des Sciences et Arts 1: 503–523.

Vilgalys R, Hester M (1990) Rapid genetic identification and mapping of enzymatically amplified ribosomal DNA from several cryptococcus species. Journal of Bacteriology 172: 4238–4246. https://doi.org/10.1128/jb.172.8.4238-4246.1990

White TJ, Bruns TD, Lee S, Taylor J (1990) Amplification and direct sequencing of fungal ribosomal RNA genes for phylogenetics. In: Innis MA, Sninsky DH, White TJ (Eds) PCR protocols: A guide to methods and applications. Academic Press Inc, New York, 315–322. https://doi.org/10.1016/B978-0-12-372180-8.50042-1

Young AM (2005) A field guide to the fungi of Austrilia. University of New South Wales Press Ltd, Sydney, 200 pp.

Zang M, Ji DG (1985) Notes on Phallaceae from the eastern Himalayan region of China. Acta Mycologica Sinica 4(2): 109–117.

Zang M, Zheng D, Hu Z (1988) A new species of the genus *Dictyophora* from China. Mycotaxon 33: 145–148.

MycoKeys 85: 127–160 (2021)
doi: 10.3897/mycokeys.85.70552
https://mycokeys.pensoft.net

RESEARCH ARTICLE

A peer-reviewed open-access journal
MycoKeys
Launched to accelerate biodiversity research

Infraspecific variation of some brown *Parmeliae* (in Poland) – a comparison of ITS rDNA and non-molecular characters

Katarzyna Szczepańska[1], Beata Guzow-Krzemińska[2], Jacek Urbaniak[1]

1 *Department of Botany and Plant Ecology, Wrocław University of Environmental and Life Sciences, pl. Grunwaldzki 24a, PL-50-363 Wrocław, Poland* **2** *Department of Plant Taxonomy and Nature Conservation, Faculty of Biology, University of Gdańsk, Wita Stwosza 59, PL-80-308 Gdańsk, Poland*

Corresponding author: Katarzyna Szczepańska (katarzyna.szczepanska@upwr.edu.pl)

Academic editor: Pradeep Divakar | Received 23 June 2021 | Accepted 20 October 2021 | Published 22 Decemeber 2021

Citation: Szczepańska K, Guzow-Krzemińska B, Urbaniak J (2021) Infraspecific variation of some brown *Parmeliae* (in Poland) – a comparison of ITS rDNA and non-molecular characters. MycoKeys 85: 127–160. https://doi.org/10.3897/mycokeys.85.70552

Abstract

Infraspecific variation of the ITS rDNA region of some brown *Parmeliae* occurring in Poland is studied and compared with non-molecular characters. Haplotype networks are used to illustrate the variability within the species. Both newly-produced sequences from Central Europe and from all over the world, downloaded from the GenBank, are used.

The number of haplotypes found for each taxon ranged from five in *Melanelia stygia* to 12 in *Melanelia hepatizon* and *Montanelia disjuncta*; however, their numbers correlate with the number of specimens tested. New haplotypes for *Melanelia agnata*, *M. hepatizon* and *Cetraria commixta* are found. Based on our 169-sample dataset, we could not infer any geographical correlation, either locally or world-wide. Many of the analysed haplotypes were widely distributed and the same haplotype was often shared between temperate and polar populations. A comparison of molecular, morphological, anatomical and chemical characters also shows no correlation.

Keywords

Cryptic species, haplotype, lichenised fungi, Parmeliaceae, phylogeny, taxonomy

Introduction

The brown *Parmeliae* (Esslinger 1977) have been an object of numerous studies (Guzow-Krzemińska and Węgrzyn 2003; Blanco et al. 2005; Crespo et al. 2010, 2011; Nelsen et al. 2011; Divakar et al. 2012; Thell et al. 2012; Leavitt et al. 2014, 2015) and, due to this exceptional attention, they are one of the best-studied assemblages in the family Parmeliaceae. These lichens are a polyphyletic group possessing foliose, a dark to medium brown thallus and usually lacking atranorin or usnic acid in the cortex (Esslinger 1977; Blanco et al. 2004).

For many years, one of the largest genera within this group was *Melanelia* Essl., segregated from *Parmelia* Ach. by Esslinger (1978) to accommodate species with brown, foliose thalli and an N– cortex layer. However, during the following years, it has been demonstrated that the genus *Melanelia* s. lat. was polyphyletic and several new genera were distinguished within it, such as *Melanelixia* O. Blanco et al., *Melanohalea* O. Blanco et al. (Blanco et al. 2004) and *Montanelia* Divakar et al. (Divakar et al. 2012). In traditional terms, brown *Parmeliae* includes other genera, such as *Allantoparmelia* (Vain.) Essl., *Pleurosticta* Petr. and some species of *Xanthoparmelia* (Vain.) Hale. Moreover, due to the historical taxonomic approach (Thell 1995; Rico et al. 2005) and the similarity in the morphological and anatomical features of thalli, *Cetraria commixta* is also referred to this group.

Our studies have focused on the saxicolous species of *Melanelia* and *Montanelia* genera. According to Otte et al. (2005), species of these genera are arctic-alpine, circumpolar and occur on silicate rocks in the mountain areas of the Northern Hemisphere, including Arctic Regions (Divakar et al. 2012). Nowadays, *Melanelia* s. str. is restricted to a small clade of saxicolous, cetrarioid lichens and includes four species: *M. agnata* (Nyl.) A. Thell, *M. hepatizon* (Ach.) A. Thell, *M. pseudoglabra* (Essl.) Essl. and *M. stygia* (L.) Essl. According to Thell (1995), these species are characterised by broadly clavate asci with a small tholus and a broad axial body, a thick, paraplectenchymatous cortex and dumb-bell-shaped pycnoconidia. *Montanelia*, representing the parmelioid clade, includes eight species: *M. disjuncta* (Erichsen) Divakar, A. Crespo, Wedin & Essl., *M. occultipanniformis* S.D. Leav., Essl., Divakar, A. Crespo & Lumbsch, *M. panniformis* (Nyl.) Divakar, A. Crespo, Wedin & Essl., *M. predisjuncta* (Essl.) Divakar, A. Crespo, Wedin & Essl., *M. saximontana* (R.A. Anderson & W.A. Weber) S.D. Leav., Essl., Divakar, A. Crespo & Lumbsch, *M. secwepemc* S.D. Leav., Essl., Divakar, A. Crespo & Lumbsch, *M. sorediata* (Ach.) Divakar, A. Crespo, Wedin & Essl. and *M. tominii* (Oxner) Divakar, A. Crespo, Wedin & Essl. (Divakar et al. 2012; Leavitt et al. 2015; Leavitt et al. 2016). The characteristic features of the *Montanelia* genus are short and narrow lobes, with flat to convex lobe margins, a non-pored epicortex, cylindrical to fusiform conidia, a medulla containing orcinol depsides and flat, effigurate pseudocyphellae (absent only in *M. sorediata*; Divakar et al. 2012). Three of these species (*M. disjuncta*, *M. panniformis* and *M. sorediata*) have broad, intercontinental distributions, with no evidence of phylogeographic substructure (Leavitt et al. 2015).

The genera *Melanelia* and *Montanelia* have been the subject of a critical revision in Poland and data concerning their distribution, ecology and morphological, anatomical and chemical features are presented in previous papers (Szczepańska et al. 2015;

Szczepańska and Kossowska 2017). However, recent molecular studies imply that both genera may include previously unrecognised species-level diversity (Divakar et al. 2012; Leavitt et al. 2014), especially within Icelandic populations of *M. stygia* (Xu et al. 2017).

One of the goals of this study was to assess the intraspecific internal transcribed spacer (ITS) rDNA variability in brown *Parmeliae* species. Investigations of genetic variation in lichen-forming symbionts have advanced considerably in recent years and resulted in interesting conclusions (Palice and Printzen 2004; Lindblom and Ekman 2006; Domaschke et al. 2012; Starosta and Svoboda 2020). Although brown *Parmeliae* appear to be well studied in taxonomic terms, there are insufficient molecular data to estimate their genetic variation. Most of the available data concern samples collected in a few regions of the world, such as Europe and North America. The North American species of this group were studied in Greenland and Canada (Leavitt et al. 2014; Leavitt et al. 2015), while samples from Europe originated mainly from the north – Iceland, Finland, Norway and Sweden (Blanco et al. 2004; Divakar et al. 2012; Xu et al. 2017). Therefore, we decided to fill in the gap in sampling and focused our study on samples collected in Central Europe. We have used phylogenetic trees and haplotype networks to investigate the extent of molecular differences between newly-generated sequences from samples collected in Central Europe (Austria, Czech Republic, Germany, Poland and Slovakia) and others originating from different geographical regions. Due to additional samplings from previously unexplored areas, it was possible to evaluate and compare the genetic variability of the studied specimens in Central Europe with samples from other regions of the world and to identify areas with the greatest haplotype diversity. In addition, we analysed morphological, anatomical and chemical characters of collected specimens to find a potential correlation between phenotypic characters and genetic variation of the studied taxa. By analysing genetic diversity and geographical distribution of identified haplotypes, as well as phenotypic characters of collected samples, we tried to better define and designate the species boundaries within analysed taxa. Special emphasis was placed on analysis of European, Greenlandic and Icelandic samples of *M. agnata* and *M. stygia* to revise the hypothesis assuming a semi-cryptic or cryptic nature of their potential species-level diversity.

Materials and methods

Taxon sampling

The study is based on collections from the AMNH, C and WRSL Herbaria, as well as the private material of Dr Maria Kossowska (hb. Kossowska). Our sampling focused on saxicolous representatives of the Parmeliaceae family occurring in Poland, with brown, foliose thalli, such as *Cetraria commixta*, *Melanelia agnata*, *M. hepatizon*, *M. stygia*, *Montanelia disjuncta* and *M. sorediata*. We also included the holotype of *Melanelia agnata* (*Platysma agnatum*; Austria, Tirol, Gerölle unter dem Gneissfelsen zum wilden see. Auf dem Kraxentrag, Tirol, Brenner 225, Aug 1871, H-NYL 36086), borrowed from Herbarium of W. Nylander in Helsinki in our analyses.

Specimens for molecular study were selected after detailed morphological and chemical analyses. Due to DNA degradation, it was not possible to use samples collected more than three years prior to the DNA extraction procedure in most cases. As the *Melanelia agnata* and *M. stygia* specimens from Greenland and Iceland were collected more than 10 years ago, we had to limit our phylogenetic analyses to ITS rDNA markers and used the sequences stored in GenBank. Before phylogenetic analysis, newly-obtained ITS rDNA sequences were subjected to a BLAST search (Altschul et al. 1997). The final ITS dataset used in this study includes 52 sequences newly generated and 117 sequences downloaded from GenBank (Table 1).

Morphology and chemistry

The morphology and anatomy of the specimens were studied in detail with dissecting and light microscopes, following routine techniques. All specimens were examined for the assessment of the morphological characters, such as lobe width and morphology (flat/convex), the appearance of the upper surface (dull/glossy), the appearance of the lower surface (light/dark), apothecia morphology (sessile/constricted), appearance and position of pycnidia (marginal/laminal), appearance and position of the pseudocyphellae (marginal/laminal), size and shape of conidia (bacilliform/bifusiform), as well as ascospore size. For light microscopy, vertical sections of apothecia were cut by hand using a razor blade and mounted in water. Hymenium and conidia measurements were made in water and ascospore measurements were made in 10% potassium hydroxide (KOH). At least ten measurements of morphological variables and measurements of 20 spores and conidia were made for each sample and their minimum and maximum values were calculated.

The TLC analyses were undertaken in A and C solvent systems using the standardised method of Culberson (1972) and following Orange et al. (2001).

DNA extraction, PCR amplification and DNA sequencing

Genomic DNA was extracted from specimens after cell disruption in a Mixer Mill MM400 (Retsch, Haan, Germany) using a CTAB method according to the standard protocol of isolation (Doyle and Doyle 1987). The quality of the isolated DNA was determined using 1% TBE agarose electrophoresis. PCR reactions were performed in 20 µl reaction tubes that contained a Dream Taq reaction buffer containing $MgCl_2$, a 0.2 mM dNTP mix, 1u DreamTaq DNA polymerase (Thermo Fisher Scientific, Waltham, MA, USA), 0.5 mM each ITS1 and ITS4 primers and 0.8 µl of total genomic DNA. The adequate annealing temperature was determined using the gradient method. The PCR programme consisted of an initial denaturation at 95 °C for 6 min, according to a previous study (Szczepańska et al. 2020), followed by 30 cycles at 95 °C for 30 sec, 51.2 °C for 45 sec, 72 °C for 45 sec, with a final extension at 72 °C for 10 min. While performing PCR, the Veriti Thermal Cycler (Life Technologies, Carlsbad, CA, USA) was used. Amplification products were separated in 1% agarose gel, photographed and compared with the DNA mass ruler (Thermo Fisher Scientific Waltham, MA, USA).

Table 1. The species and specimens used in the phylogenetic analyses and/or haplotype network analyses, sequences newly generated for this study are in bold.

Species	Year of collection	Isolate	Locality	Collector (-s)	Voucher specimens (herbarium)	GenBank no. (ITS)
Cetrariella commixta	**2007**	**36**	**Poland, Sudety Mts**	**Kossowska, M.**	**Kossowska 107 (personal herbarium)**	**MZ029708**
Cetrariella commixta	**2008**	**37**	**Poland, Sudety Mts**	**Kossowska, M.**	**Kossowska 231 (personal herbarium)**	**MZ029709**
Cetrariella commixta	**2016**	**97**	**Poland, Sudety Mts**	**Szczepańska, K.**	**Szczepańska 1137 (WRSL)**	**MZ029733**
Cetrariella commixta	**2016**	**124**	**Poland, Sudety Mts**	**Szczepańska, K.**	**Szczepańska 1184 (WRSL)**	**MZ029753**
Cetrariella commixta	**2018**	**129**	**Germany, Bayerischer Wald**	**Szczepańska, K.**	**Szczepańska 1267 (WRSL)**	**MZ029758**
Cetrariella commixta			Finland	Haikonen, V.	Haikonen 19093 (H)	AF451796
Cetrariella commixta	1996		Canada, British Columbia	Miao, V. & Taylor, T.		AF451797
Cetrariella commixta			Sweden	Wedin, M.	Wedin 8143 (UPS)	GU994554
Cetrariella commixta			Spain, Segovia	Rico, V. J.	15555 (MAF)	GU994555
Cetrariella commixta	2004	CCO 01	Sweden, Lule Lappmark		1273926 (LD)	KC990132
Cetrariella commixta		6543	Greenland, SEm, Tasilaq	Hansen, E. S.	Hansen ESH-10B.139 (C)	KF257934
Cetrariella commixta		6547	Greenland, SWm, Qeqertaq	Hansen, E. S.	Hansen ESH-09.087 (C)	KF257935
Cetrariella commixta		6567	Greenland, S, Igaliku	Hansen, E. S.	Hansen ESH-08.173 (C)	KF257936
Cetrariella commixta		6570	Greenland, SWm, Midgard	Hansen, E. S.	Hansen ES-09.030 (C)	KF257937
Cetrariella commixta		6572	Greenland, S, Aappilattoq	Hansen, E. S.	Hansen ES-04.070 (C)	KF257938
Cetrariella commixta		6573	Greenland, SWm, Qeqertaq	Hansen, E. S.	Hansen ES-09.064 (C)	KF257939
Cetrariella commixta	2014		Norway, Finnmark	Westberg, M.	O-L-195926	KY266843
Melanelia agnata	**2016**	**102**	**Poland, Karpaty Mts**	**Szczepańska, K.**	**Szczepańska 1151 (WRSL)**	**MZ029737**
Melanelia agnata	**2016**	**103**	**Poland, Karpaty Mts**	**Szczepańska, K.**	**Szczepańska 1150 (WRSL)**	**MZ029738**
Melanelia agnata	2009	6549	Greenland, SW m, Jensens Nunatakker	Hansen, E. S.	Hansen ESH-09.478 (C)	KF257940
Melanelia agnata	2009	6553	Greenland, SW m, Jensens Nunatakker	Hansen, E. S.	Hansen ESH-09.435 (C)	KF257941
Melanelia agnata	2007	6563	Greenland, N, Constable Bugt	Hansen, E. S.	Hansen ESH-07.464 (C)	KF257942
Melanelia agnata	2002	MX_MS2	Iceland, Imi	Heiðmarsson, S.	LA29683 (AMHN)	KY508672
Melanelia agnata	2005	MX_MS3	Iceland, Ino	Kristinsson, H.	LA27562 (AMHN)	KY963373
Melanelia agnata	2008	MX_MS4	Iceland, Isu	Hjaltadóttir, A.	LA30974 (AMHN)	KY508673
Melanelia agnata	2012	MX_MS5	Iceland, Ino	Heiðmarsson, S.	LA31859 (AMHN)	KY963374
Melanelia agnata	2014		Norway, Sor-Trondelag	Timdal, E.	O-L-196376	MK812394
Melanelia culbersonii			USA	Lendemer, J.	Lendemer 13821 (NY)	KR995286
Melanelia hepatizon	**2016**	**83**	**Poland, Sudety Mts**	**Szczepańska, K.**	**Szczepańska 1051 (WRSL)**	**MZ029723**
Melanelia hepatizon	**2016**	**91**	**Poland, Sudety Mts**	**Szczepańska, K.**	**Szczepańska 1120 (WRSL)**	**MZ029717**
Melanelia hepatizon	**2016**	**95**	**Poland, Sudety Mts**	**Szczepańska, K.**	**Szczepańska 1136A (WRSL)**	**MZ029731**
Melanelia hepatizon	**2016**	**96**	**Poland, Sudety Mts**	**Szczepańska, K.**	**Szczepańska 1136B (WRSL)**	**MZ029732**

Species	Year of collection	Isolate	Locality	Collector (-s)	Voucher specimens (herbarium)	GenBank no. (ITS)
Melanelia hepatizon	**2016**	**98**	**Poland, Sudety Mts**	**Szczepańska, K.**	**Szczepańska 1138 (WRSL)**	**MZ029734**
Melanelia hepatizon	**2016**	**109**	**Poland, Karpaty Mts**	**Szczepańska, K.**	**Szczepańska 1153 (WRSL)**	**MZ029741**
Melanelia hepatizon	**2016**	**110**	**Poland, Karpaty Mts**	**Szczepańska, K.**	**Szczepańska 1154A (WRSL)**	**MZ029730**
Melanelia hepatizon	**2016**	**111**	**Poland, Karpaty Mts**	**Szczepańska, K.**	**Szczepańska 1154B (WRSL)**	**MZ029743**
Melanelia hepatizon	**2016**	**113**	**Poland, Karpaty Mts**	**Szczepańska, K.**	**Szczepańska 1144 (WRSL)**	**MZ029745**
Melanelia hepatizon	**2016**	**116**	**Slovakia, Karpaty Mts**	**Szczepańska, K.**	**Szczepańska 1146 (WRSL)**	**MZ029746**
Melanelia hepatizon	**2016**	**117**	**Slovakia, Karpaty Mts**	**Szczepańska, K.**	**Szczepańska 1147 (WRSL)**	**MZ029747**
Melanelia hepatizon	**2016**	**119**	**Poland, Sudety Mts**	**Szczepańska, K.**	**Szczepańska 1180 (WRSL)**	**MZ029748**
Melanelia hepatizon	**2016**	**122**	**Poland, Sudety Mts**	**Szczepańska, K.**	**Szczepańska 1182 (WRSL)**	**MZ029751**
Melanelia hepatizon	**2018**	**128**	**Germany, Bayerischer Wald**	**Szczepańska, K.**	**Szczepańska 1269 (WRSL)**	**MZ029757**
Melanelia hepatizon	1996		Canada, British Columbia		Thell & Veer BC-9677 (LD)	AF141369
Melanelia hepatizon	2001	DNA-AT934	Italy, Trentino-Alto Adige (south Tirolia)	Feuerer T. & Thell A. s. n.	LD, HBG	AF451776
Melanelia hepatizon			Sweden	Wedin, M.	Wedin 6812 (UPS)	DQ980016
Melanelia hepatizon			Greenland, NWn, Siorapuluk	Hansen, E. S.	Hansen ESH-09B.164 (C)	KF257943
Melanelia hepatizon			Greenland, NWn, Qaanaaq	Hansen, E. S.	Hansen ESH-09B.026 (C)	KF257944
Melanelia hepatizon			Greenland, SEm, Tasilaq	Hansen, E. S.	Hansen ESH-10B.014 (C)	KF257945
Melanelia hepatizon			Greenland, SWm, Nuuq	Hansen, E. S.	Hansen ESH-10A.019 (C)	KF257946
Melanelia hepatizon			Greenland, S, Qaqortoq	Hansen, E. S.	Hansen ESH-08.036 (C)	KF257947
Melanelia hepatizon			Greenland, S, Igaliku	Hansen, E. S.	Hansen ESH-08.170 (C)	KF257948
Melanelia hepatizon			Greenland, S, Narssarsuag	Hansen, E. S.	Hansen ESH-08.263 (C)	KF257949
Melanelia hepatizon			Greenland, S, Igaliku	Hansen, E. S.	Hansen ESH-08.215 (C)	KF257950
Melanelia hepatizon			Greenland, SWm, Midgard	Hansen, E. S.	Hansen ESH-09.386 (C)	KF257951
Melanelia hepatizon			Greenland, SWm, Frederikshab Isblink	Hansen, E. S.	Hansen ESH-09.324 (C)	KF257952
Melanelia hepatizon			Greenland, S, Igaliku	Hansen, E. S.	Hansen ESH-08.477 (C)	KF257953
Melanelia hepatizon	2014		Norway, Finnmark	Westberg, M.	O-L-195864	KY266879
Melanelia hepatizon	2003	MH1	Iceland, IAu		LA30501 (AMHN)	KY508674
Melanelia hepatizon	2007	MH3	Iceland, IVe		LA30676 (AMHN)	KY508675
Melanelia hepatizon	2007	MH4	Iceland, IVe		LA30674 (AMHN)	KY508676
Melanelia hepatizon	2007	MH5	Iceland, IVe		LA30675 (AMHN)	KY508677
Melanelia hepatizon	2007	MH6	Iceland, IVe		LA30673 (AMHN)	KY508678
Melanelia hepatizon	2014	MH9	Iceland, INo		LA20781 (AMHN)	KY508679
Melanelia hepatizon	2013	MH10	Iceland, INv		LA30117 (AMHN)	KY508680
Melanelia hepatizon	2012	MH11	Iceland, Inv		LA31861 (AMHN)	KY963376

Species	Year of collection	Isolate	Locality	Collector (-s)	Voucher specimens (herbarium)	GenBank no. (ITS)
Melanelia hepatizon	2014		Norway, Hordaland	Timdal, E.	O-L-195807	MK812512
Melanelia hepatizon	2015		Norway, Nord-Trondelag	Bendiksby, M. et al.	O-L-201254	MK812070
Melanelia hepatizon	2013		Norway, Buskerud	Rui, S. & Timdal, E.	O-L-184723	MK812188
Melanelia stygia	**2007**	**40**	**Poland, Sudety Mts**	**Kossowska, M.**	**Kossowska 123 (personal herbarium)**	**MZ029710**
Melanelia stygia	**2009**	**42**	**Austria, Tyrol**	**Szczepańska, K.**	**Szczepańska 737 (WRSL)**	**MZ029712**
Melanelia stygia	**2016**	**94**	**Poland, Sudety Mts**	**Szczepańska, K.**	**Szczepańska 1134 (WRSL)**	**MZ029719**
Melanelia stygia	**2016**	**104**	**Poland, Karpaty Mts**	**Szczepańska, K.**	**Szczepańska 1152 (WRSL)**	**MZ029739**
Melanelia stygia	**2016**	**108**	**Poland, Karpaty Mts**	**Szczepańska, K.**	**Szczepańska 1149 (WRSL)**	**MZ029740**
Melanelia stygia	**2016**	**112**	**Poland, Karpaty Mts**	**Szczepańska, K.**	**Szczepańska 1160 (WRSL)**	**MZ029744**
Melanelia stygia	**2018**	**127**	**Czech Republic, Šumava**	**Szczepańska, K.**	**Szczepańska 1265 (WRSL)**	**MZ029756**
Melanelia stygia			Finland, Nyland	Kuusinen, M.	FIN-9714 (LD)	AF115763
Melanelia stygia			Italy	Feurerer, T & Thell, A.	DNA-AT922 (LD)	AF451775
Melanelia stygia			Finland, Enonkoski	Haikonen, V.	Haikonen 20365	AY611097
Melanelia stygia			Austria, Steiermark	Hafellner, J.	Hafellner 51658	AY611121
Melanelia stygia	2008	6551	Greenland, S, Qaqortoq	Hansen, E. S.	Hansen ESH-08.036 (C)	KF257954
Melanelia stygia	2008	6569	Greenland, S, Igaliku	Hansen, E. S.	Hansen ESH-08.478 (C)	KF257955
Melanelia stygia	1998	MX_MS1	Iceland, IAu	Kristinsson, H.	LA19972 (AMHN)	KY508681
Melanelia stygia	2014	MX_MS3	Iceland, IAu	Kristinsson, H.	LA20775 (AMHN)	KY508682
Melanelia stygia	2013	MX_MS4	Iceland, IAu	Kristinsson, H.	LA16894 (AMHN)	KY508683
Melanelia stygia	2000	MX_MS2	Iceland, IAu	Kristinsson, H.	LA28243 (AMHN)	KY963375
Melanelia stygia	2013		Norway, Buskerud	Rui, S. & Timdal, E.	O-L-184736	MK812608
Melanelia stygia	2014		Norway, Sor-Trondelag	Timdal, E.	O-L-196377	MK812312
Montanelia disjuncta	**2013**	**50**	**Poland, Sudsty Forelands**	**Szczepańska, K.**	**Szczepańska 969 (WRSL)**	**MZ029713**
Montanelia disjuncta	**2014**	**51**	**Poland, Sudety Mts**	**Szczepańska, K.**	**Szczepańska 989 (WRSL)**	**MZ029714**
Montanelia disjuncta	**2015**	**57**	**Poland, Sudety Foothills**	**Szczepańska, K.**	**Szczepańska 1023 (WRSL)**	**MZ029715**
Montanelia disjuncta	**2015**	**78**	**Poland, Sudety Mts**	**Szczepańska, K.**	**Szczepańska 1034 (WRSL)**	**MZ029716**
Montanelia disjuncta	**2015**	**79**	**Poland, Sudety Mts**	**Szczepańska, K.**	**Szczepańska 1038 (WRSL)**	**MZ029711**
Montanelia disjuncta	**2015**	**80**	**Poland, Sudety Mts**	**Szczepańska, K.**	**Szczepańska 1039 (WRSL)**	**MZ029720**
Montanelia disjuncta	**2016**	**81**	**Poland, Sudety Mts**	**Szczepańska, K.**	**Szczepańska 1047 (WRSL)**	**MZ029721**
Montanelia disjuncta	**2016**	**82**	**Poland, Sudety Mts**	**Szczepańska, K.**	**Szczepańska 1048 (WRSL)**	**MZ029722**
Montanelia disjuncta	**2016**	**85**	**Poland, Sudety Mts**	**Szczepańska, K.**	**Szczepańska 1054 (WRSL)**	**MZ029724**
Montanelia disjuncta	**2016**	**86**	**Poland, Sudety Mts**	**Szczepańska, K.**	**Szczepańska 1081 (WRSL)**	**MZ029725**
Montanelia disjuncta	**2016**	**87**	**Poland, Sudety Mts**	**Szczepańska, K.**	**Szczepańska 1082 (WRSL)**	**MZ029726**

Species	Year of collection	Isolate	Locality	Collector (-s)	Voucher specimens (herbarium)	GenBank no. (ITS)
Montanelia disjuncta	**2016**	**88**	**Poland, Sudety Mts**	**Szczepańska, K.**	**Szczepańska 1110 (WRSL)**	**MZ029727**
Montanelia disjuncta	**2016**	**89**	**Poland, Sudety Mts**	**Szczepańska, K.**	**Szczepańska 1111 (WRSL)**	**MZ029728**
Montanelia disjuncta	**2016**	**90**	**Poland, Sudety Mts**	**Szczepańska, K.**	**Szczepańska 1119 (WRSL)**	**MZ029729**
Montanelia disjuncta	**2016**	**92**	**Pland, Sudety Foothils**	**Szczepańska, K.**	**Szczepańska 1127 (WRSL)**	**MZ029755**
Montanelia disjuncta	**2016**	**93**	**Pland, Sudety Foothils**	**Szczepańska, K.**	**Szczepańska 1128 (WRSL)**	**MZ029718**
Montanelia disjuncta	**2016**	**120**	**Poland, Sudety Mts**	**Szczepańska, K.**	**Szczepańska 1181A (WRSL)**	**MZ029749**
Montanelia disjuncta	**2016**	**121**	**Poland, Sudety Mts**	**Szczepańska, K.**	**Szczepańska 1181B (WRSL)**	**MZ029750**
Montanelia disjuncta	**2016**	**123**	**Poland, Sudety Mts**	**Szczepańska, K.**	**Szczepańska 1183 (WRSL)**	**MZ029752**
Montanelia disjuncta	**2016**	**125**	**Poland, Sudety Mts**	**Szczepańska, K.**	**Szczepańska 1185 (WRSL)**	**MZ029754**
Montanelia disjuncta	**2016**	**126**	**Poland, Sudety Mts**	**Szczepańska, K.**	**Szczepańska 1230 (WRSL)**	**MZ029742**
Montanelia disjuncta	**2018**	**130**	**Czech Republic, Šumava**	**Szczepańska, K.**	**Szczepańska 1271 (WRSL)**	**MZ029759**
Montanelia disjuncta			Austria, Steiermark		Mayrhofer 13743	AY611077
Montanelia disjuncta			India		MAF-Lich 15512	GU994556
Montanelia disjuncta			United Kingdom		Coppins 637	JX974654
Montanelia disjuncta			Greenland, NWn, Siorapaluk	Hansen, E. S.	Hansen ESH-09B.363 (C)	KF257957
Montanelia disjuncta		3921	Canada, Yukon Territory	Spribille, T.	Spribille s.n.	KP771824
Montanelia disjuncta		3963	Greenland, Northwest	Hansen, E. S.	Hansen ESH-09B.051 (C)	KP771827
Montanelia disjuncta		3995	USA, Maine	Harris, R.	Harris 52938 (NY)	KP771828
Montanelia disjuncta		4503	Norway, Tromso	Bjerke, J.W.	Bjerke WP286-2 (TLE)	KP771829
Montanelia disjuncta		4851	Canada, Yukon Territory	Esslinger, T. L.	Esslinger BP94-3 (TLE)	KP771830
Montanelia disjuncta		5970	USA, Alaska	Esslinger, T. L.	Esslinger 19403 (TLE)	KP771831
Montanelia disjuncta		6575	Greenland, Northwest, Siorapaluk	Hansen, E. S.	Hansen ESH-09B.323 (C)	KP771833
Montanelia disjuncta		MDISJUNCT	Sweden, Lycksele Lappmark	Wedin, M.	Wedin 7143 (UPS)	KP771834
Montanelia disjuncta		MEDI637	United Kingdom, Scotland	Coppins, B.	Coppins s.n (MAF)	KP771835
Montanelia disjuncta		MESO773	India, Uttaranchal	Divakar, P. K.	MAF-Lich 15512	KP771837
Montanelia disjuncta	2014		Norway, Finnmark, Vadso	Haugan, R.	O-L-198675	KY266910
Montanelia disjuncta	2007	MD8	Iceland, INo		LA30657 (AMHN)	KY508686
Montanelia disjuncta			Sweden	Wedin, M.	Wedin 7143 (UPS)	DQ980015
Montanelia disjuncta			USA	Lumbsch, H. T.	Lumbsch 2010/M7 (F)	JX126181
Montanelia disjuncta			USA, Maine		Harris 55589 (NY)	KF257960
Montanelia disjuncta			USA, Alaska		Esslinger 19403 (TLE)	KF257968
Montanelia disjuncta			Canada		Goward 08	JX974658
Montanelia disjuncta			Canada, Yukon		Spribille s.n. (GZU)	KF257956
Montanelia disjuncta			Canada, Alberta		Holzinger 1061 (UBC)	KF257962
Montanelia disjuncta			Canada, British Columbia		Esslinger BP109-1 (TLE)	KF257964
Montanelia disjuncta			Canada, British Columbia		Esslinger BP97-01 (TLE)	KF257965

Species	Year of collection	Isolate	Locality	Collector (-s)	Voucher specimens (herbarium)	GenBank no. (ITS)
Montanelia disjuncta			Canada, Yukon		Esslinger BP94-2 (TLE)	KF257966
Montanelia disjuncta			Canada, Yukon		Esslinger BP94-3 (TLE)	KF257967
Montanelia disjuncta			Canada, New Brunswick		McMullin 7483 (TLE)	KF257969
Montanelia disjuncta			Canada, British Columbia		Goward 2008 (MAF)	KP771836
Montanelia disjuncta			Greenland, S, Igaliku	Hansen, E. S.	Hansen ESH-08.304 (C)	KF257958
Montanelia disjuncta			Greenland, NWn, Qaanaaq	Hansen, E. S.	Hansen ESH-09B.051 (C)	KF257959
Montanelia disjuncta			Greenland, S, Igaliku	Hansen, E. S.	Hansen ESH-08.216 (C)	KF257970
Montanelia disjuncta			Greenland, NWn, Siorapuluk	Hansen, E. S.	Hansen ESH-09B.323 (C)	KF257971
Montanelia disjuncta		3956	Greenland, Northwest	Hansen, E. S.	Hansen ESH-09B.363 (C)	KP771825
Montanelia disjuncta		3957	Greenland, South	Hansen, E. S.	Hansen ESH-08.304 (C)	KP771826
Montanelia disjuncta		6574	Greenland, South, Igaliku	Hansen, E. S.	Hansen ESH-08.216 (C)	KP771832
Montanelia disjuncta			Norway, Tromso		Bjerke WP286-2 (TLE)	KF257961
Montanelia disjuncta			India, Uttar Pradesh		Divakar 15512 (MAF-Lich)	KF257972
Montanelia disjuncta	2000	MD2	Iceland, Iau		LA28245 (AMHN)	KY963377
Montanelia disjuncta	2009	MD5	Iceland, Ino		LA31552 (AMHN)	KY963378
Montanelia disjuncta	2007	MD3	Iceland, Ino		LA30617 (AMHN)	KY508684
Montanelia disjuncta			Canada, British Columbia		Goward 10-19 (UBC)	KF257963
Montanelia disjuncta	2014		Norway, Sor-Trondelag	Timdal, E.	O-L-196357	MK811711
Montanelia disjuncta	2014		Norway, Finnmark	Timdal, E.	O-L-195590	MK811852
Montanelia disjuncta	2006	MD4	Iceland, Ino		LA27588	KY508685
Montanelia sorediata	**2016**	**100**	**Poland, Karpaty Mts**	**Szczepańska, K.**	**Szczepańska 1156 (WRSL)**	**MZ029735**
Montanelia sorediata	**2016**	**101**	**Poland, Karpaty Mts**	**Szczepańska, K.**	**Szczepańska 1155 (WRSL)**	**MZ029736**
Montanelia sorediata		4001	USA, Pennsylvania	Lendemer, J.	Lendemer 13329 (NY)	KF257978
Montanelia sorediata		4824	Canada, British Columbia	Esslinger, T.L.	Esslinger BP111-1 (TLE)	KF257979
Montanelia sorediata		4884	USA, Alaska	Esslinger, T.L.	Esslinger BP73-6 (TLE)	KF257980
Montanelia sorediata		5981	Russia, Khabarovskiy Krai	Spribille, T.	Spribille 31972 (GZU)	KF257981
Montanelia sorediata		6380	Canada, Ontario	McMullin, T.	McMullin 8139 (TLE)	KF257982
Montanelia sorediata		B_8600	Japan, Mt. Ohyama	Ohmura, Y.	Ohmura 9666 (TNS)	KM386101
Montanelia sorediata		MESO778	Sweden, Vasterbotten	Wedin, M.	Wedin 6862 (UPS)	KP771845
Montanelia sorediata		4001	USA, Pennsylvania	Lendemer, J.	Lendemer 13329 (NY)	KP771846
Montanelia sorediata		5981	Russia, Khabarovskiy Krai	Spribille, T.	Spribille 31972 (GZU)	KP771847
Montanelia sorediata	2014		Norway, Telemark	Timdal, E.	O-L-195791	MK811963
Montanelia sorediata	2014		Norway, Troms	Timdal, E.	O-L-195658	MK811965
Montanelia sorediata	2016		Norway, Buskerud	Dahl, M. S., Kistenich, S. D., Timdal, E., Toreskaas, A. K.	O-L-204941	MK811977
Montanelia sorediata		C_4670	Canada, British Columbia	Bjork, C.	Bjork 15153 (UBC)	KM386102

Bands corresponding to the ITS region were excised from the agarose gel and then purified by ethanol precipitation. Cleaned samples were sent to a sequencing service (Genomed, Warszawa, Poland). All laboratory analyses were performed at the Department of Botany and Plant Ecology at the Wrocław University of Environmental and Life Sciences.

Sequence alignment and phylogenetic analysis

The newly-generated sequences and selected representatives of brown saxicolous Parmeliaceae were aligned using the Guidance 2 server (Landan and Graur 2008; Penn et al. 2010; Sela et al. 2015) employing the MAFFT algorithm (Katoh et al. 2002) followed by elimination of terminal ends. The final alignment consisted of 117 sequences of 535 sites. Further, we used Partition Finder 2 (Lanfear et al. 2016) implemented at the CIPRES Science Gateway (Miller et al. 2010). Two different models were found for partitions: GTR+G for ITS1 and ITS2 and K80+G for the 18S and 5.8S regions.

Moreover, phylogenetic analysis of all *Melanelia* sequences was also performed. Newly-generated sequences and these downloaded from GenBank, together with representatives of *Cetraria commixta*, which were further used as an outgroup, were aligned using the Guidance 2 server (Landan and Graur 2008; Penn et al. 2010; Sela et al. 2015) employing the MAFFT algorithm (Katoh et al. 2002) followed by elimination of unreliable columns. The final alignment consisted of 76 sequences of 803 sites. Further, we used jModeltest 2.1 (Darriba et al. 2012) implemented at the CIPRES Science Gateway (Miller et al. 2010) and the K80+G model was selected.

Bayesian analysis was carried out using a Markov Chain Monte Carlo (MCMC) method, in MrBayes v. 3.2.6 (Huelsenbeck and Ronquist 2001; Ronquist and Huelsenbeck 2003) on the CIPRES Web Portal (Miller et al. 2010) using best models. Two parallel MCMC runs were performed, each using four independent chains and four million generations, sampling every 1000th tree. Posterior probabilities (PP) were determined by calculating a majority-rule consensus tree after discarding the initial 25% trees of each chain as the burn-in.

A Maximum Likelihood (ML) analysis was performed using RAxML-HPC2 v.8.2.10 (Stamatakis 2014) with 1000 ML bootstrap iterations (BS) and the GTR-GAMMAI model for both analyses. Phylogenetic trees were visualised using FigTree v. 1.4.2 (Rambaut 2012) and modified in Inkscape (https://inkscape.org/).

Haplotype networks

Newly-generated sequences of the ITS rDNA marker, together with sequences downloaded from GenBank from specimens of *Cetraria commixta*, *Melanelia agnata*, *M. hepatizon*, *M. stygia*, *Montanelia disjuncta* and *M. sorediata*, were aligned separately for each species using Seaview software (Galtier et al. 1996; Gouy et al. 2010). TCS networks (Clement et al. 2002) were created as implemented in PopART software (http://popart.otago.ac.nz). Nucleotide diversity per site was calculated using DnaSP v.6 software (Rozas et al. 2017).

Results

Phylogeny and haplotype networks

A total of 169 sequences were analysed in this study.

The RAxML tree did not contradict the Bayesian trees topologies for the strongly-supported branches and only the latter is shown with posterior probabilities. The bootstrap support values BS ≥ 70 and PP ≥ 0.95 were considered to be significant and are shown near the branches. In Fig. S1, three main, highly supported lineages representing *Melanelia* spp. (i.e. *M. agnata*, *M. hepatizon* and *M. stygia*), *Montanelia* spp. (i.e. *M. disjuncta* and *M. sorediata*) and *Cetraria commixta* were distinguished. The newly-sequenced specimens clustered together with other representatives of the species downloaded from GenBank. Amongst them, *Melanelia stygia* is not monophyletic, but forms two separate well-supported clades.

Moreover, to better understand phylogenetic relationships in the *Melanelia*, we performed additional analysis for all available ITS rDNA sequences from representatives of this genus. The Bayesian tree is presented in Fig. 1 with posterior probabilities and the bootstrap support values presented near the branches and with *Cetraria commixta* as an outgroup. In this tree, *Melanelia stygia* also forms two separate, highly-supported clades.

We constructed haplotype networks (Figs 2–7) to assess genetic variability within ITS rDNA marker for each species, including newly-collected specimens and data were downloaded from GenBank. The number of haplotypes found for each taxon ranged from five (in *Melanelia stygia*) to 12 (in *Melanelia hepatizon* and *Montanelia disjuncta*); however, their numbers seem to be correlated with the abundance of specimens tested, which ranged from 10 (in *Melanelia agnata*) to 67 (in *Montanelia disjuncta*). Moreover, we also calculated nucleotide diversity for each dataset and found lower values for *Montanelia disjuncta* and *Cetraria commixta* (0.00380 and 0.00405, respectively) and higher values for *Melanelia agnata*, *M. hepatizon* and *M. stygia* (0.01552, 0.01421 and 0.01418, respectively) (Table 2).

Characteristics of the studied species

***Cetraria commixta* (Nyl.) Th. Fr.**

Lichenographia Scandinavica 1:109 (1871) ≡ *Platysma commixtum* Nyl., Synopsis methodica lichenum 1:310 (1860) ≡ *Melanelia commixta* (Nyl.) A. Thell, Nova Hedwigia 60:417 (1995) ≡ *Cetrariella commixta* (Nyl.) A. Thell & Kärnefelt, Mycological Progress 3:309 (2004).

Description. *C. commixta* is a foliose species with elongated, smooth and flat lobes, 0.25–2.5 mm broad, which are thick on the margins and rounded at the ends (Szczepańska and Kossowska 2017). Its upper surface is glossy, olive-brown to dark brown or almost black. The lower surface is pale brown, but darker in the centre, with single, dark rhizines. *C. commixta* possess rounded or slightly elongated pseudocyphellae, which are present only on the margins and edges of lobes and cylindrical, marginal pycnidia, producing

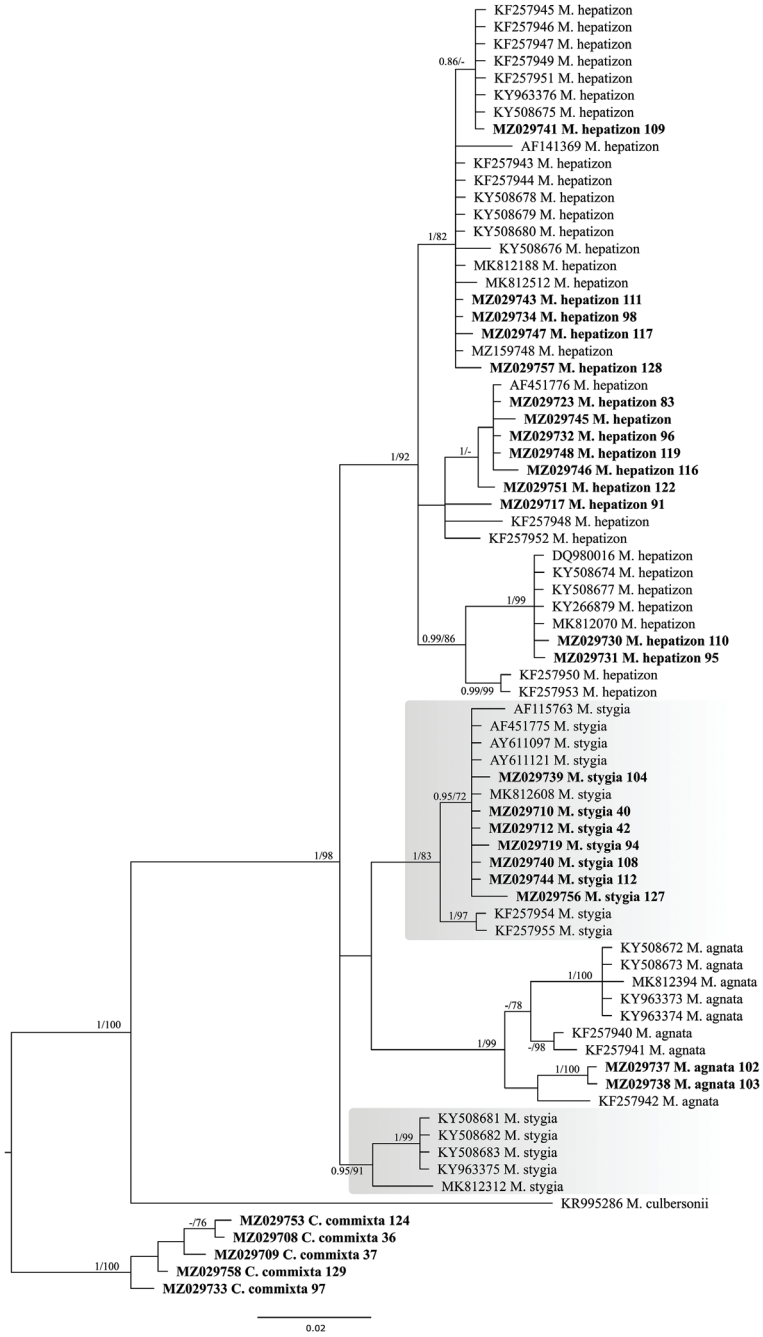

Figure 1. Phylogenetic relationships of *Melanelia* spp., based on Bayesian analysis of the ITS rDNA dataset. Posterior probabilities and Maximum Likelihood bootstrap values are shown near the internal branches. Newly-generated sequences are additionally described with isolate numbers following the species names and are marked in bold. GenBank accession numbers of sequences downloaded from GenBank are listed on the tree with species names.

hyaline, citriform conidia (3–4 × 1–1.5 µm). Apothecia are marginal, constricted at base, 0.2–7 mm diam., with hyaline, ellipsoid to oblong-ellipsoid ascospores (6–8 × 4–6 µm).

Chemistry. α-collatolic acid (chemotype I) or no substances (chemotype III).

Distribution. *C. commixta* is a circumpolar and arctic-alpine species (Otte et al. 2005), growing mainly in mountain sites, in open places with high precipitation, on natural acid, siliceous rocks in North America and Europe. Available molecular data concern samples collected in North America (Canada, Greenland), as well as North (Finland, Norway, Sweden) and West (Spain) Europe.

Haplotypes differentiation. We identified seven different haplotypes (Fig. 2, Table 2) within *C. commixta* (n = 17) that differ from each other in one or two positions, except for a single Canadian sample that differs in at least eight positions. The most common haplotype was found in ten specimens occurring in Greenland and North and Central Europe, amongst them being three newly-sequenced specimens (samples 37 and 97 from Poland and sample 129 from Germany). Moreover, two Polish specimens (samples 36 and 124 from the Sudety Mountains) represent a unique haplotype that differs from the most common one in a single position. Five haplotypes identified in our dataset were represented by single specimens originating from Greenland (3 haplotypes), Canada or Spain.

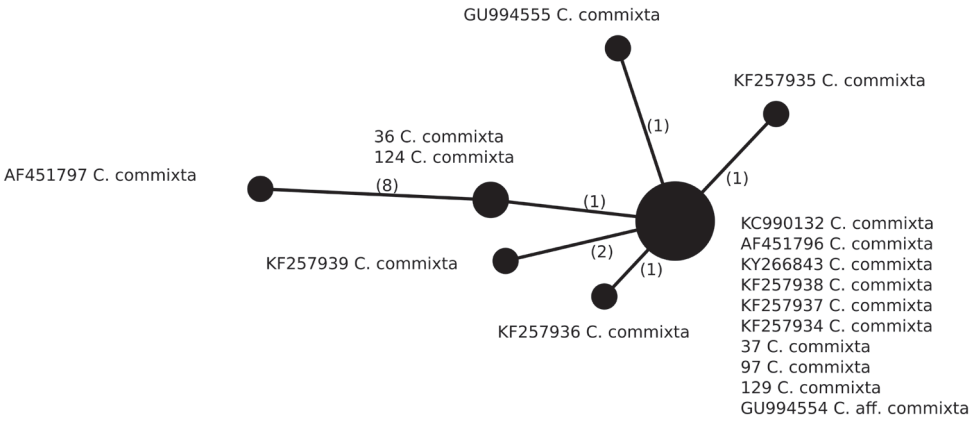

Figure 2. Haplotype network, based on ITS rDNA sequences from specimens of *Cetraria commixta*. Newly-generated sequences are described with isolate numbers preceding the species names. Sequences downloaded from GenBank are described with their accession numbers. Mutational changes are presented as numbers in brackets near lines between haplotypes.

Melanelia agnata (Nyl.) A. Thell

Nova Hedwigia 60:416 (1995) ≡ *Platysma agnatum* Nyl., Flora, Jena 60:562 (1877) ≡ *Cetraria agnata* (Nyl.) Kristinsson, Lichenologist 6:144 (1974).

Description. *M. agnata* has foliose thallus with flat, smooth, 0.25–2 mm broad lobes which are thicker on the margins and rounded at the ends (Szczepańska and Kossowska

Table 2. List of haplotypes identified in this study and their geographical distribution. Nucleotide diversity for each species is also presented, and the newly generated sequences are in bold.

Haplotypes number	North America	North Europe	Central Europe	West Europe	Asia	Nucleotide diversity
			Cetraria commixta			
1	KF257934 Greenland KF257937 Greenland KF257938 Greenland	AF451796 Finland KY266843 Norway KC990132 Sweden GU994554 Sweden	**37 Poland** **97 Poland** **129 Germany**			0.00405
2			**36 Poland** **124 Poland**			
3	AF451797 Canada					
4	KF257939 Greenland					
5	KF257936 Greenland					
6	KF257935 Greenland					
7				GU994555 Spain		
			Melanelia agnata			
1		KY508672 Iceland KY508673 Iceland KY963373 Iceland KY963374 Iceland				0.01552
2			**102 Poland** **103 Poland**			
3	KF257940 Greenland					
4	KF257941 Greenland					
5	KF257942 Greenland					
6		MK257942 Norway				
			Melanelia hepatizon			
1	KF257943 Greenland KF257944 Greenland	KY508678 Iceland KY508680 Iceland KY508679 Norway MK812188 Norway	**98 Poland** **111 Poland** **128 Germany**			0.01421
2	KF257945 Greenland KF257946 Greenland KF257947 Greenland KF257949 Greenland KF257951 Greenland	KY508675 Iceland KY508676 Iceland	**109 Poland**			
3		KY508674 Iceland KY508677 Iceland KY266879 Iceland KY266879 Norway DQ980016 Sweden	**95 Poland** **110 Poland**			
4			**83 Poland** **96 Poland** **113 Poland** **116 Slovakia** **119 Poland** **122 Poland**	AF451776 Italy		
5	KF257950 Greenland KF257953 Greenland					
6	KF257952 Greenland					
7	KF257948 Greenland					
8	AF141369 Canada					
9		KY963376 Iceland				
10		MK812512 Norway				
11			**91 Poland**			
12			**117 Slovakia**			

Haplotypes number	North America	North Europe	Central Europe	West Europe	Asia	Nucleotide diversity
			Melanelia stygia			
1		AY611097 Finland MK812608 Norway	AY611121 Austria **40 Poland** **42 Austria** **94 Poland** **104 Poland** **108 Poland** **112 Poland** **127 Czech Republic**	AF451775 Italy		0.01418
2		KY508681 Island KY508682 Island KY508683 Island KY963375 Island				
3	KF257954 Greenland KF257955 Greenland					
4		AF115763 Finland				
5		MK812312 Norway				
			Montanelia disjuncta			
1	KF257964 Canada KF257967 Canada KF257969 Canada KP771830 Canada JX126181 USA	KY963378 Iceland KF257961 Norway KP771829 Norway KP771834 Sweden	AY611077 Austria **50 Poland** **51 Poland** **57 Poland** **80 Poland** **81 Poland** **82 Poland** **85 Poland** **86 Poland** **87 Poland** **88 Poland** **93 Poland** **121 Poland** **125 Poland** **126 Poland** **130 Czech Republic**		GU994556 India KF257972 India KP771837 India	0.00380
2	KF257962 Canada KF257965 Canada KF257966 Canada KP771832 Greenland KF257958 Greenland KF257970 Greenland KP771826 Greenland	KY963377 Iceland KY266910 Norway DQ980015 Sweden	**90 Poland** **120 Poland**			
3	KF257957 Greenland KF257971 Greenland KP771825 Greenland KP771833 Greenland	KY508684 Iceland KY508685 Iceland KY508686 Iceland				
4	-	JX974654 United Kingdom KP771835 United Kingdom	**78 Poland** **79 Poland** **89 Poland** **92 Poland** **123 Poland**			

Haplotypes number	North America	North Europe	Central Europe	West Europe	Asia	Nucleotide diversity
5	KF257956 Canada KP771824 Canada					
6	JX974658 Canada KP771836 Canada					
7	KF257963 Canada					
8	KF257959 Greenland KP771827 Greenland					
9	KF257968 USA KP771831 USA					
10	KF257960 USA KP771828 USA					
11		MK811852 Norway				
12		MK811711 Norway				
			Montanelia sorediata			
1		MK811977 Norway MK811965 Norway GU994557 Sweden KP771845 Sweden	**100 Poland**			0.00830
2	KF257978 USA KP771846 USA				KF257981 Russia KP771847 Russia KM386101 Japan	
3	KF257980 USA		**101 Poland**			
4	KM386102 Canada KF257982 Canada					
5	KF257979 Canada					
6		MK811963 Norway				

2017). The upper surface is glossy, olive-brown to dark brown. The lower surface is pale brown to dark brown in the centre, with single, dark rhizines. *M. agnata* possess pseudocyphellae which are larger on the lobe margins and smaller, punctiform on the upper surface of the lobes. Pycnidia are mainly marginal to laminal, partially immersed and globose with hyaline bacilliform conidia (4.5–5.5 × 1 μm). Apothecia are not seen in examined material.

Chemistry. No secondary metabolites were detected by TLC.

Distribution. *M agnata* is a rare taxon occurring in arctic and boreal regions in North America and Europe, growing in open stands on siliceous and basalt rocks (Otte et al. 2005). Available molecular data concern samples collected only in North America (Greenland) and North Europe (Iceland, Norway).

Haplotypes differentiation. Six different haplotypes were identified in *M. agnata* (n = 10), of which two Polish specimens, collected in the Karpaty Mountains, have the same, not previously known, haplotype (Fig. 3, Table 2). It differs from other haplotypes in at least seven positions. However, the remaining specimens originate from Greenland, Iceland or Norway and no other samples from Central Europe have been sequenced until now. Four Icelandic specimens have the same haplotype, which is similar to the haplotype from Norwegian specimens. In contrast, Icelandic haplotypes differ from Greenlandic haplotypes in at least eight positions. Whether their genetic diversity supports conclusions from previous papers suggesting potentially unrecognised species lineages in the *M. agnata* genus (Leavitt et al. 2014; Xu et al. 2017) remains unresolved and should be further studied.

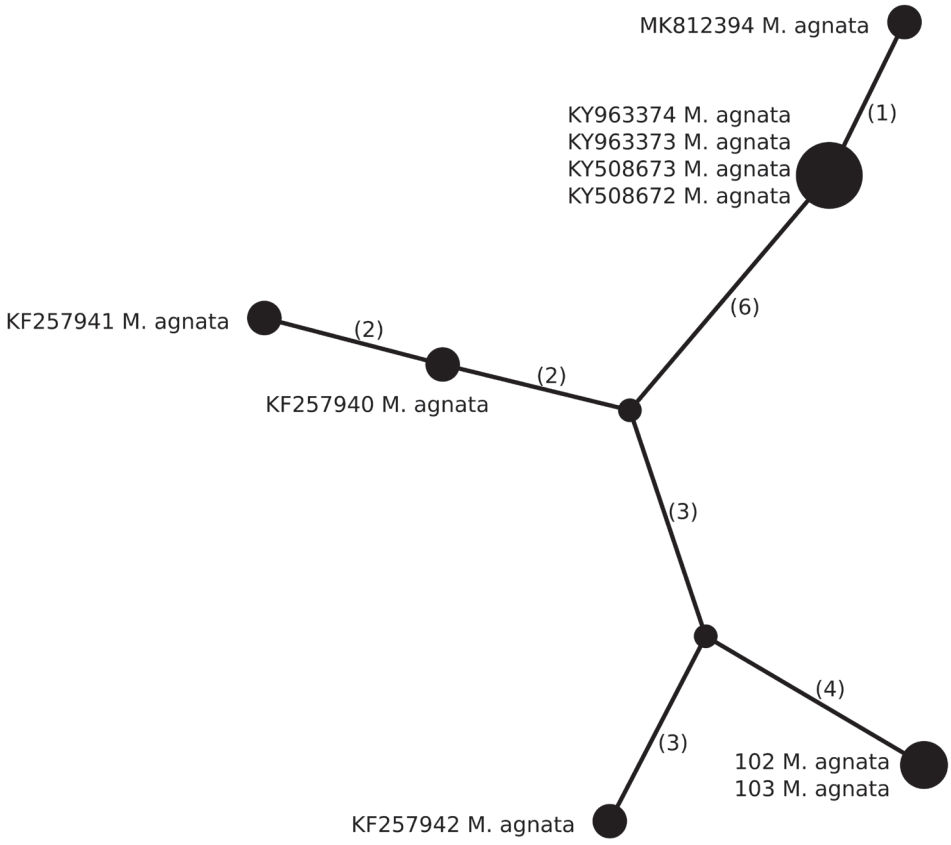

Figure 3. Haplotype network, based on ITS rDNA sequences from specimens of *Melanelia agnata*. Newly-generated sequences are described with isolate numbers preceding the species names. Sequences downloaded from GenBank are described with their accession numbers. Mutational changes are presented as numbers in brackets near lines between haplotypes.

Melanelia hepatizon (Ach.) A. Thell

Nova Hedwigia 60:419 (1995) ≡ *Lichen hepatizon* Ach., Lichenographiae Sueciae Prodromus 110 (1798) ≡ *Cetraria hepatizon* (Ach.) Vain., Termeszetrajzi Füzetek 22:278 (1899).

Description. *M. hepatizon* is foliose species with flat lobes that are 0.25–2.5 mm broad and thick at the margins (Szczepańska and Kossowska 2017). Its upper surface is glossy, brown to almost black. The lower surface is dark brown to black, paler near the margins, with single, dark rhizines. Pseudocyphellae are mainly present on the margins and edges of lobes. Pycnidia are marginal, but sometimes also laminal, sessile, globose to stalked, slightly elongated or cylindrical with hyaline, bacilliform conidia (3–5 × 1 µm). Apothecia are marginal to laminal, sessile, with hyaline, ellipsoid to oblong-ellipsoid ascospores (6–8 × 4–6 µm).

Chemistry. Stictic and norstictic acids.

Distribution. *M. hepatizon* is a circumpolar and arctic-alpine species occurring from oceanic to continental sites on siliceous rocks in North America and Europe (Otte et al. 2005). Available molecular data concern samples collected in North America (Canada, Greenland) as well as North (Iceland, Norway, Sweden) and West (Italy) Europe.

Haplotypes differentiation. A higher number of haplotypes was detected in *M. hepatizon* (n = 40), in which we identified 12 haplotypes (Fig. 4, Table 2). Amongst newly-sequenced specimens, we identified six haplotypes. Some are more common and were previously found in Greenland, Iceland, Italy, Norway or Sweden. In contrast, others were only found in newly-sequenced specimens, such as sample 91 from the Sudety Mountains in Poland and sample 117 from the Karpaty Mountains in Slovakia. However, no geographic pattern was found in the dataset.

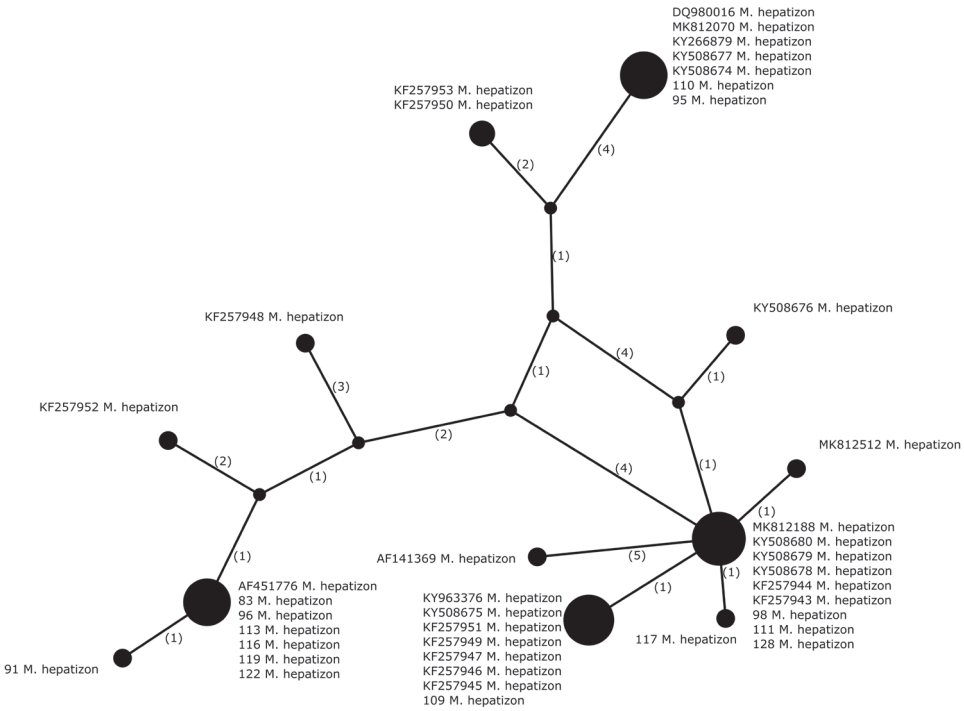

Figure 4. Haplotype network, based on ITS rDNA sequences from specimens of *Melanelia hepatizon*. Newly-generated sequences are described with isolate numbers preceding the species names. Sequences downloaded from GenBank are described with their accession numbers. Mutational changes are presented as numbers in brackets near lines between haplotypes.

Melanelia stygia (L.) Essl.

Mycotaxon 7:47 (1978) ≡ *Lichen stygius* L., Species Plantarum 2:1143 (1753).

Description. *M. stygia* has foliose thallus, composed of 0.25–1.5 mm broad, smooth and usually distinctly convex lobes (Szczepańska and Kossowska 2017). The upper

surface is glossy, dark brown to almost black. The lower surface is dark brown to black, paler near the margins, with single, dark rhizines. Pseudocyphellae in this species are numerous, rounded or slightly elongated and laminal – clearly visible on the upper surface of the lobes. Pycnidia are also common, globose, laminal and immersed with hyaline, bacilliform conidia (3.5–5 × 1 μm). Apothecia are laminal, constricted at the

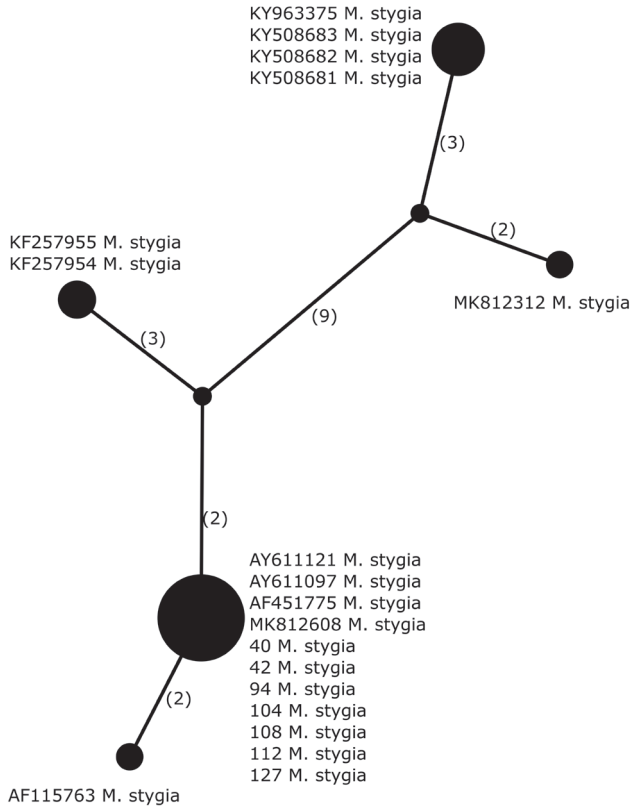

Figure 5. Haplotype network, based on ITS rDNA sequences from specimens of *Melanelia stygia*. Newly-generated sequences are described with isolate numbers preceding the species names. Sequences downloaded from GenBank are described with their accession numbers. Mutational changes are presented as numbers in brackets near lines between haplotypes.

base and 0.5–6 mm in diameter. Ascospores are hyaline, ellipsoid to oblong-ellipsoid, 6–8 × 4–6 μm in size.

Chemistry. Protocetraric and fumarprotocetraric acids (Race 1) or no substances detected (Race 6).

Distribution. *M. stygia* is a circumpolar and arctic-alpine species occurring mainly on siliceous rocks in upper mountain areas in North America and Europe (Otte et al. 2005). Available molecular data concern only a few samples collected in North America (Greenland) and North (Iceland, Finland, Norway) and West (Italy) Europe.

Haplotypes differentiation. Amongst five identified haplotypes in *Melanelia stygia* (n = 19), all newly-sequenced specimens (five from Poland, one from Austria and one from the Czech Republic) have the same haplotype, previously reported from Austria, Finland, Italy and Norway (Fig. 5, Table 2). It differs from the haplotype identified in another Finnish specimen in two positions. Two Greenlandic specimens have the same haplotype that differs from the most common one in five positions. Four Icelandic samples have an identical haplotype that differs from the Norwegian sample in five positions; however, these samples differ in at least 13 positions from other haplotypes of *M. stygia*. Moreover, these Icelandic and one Norwegian samples form a separate clade shown in Fig. 1, in contrast to the remaining specimens of *M. stygia*. These molecular data suggest that these lineages may represent phenotypically indistinguishable cryptic species.

Montanelia disjuncta (Erichsen) Divakar, A. Crespo, Wedin & Essl.

American Journal of Botany 99:2022 (2012) ≡ *Parmelia disjuncta* Erichsen, Annales Mycologici 37:78 (1939) ≡ *Melanelia disjuncta* (Erichsen) Essl., Mycotaxon 7:46 (1978).

Description. *M. disjuncta* possess foliose thallus composed of 0.6–1.2 mm broad, flat to slightly convex and glossy lobes (Szczepańska et al. 2015). Its upper surface is smooth, olive-brown to dark brown. Pseudocyphellae are small, rather indistinct and submarginal. Its characteristic feature is the presence of the soralia (0.2–0.5 mm in diameter), which are punctiform, irregular, usually capitate and arise on the surface or at the margins of the lobes. Soredia are granular to isidioid, dark, but appearing white when abraded. Pycnidia are rare, conidia are 6–7 × 1 μm. Apothecia are not seen in the examined material.

Chemistry. Perlatolic and stenosporic acids.

Distribution. *M. disjuncta* is a circumpolar species growing mainly on siliceous rocks. The geographical range of this species consists of both continental and oceanic areas of Europe and North America (Esslinger 1977; Otte et al. 2005; Hansen 2013). Available molecular data concern samples collected in North America (Canada, Greenland, USA), North (Iceland, Norway, Sweden, United Kingdom) and Central (Austria) Europe, as well as Asia (India).

Haplotypes differentiation. Twelve different haplotypes were identified in *M. disjuncta* (n = 67), of which the most common haplotype occurs in Europe, North America and Asia (Fig. 6, Table 2). The highest diversity was observed in North America (Canada, Greenland, USA), for which a total of nine different haplotypes were found, including six that were exclusive for this region. We identified three different haplotypes amongst the newly-collected samples (n = 22). The most common one also occurs in other European countries, Asia and North America. The second most common also occurs in Northern Europe and North America, while the third haplotype was previously identified in specimens collected in the

United Kingdom. Moreover, four different haplotypes were identified amongst specimens collected in Norway, while five haplotypes were identified in Canadian samples, of which three are unique to Canada. Three haplotypes were identified in samples from both Iceland and Greenland, two of which are common for these areas and one haplotype is unique to Greenland. Some haplotypes are represented by more than one sample originating from particular areas, such as Alaska and Maine (USA), the Yukon Territory (Canada) or Greenland. The haplotypes identified in our dataset originated from different geographical areas and two of the most common haplotypes are widely distributed in the Northern Hemisphere. Based on the presented sampling, we could not indicate any geographical pattern, neither locally nor worldwide.

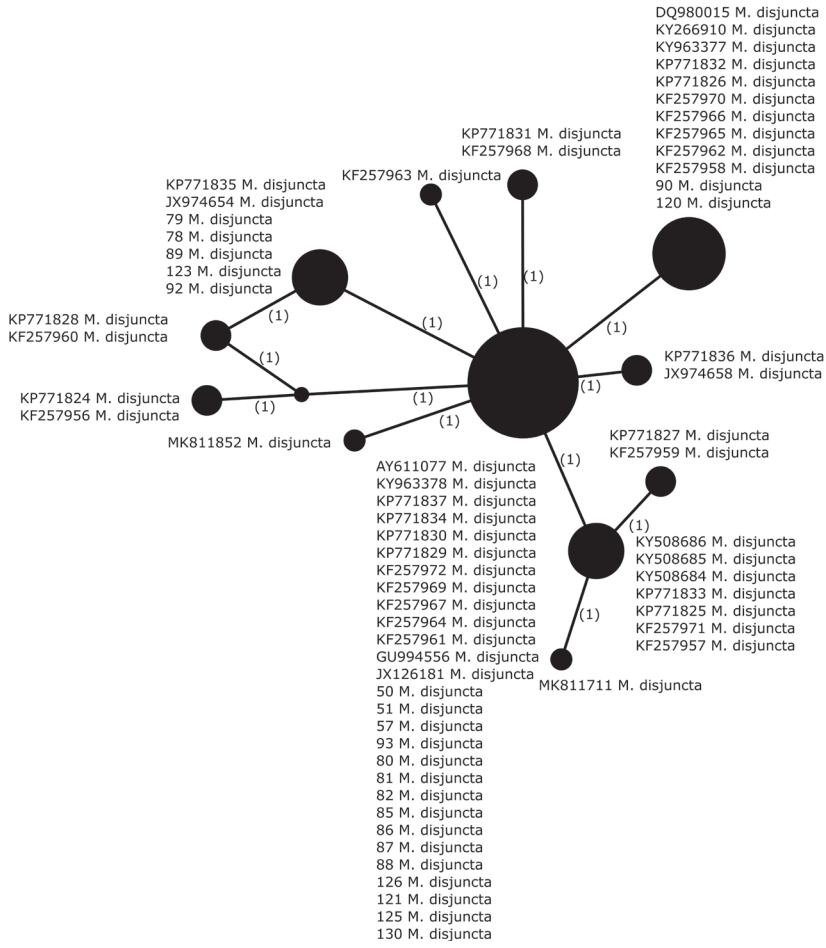

Figure 6. Haplotype network, based on ITS rDNA sequences from specimens of *Montanelia disjuncta*. Newly-generated sequences are described with isolate numbers preceding the species names. Sequences downloaded from GenBank are described with their accession numbers. Mutational changes are presented as numbers in brackets near lines between haplotypes.

***Montanelia sorediata* (Ach.) Divakar, A. Crespo, Wedin & Essl.**

American Journal of Botany 99:2023 (2012) ≡ *Parmelia stygia* var. *sorediata* Ach., Lichenographia Universalis 471 (1810) ≡ *Melanelia sorediosa* (Almb) Essl., Mycotaxon 7:47 (1978) ≡ *Melanelia sorediata* (Ach.) Goward & Ahti, Mycotaxon 28:94 (1987).

Description. *M. sorediata* is a foliose species. Its lobes are flat to slightly convex, 0.2–0.6 mm broad, distinctly rugged and pitted at the ends (Szczepańska et al. 2017). The upper surface is smooth, dull, olive brown to dark brown. Characteristic soralia arise on the ends of the main lobes or on the smaller, erect side lobes. They are usually distinctly convex and capitate with granular to isidioid, dark soredia. Pseudocyphellae and pycnidia are absent. Apothecia are not seen in the examined material.

Chemistry. Perlatolic and stenosporic acids.

Distribution. *M. sorediata* is a probably circumpolar species that prefers siliceous substrates, usually in open and well-lit places. The species is mentioned as occurring

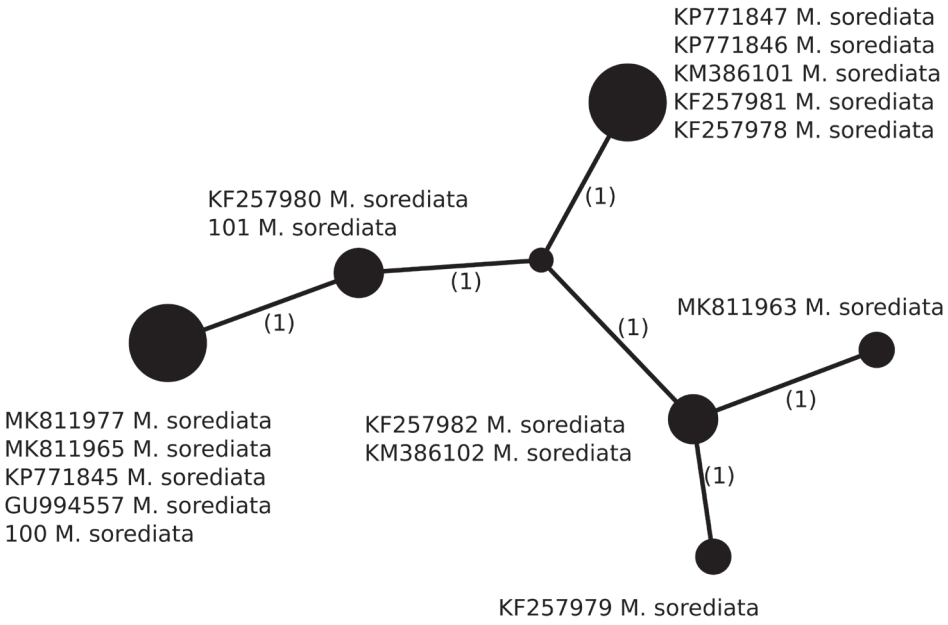

Figure 7. Haplotype network, based on ITS rDNA sequences from specimens of *Montanelia sorediata*. Newly-generated sequences are described with isolate numbers preceding the species names. Sequences downloaded from GenBank are described with their accession numbers. Mutational changes are presented as numbers in brackets near lines between haplotypes.

in North America and Europe (Esslinger 1977; Otte et al. 2005). Available molecular data concern only a few samples collected in North America (Canada, USA), North Europe (Norway, Sweden) and Asia (India).

Haplotypes differentiation. Six different haplotypes were identified in *M. sorediata* (n = 16), of which two Polish specimens, collected in the Karpaty Mountains, have two different haplotypes that differ in a single position (Fig. 7, Table 2). Interestingly, sample 101 has the same haplotype as the specimen collected in Alaska (KF257980), while sample 100 has the same haplotype as four Scandinavian specimens collected in Norway and Sweden. Another of the most common haplotypes is represented by specimens collected in Japan, Russia and the USA. Therefore, no specific geographic pattern was observed in the dataset.

Discussion

Although several studies focused on the phylogeny of brown *Parmeliae*, in the analysed datasets, there was an evident lack of molecular data concerning this group from Central Europe. The available data included only North America (mainly Greenland), Northern Europe (Scandinavian countries) and single sequences from specimens collected in Western Europe (Spain, Italy) and Asia (India, Russia). Having the opportunity to collect data from Poland, we focused on taxa occurring in this country, such as *Cetraria commixta*, *Melanelia agnata*, *M. hepatizon*, *M. stygia*, *Montanelia disjuncta* and *M. sorediata*. Additionally, in analyses, we also included newly-generated sequences from samples collected in Austria, Czech Republic, Germany and Slovakia. By supplementing the dataset with new sequences from a previously-unexplored area, we wanted to study the intraspecific internal transcribed spacer (ITS) rDNA variability of mentioned species and analyse distribution patterns of individual haplotypes. Previously, Leavitt et al. (2014) reported mean genetic distance (given as the number of nucleotide substitutions per site) in brown *Parmeliae* and found higher values in the case of *Melanelia agnata* and *M. hepatizon* (0.013) in contrast to *Cetraria commixta* and *M. stygia* (0.002 and 0.007, respectively). In this study, we found the highest nucleotide diversity in *Melanelia agnata* and *M. hepatizon* (0.01552 and 0.01421, respectively), but also in *M. stygia* (0.01418) as a result of additional sampling.

In our study, the haplotype networks illustrated that single-locus haplotypes and clades have no geographic clustering and cannot be useful in defining the species boundaries within brown *Parmeliae*. Haplotypes are dispersed amongst the sites and clades do not show apparent association with spatial location, as reported in literature data (Werth and Sork 2008; Starosta and Svoboda 2020). In addition, many of the analysed haplotypes of brown *Parmeliae* are widely distributed and, in many cases, the same haplotypes are shared between temperate and polar populations. What is more, all taxa, except *Melanelia stygia*, seem to be monophyletic and newly-sequenced specimens cluster together with other representatives of the species downloaded from

GenBank. The extremely wide geographical distribution of mycobiont haplotypes has been observed in some other species, such as *Cavernularia hultenii* (Printzen et al. 2003), *Cetraria aculeata* (Fernández-Mendoza et al. 2011) and *Cladonia subcervicornis* (Printzen and Ekman 2003). In the first two cases, this phenomenon is assigned to lichens characterised by vegetative propagation and interpreted as evidence for ancestral polymorphisms and slow genetic drift (Printzen et al. 2003). This finding conforms well with the results of our study on Parmeliaceae, which are usually sterile species, reproducing by soredia (*Montanelia*) and conidia (*Cetraria*, *Melanelia*).

Although representatives of brown *Parmeliae* are known from both Hemispheres (Otte et al. 2005), all species studied in this paper represent circumpolar distribution and occur only on northern continents. The specimens used for the analyses originated mainly from mountain areas of Poland, both the Carpathians and the Sudetes; however, the range of sampling seems to be representative for this part of Europe. The number of analysed haplotypes representing different geographical regions was comparable for each taxon; nevertheless, the number of *Melanelia agnata* and *Montanelia sorediata* samples remain very small. Due to the newly-generated molecular data covering Central Europe, we were able to compare the haplotype distribution in this area with other parts of the world. Unfortunately, the data available for discussed lichens taxa include, almost exclusively, specimens from North America and Northern Europe; the data concerning Asia and Southern Europe are not sufficient to make a reliable comparison possible. In almost all analysed taxa, stronger genetic differentiation was found amongst North American populations, with a few haplotypes unique for this part of the world, especially for Greenland. Specimens occurring in Central Europe have lower haplotype diversification and many of these haplotypes have wide geographical distribution (Table 2). Nevertheless, it seems that the number of analysed sequences is still insufficient to indicate high diversity areas (hotspots), species speciation centres or glacial refugia. Although the numbers of haplotypes correlated with the number of specimens tested, two species occurring in Poland (*Melanelia agnata* and *M. stygia*) clearly indicate a very low level of genetic diversity. Both species are rare in Poland and their distribution is limited to the high mountain regions (Szczepańska and Kossowska 2017). Low genetic diversity and limited occurrence suggest considering both taxa as critically endangered in Poland.

In recent years, it has been proved that cryptic species-level lineages are very common amongst lichen-forming fungi (Crespo and Pérez-Ortega 2009; Crespo and Lumbsch 2010; Lumbsch and Leavitt 2011). At the same time, it has been shown that phenotypic variation is not always 'sensitive' enough for delimitation and description of new taxa. Modern methods of genetic analysis are recommended as an additional tool for this purpose (Molina et al. 2011; de Paz et al. 2012; Leavitt et al. 2013; Renner 2016). At the same time, it is necessary to include other evidence, such as chemistry, ecology, geography and morphology, for the proper delimitation of lichenised fungi species (Hawksworth 1976; Dayrat 2005; Crespo and Pérez-Ortega 2009). Such careful and versatile analysis of distinct phylogenetic lineages may lead to recognising some previously-overlooked characteristics (Kroken and Taylor 2001; del Prado et al. 2007;

Frolov et al. 2016; Leavitt et al. 2016; Szczepańska et al. 2020). In the recent review paper, Lücking et al. (2021) proposed a detailed protocol for consistent taxonomy of lichen-forming fungi. The integrative taxonomy employing phylogeny, reproductive biology and phenotype should be used to delimit species (Lücking et al. 2020). Aime et al. (2021) recommended circumscription of new taxa, based on an appropriate sampling of multiple representatives from different collections for which multi-loci analyses should be performed. They also noted that description of a new species, based on single-locus phylogenetic analyses, could only be done in exceptional cases. The errors caused by contaminant sequences, laboratory mix-ups and chimeric sequences should be avoided for proper establishment of novel taxa, based on molecular data only (Lücking et al. 2021). Therefore, it is crucial to employ unlinked loci from different parts of the genome, even though the ITS rDNA marker is widely used in DNA barcoding of fungal taxa.

We analysed phenotypic diversity of samples representing individual haplotypes in our studies. However, in morphological, anatomical and chemical analyses, we observed that phenotypic characters of individuals representing different haplotypes are homogeneous and no visible distinctive features for samples with different geographic distribution were recognised. Recent molecular studies of one of the analysed genus – *Melanelia*, suggested previously unrecognised species-level diversity within this taxon (Divakar et al. 2012; Leavitt et al. 2014; Xu et al. 2017). However, the authors based their assumptions primarily on phylogenetic analyses without considering phenotypic features. Therefore, we have decided to analyse differences in morphology, anatomy and chemistry of *M. stygia* and *M. agnata* specimens originating from different geographic regions (Greenland, Iceland and Central Europe).

Melanelia agnata is a rare lichen recorded in North America and some European countries, such as Austria, Iceland, Norway, Poland, Russia, Sweden, Switzerland and Slovakia (Westberg et al. 2004; Hawksworth et al. 2008; Szczepańska and Kossowska 2017). The analysed holotype of *Melanelia agnata* is characterised by small (ca. 3.0 cm in diam.), foliose, olive-brown to dark-brown thallus, composed of flat, shiny, 0.25–2 mm broad, smooth lobes with thicker margins (Fig. 8A). Its lower surface is pale brown with single, dark rhizines. Polish (Figs. 8G and H) and Greenlandic (Fig. 8E and F) specimens comply with the type. However, Icelandic material differs in a larger thallus size (up to 10 cm in diam.) and the appearance of the lobes, which are more convex than flat, 1–5 mm broad and distinctly wrinkled (Fig. 8C). Thell (1995) made an interesting taxonomic description of *M. agnata*, in which he noted that its thallus could reach up to 10 cm diam. However, in his research, Thell (1995) analysed only a few specimens, including one from Iceland (Kristinsson 14781, GZU, LD) and treated them all as a single taxon. A similar situation applies to conidia, reaching 5–7.5 μm in *M. agnata*, according to Thell (1995). Pycnidia observed in Icelandic specimens are usually marginal (Fig. 8D), very often double and produce bifusiform conidia, 4.5–6 × 1 μm, in contrast to the type specimen, which pycnidia are simple, marginal to laminal (Fig. 8B) with smaller conidia, at 3.5–5 × 1 μm. Pseudocyphellae are always whitish, rounded or irregular, marginal

and laminal in all analysed material; they are much more abundant in specimens from Iceland (Fig. 8D). None of the Icelandic specimens had apothecia, so their anatomical analysis was impossible. All material was chemically homogeneous and no secondary metabolites were detected by thin-layer chromatography (TLC), which is consistent with other descriptions (Thell 1995; Xu et al. 2017).

Melanelia stygia is a much more common species than *M. agnata*. In Europe, it was recorded in the upper mountain areas of Austria, the Czech Republic, Germany, Great Britain, Poland, Romania, Russia, Slovakia, Switzerland and Ukraine (Hawksworth et al. 2008).

After phenotypic studies, we have concluded that all material is homogeneous and none of the analysed morphological and anatomical features coincides with geographically-distinct *M. stygia* populations (Fig. 9A–F). However, some differences may be observed in the secondary chemistry. In his paper, Esslinger (1977) recognised six chemical races within *M. stygia*. He stated that some of them are broadly distributed and others are more frequent in particular regions. All the currently-examined samples originating from Greenland and Central Europe belong to Race 1, containing fumaroprotocetraric and protocetraric acids. Specimens from Iceland represent Race 6, without secondary metabolites. Both races are known to occur in Japan, North America and Europe; however, there is a possibility that Race 6 is the only chemical Race occurring in Iceland. Production of some secondary metabolites may be induced by environmental factors (Culberson 1986; Leavitt et al. 2011) and does not always correspond with molecular data. Moreover, chemical differences can be observed within some recognised haplotype groups and even in the same haplotype (Matteucci et al. 2017). At the same time, chemical characters may be successfully used to support delimitation of lichen taxa, but in any case, they cannot be treated as an exclusive diagnostic trait (Elix et al. 2009; Spribille et al. 2011; Leavitt et al. 2013; Onut-Brännström et al. 2018; Mark et al. 2019,).

In conclusion, we can state that all of the potential species lineages within *Melanelia agnata* and *M. stygia* are cryptic, with very slight morphological, anatomical and chemical variation. We were unable to distinguish any distinctive feature that could be considered diagnostic and useful for the delimitation of new species, except molecular variation. The phenotypic differences mentioned above may reflect environmental or climate conditions, such as temperature, light, humidity or substrate and may not be connected with genetic differences. However, this study was limited to a small number of samples and one genetic marker, ITS; therefore, we refrain from describing new species because further study is pending. We suggest that an extended phylogeographic study is necessary and an increase in the number of herbarium specimens would probably give additional information. Even though our analyses complement the knowledge on lichens in Central Europe, many areas remain insufficiently explored. Additional sampling from Asia and Southern Europe may bring new data on the phylogenetic and phenotypic diversity of species from the brown *Parmeliae* group.

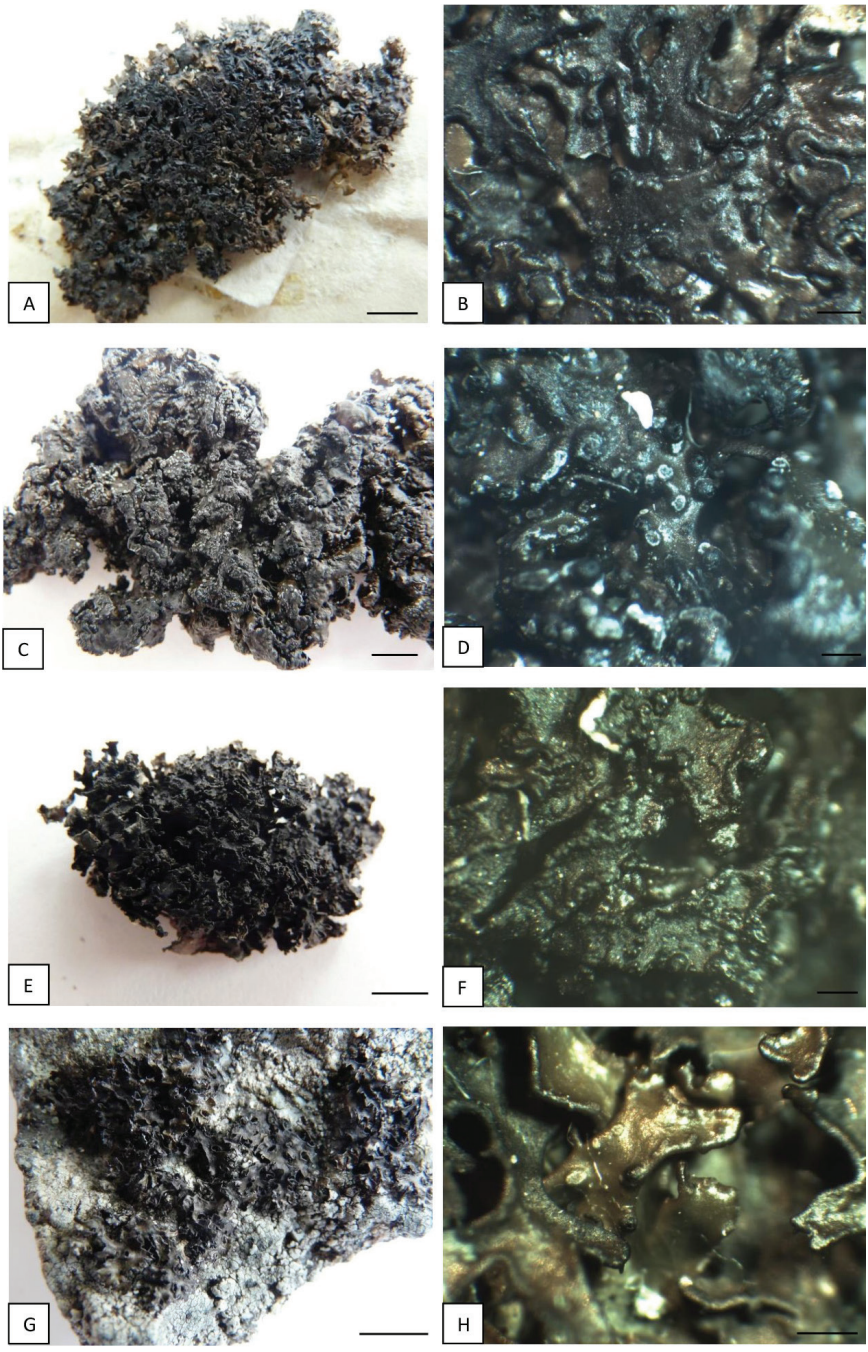

Figure 8. *Melanelia agnata* specimens treated **A** *Melanelia agnata* H-NYL 36086 (holotype) **B** *Melanelia agnata*, H-NYL 36086 (holotype) **C** *M. agnata*, AMNH 27562 (Iceland) **D** *M. agnata*, AMNH 30974 (Iceland) **E** *M. agnata*, C 19019 (Greenland) **F** *M. agnata*, C 19019 (Greenland) **G** *M. agnata*, Szczepańska 1050, WRSL (Poland) **H** *M. agnata*, Szczepańska 1050, WRSL (Poland). Scale bars: 0.5 cm (**A, C, E, G**); 0.5 mm (**B, D, F**); 1 mm (**H**).

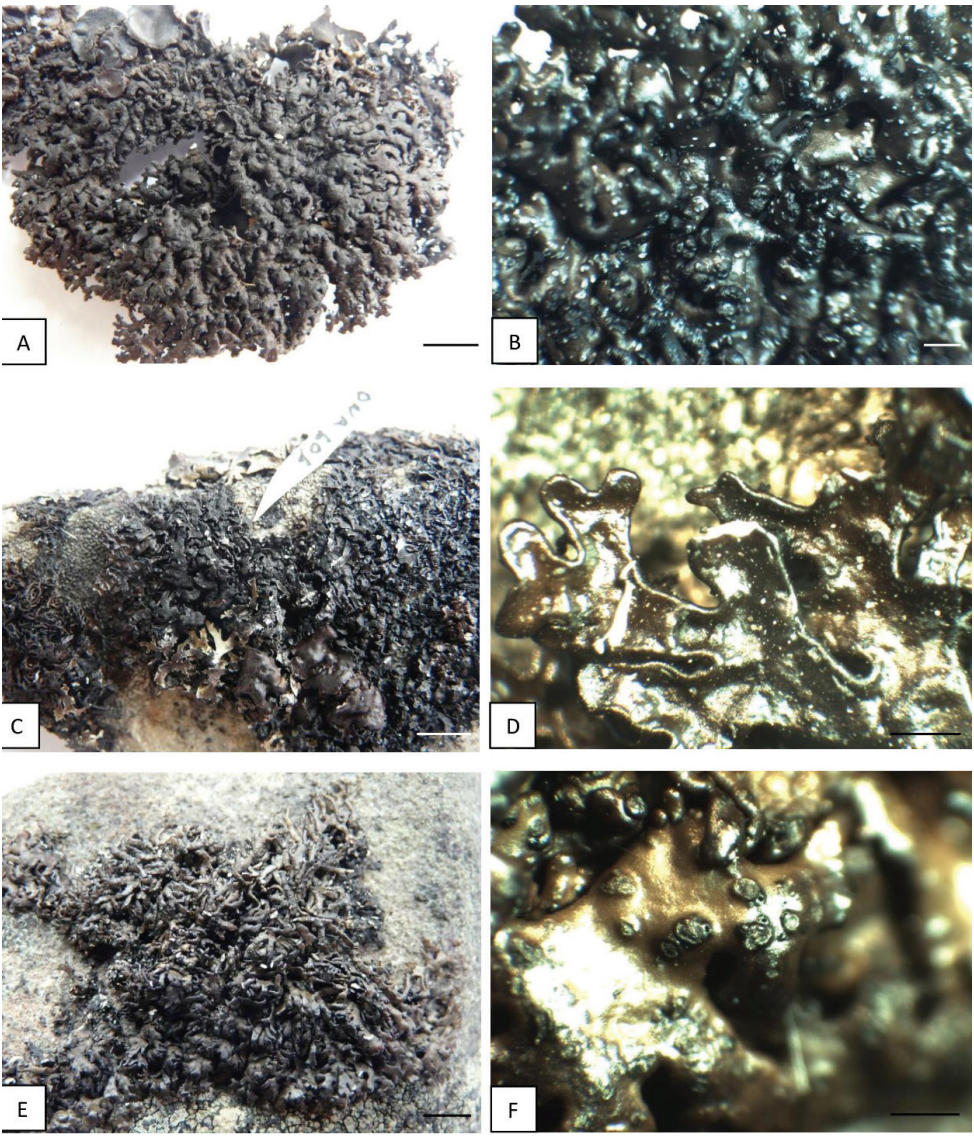

Figure 9. *Melanelia stygia* specimens treated **A** *M. stygia*, AMNH 28243 (Iceland) **B** *M. stygia*, AMNH 16894 (Iceland) **C** *M. stygia*, C 19893 (Greenland) **D** *M. stygia*, C 19893 (Greenland) **E** *M. stygia*, Szczepańska 1160, WRSL (Poland) **F** *M. stygia*, Szczepańska 737, WRSL (Austria). Scale bars: 0.5 cm (**A, C, E**);1 mm (**B, D**); 0.5 mm (**F**).

Acknowledgements

The curators of AMNH, C and H, are gratefully acknowledged for the loan of specimens. The authors are also very grateful to the reviewers for their valuable comments and improvements to the manuscript. The publication is financed under the Leading Research Groups support project from the subsidy increased for the period

2020–2025 in the amount of 2% of the subsidy referred to Art. 387 (3) of the Law of 20 July 2018 on Higher Education and Science, obtained in 2019.

References

Aime MC, Miller AN, Aoki T, Bensch K, Cai L, Crous PW, Hawksworth DL, Hyde KD, Kirk PM, Lücking R, May TW, Malosso E, Redhead SA, Rossman AY, Stadler M, Thines M, Yurkov AM, Zhang N, Schoch CL (2021) How to publish a new fungal species, or name, version 3.0. IMA Fungus 12: e11. https://doi.org/10.1186/s43008-021-00063-1

Altschul SF, Madden TL, Schäffer AA, Zhang J, Zhang Z, Miller W, Lipman J (1997) Gapped BLAST and PSI-BLAST: a new generation of protein database search programs. Nucleic Acids Research 25: 3389–3402. https://doi.org/10.1093/nar/25.17.3389

Blanco O, Crespo A, Divakar PK, Esslinger TL, Hawksworth DL, Lumbsch H (2004) *Melanelixia* and *Melanohalea*, two new genera segregated from *Melanelia* (Parmeliaceae) based on molecular and morphological data. Mycological Research 108: 873–884. https://doi.org/10.1017/S0953756204000723

Blanco O, Crespo A, Divakar PK, Elix JA, Lumbsch HT (2005) Molecular phylogeny of parmotremoid lichens (Ascomycota, Parmeliaceae). Mycologia 97: 150–159. https://doi.org/10.1080/15572536.2006.11832848

Clement M, Snell Q, Walker P, Posada D, Crandall K (2002) TCS: Estimating gene genealogies. Parallel and Distributed Processing Symposium, International Proceedings 2: e184. https://doi.org/10.1109/IPDPS.2002.1016585

Crespo A, Pérez-Ortega S (2009) Cryptic species and species pairs in lichens: a discussion on the relationship between molecular phylogenies and morphological characters. Anales del Jardín Botánico de Madrid 66: 71–81. https://doi.org/10.3989/ajbm.2225.

Crespo A, Lumbsch HT (2010) Cryptic species in lichen-forming fungi. IMA fungus 1: 167–170. https://doi.org/10.5598/imafungus.2010.01.02.09

Crespo A, Divakar PK, Hawksworth DL (2011) Generic concepts in parmelioid lichens, and the phylogenetic value of characters used in their circumscription. Lichenologist (London, England) 43: 511–535. https://doi.org/10.1017/S0024282911000570

Crespo A, Kauff F, Divakar PK, del Prado R, Pérez-Ortega S, Amo de Paz G, et al. (2010) Phylogenetic generic classification of parmelioid lichens (Parmeliaceae, Ascomycota) based on molecular, morphological and chemical evidence. Taxon 59: 1735–1753. https://doi.org/10.1002/tax.596008

Culberson CF (1972) Improved conditions and new data for identification of lichen products by standardized thin-layer chromatographic method. Journal of Chromatography A72: 113–125. https://doi.org/.10.1016/0021-9673(72)80013-X.

Culberson WL (1986) Chemistry and sibling speciation in the lichen-forming fungi: ecological and biological considerations. Bryologist 89: 123–131. https://doi.org/10.2307/3242752

Darriba D, Taboada GL, Doallo R, Posada D (2012) jModelTest 2: more models, new heuristics and parallel computing. Nature Methods 9: e772. https://doi.org/10.1038/nmeth.2109

Dayrat B (2005) Towards integrative taxonomy. Biological Journal of the Linnean Society 85: 407–417. https://doi.org/10.1111/j.1095-8312.2005.00503.x

de Paz GA, Cubas P, Crespo A, Elix JA, Lumbsch HT (2012) Transoceanic dispersal and subsequent diversification on separate continents shaped diversity of the *Xanthoparmelia pulla* group (Ascomycota). PLoS ONE 7(6): e39683. https://doi.org/10.1371/journal.pone.0039683

del Prado R, Ferencová Z, Armas-Crespo V, de Paz GA, Cubas P, Crespo A (2007) The arachiform vacuolar body: an overlooked shared character in the ascospores of a large monophyletic group within Parmeliaceae (*Xanthoparmelia* clade, Lecanorales). Mycological Research 111: 685–692. https://doi.org/10.1016/j.mycres.2007.04.002

Divakar PK, Del-Prado R, Lumbsch HT, Wedin M, Esslinger TL, Leavitt SD, Crespo A (2012) Diversification of the newly recognized lichen-forming fungal lineage *Montanelia* (Parmeliaceae, Ascomycota) and its relation to key geological and climatic. American Journal of Botany 99: 2014–2026. https://doi.org/10.3732/ajb.1200258

Domaschke S, Fernandez-Mendoza FA, García M, Martín M, Printzen C (2012) Low genetic diversity in Antarctic populations of the lichen-forming ascomycete *Cetraria aculeata* and its photobiont. Polar Research 31(1): e17353. https://doi.org/10.3402/polar.v31i0.17353

Doyle JJ, Doyle JL (1987) A rapid DNA isolation procedure for small quantities of fresh leaf tissue. Phytochemical Bulletin 19: 11–15.

Elix JA, Corush J, Lumbsch HT (2009) Triterpene chemosyndromes and subtle morphological characters characterise lineages in the *Physcia aipolia* group in Australia (Ascomycota). Systematics and Biodiversity 7: 479–487 https://doi.org/10.1017/S1477200009990223.

Esslinger TL (1977) A chemosystematic revision of the brown Parmeliae. Journal of the Hattori Botanical Laboratory 42: 1–211.

Esslinger TL (1978) A new status for the brown Parmeliae. Mycotaxon 7: 45–54.

Fernández-Mendoza F, Domaschke S, García MA, Jordan P, Martín MP, Printzen C (2011) Population structure of mycobionts and photobionts of the widespread lichen *Cetraria aculeata*. Molecular Ecology 20: 1208–1232. https://doi.org/10.1111/j.1365-294X.2010.04993.x

Frolov I, Vondrá J, Fernández-Mendoza F, Wilk K, Khodosovtsev A, Halıcı MG (2016) Three new, seemingly-cryptic species in the lichen genus *Caloplaca* (Teloschistaceae) distinguished in two-phase phenotype evaluation. In Annales Botanici Fennici 53: 243–262. https://doi.org/10.5735/085.053.0413

Galtier N, Gouy M, Gautier C (1996) SEAVIEW and PHYLO_WIN: two graphic tools for sequence alignment and molecular phylogeny. Computational Applied Biosciences 12: 543–548. https://doi.org/10.1093/bioinformatics/12.6.543

Gouy M, Guindon S, Gascuel O (2010) SeaView version 4: a multiplatform graphical user interface for sequence alignment and phylogenetic tree building. Molecular Biology and Evolution 27: 221–224. https://doi.org/10.1093/molbev/msp259

Guzow-Krzemińska B, Węgrzyn G (2003) A preliminary study on the phylogeny of the genus *Melanelia* using nuclear large subunit ribosomal DNA sequences. Lichenologist 35: 83–86. https://doi.org/10.1006/lich.2002.0429

Hansen ES (2013) Lichens from three localities in Central West Greenland with notes on their climatic preferences. Botanica Lithuanica 19: 28–36. https://doi.org/10.2478/botlit-2013-0004

Hawksworth DL (1976) Lichen chemotaxonomy. In: Brown DH, Hawksworth DL, Bailey RH (Eds) Lichenology: progress and problems. Academic Press, London, 139–184.

Hawksworth DL, Blanco O, Divakar PK, Ahti T, Crespo A (2008) A first checklist of parmelioid and similar lichens in Europe and some adjacent territories, adopting revised generic circumscriptions and with indications of species distributions. Lichenologist 40: 1–21. https://doi.org/10.1017/S0024282908007329

Huelsenbeck JP, Ronquist F (2001) MrBayes: Bayesian inference of phylogenetic trees. Bioinformatics 17: 754–755. https://doi.org/10.1093/bioinformatics/17.8.754

Katoh K, Misawa K, Kuma K, Miyata T (2002) MAFFT: a novel method for rapid multiple sequence alignment based on fast Fourier transform. Nucleic Acids Research 30: 3059–3066. https://doi.org/10.1093/nar/gkf436

Kroken S, Taylor JW (2001) A gene genealogical approach to recognize phylogenetic species boundaries in the lichenized fungus *Letharia*. Mycologia 93: 38–53. https://doi.org/10.1080/00275514.2001.12061278

Landan G, Graur D (2008) Local reliability measures from sets of co-optimal multiple sequence alignments. Pacific Symposium on Biocomputing 13: 15–24.

Lanfear R, Frandsen PB, Wright AM, Senfeld T, Calcott B (2016) PartitionFinder 2: new methods for selecting partitioned models of evolution for molecular and morphological phylogenetic analyses. Molecular Biology and Evolution 34: 772–773. https://doi.org/10.1093/molbev/msw260

Leavitt SD, Divakar PK, Ohmura Y, Wang L-S, Esslinger TL, Lumbsch HT (2015) Who's getting around? Assessing species diversity and phylogeography in the widely distributed lichen-forming fungal genus *Montanelia* (Parmeliaceae, Ascomycota). Molecular Phylogenetics and Evolution 90: 85–96. https://doi.org/10.1016/j.ympev.2015.04.029

Leavitt SD, Fankhauser JD, Leavitt DH, Porter LD, Johnson LA, Clair LLS (2011) Complex patterns of speciation in cosmopolitan "rock posy" lichens-Discovering and delimiting cryptic fungal species in the lichen-forming *Rhizoplaca melanophthalma* species-complex (Lecanoraceae, Ascomycota). Molecular Phylogenetics and Evolution 59: 587–602. https://doi.org/10.1016/j.ympev.2011.03.020

Leavitt S, Fernández-Mendoza F, Pérez-Ortega S, Sohrabi M, Divakar P, Lumbsch T, Clair LLS (2013) DNA barcode identification of lichen-forming fungal species in the *Rhizoplaca melanophthalma* species-complex (Lecanorales, Lecanoraceae), including five new species. MycoKeys 7: 1–22. https://doi.org/10.3897/mycokeys.7.4508.

Leavitt SD, Esslinger TL, Hansen ES, Divakar PK, Crespo A, Loomis BF, Lumbsch HT (2014) DNA barcoding of brown Parmeliae (Parmeliaceae) species: a molecular approach for accurate specimen identification, emphasizing species in Greenland. Organisms Diversity & Evolution 14: 11–20. https://doi.org/10.1007/s13127-013-0147-1

Leavitt SD, Esslinger TL, Divakar PK, Crespo A, Lumbsch HT (2016) Hidden diversity before our eyes: Delimiting and describing cryptic lichen-forming fungal species in camouflage lichens (Parmeliaceae, Ascomycota). Fungal Biology 120: 1374–1391. https://doi.org/10.1016/j.funbio.2016.06.001

Lindblom L, Ekman S (2006) Genetic variation and population differentiation in the lichen-forming ascomycete *Xanthoria parietina* on the island Storfosna, central Norway. Molecular Ecology 15: 1545–1559. https://doi.org/10.1111/j.1365-294X.2006.02880.x

Lumbsch HT, Leavitt SD (2011) Goodbye morphology? A paradigm shift in the delimitation of species in lichenized fungi. Fungal Diversity 50: 59–72. https://doi.org/10.1007/s13225-011-0123-z

Lücking R, Aime MC, Robberts B, Miller AN, Ariyawansa HA, Aoki T, Cardinali G, Crous PW, Druzhinina IS, Geiser DM, Hawksworth DL, Hyde KD, Irinyi L, Jeewon R, Johnston PR, Kirk PM, Malosso E, May TW, Meyer W, Öpik M, Robert V, Stadler M, Thines M, Vu D, Yurkov AM, Zhang N, Schoch CL (2020) Unambiguous identification of fungi: where do we stand and how accurate and precise is fungal barcoding? IMA Fungus 11: e14. https://doi.org/10.1186/s43008-020-00033-z

Lücking R, Leavitt SD, Hawksworth DL (2021) Species in lichen-forming fungi: balancing between conceptual and practical considerations, and between phenotype and phylogenomics. Fungal Diversity. https://doi.org/10.1007/s13225-021-00477-7

Mark K, Randlane T, Thor G, Hur JS, Obermayer W, Saag A (2019) Lichen chemistry is concordant with multilocus gene genealogy in the genus *Cetrelia* (Parmeliaceae, Ascomycota). Fungal Biology 123: 125–139. https://doi.org/10.1016/j.funbio.2018.11.013

Matteucci, E, Occhipinti A, Piervittori R, Maffei ME, Favero-Longo SE (2017) Morphological, secondary metabolite and ITS (rDNA) variability within usnic acid-containing lichen thalli of *Xanthoparmelia* explored at the local scale of rock outcrop in W-Alps. Chemistry & Biodiversity 14: e1600483. https://doi.org/10.1002/cbdv.201600483

Miller MA, Pfeiffer W, Schwartz T (2010) Creating the CIPRES Science Gateway for inference of large phylogenetic trees. In: Proceedings of the Gateway Computing Environments Workshop (GCE), 14 November 2010, New Orleans, 1–8. https://doi.org/10.1109/GCE.2010.5676129

Molina M, Del-Prado R, Divakar PK, Sánchez-Mata D, Crespo A (2011) Another example of cryptic diversity in lichen-forming fungi: the new species *Parmelia mayi* (Ascomycota: Parmeliaceae). Organisms Diversity & Evolution 11: 331–342. https://doi.org/10.1007/s13127-011-0060-4

Nelsen MP, Chavez N, Sackett-Hermann E, Thell A, Randlane T, Divakar PK, Rico VJ, Lumbsch HT (2011) The cetrarioid core group revisited (Lecanorales: Parmeliaceae). Lichenologist 43: 537–551. https://doi.org/10.1017/S0024282911000508

Onut-Brännström I, Johannesson H, Tibell L (2018) *Thamnolia tundrae* sp. nov., a cryptic species and putative glacial relict. Lichenologist 50: 59–75 https://doi.org/10.1017/S0024282917000615.

Orange A, James PW, White FJ (2001) Microchemical methods for the identification of lichens. London: British Lichen Society.

Otte V, Esslinger TL, Litterski B (2005) Global distribution of the European species of the lichen genus *Melanelia* Essl. Journal of Biogeography 32: 1221–1241. https://doi.org/10.1111/j.1365-2699.2005.01268.x

Palice Z, Printzen C (2004). Genetic variability in tropical and temperate populations of *Trapeliopsis glaucolepidea*: evidence against long range dispersal in a lichen with disjunct distribution. Mycotaxon 90: 43–54.

Penn O, Privman E, Ashkenazy H, Landan G, Graur D, Pupko T (2010) GUIDANCE: a web server for assessing alignment confidence scores. Nucleic Acids Research 38(Web Server issue): W23–W28. https://doi.org/10.1093/nar/gkq443

Printzen C, Ekman S (2003) Local population subdivision in the lichen *Cladonia subcervicornis* as revealed by mitochondrial cytochrome oxidase subunit 1 intron sequences. Mycologia 95: 399–406. https://doi.org/10.1080/15572536.2004.11833084

Printzen C, Ekman S, Tønsberg T (2003) Phylogeography of *Cavernularia hultenii*: evidence for slow genetic drift in a widely disjunct lichen. Molecular Ecology 12: 1473–1486. https://doi.org/10.1046/j.1365-294X.2003.01812.x

Rambaut A (2012) FigTree v.1.4.2. http://tree.bio.ed.ac.uk/software/figtree/

Renner SS (2016) A return to Linnaeus's focus on diagnosis, not description: The use of DNA characters in the formal naming of species. Systematic Biology 65(6): 1085–1095. https://doi.org/10.1093/sysbio/syw032

Rico VJ, van den Boom PP, Barrasa JM (2005) Morphology, chemistry and distribution of *Melanelia sorediella* (Parmeliaceae) and similar species in the Iberian Peninsula. Lichenologist 37: 199–215. https://doi.org/10.1017/S0024282905014830

Ronquist F, Huelsenbeck JP (2003) MrBayes 3: Bayesian phylogenetic inference under mixed models. Bioinformatics 19: 1572–1574. https://doi.org/10.1093/bioinformatics/btg180

Rozas J, Ferrer-Mata A, Sánchez-DelBarrio JC, Guirao-Rico S, Librado P, Ramos-Onsins SE, Sánchez-Gracia A (2017) DnaSP 6: DNA Sequence Polymorphism Analysis of Large Datasets. Molecular Biology and Evolution 34: 3299–3302. https://doi.org/10.1093/molbev/msx248

Sela I, Ashkenazy H, Katoh K, Pupko T (2015) GUIDANCE2: accurate detection of unreliable alignment regions accounting for the uncertainty of multiple parameters. Nucleic Acids Research 43(Web Server issue): W7–W14. https://doi.org/10.1093/nar/gkq443

Spribille T, Klug B, Mayrhofer H (2011) A phylogenetic analysis of the boreal lichen *Mycoblastus sanguinarius* (Mycoblastaceae, lichenized Ascomycota) reveals cryptic clades correlated with fatty acid profiles. Molecular Phylogenetics and Evolution 59: 603–614. https://doi.org/10.1016/j.ympev.2011.03.021

Stamatakis A (2014) RAxML Version 8: A tool for phylogenetic analysis and post-analysis of large phylogenies. Bioinformatics 30: 1312–1313. https://doi.org/10.1093/bioinformatics/btu033

Starosta J, Svoboda D (2020) Genetic variability in the *Physconia muscigena* group (Physciaceae, Ascomycota) in the Northern Hemisphere. Lichenologist 52: 305–317. https://doi.org/10.1017/S0024282920000134

Szczepańska K, Kossowska M (2017) *Cetrariella commixta* and the genus *Melanelia* (Parmeliaceae, Ascomycota) in Poland. Herzogia 30: 272–288. https://doi.org/10.13158/heia.30.1.2017.272

Szczepańska K, Pruchniewicz D, Sołtysiak J, Kossowska M (2015) Lichen-forming fungi of the genus *Montanelia* in Poland and their potential distribution in Central Europe. Herzogia 28: 697–712. https://doi.org/10.13158/heia.28.2.2015.697

Szczepańska K, Urbaniak J, Śliwa L (2020) Taxonomic recognition of some species-level lineages circumscribed in nominal *Rhizoplaca subdiscrepans* s. lat. (Lecanoraceae, Ascomycota). PeerJ 8: e9555.

Thell A (1995) A new position of the *Cetraria commixta* group in *Melanelia* (Ascomycotina, Parmeliaceae). Nova Hedwigia 60: 407–422.

Thell A, Crespo A, Divakar PK, Kärnefelt I, Leavitt SD, Lumbsch HT, Seaward MRD (2012) A review of the lichen family Parmeliaceae – history, phylogeny and current taxonomy. Nordic Journal of Botany 30: 641–664. https://doi.org/10.1111/j.1756-1051.2012.00008.x

Werth S, Sork VL (2008) Local genetic structure in a North American epiphytic lichen, *Ramalina menziesii* (Ramalinaceae). American Journal of Botany 95: 568–576. https://doi.org/10.3732/ajb.2007024

Westberg M, Kärnefelt I, Thell A (2004) *Melanelia agnata*, an overlooked species, new to Sweden. Graphis Scripta 16(1): 23–27.

Xu M, Heidmarsson S, Thorsteinsdottir M, Eiriksson FF, Omarsdottir S, Olafsdottir ES (2017) DNA barcoding and LC-MS metabolite profiling of the lichen-forming genus *Melanelia*: Specimen identification and discrimination focusing on Icelandic taxa. PLoS ONE 12(5): e0178012. https://doi.org/10.1371/journal.pone.0178012

Supplementary material 1

Figure S1

Authors: Katarzyna Szczepańska, Beata Guzow-Krzemińska, Jacek Urbaniak

Data type: Images.

Explanation note: Phylogenetic relationships of brown Parmeliae, based on Bayesian analysis of the ITS rDNA dataset. Posterior probabilities and Maximum Likelihood bootstrap values are shown near the internal branches. Newly-generated sequences are described with isolate numbers preceding the species names and are marked in bold. GenBank accession numbers of sequences downloaded from GenBank are listed on the tree with species names.

Link: https://doi.org/10.3897/mycokeys.85.70552.suppl1

MycoKeys 85: 161–172 (2021)
doi: 10.3897/mycokeys.85.73405
https://mycokeys.pensoft.net

RESEARCH ARTICLE

A peer-reviewed open-access journal
MycoKeys
Launched to accelerate biodiversity research

Azygosporus gen. nov., a synapmorphic clade in the family Ancylistaceae

Yue Cai[1,2*], Yong Nie[2,3*], Heng Zhao[5], ZiMin Wang[3], ZhengYu Zhou[3], XiaoYong Liu[4], Bo Huang[2]

1 *College of Biology, Food and Environment, Hefei University, Hefei, 230601, China* **2** *Anhui Provincial Key Laboratory for Microbial Pest Control, Anhui Agricultural University, Hefei 230036, China* **3** *School of Civil Engineering and Architecture, Anhui University of Technology, Ma'anshan 243002, China* **4** *College of Life Sciences, Shandong Normal University, Jinan 250014, China* **5** *Institute of Microbiology, School of Ecology and Nature Conservation, Beijing Forestry University, Beijing 100083, China*

Corresponding author: Bo Huang (bhuang@ahau.edu.cn), XiaoYong Liu (liuxiaoyong@im.ac.cn)

Academic editor: Kerstin Voigt | Received 24 August 2021 | Accepted 30 October 2021 | Published 31 December 2021

Citation: Cai Y, Nie Y, Zhao H, Wang Z, Zhou Z, Liu X, Huang B (2021) *Azygosporus* gen. nov., a synapmorphic clade in the family Ancylistaceae. MycoKeys 85:161–172. https://doi.org/10.3897/mycokeys.85.73405

Abstract

The fungal genus *Conidiobolus* sensu lato was delimited into four genera based on morphology and phylogeny. However, the taxonomic placement of *C. parvus* has not been determined until now. Here, we show that *C. parvus* belongs to a distinct lineage based on mitochondrial (mtSSU) and nuclear (*TEF1* and nrLSU) phylogenetic analyses. Phylogenetic analyses further revealed a new species as sister to *C. parvus*. We identified a synapomorphy uniting these lineages (azygospore production) that was not observed in other allied genera of the family Ancylistaceae, and erected a new genus *Azygosporus* **gen. nov.** for this monophyletic group, with a new combination, *A. parvus* **comb. nov.** as the type species. Within *Azygosporus*, the novel species *A. macropapillatus* **sp. nov.** was introduced from China based on morphological characteristics and molecular evidence, which is characterized by its prominent basal papilla, in comparison to other closely related species, measuring 7.5–10.0×5.0–10.0 μm. Our study resolved the phylogenetic placement of *C. parvus* and improved the taxonomic system of the Ancylistaceae family.

Keywords

Entomophthorales, resting spores, saprophytic fungi, taxonomy

* These authors contribute equally to this study and share the first author.

Introduction

Conidiobolus is the largest genus within the family Ancylistaceae, and includes mainly saprotrophs occurring in soil and plant debris, but also parasites of insects and animals (Vilela et al. 2010; Gryganskyi et al. 2012). After decades of study on more than 35 American and Indian *Conidoioblus* taxa (Drechsler 1952, 1953, 1954, 1955a, b, 1957, 1960, 1962; Srinivasan and Thirumalachar 1961, 1962a, b, 1967, 1968b), a numerical taxonomy was proposed that included 27 distinct species (King 1976a, b, 1977). Subsequently, the genus *Conidiobolus* was divided into three subgenera according to secondary conidia types (Ben-Ze'ev and Kenneth 1982). However, these morphologies can be difficult to distinguish and possess limited phylogenetic information that has limited our understanding of the evolution of *Conidiobolus* (Humber 1989). Since the division of *Conidiobolus*, several singe- and multi-locus phylogenetic analyses of the genus have shown that the proposed groups are polyphyletic (Jensen et al. 1998; Gryganskyi et al. 2013; Nie et al. 2018). The latest taxonomic revision of *Conidiobolus*, based on morphology and four genetic loci, revealed four lineages, and four genera (*Capillidium*, *Conidiobolus* sensu stricto, *Microconidiobolus* and *Neoconidiobolus*) were established (Nie et al. 2020a).

In addition to the size of primary conidia and the type of secondary conidia, resting spores are another character with taxonomic importance for recognizing *Conidiobolus* species (Humber 1997). Until now, four styles of resting spores have been reported: villose spores in *C. coronatus* and *C. lunulus* (Nie et al. 2020a; Goffre et al. 2020), zygospores and chlamydosporus in most members (King 1977; Nie et al. 2020a), and azygospores found only in *C. parvus* (Drechsler 1962; King 1977). Consequently, the taxonomic status of *C. parvus* remained uncertain, as a monotypic lineage in the most recent phylogeny analysis (Nie et al. 2020a, b).

Previous phylogenetic analyses have shown that is it not only *Conidiobolus parvus* that has questionable taxonomic placement. Our recent research has indicated that *C. lampragues* and *C. nanodes* should be assigned into the genus *Neoconidiobolus* (Nie et al. 2021). In this article, we describe a new genus, *Azygosporus* gen. nov., and a new species, *A. macropapillatus* sp. nov., and compare them to other allied taxa. We construct a multilocus (nrLSU, mtSSU, and *TEF1*) phylogeny that supports morphological results and confirm the treatment of ex-type cultures of *C. parvus* as a new combination in *Azygosporus* gen. nov., named *A. parvus* (Drechsler) B. Huang & Y. Nie, comb. nov.

Materials and methods

Isolates and morphology

Plant debris was collected from Tiantangzhai National Forest Parks (31°17'48" N, 115°78'18") and Fangtang (30°30'57" N, 118°42'17" E), Anhui Province, China. Isolations were carried out using the canopy-plating approach (King 1976a). A Petri dish

with potato dextrose agar (PDA; potato 200 g, dextrose 20 g, agar 20 g, H_2O 1000 ml) was inverted over the plant debris and incubated at 21 °C. We surveyed the PDA canopy daily for entomophthoroid fungi, which were transferred to new PDA for purification when detected. Morphological characters of mycelia, primary conidiophores, primary and secondary conidia, and resting spores were described with the method of King (1976a). The length and width of 35 primary conidia, 35 conidiophores and 50 azygospores were measured using an Olympus BX50 research microscope, and then photographed by an Olympus DP25 microscope-camera. Meanwhile, we observed the morphology of secondary conidia grown on 2% agar plates (agar 20 g, H_2O 1000 ml) under a light microscope (Olympus BX50, Japan). The living culture was deposited in the Research Center for Entomogenous Fungi of Anhui Agricultural University, Anhui Province, China (RCEF), and duplicated in the China General Microbiological Culture Collection Center, Beijing, China (CGMCC). The dried cultures were deposited in the Herbarium Mycologicum Academiae Sinicae, Beijing, China (HMAS).

DNA extraction, PCR amplification and sequencing

Fungal mycelia were incubated on PDA for 7 d at 21 °C. Total genomic DNA was extracted from fresh fungal mycelia by using a CTAB method followed Watanabe et al. (2010). We targeted three genetic loci for phylogenetic analyses: the large subunit of the nuclear ribosomal RNA (nrLSU), the small ribosomal subunit of the mitochondria (mtSSU), and translation elongation factor 1-alpha gene 1 (*TEF1*) were used for phylogenetic analysis. Details of the PCR primers and reactions can be found in Nie et al. (2020b). PCR products were purified according to the manufacturer protocol of Bioteke's Purification Kit (Bioteke Corporation, Beijing, China). The sequences of the PCR products were determined on both strands by using dideoxy-nucleotide chain termination on an ABI 3700 automated sequencer at Shanghai Genecore Biotechnologies Company (Shanghai, China). Sequence chromatograms were proofread and assembled with Geneious 9.0.2 (http://www.geneious.com) and the nine new nucleotide sequences were deposited in GenBank (Table 1).

Phylogenetic analyses

We downloaded nrLSU, mtSSU, and *TEF1* sequences of 5 *Capillidium* species, 19 *Conidiobolus* s.s. strains, four *Microconidiobolus* strains, 12 *Neoconidiobolus* species, *C. parvus*, and two outgroup taxa (*Entomophthora muscae* and *Erynia conica*) from GenBank. Individual sequences of each locus were aligned using MUSCLE 3.8.31 (Edgar 2004) and concatenated matrices were assembled by SequenceMatrix 1.7.8 (Vaidya et al. 2011). We partitioned the concatenated matrix by selecting the best model of sequence evolution for each gene according to the Akaike Information Criterion (AIC) using Modeltest 3.7 (Posada and Crandall 1998). We then conducted a Maximum Likelihood (ML) phylogenetic analysis using the best model using RAxML 8.1.17 with 1000 bootstrap replicates (Stamatakis 2014). We

Table 1. Accession information for samples used in phylogenetic analyses.

Species	Strains*	GenBank accession numbers		
		nucLSU	*TEF1*	mtSSU
Azygosporus macropapillatus	RCEF 4444	MZ542004	MZ555648	MZ542277
A. macropapillatus	RCEF 6334	MZ542005	MZ555649	MZ542278
A. macropapillatus	CGMCC 3.16068 (T)	MZ542006	MZ555650	MZ542279
A. parvus	ATCC 14634 (T)	KX752051	KY402207	MK301192
Capillidium adiaeretum	CGMCC 3.15888	MN061284	MN061481	MN061287
Ca. bangalorense	ARSEF 449 (T)	DQ364204	–	DQ364225
Ca. heterosporum	RCEF 4430	JF816225	JF816239	MK301183
Ca. lobatum	ATCC 18153 (T)	JF816218	JF816233	MK301187
Ca. rhysosporum	ATCC 12588 (T)	JN131540	JN131546	MK301195
Conidiobolus bifurcatus	CGMCC 3.15889 (T)	MN061285	MN061482	MN061288
C. brefeldianus	ARSEF 452 (T)	EF392382	–	EF392495
C. chlamydosporus	ATCC 12242 (T)	JF816212	JF816234	MK301178
C. coronatus	NRRL 28638	AY546691	DQ275337	–
C. dabieshanensis	CGMCC 3.15763 (T)	KY398125	KY402206	MK301180
C. firmipilleus	ARSEF 6384	JX242592	–	JX242632
C. gonimodes	ATCC 14445 (T)	JF816221	JF816226	MK301182
C. humicolus	ATCC 28849 (T)	JF816220	JF816231	MK301184
C. iuxtagenitus	ARSEF 6378 (T)	KC788410	–	–
C. khandalensis	ATCC 15162 (T)	KX686994	KY402204	MK301185
C. lichenicolus	ATCC 16200 (T)	JF816216	JF816232	MK301186
C. marcosporus	ATCC 16578 (T)	KY398124	KY402209	MK301188
C. megalotocus	ATCC 28854 (T)	MF616383	MF616385	MK301189
C. mycophagus	ATCC 16201 (T)	JX946694	JX946698	MK301190
C. mycophilus	ATCC 16199 (T)	KX686995	KY402205	MK301191
C. polyspermus	ATCC 14444 (T)	MF616382	MF616384	MK301193
C. polytocus	ATCC 12244 (T)	JF816213	JF816227	MK301194
C. taihushanensis	CGMCC 3.16016 (T)	MT250088	MT274290	MT250086
C. variabilis	CGMCC 3.16015 (T)	MT250087	MT274289	MT250085
Erynia conica	ARSEF 1439	EF392396	–	EF392506
Entomophthora muscae	ARSEF 3074	DQ273772	DQ275343	–
Microconidiobolus nodosus	ATCC 16577 (T)	JF816217	JF816235	MK333391
M. paulus	ARSEF 450 (T)	KC788409	–	–
M. terrestris	ATCC 16198 (T)	KX752050	KY402208	MK301199
M. undulatus	ATCC 12943 (T)	JX946693	JX946699	MK301201
Neoconidiobolus couchii	ATCC 18152 (T)	JN131538	JN131544	MK301179
N. kunyushanensis	CGMCC 3.15890 (T)	MN061286	MN061483	MN061289
N. lamprauges	CBS 461.97	MH874268	–	–
N. lachnodes	ARSEF 700	KC788408	–	–
N. mirabilis	CGMCC 3.17763 (T)	MH282852	MH282853	MK333392
N. nanodes	CBS 154.56 (T)	MH869096	–	–
N. osmodes	ARSEF 79	EF392371	–	DQ364219
N. pachyzygosporus	CGMCC 3.17764 (T)	KP218521	KP218524	MK333393
N. sinensis	RCEF 4952 (T)	JF816224	JF816238	MK301196
N. stilbeus	RCEF 5584 (T)	KP218522	KP218525	MK301197
N. stromoideus	ATCC 15430 (T)	JF816219	JF816229	MK301198
N. thromboides	ATCC 12587 (T)	JF816214	JF816230	MK301200

*ARSEF, ARS Entomopathogenic Fungus Collection (Ithaca, U.S.A.). ATCC, American Type Culture Collection (Manassas, U.S.A). CBS, Westerdijk Fungal Biodiversity Institute (Utrecht, The Netherlands). CGMCC, China General Microbiological Culture Collection Center (Beijing, China). FSU, Jena Microbial Resource Collection (Friedrich-Schiller-University of Jena, Germany). NRRL, ARS Culture Collection (Peoria, U.S.A). RCEF, Research Center for Entomogenous Fungi (Hefei, China). T = ex-type.

also built a phylogeny using Bayesian Inference (BI) with MrBayes 3.2.2 (Ronquist and Huelsenbeck 2003). We ran four Markov chains for 400,000 generations, sampling every 100th generation, and chains were run until the standard

deviation of split frequencies fell below 0.01. Maximum Parsimony (MP) analyses were performed with PAUP* 4.0b10 (Swofford 2002) using the heuristic research option with random stepwise addition, random taxon addition of sequences, tree bisection and reconnection (TBR) as the branch swapping algorithm, and 1000 replicates. All characters were weighted equally and character state transitions were treated as unordered. Parameters measured for parsimony included tree length (TL), consistency index (CI), rescaled consistency index (RC), retention index (RI), and homoplasy index (HI). The sequence matrix was deposited at TreeBase (No. S28467). Phylogenetic trees were viewed in TreeView (Page 1996) and edited in FigTree 1.4 (Rambaut 2012).

Results

Phylogenetic analyses

The total alignment length of the 46 taxa was 2,002: nrLSU, 1–1,095; *TEF1*, 1,096–1,597; and mtSSU, 1,598–2,002. The concatenated matrix contained 957 parsimony-informative and 225 parsimony-uninformative sites. The MP tree had a length of 5,463 with CI = 0.3815, RC = 0.2467, RI = 0.6404, and HI = 0.6471. We found that the optimal model of sequence evolution for nrLSU and *TEF1* were GTR+I+G4, while TVM+I+G4 was selected for mtSSU, and the resulting BI, ML, and MP trees had similar topologies; the ML tree was selected to represent the phylogeny with MP/ML/BI support values (Fig. 1). Samples from *Azygosporus macropapillatus* sp. nov. were sister to *C. parvus* (= *A. parvus*) in a single clade mostly related to the genus *Conidiobolus* s.s. in the phylogenetic tree. Both the clades of *Azygosporus* gen. nov. and *A. macropapillatus* sp. nov. were monophyletic with strong support (100/100/1.00).

Taxonomy

***Azygosporus* B. Huang & Y. Nie, gen. nov.**
MycoBank No: 840849

Etymology. Referring to produce azygospores.

Type species. *Azygosporus parvus* (Drechsler) B. Huang & Y. Nie.

Description. Mycelia colorless. Primary conidiophores simple, bearing single primary conidia. Primary conidia forcibly discharged multinucleate, colourless, globose to subglobose, small, less than 22.5 μm. Producing only globose or subglobose replicative conidia, similar to and smaller than primary conidia. Azygospores formed in the middle region of the old hyphal segments. Mature azygospores colourless or yellowish, smooth, without thickening or less thickening (0.5–1.2 μm).

Notes. *Azygosporus* is strongly supported as monophyletic and is distinguished from other Ancylistaceae lineages by the synapomorphy of azygospore production.

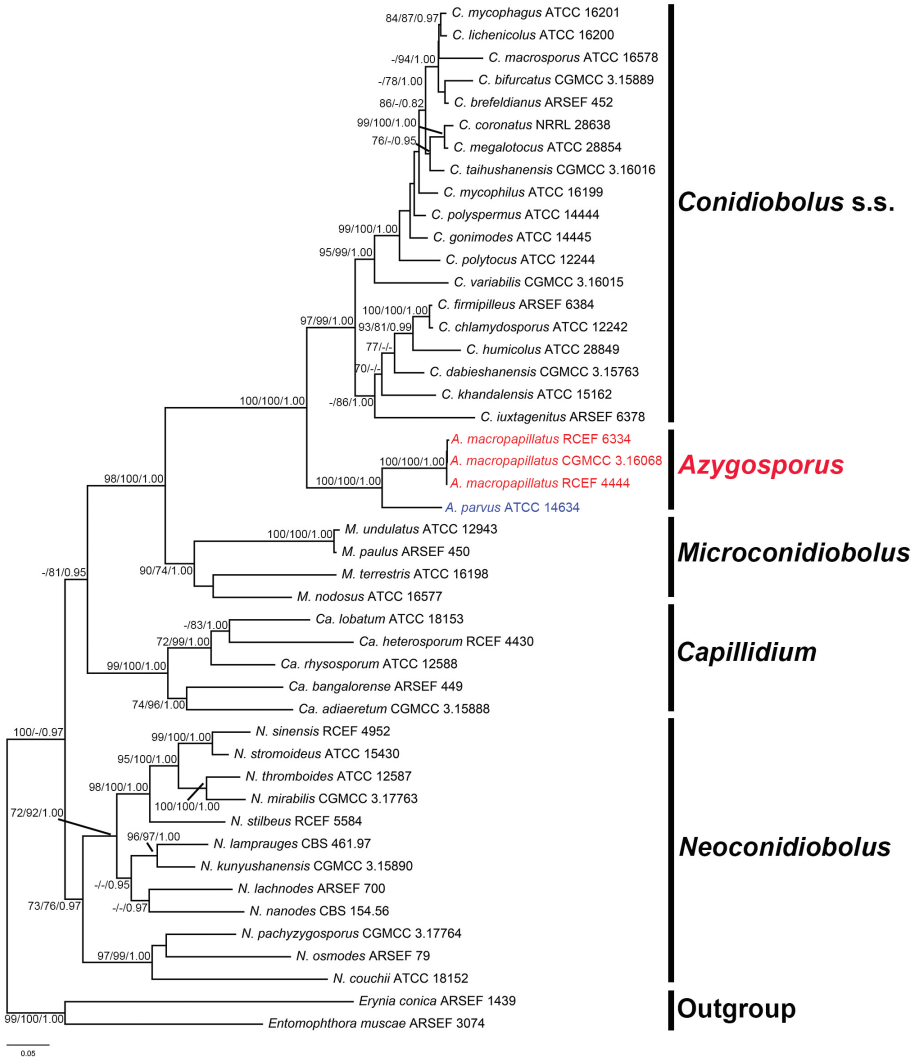

Figure 1. ML tree of *Coniobolus* s.l. using nrLSU + *TEF1* + mtSSU sequences. *Entomophthora muscae* and *Erynia conica* are selected as outgroups. Support for each node is shown as MP bootstrap support/ML bootstrap support/Bayesian posterior probability (MPBS/MLBS/BPP) for nodes with MPBS ≧ 70%, MLBS ≧ 70%) and BPP ≧ 0.95. The new genus, *Azyosporus*, and new species, *A. macropapillatus*, are shown in red, and the new combination is shown in blue.

Therefore, we classify this lineage as a new genus, named *Azygosporus* gen. nov. *Azygosporus* currently contains only two members: *C. parvus* (= *A. parvus*) and *A. macropapillatus* sp. nov. (Fig. 1). Morphologically, *Azygosporus* is most similar to *Microconidiobolus*, which forms small primary conidia (less than 22.5 µm) (Table 2). However, the synapomorphy of azygospore production clearly distinguishes *Azygosporus* from *Microconidiobolus* and other allied genera of the family.

Table 2. Morphological measurements of *A. macropapillatus* and other related species.

Species	Growth rate (mm/d) at 21°C on PDA	Diameter of mycelia (μm)	Primary conidiophores (μm)	Primary conidia (μm)	Basal papilla (μm)	Resting spores (μm)	References
A. macropapillatus	5.7–7.7	3.0–7.5	37.0–150.0×5.0–8.5	16.5–22.5×12.0–19.0	7.5–10.0×5.0–10.0	azygosporus, 25.0–30.0×27.0–34.0	This article
A. parvus	1.5	1.4–8.0 (3.5–5)	15.0–30.0×3.0–8.0	6.0–20.0×4.5–17.0	1.5–6.0×1.5–4.5	azygosporus, 20.0–25.0×8.0–20.0	Drechsler 1962
M. nodosus	7.1	3.5–6.5	30.0–50.0	17.0–22.0×13.0–16.0	2.5–5.0×1.5–2.5	chlamydosporus	Srinivasan and Thirumalachar 1967; King 1977
M. paulus	1.3–3.3	1.5–7.0 (4.0–5.0)	15.0–30.0×3.5–7.0	5.0–19.0×4.0–14.0	2.0–7.0×1.0–5.0	zygosporus, 10.0–15.0	Drechsler 1957
M. terrestris	2.6	2.8–4.5	15.0–80.0 ×3.0–5.0	8.0–12.0	2.0–4.0×1.5–2.0	chlamydosporus	Srinivasan and Thirumalachar 1968a; King 1977
N. lamprauges	less than 5.0	3.0–8.0 (4.0–7.0)	25.0–100.0 (25.0–50.0)×4.0–8.0 (5.0–15.0)	15.0–22.0×12.5–20.0	2.5–7.0×1.5–4.0	zygosporus, 12.0–18.0	Drechsler 1953
N. kunyushanensis	8.3–10.0	3.5–9.0	62.0–121.0×7.0–12.0	15.0–21.0×13.0–17.0	4.0–8.0×1.0–4.0	zygosporus, 12.0–25.0	Nie et al. 2021
N. pachyzygosporus	12.0	3.0–14.0	34.0–156.0×6.0–12.0	15.5–23.0×11.0–18.0	3.0–5.0×1.0–4.0	zygosporus, 15.0–25.0	Nie et al. 2018

***Azygosporus parvus* (Drechsler) B. Huang & Y. Nie, comb. nov.**
MycoBank No: 840850

Conidiobolus parvus Drechsler, Bull. Torrey bot. Club 89: 233 (1962) Basionym.

Description. Refer to Drechsler (1962).

Host and distribution. Isolated from decaying leaves in Maryland, United States.

Notes. The ex-type living culture is ATCC 14634 (United States, Maryland, Cumberland, 4 November 1962, Drechsler). It was reported to produce azygospores in *Conidiobolus* (King 1977); therefore, we recognize it as the type species of the genus *Azygosporus* gen. nov.

***Azygosporus macropapillatus* B. Huang & Y. Nie, sp. nov.**
MycoBank No: 840548
Fig. 2

Etymology. *macropapillatus* (Lat.), named by its prominent basal papilla.

Host and known distribution. Isolated from plant debris and mosses in Anhui Province, China.

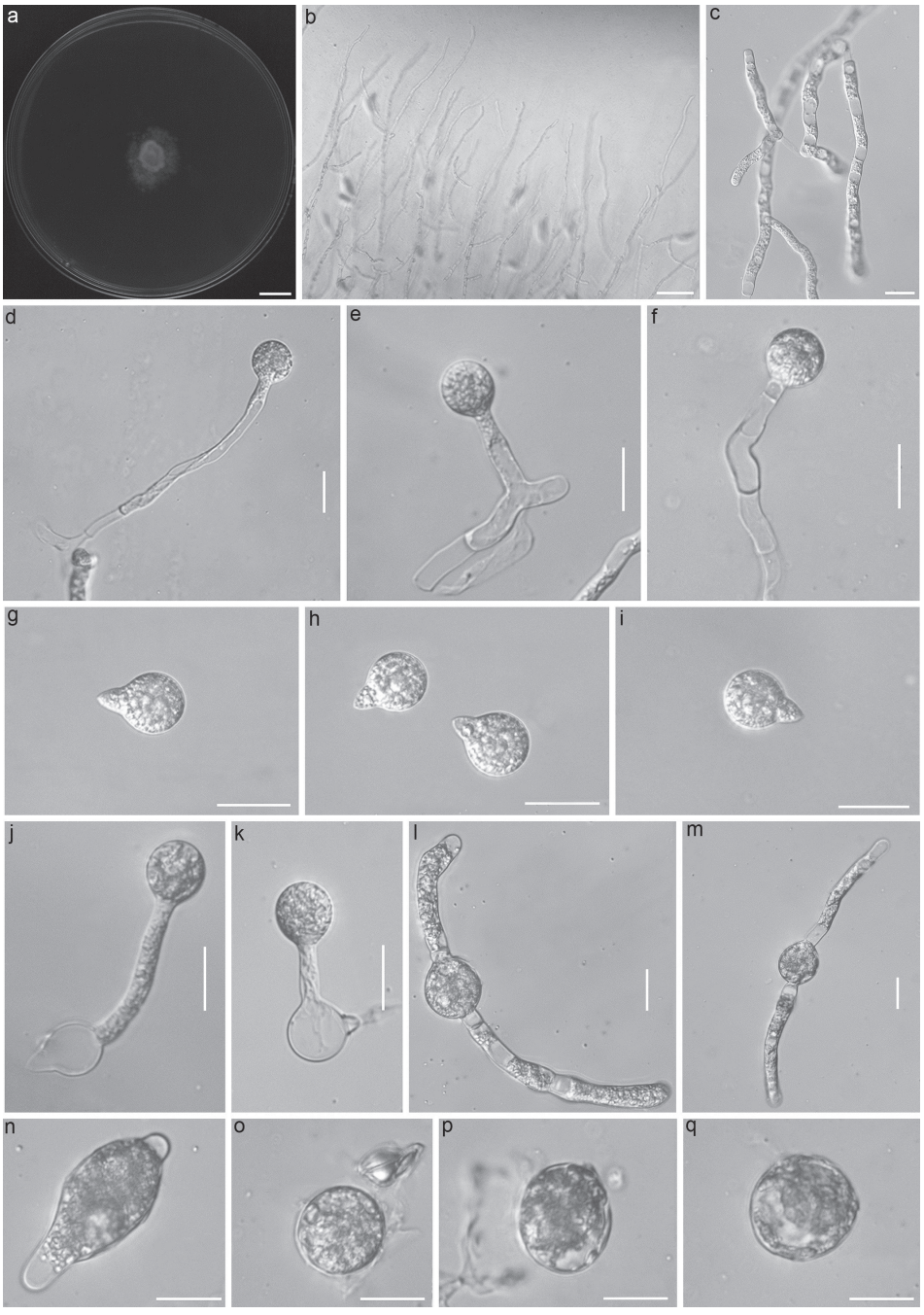

Figure 2. Morphological characters of *Azygosporus macropapillatus*: a) colony on PDA after 3 d at 21 °C, b) mycelia rarely branched at the colony edge, c-f) primary conidiophores bearing primary conidia, g-h) Primary conidia with prominent basal papillum, j-k) secondary conidia arising from primary conidia, i-m) azygospores formed in the middle region of the old hyphal segment, n) immature azygospore, and o-q) mature azygospores. Scale bars: a) 10 mm, b) 100 μm, and c-q) 20 μm.

Type specimens examined. China, Anhui Province, Ningguo City, Fangtang Town, 30°30'57" N, 118°42'17" E, from plant debris, 12 Nov 2020, *Y. Nie*, HMAS 350621, holotype, culture ex-holotype *CGMCC 3.16068* (= *RCEF 6680*). GenBank: nrLSU = MZ542006; *TEF1* = MZ555650; mtSSU = MZ542279.

Additional specimens examined. China, Anhui Province, Jinzhai County, Tiantangzhai National Forest Park, 31°20'68" N, 115°81'25" E, from mosses, 6 Nov 2008, *C.F. Wang*, culture *RCEF 4444*. GenBank: nrLSU = MZ542004; *TEF1* = MZ555648; mtSSU = MZ542277. China, Anhui Province, Jinzhai County, Tiantangzhai National Forest Park, 31°17'34" N, 115°78'13" E, from plant debris, 3 Dec 2015, *Y. Nie* and *X.X. Tang*, culture *RCEF 6334*. GenBank: nrLSU = MZ542005; *TEF1* = MZ555649; mtSSU = MZ542278.

Description. Colonies white, reaching ca 17.0–23.0 mm diameter on PDA after 3 d at 21°C. Mycelia colorless, 3.0–7.5 µm wide, usually unbranched at the colony edge. Primary conidiophores colorless, without widening upward near the tip, unbranched and producing a single conidium, 37.0–150.0 × 5.0–8.5 µm. Primary conidia forcibly discharged, colorless, subglobose, 12.0–19.0 µm wide and 16.5–22.5 µm long, most primary conidia possessed a prominent basal papilla 5.0–10.0 µm wide and 7.5–10.0 µm long. Secondary conidia arising from the primary ones with a similar shape and a smaller size. Resting spores (azygospores) observed after 10 d, and the young spores formed in the middle region of the old hyphal segments. The young spores enlarge gradually to form mature azygpspores with less thickening. Mature azygospores colorless, subglobose 25.0–30.0 × 27.0–34.0 µm with a wall 0.5–1.0 µm thick.

Notes. Morphologically, *Azygosporus macropapillatus* sp. nov. has conidial dimensions similar to six *Conidiobolus* s.l. species without capilliconidia and microconidia: *C. parvus*, *M. nodosus*, *M. paulus*, *N. kunyushanensis*, *N. lamprauges*, and *N. pachyzygosporus* (Drechsler 1953, 1957, 1962; Srinivasan and Thirumalachar 1967; Nie et al. 2018, 2021). However, *A. macropapillatus* sp. nov. produces a prominent basal papilla of primary conidia that differs from other related species (see detailed morphological comparisons in Table 2). *A. macropapillatus* sp. nov. forms azygospores most closely resembling those of *C. parvus* (= *A. parvus*), which is its closest known relative with robust support (100/100/1.00). *A. macropapillatus* sp. nov. is distinguished from *C. parvus* (= *A. parvus*) by its longer primary conidiophore and its prominent basal papilla.

Discussion

The genus *Microconidiobolus*, typified by *M. paulus*, was recently established as a monotypic genus based on its small discharged primary conidia (less than 20 µm) (Nie et al. 2020a). Besides the species shown in Table 2, we note that overlapping small primary conidial dimensions occur in other related genera such as, *Capillidium pumilum* (7.3–14 × 9–18 µm) (Drechsler 1955a) and *Conidiobolus khandalensis* (15–18 × 17–21 µm) (Srinivasan and Thirumalachar 1962b). Therefore, taxonomic definitions in this fungal group, as in all life, should be revised to follow phylogenetic relationships. Phylogenetically, *Ca. pumilum* and

C. khandalensis were distinct from *Microconidiobolus* spp. and *C. parvus* (= *A. parvus*) (Nie et al. 2018; 2020a). However, our previous phylogeny recovered *C. parvus* (= *A. parvus*) as distinct lineage within *Conidiobolus* s.s. (Nie et al. 2018; 2020b), but its taxonomic placement was uncertain due to its affinity with members of *Microconidiobolus*.

The phylogeny presented here (Fig. 1) is congruent with previous studies (Nie et al. 2018; 2020b) that investigated the placement of *C. parvus* (= *A. parvus*). Here, we demonstrate that *C. parvus* (= *A. parvus*) is sister to a new taxon, *A. macropapillatus* sp. nov., in a clade most closely related to *Conidiobolus* s.s., which we name *Azygosporus*. The primary character distinguishing *Azygosporus* from *Conidiobolus* s.s. is the production of microspores. Furthermore, *Azygosporus* can be distinguished from the related genus *Microconidiobolus*, by the production of azygospores, while members of *Microconidiobolus* form zygospores or chlamydospores. Azygospores were not observed in other related genera of the family Ancylistaceae. Consequently, we proposed a new genus, *Azygosporus* gen. nov., based on morphology and phylogeny. In addition, *C. parvus* (= *A. parvus*) was recognized as a new combination in the genus *Azygosporus* gen. nov. and introduced *A. macropapillatus* sp. nov. by its prominent basal papilla.

For decades, most published *Conidiobolus* species had been described by only one strain, with the exception of some pandemic species (e.g., *C. coronatus*, *N. osmodes*, and *N. thromboides*) (Nie et al. 2021). Unfortunately, the type species *C. utriculosus* Brefeld, along with other important ex-types are missing, which makes it difficult to determine the exact taxonomic placement of some questionable *Conidiobolus* spp. Expanding our descriptions of fungal diversity and improving the taxonomic system of this fungal group are continuing goals. Herein, we introduced a new genus and a new species, which are contributions to fungal taxonomy.

Acknowledgements

The authors are grateful to Dr. Ian Gilman (Yale University) for improving the manuscript. Mrs. C.F. Wang and Mrs. X.X. Tang (Anhui Agricultural University) are acknowledged for helping with specimen collection and molecular work.

This work was supported by the National Natural Science Foundation of China (Nos. 31900008, 30770008 and 31970009) and the Natural Science Foundation of Anhui Province (No. 2108085MH318).

References

Ben-Ze'ev IS, Kenneth RG (1982) Features-criteria of taxonomic value in the Entomophthorales: I. A revision of the Batkoan classification. Mycotaxon 14: 393–455.

Drechsler C (1952) Widespread distribution of *Delacroixia coronata* and other saprophytic Entomophthoraceae in plant detritus. Science 115: 575–576. https://doi.org/10.1126/science.115.2995.575

Drechsler C (1953) Three new species of *Conidiobolus* isolated from leaf mold. J Wash Acad Sci 43(2): 29–34.

Drechsler C (1954) Two species of *Conidiobolus* with minutely ridged zygospores. Am J Bot 41: 567–575. https://doi.org/10.1002/j.1537-2197.1954.tb14380.x

Drechsler C (1955a) A small *Conidiobolus* with globose and with elongated secondary conidia. Journal of Washington Academy of Sciences 45(4): 114–117.

Drechsler C (1955b) Three new species of *Conidiobolus* isolated from decaying plant detritus. Am J Bot 42(5): 437–443. https://doi.org/10.1002/j.1537-2197.1955.tb11144.x

Drechsler C (1957) Two small species of *Conidiobolus* forming lateral zygospores. Bulletin of the Torrey Botanical Club 84(4): 268–280. https://doi.org/10.2307/2482673

Drechsler C (1960) Two new species of *Conidiobolus* found in plant detritus. Am J Bot 47: 368–377. https://doi.org/10.1002/j.1537-2197.1960.tb07138.x

Drechsler C (1962) A small *Conidiobolus* with resting spores that germinate like zygospores. Bulletin of the Torrey Botanical Club 89(4): 233–240. https://doi.org/10.2307/2483199

Gryganskyi AP, Humber RA, Smith ME, Miadlikovska J, Wu S, Voigt K, Walther G, Anishchenko IM, Vilgalys R (2012) Molecular phylogeny of the Entomophthoromycota. Mol Phylogenet Evol 65: 682–694. https://doi.org/10.1016/j.ympev.2012.07.026

Gryganskyi AP, Humber RA, Smith ME, Hodge K, Huang B, Voigt K, Vilgalys R (2013) Phylogenetic lineages in Entomophthoromycota. Persoonia 30: 94–105. https://doi.org/10.3767/003158513X666330

Goffre D, Jensen AB, Lopez Lastra CC, Humber RA Folgarait PJ (2020) *Conidiobolus lunulus*, a new entomophthoralean species isolated from leafcutter ants. Mycologia 113(1): 56–64. https://doi.org/10.1080/00275514.2020.1816387

Humber RA (1989) Synopsis of a revised classification for the Entomophthorales (Zygomycotina). Mycotaxon 34: 441–460. https://doi.org/10.1098/rspa.1937.0056

Humber RA (1997) Fungi: identification. In: Lacey LA (Ed.) Manual of techniques in insect pathology. Academic Press, London

Jensen AB, Gargas A, Eilenberg J, Rosendahl S (1998) Relationships of the insect-pathogenic order Entomophthorales (Zygomycota, Fungi) based on phylogenetic analyses of nucleus small subunit ribosomal DNA sequences (SSU rDNA). Fungal Genetics and Biology 24(3): 325–334. https://doi.org/10.1006/fgbi.1998.1063

King DS (1976a) Systematics of *Conidiobolus* (Entomophthorales) using numerical taxonomy I. Taxonomic considerations. Can J Bot 54: 45–65. https://doi.org/10.1139/b76-008

King DS (1976b) Systematics of *Conidiobolus* (Entomophthorales) using numerical taxonomy II. Taxonomic considerations. Can J Bot 54: 1285–1296. https://doi.org/10.1139/b76-141

King DS (1977) Systematics of *Conidiobolus* (Entomophthorales) using numerical taxonomy III. Descriptions of recognized species. Can J Bot 55: 718–729. https://doi.org/10.1139/b77-086

Nie Y, Qin L, Yu DS, Liu XY, Huang B (2018) Two new species of *Conidiobolus* occurring in Anhui, China. Mycol Prog 17(10): 1203–1211. https://doi.org/10.1007/s11557-018-1436-z

Nie Y, Yu DS, Wang CF, Liu XY, Huang B (2020a) A taxonomic revision of the genus *Conidiobolus* (Ancylistaceae, Entomophthorales): four clades including three new genera. Mycokeys 66: 55–81. https://doi.org/10.3897/mycokeys.66.46575

Nie Y, Cai Y, Gao Y, Yu DS, Wang ZM, Liu XY, Huang B (2020b) Three new species of *Conidiobolus* sensu stricto from plant debris in eastern China. MycoKeys 73: 133–149. https://doi.org/10.3897/mycokeys.73.56905

Nie Y, Wang ZM, Liu XY, Huang B (2021) A morphological and molecular survey of *Neoconidiobolus* reveals a new species and two new combinations. Mycol Prog 20: 1233–1241. https://doi.org/10.1007/s11557-021-01720-w

Page RD (1996) TREEVIEW: an application to display phylogenetic trees on personal computers. Comput Appl Biosci 12: 357–358 https://doi.org/10.1093/bioinformatics/12.4.357

Posada D, Crandall KA (1998) MODELTEST: testing the model of DNA substitution. Bioinformatics 14: 817–818. https://doi.org/10.1093/bioinformatics/14.9.817

Rambaut A (2012). FigTree version 1.4.0. Available at http://tree.bio.ed.ac.uk/software/figtree/

Ronquist F, Huelsenbeck JP (2003) MRBAYES 3: Bayesian phylogenetic inference under mixed models. Bioinformatics 19: 1572–1574. https://doi.org/10.1093/bioinformatics/btg180

Srinivasan MC, Thirumalachar MJ (1961) Studies on species of *Conidiobolus* from India-I. Sydowia, Annales Mycologici 15: 237–241.

Srinivasan MC, Thirumalachar MJ (1962a) Studies on species of *Conidiobolus* from India-II. Sydowia, Annales Mycologici 16: 60–66.

Srinivasan MC, Thirumalachar MJ (1962b) Studies on species of *Conidiobolus* from India-III. Mycologia 54(6): 685–693. https://doi.org/10.2307/3756504

Srinivasan MC, Thirumalachar MJ (1967) Evaluation of taxonomic characters in the genus *Conidiobolus* with a key to known species. Mycologia 59: 698–713. https://doi.org/10.2307/3757098

Srinivasan MC, Thirumalachar MJ (1968a) Studies on species of *Conidiobolus* from India V. Mycopathologica et Mycologia Applicata 36: 341–346. https://doi.org/10.1007/BF02050380

Srinivasan MC, Thirumalachar MJ (1968b) Two new species of *Conidiobolus* from India. J Mitchell Soc 84: 211–212.

Stamatakis A (2014) RAxML version 8: A tool for phylogenetic analysis and post-analysis of large phylogenies. Bioinformatics 30(9): 1312–1313. https://doi.org/10.1093/bioinformatics/btu033

Swofford DL (2002) PAUP*: Phylogenetic analysis using parsimony (*and other methods), Version 4.0b10. Sinauer Associates, Sunderland.

Vaidya G, Lohman DJ, Meier R (2011) SequenceMatrix: concatenation software for the fast assembly of multi-gene datasets with character set and codon information. Cladistics 27(2): 171–180. https://doi.org/10.1111/j.1096-0031.2010.00329.x

Vilela R, Silva SMS, Correa FR, Dominguez E, Mendoza L (2010) Morphologic and phylogenetic characterization of *Conidiobolus lamprauges* recovered from infected sheep. J Clin Microbiol 48: 427–432. https://doi.org/10.1128/JCM.01589-09

Watanabe M, Lee K, Goto K, Kumagai S, Sugita-Konishi Y, Hara-Kudo Y (2010) Rapid and effective DNA extraction method with bead grinding for a large amount of fungal DNA. J Food Prot 73(6): 1077–1084. https://doi.org/10.4315/0362-028X-73.6.1077